INTEGRATED DYNAMIC SIMULATION OF LARGE THERMAL SYSTEMS

D.C. Arndt

Presented in partial fulfilment
of the requirements for the degree

PHILOSOPHIAE DOCTOR

in the Faculty of Engineering
Department of Mechanical Engineering
University of Pretoria
Pretoria

November 2000

ABSTRACT

Title: Integrated dynamic simulation of large thermal systems

Author: Deon Arndt

Supervisor: Prof. E.H. Mathews

Department: Mechanical and Aeronautical Engineering

Degree: Philosophiae Doctor

Search terms: Thermal building simulation; HVAC system simulation; Control simulation; System simulation verification; System simulation applications; Energy-efficient control; Mine cooling plant simulation; Mine pumping system simulation; Demand side Management; Component models; Simulation procedures.

Studies concluded that more that 10% of all energy consumed in the world is expended by building air-conditioning systems. Energy efficiency in building and HVAC (Heating, Ventilating and Air-conditioning) design is therefore exceptionally important. A cost-effective way to improve the energy efficiency of a HVAC system, without compromising indoor comfort, is by implementing better control.

System energy cost savings of up to 50% can be realised by optimising the system operating control strategies with direct payback periods of less than a year. However, when changing the operating strategy of a system it is often difficult to predict the resulting changes in system energy consumption and indoor comfort. To achieve these predictions, a dynamic simulation tool, which can efficiently and accurately simulate the building with the HVAC and control system in an integrated fashion, is required.

Extensions to the integrated tool QUICKcontrol is therefore proposed to suite the needs of the energy service contractor. QUICKcontrol still has many shortcomings in the availability of component models for certain equipment commonly used in building systems today. New dynamic component models were therefore derived in this study.

ABSTRACT

The accuracy and applicability of integrated building and natural ventilation modelling is illustrated in animal housing facilities. The predicted results obtained during this study were satisfactory to use these models with confidence in this type of building applications.

The applicability of building, HVAC system and control simulations was illustrated in conference facilities. The results obtained show the value of integrated building and system simulation in the evaluation of energy cost saving inventions in commercial buildings.

The mining and industrial sectors in South Africa consume about 40% of ESKOM's total electrical energy production. Mines alone use nearly 20% of the electricity provided by ESKOM. Ventilation and cooling (VC) systems are responsible for approximately 25% or R750 million of this energy. It will therefore be beneficial if the mines can be more energy clever in order to reduce their VC operating costs.

The use of an extended integrated building and system simulation tool was therefore realised to investigate the potential for energy cost savings in mine VC applications. To extend QUICKcontrol for the simulation of other large thermal systems found in mining and industrial applications, new component models and simulations procedures were developed.

Two case studies were performed with the extended tool to illustrate its applicability in thermal systems other than building systems. The potential for Demand Side Management (DSM) on a surface cooling plant and an underground clear water-pumping system was investigated.

Satisfactory results were obtained during the two investigations to utilise this extended tool with confidence in practice. With more extensions to the tool it should be possible to investigate the potential for energy cost saving on any other thermal industrial applications.

SAMEVATTING

Titel: Integrated dynamic simulation of large thermal systems

Outeur: Deon Arndt

Leier: Prof. E.H. Mathews

Departement: Meganiese en Lugvaartkundige Ingenieurswese

Graad: Philosophiae Doctor

Sleutelterme: Thermal building simulation; HVAC system simulation; Control simulation; System simulation verification; System simulation applications; Energy-efficient control; Mine cooling plant simulation; Mine pumping system simulation; Demand side Management; Component models; Simulation procedures.

Volgense internasionale studies verbruik lugversorgingsstelsels 10% van die wêreld se energie. Energie effektiewe geboue en lugversorgingsstelsels is dus baie belangrik. 'n Goedkoop wyse om die energieverbruik van 'n lugversorgingsstelsel te verlaag, sonder om die behaaglikheid van die gebou te beïnvloed, is om beter stelselbeheer te implimenteer.

Stelselenergie bespaarings van 50% kan verkry word deur die beheer van die stelsel te optimeer met 'n direkte terug betaal tydperk van minder as een jaar. Dit is egter moeilik om die verandering in stelselenergie en behaaglikheid te voorspel wanneer die beheer verander word. Sagteware wat die gebou en die stelsel geïntegreerd kan simuleer is nodig om hierdie veranderings akkuraat te voorspel.

Veranderings aan die simulasie-sagteware QUICKcontrol word in hierdie tesis voorgestel om die gebruikersvoorwaardes van die energie-konsultant te bevredig. Daar is egter nog 'n tekort in komponentmodelle van toerusting wat algemeen gebruik word in geboue. Nuwe modelle is daarom afgelei vir sommige van hierdie toerusting.

SAMEVATTING

Die akkuraatheid en die toepaslikheid van geïntegreerde gebou en natuurlike ventilasie modellering word geïllustreer in dierebehuising. Bevredigende resultate is tydens hierdie studie verkry en die modelle kan dus met sekerheid in die bedryf gebruik word.

Die toepaslikheid van geïntegreerde gebou en stelselsimulasie word verder geïllustreer in konferensielokale. Die resultate van hierdie studie wys die waarde van geïntegreerde simulasie tydens gebou energie besparings projekte.

Die mynboubedryf en industriële sektor van Suid Afrika verbruik ongeveer 40% van ESKOM se totale beskikbare energie. Die myne alleen verbruik ongeveer 20% van hierdie totale energie. Ventilasie en Verkoeling (VV) in myne is verder verantwoordelik vir 25%, of R750 miljoen, van hierdie energie. Die myne kan dus hul VV bedryfsuitgawes verminder deur energie meer effektief te gebruik.

Die gebruik van geïntegreerde gebou en stelsel sagteware om die potensiaal vir energie koste besparings in die mynboubedryf en industriële sektor te bepaal, is besef. Nuwe modelle en prosedures is ontwikkel om QUICKcontrol aan te pas vir die simulering van termiese mynstelsels en ander termiese industriele-stelsels.

QUICKcontrol is gebruik tydens twee gevalle studies om die toepaslikheid daarvan in ander velde te illustreer. Die potensiaal vir aanvraagkantbeheer op 'n myn verkoelingsaanleg en 'n myn pompstelsel is ondersoek.

Bevredigende resultate is verkry tydens die twee studies met QUICKcontrol. Die sagteware kan dus met sekerheid gebruik word in hierdie bedryf. Met verdere sagteware veranderings sal dit in die toekoms moontlik wees om die potensiaal vir energie koste besparings van enige termiese-stelsels in die industriële sektor te bepaal.

ACKNOWLEDGEMENTS

I would like to express my gratitude to Prof. E.H. Mathews for the opportunity to perform this study. His guidance throughout has been of great value and I am grateful for his contribution to my development.

Many thanks also to the following people whose contributions throughout the course of this study have been invaluable:

- All my colleagues at the Centre for Experimental and Numerical Thermoflow for their input,
- Transfer of Energy, Momentum and Mass International (Pty) Ltd. for the use of their simulation software QUICKcontrol.

A very special word of thanks goes out to my family and friends for their constant support. This study is dedicated to my parents for their encouragement, love and support throughout my life.

Finally, all thanks to my Creator without whom none of this would have been possible. Thank you Lord, for your endless blessings.

PREAMBLE

This dissertation consists of two parts. Each part has its own introduction, main body and closure. The first part describes integrated dynamic simulation of thermal building systems and the second part deals with mining and industrial thermal systems.

The second part of the dissertation is an extension to the first part to investigate the use of building and HVAC systems simulation programs in applications other than building applications. Each part can be seen as a separate part and can therefore be read on its own. However it will make more sense to read part one before part two.

TABLE OF CONTENTS

CHAPTER 3 APPLICATION 1: ANIMAL HOUSING FACILITIES

CHAPTER 4 APPLICATION 2: CONFERENCE FACILITIES

CHAPTER 5 CLOSURE

PART 2: OTHER THERMAL SYSTEMS

CHAPTER 6 INTRODUCTION

CHAPTER 7 NEW THERMAL MODELS

LIST OF FIGURES

LIST OF TABLES

CHAPTER 1

INTRODUCTION

Studies concluded that more that 10% of all energy consumed in the world is expended by building air-conditioning systems. Energy efficiency in building and HVAC design is therefore exceptionally important. A cost-effective way to improve the energy cost efficiency of a HVAC system, without compromising indoor comfort, is by implementing better control. System energy cost savings of up to 50% can be realised by optimising the system operating control strategies with direct payback periods of less than a year. However, when changing the operating strategy of a system it is often difficult to predict the resulting changes in system energy consumption and indoor comfort. To achieve these predictions, a dynamic simulation tool, which can efficiently and accurately simulate the building with the HVAC and control system in an integrated fashion, is required. Extensions to the integrated tool QUICKcontrol are therefore proposed to suite the needs of the energy service contractor. These proposals can be implemented to achieve an efficient integrated simulation tool to be used as standard procedure in practice.

NOMENCLATURE

C	Thermal capacity (J/kgK)
Q	Heat source (W)
R	Thermal resistance across the surface (K/W)
T	Temperature (°C)

Subscripts

a	Air
c	convective
e	Envelope
hm	high mass
i	inside
lm	low mass
o	outside
r	radiative
s	solar air/surface

1.1 THE NEED FOR AN INTEGRATED TOOL

According to international studies[1], building operational costs account for 37% of the total world primary energy consumption. In the UK[2] building operation is the second largest industry and is responsible for 18% of the energy use. For the energy-intensive USA it is estimated[3] that some 36% of the country's energy supply is consumed in buildings. It is a clear fact that a large percentage of the total energy consumption of the world is used in buildings.

An analysis of the building sector for the UK[4] showed that housing accounts for 65%, the commercial and public buildings for 29% and industrial buildings for approximately 6% of the energy expenditures. In the USA[5] it is speculated that the energy consumption in commercial buildings amounts to approximately 13% of all USA energy use.

Studies in South Africa[6] have shown that 20% of the total municipal electrical energy consumption is utilised in commercial buildings. Although the energy use of the housing and industrial sectors is the largest, the potential for energy savings is probably the greatest in the existing stock of commercial buildings.

According to a 1988 report by Geller[7], commercial buildings at that time showed the highest growth in energy consumption of all sectors of the economy. Forecasts at that time showed that air-conditioning would be one of the end-use categories that would show the highest percentage growth between 1985 and 2010, mainly due to increases in commercial floor space.

In the now defunct USSR[1] approximately 25% of the total energy consumption is spent annually on air-conditioning. Considering the energy delivered in Western Europe[2], we see that 9% is attributed to iron and steel production, 21% to transportation, 2% to agriculture, 16% to the manufacturing industries and a massive 52% - more than all the other demands put together - is consumed to maintain acceptable conditions within their building stock.

In the USA[8] HVAC systems account for 80 % of the commercial energy consumption of

15% of the nations primary annual energy use. In South Africa studies[7] have shown that 65% of the energy in the commercial sector is used for air-conditioning. Rousseau and Mathews[9] concluded that more that 10% of all energy consumed in the world is expended by building air-conditioning systems. Energy efficiency in building and HVAC design is therefore exceptionally important.

Energy audits in Australia[10] have shown that retrofitting existing buildings could reduce energy use for space heating and cooling by up to 35%. In new buildings savings of up to 50% could be achieved. Estimates by the UK Department of Energy[3] suggest that better design of new buildings could result in a 50% reduction in energy consumption and that retrofitting in existing buildings could yield energy reductions of 25%.

In the USA[5] a study of over 1 700 building energy retrofits reports annual savings of 18% of whole building energy usage with an average payback time of 3,1 years. Optimistic sources estimate energy savings as high as 70% or more through the use of improved design and management practices, as well as through retrofit projects of existing commercial buildings[11].

It is more commonly agreed that energy savings of around 30% may be realised through the use of improved design and management practices as well as through retrofit projects of existing commercial buildings[12]. Energy saving retrofits have proven effective at reducing energy costs for buildings and moderating total energy consumption growth.

Energy saving measures on HVAC systems must never compromise indoor air quality (IAQ) in buildings at any time. The reason is that IAQ has a direct effect on the productivity of the occupants[13]. The cost associated with poor IAQ far outweigh savings due to reduced energy consumption[14].

A cost-effective way to improve the energy cost efficiency of a HVAC system, without compromising indoor comfort, is by implementing better control. System energy cost savings of up to 50% can be realised by optimising the system operating control strategies with direct payback periods of less than a year[15].

This ratio of savings to payback periods should be very attractive to Energy Service Contractors and HVAC designers. However, when changing the operating strategy of a system it is often difficult to predict the resulting changes in system energy consumption and indoor comfort. To achieve these predictions, a dynamic simulation tool, which can efficiently and accurately simulate the building with the HVAC and control system in an integrated fashion, is required.

There are many building and system energy simulation tools available in the world today but most of them are only used for research[16],[17] and not in practise as standard procedure where time is of the essence. The main reasons are that they are time consuming and difficult to use.

1.2 REQUIREMENTS FOR AN INTEGRATED TOOL

The user requirements for a building and system simulation tool, which can efficiently predict the effect of control strategies on energy consumption and indoor comfort, is discussed in this section. There is no sense in developing any new integrated simulation tools if the requirements of the user are not satisfied. These tools should be developed for the energy contractor and HVAC designer in practice and not for the research community.

Most simulation tools do no satisfy the requirements of the user in practice because they are developed by research institutions[16] for their own needs. This normally results in a tool that is very difficult and time consuming to use. Only "PhDs" can efficiently achieve realistic results with them. Most of the time these tools are very unstable when inexperienced users perform simulations.

User requirements that satisfy the needs of the energy service contractor and HVAC designer are identified in this section. These requirements were obtained from experienced Energy Service Companies, TEMM International[18], ESKOM[19], and Econoler International[20]. An evaluation by TEMM International and ESKOM of the two software packages VisualDOE and QUICKcontrol is shown in Appendix E. Proposed methods and procedures are furthermore discussed to satisfy each of these user requirements.

1.2.1 Building

Any building structure:

The tool must have the flexibility for the construction of any building zone found in the building sector world-wide. This implies the combination of any surfaces, materials, dimensions, orientation, climate, mechanical ventilation, natural ventilation, infiltration and internal loads.

To allow for any building, the construction of an unlimited number of building zones must be possible. The same applies for the number of surfaces. An extendable database is therefore necessary to add new building materials. The building model must further allow for the integration of natural and mechanical ventilation.

To integrate ventilation models (ventilation air from the HVAC system) into the building model, a method which predicts the indoor air temperatures (passive building model) and not heat loads to a set temperature[22] must be utilised. This is necessary for the calculation of transient indoor air temperature profiles caused by the environment, thermal mass of the structure and the influence of the HVAC system. Load calculation methods will therefore not be sufficient to model the performance of building zones in an integrated control simulation tool.

Fast and easy construction:

Fast and easy construction of the building envelope with its daily user profiles is important. A building zone must be constructed within minutes without the availability of detailed building drawings. Detailed data and drawings are not always available during the concept stages of new designs and for existing buildings during retrofit projects.

Typical used surface types must be available in a pre-constructed database for fast building construction. The user must only be asked for the input data which is sensitive to the thermal performance of the building[21]. Thermal mass, position of insulation and the orientation of large glazing facades are some of the sensitive building inputs.

Availability of input data:

The user must never be asked for input data that is not freely available or not understandable. This applies to the entire building input phase. The ideal would be to set-up the building model on a portable computer during a walk-through investigation of the building.

The user must not be confronted with complex technical data during the building construction phase. For example, the user should be asked for a listed colour rather than an absorptance value of an outside surface. The user must be given set choices (orientation, building shape, transparent surfaces, dimensions and surface structure) during the construction phase to prevent the input of unnecessary data, which will have a small effect on the performance of the building[21].

Verification and calibration:

The simulation tool must allow for easy and fast verification and calibration of the thermal performance of the building zones with measurements during retrofit projects. This is necessary for the calculation of accurate and realistic energy cost savings.

The simulation tool must therefore be component-based where each zone is represented by a separate component. This is necessary to identify the inside condition profiles of each zone over time for easy and fast verification. Building conditions must be calculated at any time intervals to validate the dynamic response of the building and system.

Output:

Temperature and relative humidity output trends over 24-hours for each day of the year must be available. These trends are necessary to obtain the effect of operating strategies, time constants of the system and limited capacity of the system components on the indoor comfort over time.

The building model must be dynamic to calculate the transient response of the building conditions over time. To investigate the effect of control and system capacity the building

must be solved with all the other components in an integrated fashion.

1.2.2 HVAC system

Any system configuration:

The tool must have the flexibility to configure any system type found in the building industry world-wide. There must be no restrictions for the user regarding the number of system components and the sequence of the components in the system.

The simulation tool must therefore be component-based to configure any system type intuitively from the real system. The feature that allows the user to add any new component models is important for future technologies.

Fast and easy configuration:

Fast and easy system configuration is very important. A HVAC system must be configured within tens of minutes directly from a schematic drawing of the system. The procedure must therefore be intuitive and the system model must be a replica of the schematic drawing. This implies that each component in the simulation tool can be identified with the respective component of the real system at the same location.

The tool must make use of a drag and drop interface for the fast and easy configuration of a new system. It must allow for typical pre-constructed system units (fan coil units) and total system types to decrease the time of input.

Availability of input data:

The user must never be asked for system component input data that is not freely available or not understandable. The ideal would be to configure each component from data of only one operating point, freely available from the manufacturer or measurements from an existing system.

Component models must therefore be a combination of fundamental principles and empirical correlation coefficients for "real life" simulations and to minimise the required input data[22]. Scale factors and typical system curves must be used to obtain regression coefficients of the component models from only one given operating point.

Appendix A illustrates the use of typical system curves to scale a simulation model to fit through one known operating point. This point can either be from the manufacturer (for new equipment) or measurements (for old equipment).

Verification and calibration:

The tool must allow for easy and fast verification and calibration of the thermal performance of all the system components with measurements during retrofit projects. This is necessary to ensure the performance of each system component due to performance losses over the years. This is very important for the calculation of accurate and realistic energy cost savings and the effect these losses are going to have on the indoor comfort.

The tool must therefore be fully component-based to identify the problem areas during verification and calibration. The components that do not perform according to the original specifications can now be identified and calibrated. By doing this the accurate performance of each component in a retrofit energy simulation can be ensured for realistic predictions.

System outputs:

System condition output trends for each component over 24-hours for each day of the year must be available. These trends are necessary to obtain the effect of operating strategies, time constants of the system and limited capacity of the system components on the indoor comfort over time. Power consumption trends of each component over 24-hours for each day of the year are important. This is necessary for energy cost calculation when investigating the viability of time of use tariffs.

The system models must therefore be dynamic to calculate the transient response of the system conditions and power consumption over time. To investigate the effect of control and

system capacity, the building must be solved with all the other components in an integrated fashion.

1.2.3 Controls

Any control strategy:

Any system component must have the option to be controlled from a sensor anywhere in the system. All the sensor types used in the building industry must be available. The same applies for controller types utilised in the building sector.

Any component, sensor and controller combination must be possible. The sensors and controllers must therefore also be component-based to allow for any control strategy.

Fast and easy configuration:

The tool must allow for fast and easy configuration of control systems. A control system must be configured within minutes directly from a schematic drawing of the control system. The procedure must therefore be intuitive and the control system in the simulation tool must be a replica of the schematic drawing. This implies that each controller and sensor in the simulation tool can be identified with the respective components of the real system at the same locations.

The tool must therefore make use of a drag and drop interface for the fast and easy configuration of any new control system. Typical pre-constructed control units (economiser cycles) will decrease the time of input.

1.2.4 Simulations procedure:

Fast and stable solutions are one of the most important requirements of any simulation user. There is nothing more frustrating than a slow unstable simulation tool. Both these requirements are important in the industry where time is of the essence. It is therefore

important to obtain a balance between the two. Fast unstable simulations can easily outweigh the total simulation time utilised by slow stable solutions.

One method to decrease simulation execution time and increase stability is to utilise an explicit equation philosophy on component level. The ideal for an integrated simulation tool is to use only explicit equations to calculate component outputs. This also applies to the building model. Each building zone must therefore be a set of explicit equations de-coupled from other adjacent building zones.

Using this approach will eliminate the use of any solvers and numerical iterations to calculate the output conditions of the system components. The advantages are two fold: explicit equations are exact and will always produce an answer. The elimination of iterations will ensure faster simulations and decrease simulation time.

The approach where flow is specified explicitly by certain components in a flow network and not solved implicitly for each time step will further improve the stability and decrease simulation time. Only an integrated implicit solver to obtain the conditions in a configuration with closed-loops is therefore necessary. This calculation procedure will now be the only procedure for which a solution cannot always been ensured for all the calculations during a simulation. This is only true when all the component models are already explicit.

1.3 EXISTING SIMULATION TOOLS

There are many building and system analysis tools available in the world today. These tools can be grouped into two types[23]: Energy analysis tools and system simulation tools. The primary function of energy analysis programs is to calculate system energy consumption. Various HVAC systems can be compared to reveal the system with the lowest energy consumption. These tools are normally based on load calculation methods from where system energy is calculated by simplified models.

System simulation tools endeavour to predict the dynamic response of the HVAC system and the building, i.e. indoor air conditions, system operation points and energy usage. In general these tools are component-based[24] which makes them more flexible with fewer restrictions

placed on the applicability.

Some of the well-known energy analysis tools are: BLAST[25], DOE-2[26], VisualDOE[27], E-CUBE[28], AXCESS[29], COM-TECH[30], HAP E-20[31], HAP 40[32], TAS[33], TRACE[34], ENERPAS[35], ENERWIN[36], and BSIM2000[37]. Of these, DOE-2 (Visual DOE) is probably the most popular and comprehensive, while TAS is the most user-friendly[24].

System simulation tools include APACHE[38], CABERETS[39], HVACSIM+[40], HVAC-DYNAMIC[41], SPARK[42], TRNSYS[43], GEMS[44] and QUICKcontrol[23].

These energy analysis tools found in the literature do not satisfy the most important technical requirements identified for control simulation, i.e. the complete integration of the building, HVAC system and its control[23].

Many of these tools perform calculations in three sequential steps[22]. The first step is the calculation of the loads which accounts for the thermal performance of the building at a specified fixed indoor air temperature. The second step is the secondary systems calculation, which describes the thermodynamic behaviour of different elements in the air-handling units such as fans, heat exchangers. The third set is the plant calculation, which simulates the primary energy conversion equipment such as boilers and chillers.

This means the effects of control, limited system capacity and the thermal mass of the building structure on indoor comfort are not accounted for. In real life controllers cannot keep the indoor or any system setpoints exactly at the right conditions. In some programs, like DOE-2, an overload is reported when the indoor air temperature cannot be maintained.

Even though system simulation programs cater for detailed simulation of the secondary system or air-handling units on a component base, and some even take into account the important interaction between the building and the secondary system, many of them are still not fully integrated[23].

A separate load calculation model based on the response factor method is, for example, used

to determine the loads that are used in the building model of HVACSIM+. No load modelling is attempted with the system simulation. Thus the problem of varying indoor temperature will still be experienced[24].

QUICKcontrol[23] and TRNSYS[43] were found to be the closest to the philosophy and the requirements identified by the author. QUICKcontrol was funded and developed by TEMM International specifically for "real life" control simulation. TRNSYS, developed by the Solar Energy Lab (SEL) at the University of Wisconsin-Madison performs detailed analyses of systems whose behaviour is dependent on the passage of time.

Both these programs are dynamic and fully integrated which satisfy two important requirements identified by the author. They are further component-based for the configuration of any building and system type. However these two simulation tools are very difficult and time consuming to use.

Furthermore, stable solutions are difficult to obtain by the inexperienced user when solving rather large complex systems. However, these tools have the potential to be used as basis for the development of a new tool, which will satisfy the requirements discussed previously.

There is still a shortage in component models in QUICKcontrol of typical used HVAC equipment in the building sector. Many of the existing component models are not explicit and therefore do not satisfy this requirement as expressed by the author.

A new integrated tool, which is based on QUICKcontrol, is proposed in the following section to satisfy the identified requirements. The tool is discussed under the headings: building model, HVAC components, control components and simulation procedures. These sections also include proposals on user inputs to minimise input data for fast efficient use.

1.4 THE NEW SIMULATION TOOL

1.4.1 Building model

An electrical analogy derived by Van Heerden[24] is used to model the heat transfer processes in the building for the accurate prediction of the thermal performance of the building zones. The reason for the use of this model is to simulate the building zones with the air-conditioning plant and its controls in an integrated fashion.

The model makes use of a six-node electric circuit to simulate the different heat flow paths. A schematic layout of the zone model electrical analogy is displayed in Figure 1.1.

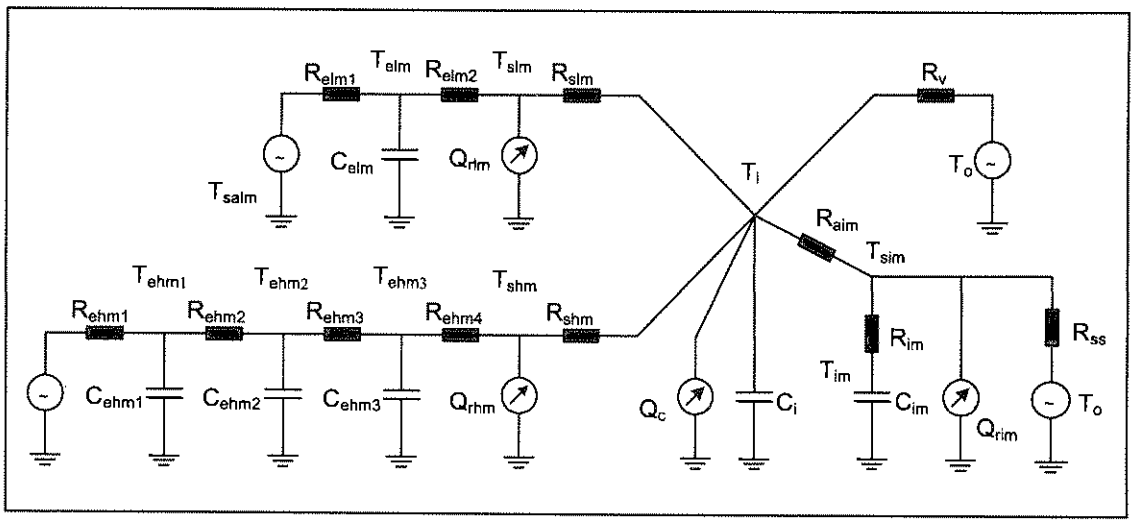

Figure 1.1: Zone model electrical analogy

The air node of the electric circuit is treated as a separate node, and its capacitance (C_i) is simply calculated by:

$$C_i = Vol\rho C_p \tag{1.1}$$

where Vol is the zone volume, ρ is the air density and C_p is the specific heat capacity of the air. The ventilation, infiltration and environmental control are all treated separately and the resistance is given as:

$$R_v = \frac{1}{Vol\rho C_p(ACS)} \tag{1.2}$$

where ACS is the air changes per second. All the internal masses are combined and treated as a single capacitor, including the floor (C_{im}). The heat gains through the floor are treated separately with the steady state resistance R_{ss}.

Provision is made in the model for two structural heat flow paths, namely a low mass path (single node - glass, fenestration and other low mass structures), and a high mass path (triple node). The thermal resistances and capacitances for the high and low mass path are determined by optimisation.

The analytical solution in the frequency domain is determined from the theory derived by Davies[46]. The response of the electric analogy is then matched to the analytical solution by selecting values for R and C.

Convective heat gains (Q_c) act directly on the air node. Radiative heat gains (Q_r) are weighed according to surface area and act directly on the surface. The governing equations for the complete circuit can be derived by adding the currents at each node.

In total the circuit contains nine nodes. Six of the nodes are associated with capacitors and the other three with surfaces. The differential equations resulting at the nodes containing capacitors can be discretisized using a forward differencing scheme.

The use of the heat balances at the surfaces contribute three algebraic equations containing the surface temperature terms. The resultant nine equations must be solved simultaneously at each time step. The relevant psychrometric relationships are employed in the building model to deal with the moist air properties.

At first it might sound like a formidable task to solve the building model, but fortunately the resultant matrix is sparse with an almost tri-diagonal structure. The matrix can therefore be inverted by Guass-elimination beforehand and the coefficients can be calculated once since the coefficients remain constant. At each time step only the backward substitution needs to

be done to solve the model. Therefore the building model is explicit and can be solved quickly and efficiently.

Each building zone is treated as a separate component model with pipe elements linked to the HVAC system (R_v) and the climate (T_o, T_{sa}). This model therefore satisfies the requirements identified by the author for efficient integrated control simulation.

Ellis[21] introduced a philosophy where the building input per zone is minimised to only a single input screen. The philosophy is to include only the building data, which is critical when modelling the thermal performance of building zones. Most of this building data can further be stored in a pre-constructed database for fast and efficient zone construction. This philosophy is implemented to obtain the parameters of the building model introduced above.

1.4.2 System component models

The HVAC component models derived by Rousseau[22] link inputs and outputs of the basic thermodynamical variables in the system. They are based on simplified fundamental principals combined with correlation coefficients derived from discrete empirical data.

The models are fully component-based and allow simulation of a wide range of operating conditions. The calculation of the energy consumption of each component is included in each model. The correlation coefficients for a specific make and model can be derived from data obtained from measurements or manufacturers' data sheets.

Each component model is configured so that it calculates the thermodynamic output states of the fluids flowing through it, given the input states. The simulation tool makes use of the following component types based on the combinations of fluids that can flow through the component:

- Air only (fan - one inlet and one outlet; air converge - multiple inlets and one outlet; air diverge - multiple outlets and one inlet).
- Water only (pump - one inlet and one outlet; water converge - multiple inlets and one outlet; water diverge - multiple outlets and one inlet).

- Air and water (air-cooled chiller - water flowing through the evaporator and air through the condenser; cooling or heating water coil - water passing through the tubes and air on the outside; Cooling towers - air passing through a water spray).
- Air and air (air-cooled DX air-conditioner - air passing through the evaporator and the condenser).
- Water and water (water-cooled chiller - water flowing through the evaporator and the condenser).

All the models are assumed to be isolated from the environment save for the flow in and out and the power supplied. All the processes are therefore assumed to be adiabatic since no heat will be transferred to or from the environment. The equations of these components can be seen in Appendix A.

The models derived by Rousseau are steady state models and the dynamics of the components and the flow in the pipes and ducts are not considered. These dynamics cannot be ignored if the purpose is to simulate the effect of the control parameters.

To simulate these dynamic effects Van Heerden[24] has introduced a simple time constant approach. The user is responsible for supplying the time constants. The following approach is used:

$$\tau \frac{d\psi}{dt} = function(\text{model input parameters}) \tag{1.3}$$

with τ the time constant of the model and ψ one of the output parameters of the model. For component models where dynamic effects are caused by the heat capacity of the heat transfer surfaces, the following relation can be used to obtain the time constant, τ:

$$\tau = \frac{C_{surfaces}}{mc_p + UA} \tag{1.4}$$

The relevant psychrometric relationships are employed in all models dealing with moist air properties. All the models derived by Rousseau are component-based but not all of them are explicit. Some of the components need solvers to solve systems of non-linear equations

simultaneously. New equations for some of these models must therefore be derived to be explicit (chapter 2) to satisfy the component requirements identified by the author for an efficient simulation.

The approach where regression coefficients from empirical data are used for system models is only efficient if enough operating conditions can be obtained to characterise the performance. In many cases only one operating point is freely available from the supplier. Sometimes there is no performance data available for certain equipment during retrofit projects. The ideal situation will therefore be to obtain a new model from only one operating point.

Scaling of curves from typical system types can be implemented into the tool to fit one measured or catalogue operating point. A typical system performance curve can therefore be scaled up and down to fit through the one given operating point. Examples of typical system curves of various component types are shown in Appendix A.

This method will improve the efficiency of system component input and will satisfy one of the important user requirements identified by the author. It is very frustrating and time consuming if certain simulation input data is unavailable or difficult to find. Inefficient user input can make or break the use of a simulation tool as standard procedure in practice.

1.4.3 Control models

At present QUICKcontrol makes provision for PID (Proportional, Integral, Derivative), on/off and step controllers. These controllers are used in most HVAC applications. With these controllers any measurable condition can be controlled from a sensor.

The controllers can be linked to any sensor available in the simulation tool for a feedback signal. The controllers can control all the controllable variables of the components, including the ventilation rates of the building zones. These variables include water flow rates, air flow rates, steam flow rates and load capacities.

Controller output at each step is only dependent on the previous time step values. This considerably reduces the complexity of the solution algorithm. From a system point of view

this implies that the controller acts as a controller that has a sample corresponding to the system integration time step size.

There are also energy management systems included in the simulation tool. With these, system energy consumption can be reduced by more energy-efficient control. The simulation tool provides the following energy management strategies:

- Setpoint-related energy management systems (temperature reset, zero energy band control, enthalpy economiser cycle and adaptive comfort control).
- Advanced energy management strategies (demand limiting, duty cycling, load resetting, optimal start-stop and CO_2 control).

These energy management strategies are discussed in reference [24].

1.4.4 Simulation procedure

After the models for all the components have been found for a given configuration, they need to be solved numerically and in the correct order. To set up a given configuration, a graphical user interface is used. The various components that make up a system can be dragged and dropped into position. Connections between these can be established by graphically inserting the connections.

A simulation procedure introduced by Van Heerden[24] is utilised to determine the solution order. Graph theory[47] is used to transform any ducting or piping system into a tree, identify the minimum unknowns and the order in which the components have to be solved. The resulting equations of this procedure have to be solved by an iterative procedure. Methods to solve these equations efficiently are discussed in detail by Van Heerden and are used in the simulation tool.

1.5 CONTRIBUTIONS OF THIS STUDY

The following contributions have been made by this study:

- User requirements, for the efficient use of system simulation tools, have been identified to satisfy the needs of the energy service contractor and HVAC designer.

- Methods and procedures are proposed to satisfy the needs identified for the energy service contractor and HVAC designer.

- Extensions to the simulation software QUICKcontrol are proposed for the efficient use in practise as standard procedure during projects.

- The derivation of new explicit component models not available in QUICKcontrol and commonly used in building systems.

- The practical applicability of integrated building and natural ventilation simulation is illustrated in a passive building case study.

- The practical applicability of integrated building, HVAC system and control simulation is illustrated in an energy cost savings case study.

1.6 OUTLINE OF THIS STUDY

The needs, trends and requirements of an efficient integrated building, HVAC and control simulation tool are discussed in chapter 1. Extensions to QUICKcontrol are proposed to satisfy the requirements of the energy service contractor and HVAC designer in practice.

There are many shortages in system component models in QUICKcontrol of equipment commonly used in the building sector. New explicit models for variable speed control on pumps, heat recovery systems, air ducts, boiler/tank/coil combinations and animal heat

generation are therefore derived in chapter 2.

The applicability of integrated building and natural ventilation simulation is illustrated in chapter 3. A case study was conducted on animal housing facilities to investigate the use of integrated simulation in these applications.

The applicability of integrated building, HVAC system and control simulation is illustrated in chapter 4. A case study was conducted on conference facilities to obtain the potential for energy cost savings by improving the operation of the HVAC system.

Chapter 5 briefly summarises this part of the study and proposes recommendations for future work.

1.7 REFERENCES

[1] VA Drozdov, YU A Matrosov, YU A Tabunschikov, The main trends in energy savings in buildings - Theory and practice in USSR, Energy and Buildings, 1989.

[2] JA Clarke, TW Maver, Advanced Design Tools for Energy Conscious Building Design: Development and Dissemination, Building and Environment, Vol.26 No.1, pp. 25-34, 1991.

[3] AH Rosenfeld, R. Bevington, Energy for Buildings and Homes, Scient. Amer., September, pp. 39-45, 1990.

[4] AH Birtles, Getting Energy Efficiency Applied in Buildings, Building Research Establishment, Watford WD2 7JR, UK.

[5] JK Kissock, DE Clardige, JS Haberl, TA Reddy, Measuring retrofit savings for the Texas Loanstar Program: Preliminary methodology and results, Solar Engineering, Vol.1, ASME, 1992.

[6] JJ Anderssen, Cape Town Electric Load Study and End Use Segmentation, Seminar and main Steering committee meeting for DSM and related projects, 27 April 1993.

[7] HS Geller, Commercial building Equipment Efficiency - A state of the art review,

ACEEE, May 1988.

[8] CR Miró, J.E. Cox, DOE-Sponsored study provides energy efficiency recommendations, ASHRAE Journal, February 1994.

[9] PG Rousseau, E.H. Mathews, Needs and Trends in Integrated Building and HVAC Thermal Design Tools, Building and Environment, Vol.28, No.4 pp.439-452, 1993.

[10] C Jones, Australia has a huge untapped resource - energy wasted through inefficiency, Engineers Australia, June 1989.

[11] L Aires-Barros, The energy efficiency revolution: formula for success, Int. J Global Energy Issues, pp.111-116, 1990.

[12] JA Clarke, Energy Simulation in Building Design, Adam Hilger, Bristol, 1985.

[13] J.E. Woods, Cost avoidance and productivity in owning and operating buildings, Occupational Medicine, State of the art reviews, Vol. 4, No. 4, January 1989.

[14] E. Sterling, C. Collett, S. Turner and C. Downing, Commissioning to avoid indoor air quality problems, Proc. ASHRAE Transactions: Symposia, pg. 867, January 1994.

[15] EH Mathews, DC Arndt, CB Piani, E van Heerden, Developing cost efficient control strategies to ensure optimal energy use and sufficient indoor comfort, Applied Energy, Vol.66, pp.135-159, 2000.

[16] JA Clark, Building energy simulation: the state of the art, Solar & Wind Technology, Vol. 6(4), pp. 345-355, 1989.

[17] D Newton, R James and D Bartholomew, Building energy simulation – a user's perspective, Energy and Buildings, Vol. 10, pp. 241-247, 1988.

[18] TEMM International (Pty) Ltd, PO Box 13517, Hatfield, 0028, Pretoria, South Africa.

[19] ESKOM (DSM), Electricity Demand Department, PO Box 1091, Johannesburg, 2000, South Africa.

[20] ECONOLER International, 253 rue St-Paul, Bureau 200, Quebec (Oc), Canada, G1K 8C1.

[21] MW Ellis, New simplified thermal and HVAC design tools, *PhD thesis,* Faculty of Engineering, University of Pretoria, Pretoria, 1999.

[22] PG Rousseau, Integrated building and HVAC thermal simulation, *PhD thesis,* Faculty of Engineering, University of Pretoria, Pretoria, 1994.

[23] EH Mathews, E van Heerden and DC Arndt, A tool for integrated HVAC, building, energy and control analysis Part 1: overview of QUICKcontrol, Building and Environment, Vol. 34, pp. 429-449, 1999.

[24] E van Heerden, Integrated simulation of building thermal performance, HVAC system and control, *PhD thesis,* Faculty of Engineering, University of Pretoria, Pretoria, 1997.

[25] LK Lawrie, Day-to-day use of energy analysis software, Energy Engineering, Vol. 89, pp. 41-51, 1992.

[26] B Birdsall, WF Buhl, KL Ellington, AE Erdam, FC Winkelmann, Overview of the DOE-2 building energy analysis program, Technical report, Simulation Research Group, Lawrence Berkeley Laboratory, University of California, Berkeley, California, 94720, 1990.

[27] VisualDOE, http://www.eley.com, Eley Associates, 142 Minna Street, San Francisco, California, 94105, USA.

[28] D Pedreya, V Bush, PC-CUBE simulates hourly electric demand and energy consumption, Energy Engineering, Vol. 89, pp. 23-37, 1992.

[29] RH Howell, HJ Sauer, Energy efficiency and conservation of building HVAC system using the AXCESS energy analysis, In Second Annual Conference on ENERGY, Rolla, pp. 7-9, 1975.

[30] KE Fuller, I Rohmund, Contech for commercial building system analysis, Energy Engineering, Vol. 89, pp. 6-22, 1992.

[31] Climatisation and Development Group, Overview of the hourly analysis program, Carrier, 12 Ruede Paris-78230, LE PECQ, 1992, Available from Carrier SA.

[32] HAP (Hourly Analysis Program) v4.0, http://www.carrier-commercial.com, Carrier Corporation, Software Systems, TR-1, Room 250, P.O. Box 4808, Syracuse, New York 13221, USA.

[33] MCB Gough, Component based building energy system simulation, International Journal of Ambient Energy, Vol. 7, pp. 137-143, 1986.

[34] J Althof, Marketing and productivity opportunities of computer aided system design, Energy Engineering, Vol. 84, pp. 4-29, 1987.

[35] ENERPASS, http://www.enermodal.com, Enermodal Engineering, 650 Riverbend Drive, Kitchener, Ontario, Canada.

[36] ENER-WIN, http://archone.tamu.edu/~energy/enerwin.htm, College of Architecture, Texas A&M University, College Station, Texas 77843-3137, USA.

[37] BSim2000, http://www.sbi.dk, Danish Building Research Institute, P.O.Box 115, Hoersholm, DK-2970, Denmark.

[38] SJ Irving APACHE – an integrted approach to thermal an HVAC system analysis, International Journal of Ambient Energy, Vol.7, pp. 129-136, 1986.

[39] AE Samual, TH Chia, Simulation of the full and part load energy consumption of HVAC systems of buildings, Building and Environment, Vol. 18, pp. 207-218, 1983.

[40] C Park, DR Clark, GE Kelly, HVACSIM Buildings, Systems and Equipment Simulation Program: Building Loads Calculation, Gaithersburg, MD 20899, 1986.

[41] M Heintz, O Ogard, Vnovakovic, G Brustad, HVAC-DYNAMIC – a training simulator for dynamic analysis of HVAC plants, Modelling, Identification and Control, Vol. 10, pp. 159-164, 1989.

[42] SPARK (Simulation Problem Analysis and Research Kernel), http://simulationresearch.lbl.gov, Lawrence Berkeley National Laboratory, Mail Stop 90-3147, 1 Cyclotron Road, Berkeley, California 94720, USA.

[43] WA Beckman, L Broman, A Fiksel, SA Klein, E Lindberg, M Schuler, J Thornton, TRNSYS the most complete solar energy system modelling and simulation software,

In AAM Saying, editor, Renewable Energy Climate, Change Energy and Environment: World Renewable Energy Congress, Reading, UK, 1994.

[44] F Winkelmann, Advances in building energy simulation in North America, Energy and Buildings, Vol. 10, pp. 161-173, 1988.

[45] VI Hanby and AJ Dil, Error prediction in Markov models of building/HVAC systems, Applied Mathematical Modelling, Vol. 8, No. 8, pp. 608-613, 1996.

[46] M.G. Davies, Transmission and storage characteristics of walls experiencing sinusoidal excitation, Applied Energy, Vol. 12, pp. 269-316, 1982.

[47] R Tarjan, Depth search and linear graph algorithms, SIAM Journal of Computing, Vol. 1, No. 2, pp. 146-160, 1972.

CHAPTER 2

NEW BUILDING AND HVAC MODELS

QUICKcontrol still has many shortcomings in the availability of component models for certain equipment commonly used in building systems today. Most existing component models do not satisfy the requirements and the philosophy of the author. New dynamic component models for variable speed control on pumps and fans, heat recovery systems, air ducts, boiler/tank/coil combinations and animal heat loads were derived in this chapter. The equations of these models are all explicit equations to calculate the outlet conditions directly from the inlet conditions without the use of solvers.

NOMENCLATURE

A	Area (m^2)
cp	Specific heat capacity (J/kg.K)
D	Impeller diameter (m)
h	Enthalpy (J/kg)
hc	Convection coefficient ($W/m^2.K$)
L	Length (m)
m	Fluid mass flow rate (kg/s)
n	RPM
P	Perimeter (m)
Pwr	Power Input (Watt)
Q	Heat Input (Watt)
t	Time (s)
T	Temperature (°C)
U	Heat transfer coefficient ($W/m^2.K$)
vol	Volume (m^3)
η	Efficiency
ρ	Density (kg/m^3)
ΔP	Pressure difference (Pa)

Subscripts

a	Air
c	Coil/Cold fluid
d	Dry conditions
h	Hot fluid
i	Inlet
o	Outlet
s	Storage tank fluid
ss	Steady state value

2.1 INTRODUCTION

QUICKcontrol has many shortcomings in the availability of component models for certain equipment commonly used in building systems today. New building and system component models are therefore derived in this chapter. Most existing component models do not satisfy the requirements and the philosophy of the author and therefore the new models.

As mentioned previously all mathematical models' equations must be dynamic explicit equations, which obtain outlet conditions directly from inlet conditions. This is very important to achieve a fast and robust integrated simulation of a large thermal system. The use of solvers on component level must therefore be eliminated completely. The models must utilise a time step approach where the inlet and outlet conditions are constant for the time step period.

A component model in a large dynamic complex system integrated with control can never be too simple for fast stable solutions. The models must further be a combination of fundamental principles and empirical regressions for "real life" simulation. When a model makes use of empirical data the number of input values must be minimised to make the input practical and quick for the user.

Regressions must be obtained from either catalogue or measured data. It is often difficult or time consuming to obtain many operating points and therefore theory must be combined with empirical relationships to obtain a model with scaling from these points. The ideal will be to obtain a model from only one measured or catalogue operating point.

New dynamic component models for variable speed control on pumps and fans, heat recovery systems, air ducts, boiler/tank/coil combinations and animal heat loads were derived in the following sections. These models satisfy the requirements discussed here.

2.2 VARIABLE SPEED DRIVES

2.2.1 Description

Variable speed control on fans and pumps in HVAC applications is a well-known measure to save on system energy consumption. Two typical control methods are: controlling the speed to maintain a constant static pressure difference over a pump or a fan when valves or dampers are respectively utilised for variable flow control in a flow network (Figure 2.1). A second strategy is to regulate a certain condition (temperature, enthalpy, etc.) which is flow dependent in a flow network by varying directly the speed of the pump or fan (Figure 2.2).

Variable speed motors or variable speed drives may be used when frequent or continuous variations are desired. These methods have a high initial cost but can reduce power consumption considerably in large variable flow networks.

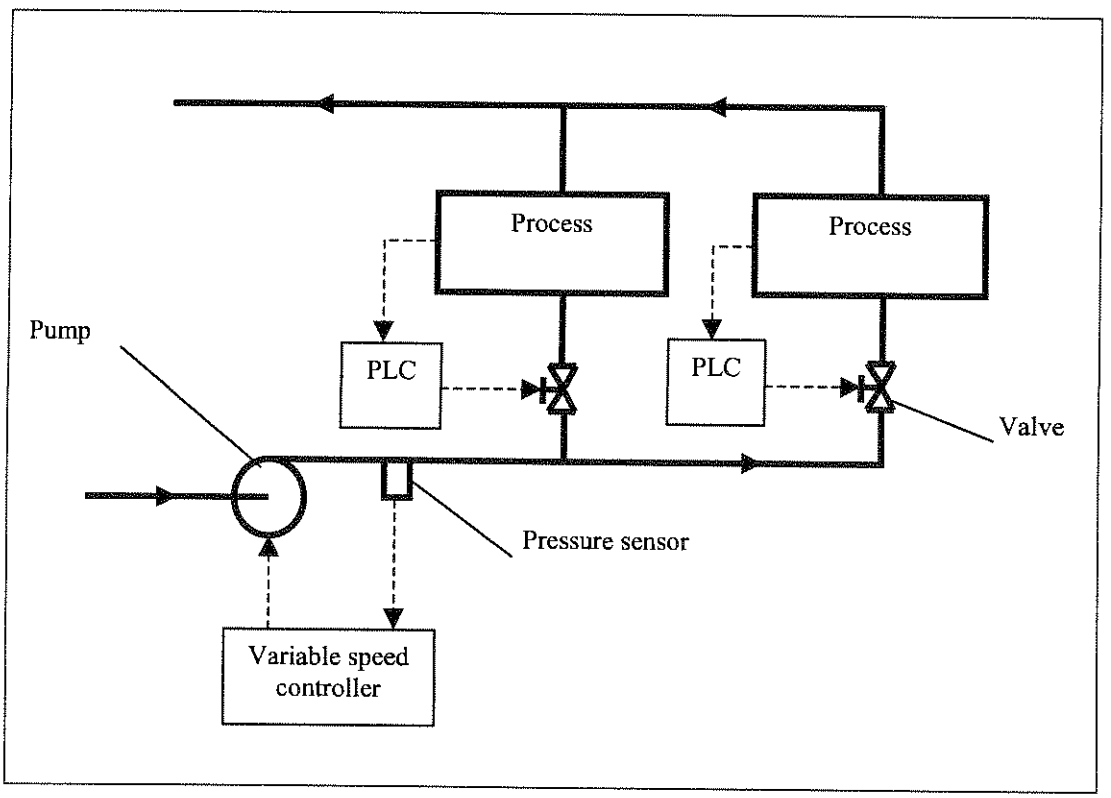

Figure 2.1: Pressure control

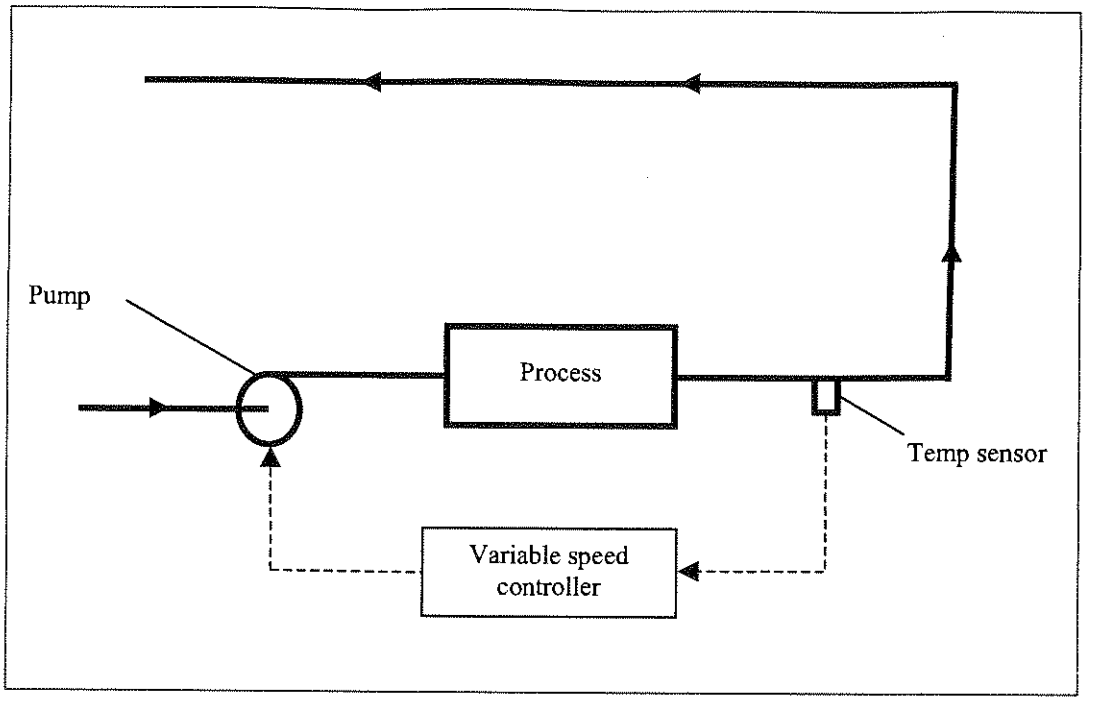

Figure 2.2: Temperature control

A mathematical model to simulate the performance of variable speed pumps and fans in flow networks where flow is set by certain elements and not solved is derived in the following section.

2.2.2 Mathematical model

It is quite a formidable task to set-up a complex theoretical flow network with the correct variable flow resistances and to solve it to predict the correct flows in all the branches for each time step in a dynamic system simulation tool. Therefore many system simulation tools utilise the approach where flow is specified in the branches by valves, pumps, dampers and fans and not calculated for each time step[1].

The problem is however to calculate the effect that variable speed control has on the performance of pumps and fans when flow is specified and not calculated. The following method can be used for the two scenarios shown in Figure 2.1 and Figure 2.2.

The two well-known non-dimensional variables K_f and K_h can be used to characterise the performance of pumps (fans):

$$K_f = \frac{m}{\rho n D^3}$$
$$K_h = \frac{\Delta P_{total}}{\rho n^2 D^2} \tag{2.1}$$

K_h can be written as a function of K_f by using a simple polynomial regression:

$$K_h = a_0 + a_1 K_f + a_2 K_f^2 + ... + a_k K_f^k \tag{2.2}$$

The efficiency of the pump as a function of K_f can be expressed as:

$$\eta_{pump} = b_0 + b_1 K_f + b_2 K_f^2 + ... + b_k K_f^k \tag{2.3}$$

The pump's motor power can now be calculated for any given mass flow rate with the following equation:

$$Pwr = \frac{m \Delta P_{total}}{\rho \eta_{pump} \eta_{motor}} \tag{2.4}$$

and the leaving fluid temperature T_o due to the pump inefficiencies with:

$$Q = \frac{(1 - \eta_{pump}) m \Delta P_{total}}{\rho \eta_{pump}}$$
$$T_o = T_i + \frac{Q}{m c_p} \tag{2.5}$$

For the scenario in Figure 2.1 the PLCs control a process by changing the supply flow rate to maintain a certain condition. If, for example, one of the PLCs reduce the process flow by closing the valve slightly, the system curve in Figure 2.3 will change from curve 1 to 2. The pump pressure and therefore the system power consumption will increase. To maintain a constant pressure over the pump the speed of the pump can be controlled and reduced to RPM 2.

The PLC will now open the valve slightly to ensure the correct flow to maintain the certain condition in the process. The system curve will now change to curve 3. This will not only ensure a constant pressure over the system but will reduce the power consumption of the pump.

This scenario can be modelled without solving the network. The flow needed to maintain the condition in the process can be specified by the valve. With the pressure over the pump and the flow through the pump (total flow through the two valves) known, n (RPM 2) can be calculated by substituting Eq. (2.1) into Eq. (2.2). The pump power consumption, Pwr and T_o can now be calculated by using Eq. (2.3) to Eq. (2.5).

With this method the flow through the process branches can be set by the valves for a certain condition, the flow can be added to obtain the flow through the pump and the needed pump speed can be calculated for the specified flow rates and constant pressure.

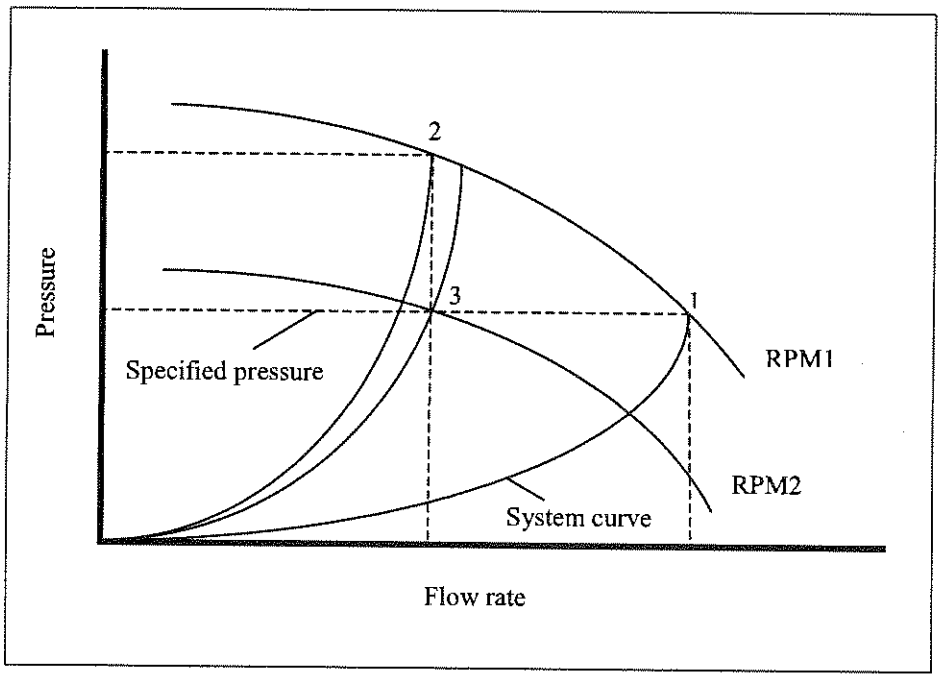

Figure 2.3: Constant pressure

For the scenario in Figure 2.2 flow through the process can for example be reduced by directly changing the speed of the pump to maintain a certain condition.

The system curve in Figure 2.4 will stay unchanged and the working point will move from point 1 to point 3. If the flow was reduced by changing the system curve (closing of a valve),

the pressure would have increased to point 2. Speed control reduces the pump pressure and therefore the power consumption.

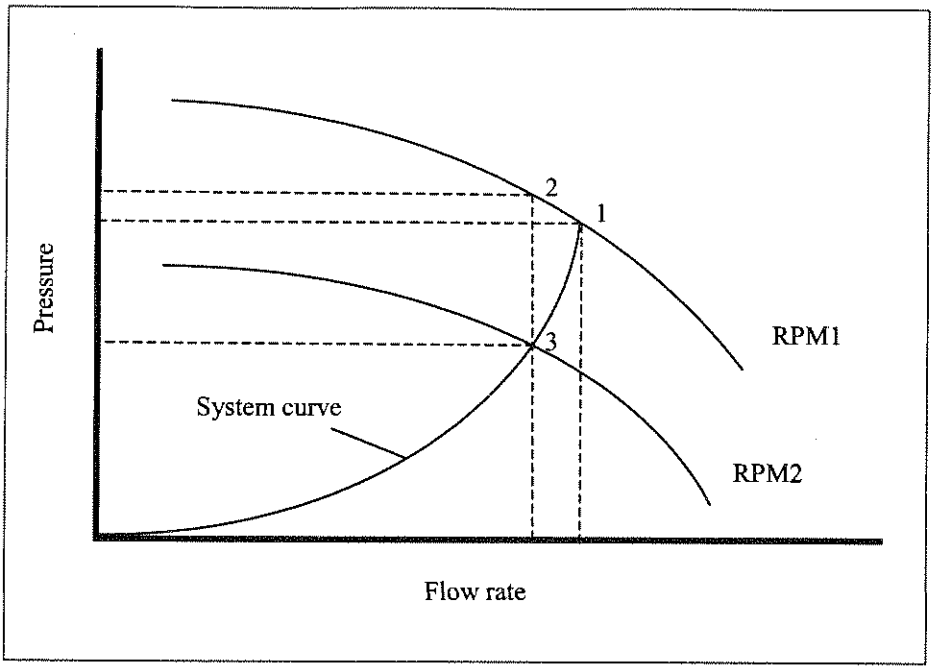

Figure 2.4: Direct control

To model this scenario without solving the flow network a simplified system curve must be obtained. The curve in Figure 2.4 can easily be obtained by a one point 2^{ed} order curve fit through any given flow rate (m) and pressure difference (ΔP) over the pump to give:

$$\Delta P = c\left(\frac{m}{\rho}\right)^2 \tag{2.6}$$

Only a one point measurement or theoretical calculation is therefore needed to obtain the coefficient c. For any given flow rate m the pressure over the pump can be calculated. With P_{total} known and by substituting Eq. (2.1) into Eq. (2.2), n (RPM) can be calculated. The pump power consumption, Pwr and T_o can now be obtained by using Eq. (2.3) to Eq. (2.5).

These methods allow for speed control modelling on pumps (fans) without solving a dynamic flow network. An algorithm to simulate flow, and control flow, in a large flow network is discussed in section 7.5.

2.3 HEAT RECOVERY SYSTEMS

2.3.1 Description

In large commercial applications considerable quantities of air is extracted to the environment because of the introduction of outdoor ventilation air. Considerable savings in energy can be realised if the heat energy from the interior spaces can be recovered to heat up the colder outside air during winter. The same applies during summer when cold exhaust air can be used to cool down hot outside air to save energy.

Heat energy can also be recovered from waste water in cooling and heating applications. Redistribution of heat energy within a building can therefore be accomplished through the use of air-to-air or water-to-water heat exchanger types. The most common and efficient heat exchanger configurations used in building applications are plate counter flow and cross-flow types.

Dynamic mathematical models for dry air-to-air and water-to-water heat exchangers are derived in the following section.

2.3.2 Mathematical model

Integrated dynamic modelling of a large complex thermal system can be simplified by using explicit equations to calculate outlet conditions of any component directly from the inlet conditions. In any heat exchanger heat is transferred from the hot fluid, entering at temperature T_{hi} to the cold fluid, entering at temperature T_{ci}. The exit temperatures are T_{ho} and T_{co} respectively.

Two fundamental equations describe the working of a heat exchanger: the heat balance and the heat transfer rate equation. The heat balance is given by:

$$m_h c_{ph}(T_{hi} - T_{ho}) = m_c c_{pc}(T_{co} - T_{ci}) \tag{2.7}$$

Many methods are available to model the thermal performance of heat exchangers. Both the logarithmic-mean-temperature and effectiveness[2] methods are not suitable for simulation where a numerical algorithm must search for an integrated solution in a complex system. With the logarithmic-mean-temperature method the search may wander into a region where the argument of the logarithmic function is negative.

With the effectiveness method, the solution procedure might have to adjust the flow so that the minimum capacity flux changes from the one stream to the other, and the resultant numerical discontinuity causes problems for the searching algorithm. To avoid these and other problems, Shah and Mueller[3] discuss two further methods: the $(P\text{-}N_{tu})$ and $(\Psi\text{-}P)$ method, which do not make use of the minimum capacity flux concept.

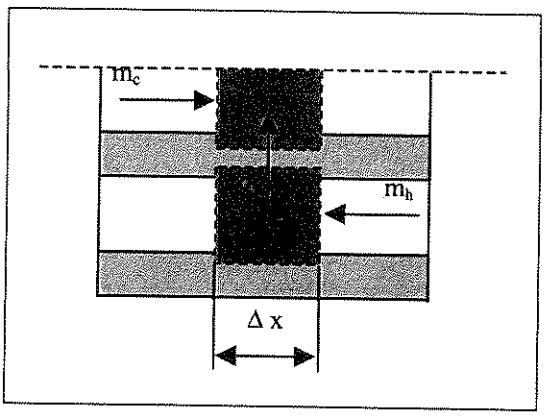

Figure 2.5: Hot and cold fluid control volumes for a counter-flow heat exchanger

Another alternative explicit method[4] is presented here on a counter flow configuration. A heat balance on the two streams in Figure 2.5 gives:

$$UP\Delta x(T_h - T_c) = C_c \Delta T_c$$
$$UP\Delta x(T_h - T_c) = C_h \Delta T_h \qquad (2.8)$$

where ΔT is the incremental increase in the temperature and $C = mc_p$ the flow thermal capacity. Dividing Eq. (2.8) by Δx, and letting $\Delta x \to 0$ gives:

$$C_c \frac{dT_c}{dx} = UP(T_h - T_c)$$
$$C_h \frac{dT_h}{dx} = UP(T_h - T_c)$$

(2.9)

If these two equations are subtracted from each other and solved for the length L when UP and specific heats are assumed to be constant, the result is:

$$\frac{T_{hi} - T_{co}}{T_{ho} - T_{ci}} = \exp\left[-UPL\left(\frac{1}{C_c} - \frac{1}{C_h}\right)\right]$$

(2.10)

The heat balance equation Eq. (2.7) can be solved for the cold fluid exit temperature:

$$T_{co} = (T_{hi} - T_{ho})\frac{C_h}{C_c} + T_{ci}$$

(2.11)

If Eq. (2.11) is substituted into Eq. (2.10) and the result is solved it is found that:

$$T_{ho} = \frac{(1-r)}{(\Gamma - r)}T_{hi} + \frac{(\Gamma - 1)}{(\Gamma - r)}T_{ci}$$
$$T_{co} = \frac{(\Gamma - 1)r}{(\Gamma - r)}T_{hi} + \frac{(1-r)\Gamma}{(\Gamma - r)}T_{ci}$$

Where $$r = \frac{C_h}{C_c}, \; r \neq 1$$

and $$\Gamma = \exp\left[-UPL\left(\frac{1}{C_c} - \frac{1}{C_h}\right)\right]$$

(2.12)

The outlet temperatures for a counter-flow heat exchanger can now be calculated with the explicit equation Eq. (2.12) from the inlet temperatures. It will also be easy to derive an equation of a parallel heat exchanger by using the same method. For more complex heat exchanger types like single pass cross-flow exchangers Mueller charts (Ψ-P)[3] can be used to obtain explicit equations by curve fits.

Mueller introduced a method that combines all the variables of the LMTD and the ε-NTU methods and eliminates their limitations for a hand solution. A two dimensional curve fit through the Mueller chart of a single-pass cross-flow exchanger for the hot fluid unmixed, and the other mixed, gives:

$$\frac{T_{ho}-T_{hi}}{T_{ci}-T_{hi}} = [0.295735r^{1.4} - 0.758704r + 0.72661][\exp(-0.660909\Gamma)] + \exp(-0.04965\Gamma) - 0.61666$$

$$\Gamma = \frac{C_h}{UA}, \Gamma \leq 2$$

$$r = \frac{C_h}{C_c}, r \leq 4 \qquad (2.13)$$

The leaving fluid temperature of the hot fluid can now be calculated explicitly from the entering fluid temperatures by solving Eq. (2.13). With T_{ho} known, T_{co} can be calculated by solving the energy balance equation Eq. (2.7). The Mueller chart with the curve fit can be seen in Figure 2.6.

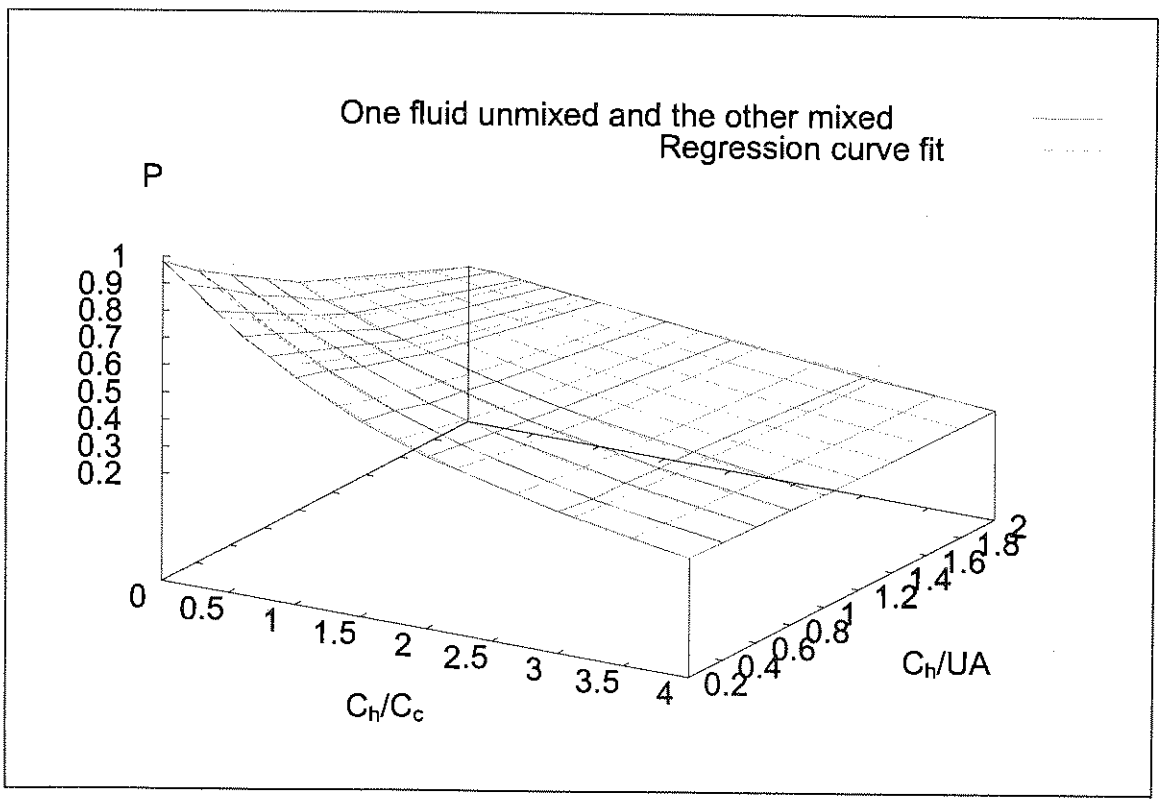

Figure 2.6: Mueller chart and curve fit of a single–pass cross-flow exchanger for the hot fluid unmixed and the other mixed

In figure 2.6: $$P = \frac{T_{ho} - T_{hi}}{T_{ci} - T_{hi}}$$

An explicit equation for a single-pass cross-flow exchanger with both fluids unmixed is derived in the same manner discussed and gives:

$$\frac{T_{ho} - T_{hi}}{T_{ci} - T_{hi}} = [-0.00187r^5 - 0.320757r^{1.1} + 1.070107][\exp(-0.880466\Gamma)] - [0.039611\ln(\Gamma) - 0.088206] + 0.088206$$

$$\Gamma = \frac{C_h}{UA}, 0.3 \le \Gamma \le 2$$

$$r = \frac{C_h}{C_c}, 0.3 \le r \le 2 \qquad (2.14)$$

The Mueller chart and the curve fit are displayed in Figure 2.7.

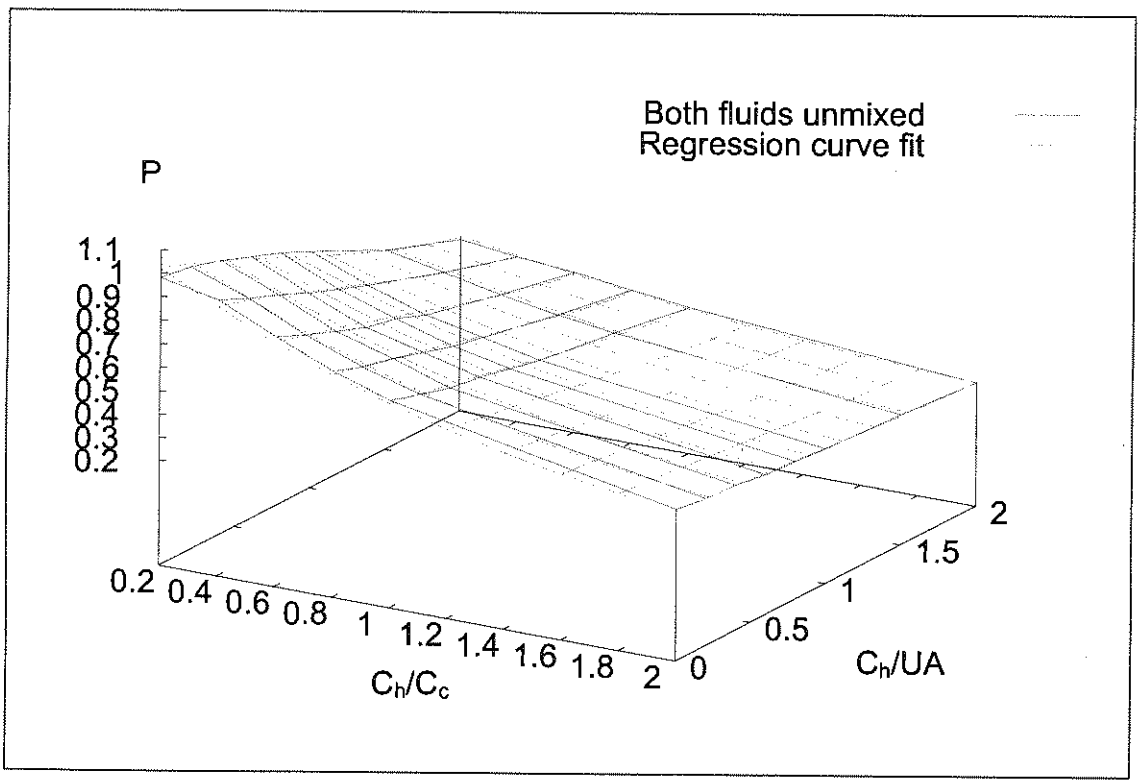

Figure 2.7: Mueller chart and curve fit of a single-pass cross-flow exchanger with both fluids unmixed

Since plate counter and cross-flow heat exchangers are most commonly used in heat recovery systems, these steady state equations should be satisfactory for dynamic simulation due to the

low thermal capacitance of their heat transfer plates. However the following time constant approach can be used to simulate the dynamic effects of heat exchangers:

$$T_o = T_{oss} + (T_o^0 - T_{oss}) \exp\left(\frac{-\delta t}{\tau}\right)$$

$$\tau = \frac{C_{plates}}{UPL} \tag{2.15}$$

Where T_{oss} is the steady state temperature, T_o^0 is the outlet temperature at the previous time step, δt is the time step size and C_{plates} is the heat capacity of the heat transfer plates. Further advantages of this explicit method will be illustrated in some of the sections that follow where heat and mass transfer are relevant.

2.4 AIR DUCTS

2.4.1 Description

The main purpose of air duct or conduit systems in HVAC applications are to deliver a specified amount of air at a specific air condition to the conditioned building space at the lowest capital and operating cost. Thermal insulation on air ducts of large air distribution systems can result in worthwhile savings on heating and cooling energy.

Thermal insulation can also prevent inside condensation when the air inside is warmer than the ambient temperature or outside condensation when the inside air is cooler than the outside. It is therefore important to model the thermal performance of long air ducting systems correctly in energy and new design simulations. The model must predict condensation and therefore include heat and mass transfer.

2.4.2 Mathematical model

The model must allow for dry and wet inside surfaces. Parts of the inside surface will be wet due to condensation when the surface temperature is lower than the dewpoint temperature of the inlet air. This scenario can be viewed in Figure 2.8.

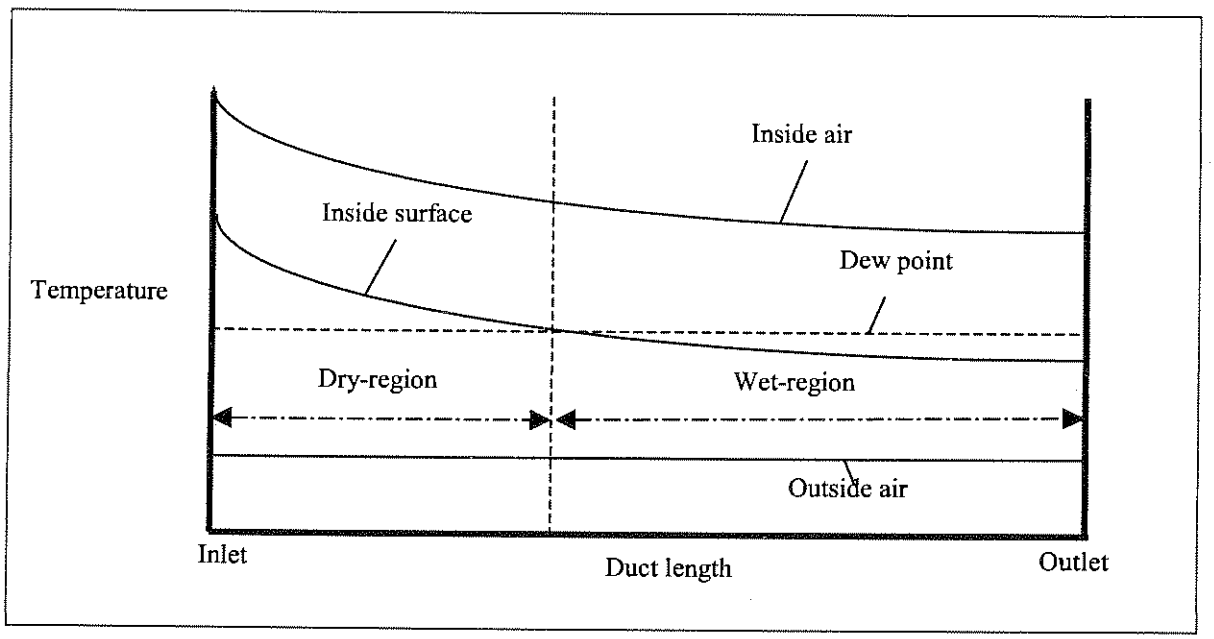

Figure 2.8: Inside air temperature profile of a duct

For the dry part in the graph only heat transfer will occur and the steady state equation for a single stream heat exchanger[2] can be used to calculate the outlet conditions:

$$\frac{(T_{ai} - T_{ao})}{(T_{ai} - T_{ambient})} = \varepsilon \tag{2.16}$$

where $$\varepsilon = 1 - \exp(\frac{-U_d P_d L_d}{m_a cp_a})$$

Lombard[4] introduced an analogy where heat and mass transfer are accounted for by using the same explicit heat exchanger equations derived in section 2.3. The rules for the analogy are:

- The driving potential is $(h_h - h_c) = (h_h - \phi T_c)$

- The effective resistance from the hot to the cold fluid is $U_e = \dfrac{Uhc_h}{Uc_{ph} + hc_h\phi}$

- The effective mass flow of the cold fluid is $m_{ce} = (c_{pc}/\phi)m_c$

Where $\phi = h_s/T_s$, h_s and T_s are the saturation enthalpy and temperature respectively at the inside surface temperature. This saturation curve is very nearly linear in the range 7 to 20°C range[4]. U is the combined heat transfer coefficient of the wall and cold fluid convection coefficients. If this analogy is implemented into the single stream heat exchanger Eq. (2.16) it gives:

$$\frac{(h_{ai} - h_{ao})}{(h_{ai} - \phi T_{ambient})} = 1 - \exp\left(\frac{-U_e PL}{m_a cp_a}\right) \tag{2.17}$$

Eq. (2.17) can be solved to calculate the outlet enthalpy from the inlet enthalpy for the wet part of the duct where the inside surface temperature is lower than the air dewpoint temperature. The outlet temperature can now be calculated by using a straight-line through (T_{ai}, h_{ai}) and (T_{so}, h_{so}) showed in Figure 2.9. T_{so} is the saturation temperature and h_{so} the saturation enthalpy at the duct inside surface outlet.

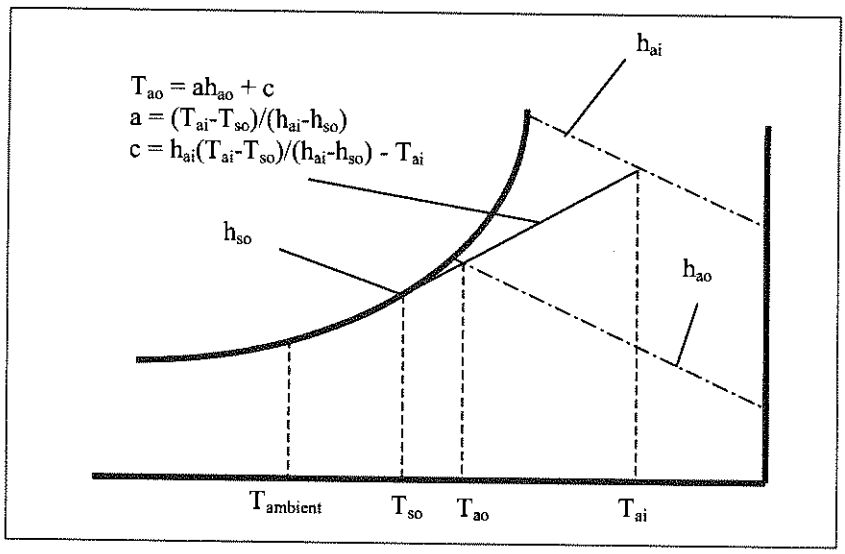

Figure 2.9: Straight-line process

To solve the thermal performance of an air duct segment, first apply Eq. (2.16) to calculate the outlet temperature. If T_{ao} is above the dewpoint temperature of the air, no condensation will occur and the heat transfer surface will be dry. T_{ao} will then be the outlet temperature of

this segment. When T_{ao} is below the inlet dewpoint temperature the duct segment is partly dry and partly wet.

To calculate the transition distance from the inlet, divide the duct into two and calculate the air temperature at this mid point with Eq. (2.16). The inside surface temperatures at the inlet, mid and outlet points can now be calculated by:

$$T_s = (T_a - T_{ambient})\left(\frac{hc_i}{hc_i + U_{wall}}\right) + T_{ambient} \tag{2.18}$$

A second order curve can be fitted through the three surface temperature points as a function of the duct length ($T = f(L)$). This equation can be solved with $T = T_{dewpoint}$ and the transition point can be calculated. Eq. (2.16) can now be solved to obtain the outlet temperature at the transition point for the dry part. This condition can now be used as inlet condition for the wet part and the outlet conditions can be solved by Eq. (2.17).

Since ducts are usually made of metal sheets these steady state equations should be satisfactory for dynamic simulation due to the low thermal capacitance of their material. However the following time constant approach can be used to simulate the dynamic effects of air ducts:

$$T_o = T_{oss} + (T_o^0 - T_{oss})\exp\left(\frac{-\delta t}{\tau}\right)$$

$$\tau = \frac{C_{wall}}{mc_p + UPL} \tag{2.19}$$

where T_{oss} is the steady state temperature, T_o^0 is the outlet temperature at the previous time step and C_{wall} is the heat capacity of the duct material.

2.5 BOILER/TANK/COIL COMBINATIONS

2.5.1 Description

Boilers and thermal storage tanks are very commonly used in district cooling and central heating applications. Many boiler, storage tank and coil combinations are used in practice to satisfy specific user requirements. Figure 2.10 displays a schematic drawing of an electric boiler/tank/coil combination.

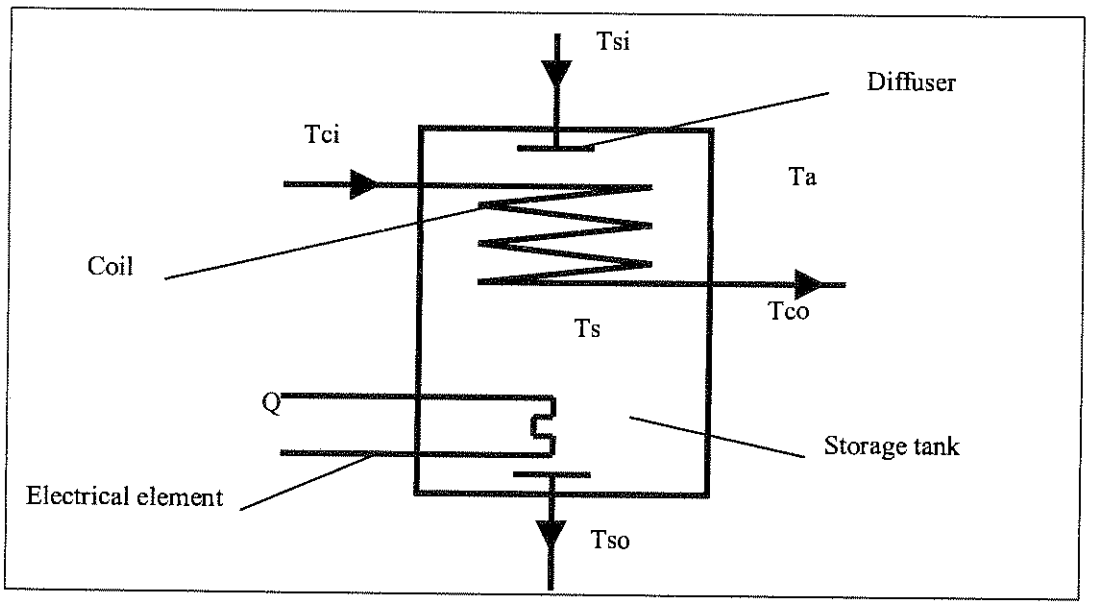

Figure 2.10: Boiler/tank/coil combination

This system has numerous applications. It can firstly be used as a stratification tank to store thermal energy in heating and cooling systems to reduce operating costs and plant capacities. For example, in a chilled water application two volumes of water must be held separately: a cool volume with unused capacity and a warm, discharged volume.

During a discharge cycle, water is withdrawn from the cooler volume, heated by a cooling load, and returned to the warmer volume. During a charge cycle, water is removed from the warmer volume, cooled by a refrigeration plant, and returned to the cooler volume.

The most widely used and economical technology is to store both volumes in the same tank with separation[5]. This separation is maintained by natural stratification. Diffusers at the

top and the bottom of the tank are responsible for and designed to minimise thermal blending. It is therefore important to model natural stratification correctly in such an application.

In central heating systems, a storage tank can be combined with an electrical resistance element, furnace or combustion chamber to supply heat to the tank. Heat can also be transferred to the water in the tank or extracted via a coil inside the tank. This type of combination is commonly used in central space heating and domestic hot water applications.

The space heating system will typically be linked to the water inside the tank (T_{so} and T_{si} in Figure 2.10) and the domestic hot water system to the coil. The mathematical model derived and described in the following section must therefore allow for these scenarios.

2.5.2 Mathematical model

Let's first look at the scenario where the tank is combined with an electrical element, furnace or a combustion chamber. When a heat source is present in the form of a coil or heating element, one can assume a constant water temperature inside the tank. This implies 100% mixing due to convection inside caused by the heat source. An energy balance on the system in Figure 2.10 can therefore be written as:

$$C\frac{dT_s}{dt} = U_s A_s (T_a - T_s) + m_c cp_c (T_{ci} - T_{co}) + m_s cp_s (T_{si} - T_s) + Q \tag{2.20}$$

where $C = \rho_s cp_s vol_s$.

The heat transfer process between the water in the tank (T_s) and the coil (T_c) can be calculated with the single stream heat exchanger equation[2] if assumed that T_s is constant over a short time period δt. The thermal mass of the coil material is very small compared to the water in the tank thus a steady state equation will be satisfactory.

$$\frac{(T_{ci} - T_{co})}{(T_{ci} - T_s)} = \varepsilon \tag{2.21}$$

where $$\varepsilon = 1 - \exp(\frac{-U_c A_c}{m_c cp_c})$$

The U_c value can be taken as the outside heat transfer coefficient on the coil as a empirical function of T_s-T_{ci} ($f(T_s$-$T_{ci})$). Ts can now be solved by substituting Eq. (2.21) into Eq. (2.20), separating the variables and using the initial values $T_s = T_s^o$ at $t = 0$:

$$T_s = \frac{1}{a}\left[(aT_s^o - b)\exp(\frac{-a\delta t}{C_{mix}}) + b\right] \tag{2.22}$$

where $$a = U_s A_s + m_s cp_s + m_c cp_c \varepsilon$$

and $$b = U_s A_s T_a + m_s cp_s T_{si} + m_c cp_c \varepsilon T_{si} + Q$$

With T_s now known T_{co} can be solved:

$$T_{co} = \varepsilon(T_s - T_{ci}) + T_{ci} \tag{2.23}$$

The heat capacity Q for any type of boiler can be taken as a function of the tank water temperature ($T_s^{t-\delta t}$) at the previous time step. The same applies for the power input (electrical or fuel).

$$\begin{aligned} Q &= f(T_s^{t-\delta t}) \\ Pwr &= f(T_s^{t-\delta t}) \end{aligned} \tag{2.24}$$

It should be easy to obtain these functions by curve fits through the suppliers' catalogue data or measured data.

If there are no heat sources present in the tank natural stratification will occur. However thermal separation between the warm and cool water in the tank is imperfect. Heat is transferred between the warm and cool water via mixing and conduction.

In a storage tank heat gain from the environment through tank walls is reduced to negligible levels by insulation. The conductive heat transfer between warm and cool water within the tank is also quite small over the course of an operating cycle. Convection due to density differences between the warm and cool volumes will be small if the warm volume is kept on top of the cool volume. Mixing near the inlet is therefore the dominant[5] process and a good mixing model is essential for the accurate simulation of stratified tank performance.

A one-dimensional finite difference approach[6],[7] can be used to model natural stratification in a storage tank. The tank can be divided in to two volumes: a mixing volume (segment *s1* to *sm*) at the inlet diffuser and a second volume (Segment *sm+1* to *sn*) where no mixing occurs. Figure 2.11 displays the two volumes.

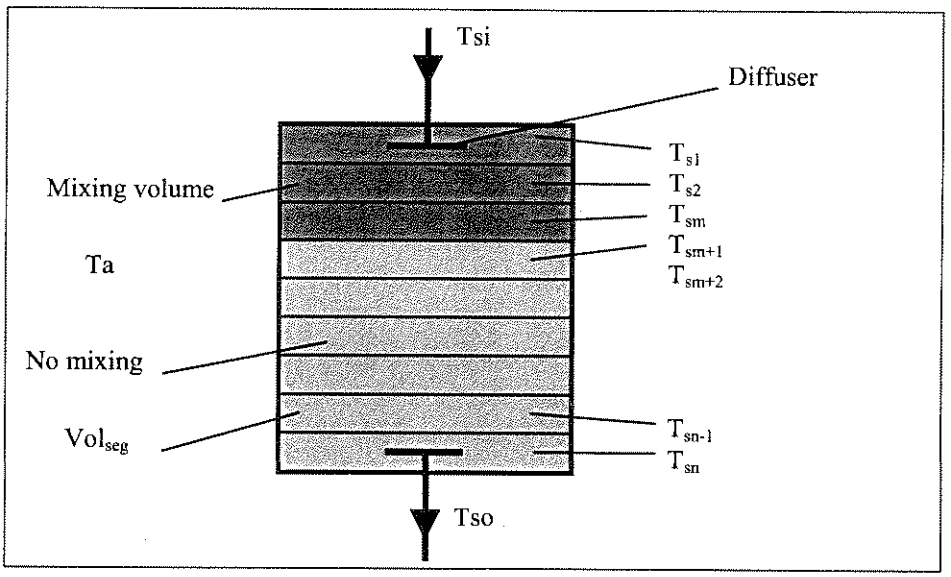

Figure 2.11: One-dimensional finite difference model for a stratified storage tank

The temperature of the water in all the segments of the mixing volume is assumed to be the same and an energy balance on the volume gives:

$$C_{mix}\frac{dT_s}{dt} = U_{mix}A_{mix}(T_a - T_s) + m_s cp_s (T_{si} - T_s) \tag{2.25}$$

where $C_{mix} = \rho_s cp_s vol_{mix}$. The variables in Eq. (2.25) can be separated and the equation solved with $T_s = T_s^o$ at $t = 0$:

$$T_s = \frac{1}{a}\left[(aT_s^o - b)\exp(\frac{-a\delta t}{C_{mix}}) + b\right] \tag{2.26}$$

where $$a = U_{mix}A_{mix} + m_s cp_s$$

and $$b = U_{mix}A_{mix}T_a + m_s cp_s T_{si}$$

If no conduction and no mixing[5] is assumed between the segments *sm+1* to *sn* the convection term can be eliminated and an energy balance on segment *j* gives:

$$C_{seg}\frac{dT_{sj}}{dt} = U_{sj}A_{sj}\left(T_a - T_{sj}\right) \tag{2.27}$$

where $C_{seg} = \rho_s cp_s vol_{seg}$. The variables in Eq. (2.27) can be separated and the equation solved with $T_{sj} = T_{sj}^{o}$ at $t = 0$:

$$T_{sj} = (T_{sj}^{o} - T_a)\exp(\frac{-U_{sj}A_{sj}\delta t}{C_j}) + T_a \tag{2.28}$$

The two equations derived respectively for the mixing segments and non-mixing segments can now be used in the following algorithm to solve the performance of the tank over time using a time step approached:

$$\delta t = \frac{vol_{seg}\rho_s}{m_s}$$

δt is therefore the time it takes the water to flow through one of the segments.

for j = 1 to m do (mixing segments)

$$T_{ave} = \frac{\sum_{j=1}^{j=m} T_{sj}^{t-\delta t}}{m}$$

$$T_{sj} = \frac{1}{a}\left[(aT_{ove} - b)\exp(\frac{-a\delta t}{C_{mix}}) + b\right]$$

where $a = U_{mix}A_{mix} + m_s cp_s$

and $b = U_{mix}A_{mix}T_a + m_s cp_s T_{si}$

(2.29)

for j = m+1 to n do (non-mixing segments)

$$T_{sj} = (T_{sj-1}^{t-\delta t} - T_a)\exp(\frac{-U_{sj}A_{sj}\delta t}{C_{seg}}) + T_a$$

where m is the number of mixing segments and n is the total number of segments in the finite element model. In the tank, segments are displaced from the inlet to the outlet at each time

step to emulate flow through the tank. A finite quasie-steady state approach is therefore used to model flow and heat transfer.

The size of the mixing volume depends mainly on the water flow rate and the diffuser design[8]. Thus for a specific tank and inlet diffuser the mixing volume or mixing fraction (m/n) can be written as a function of Half-cycle Figure of Merit ($FOM_{1/2}$). The $FOM_{1/2}$ gives a direct measure of the fraction of nominal capacity that can be delivered at a usable temperature for given charge and discharge inlet conditions. It is therefore important to model the $FOM_{1/2}$ of a storage tank correctly.

$$Fraction_{mix} = f(FOM_{1/2}) \tag{2.30}$$

where

$$FOM_{1/2} = \frac{\sum m_s cp_s |T_{si} - T_{so}| \delta t}{M_s cp_s (T_h - T_c)}\Big|_{1volume} \quad [8]$$

$$Fraction_{mix} = \frac{m}{n} \tag{2.31}$$

where T_h and T_c are the inlet temperatures of the discharge and charges cycles respectively. M is the total water mass of one tank volume.

The following function was obtained by fitting a curve through data points calculated theoretically by algorithm (2.29):

$$fraction_{mix} = -2.7131(FOM_{1/2}) + 2.7131 \tag{2.32}$$

The $FOM_{1/2}$ of a tank diffuser combination at any mass flow rate can now easily be obtained by measurements to categorise the thermal performance of the system[8]:

$$FOM_{1/2} = f(m_s) \tag{2.33}$$

The thermal performance of a stratified storage tank will therefore be characterised by the measured $FOM_{1/2}$.

2.6 ANIMAL HEAT LOADS

2.6.1 Description

Animal performance (growth, egg or milk production, wool growth, and reproduction) and their conversion of feed to useful products are closely tied to the thermal environment[9]. For each homeothermic species, an optimum thermal environment permits necessary and desirable body factions with minimum energetic input.

Thus it has become important to construct low capital and energy efficient housing facilities to maintain an optimal thermal environment for animals. However to optimise the design of these facilities it is necessary to integrate animal heat loads in passive building and system analysis tools. A general animal heat load model is derived in the following section.

2.6.2 Mathematical model

Animal heat production rates are primarily a function of ambient temperature, animal specie and animal size[10]. All three factors have a definite effect on heat production rates but detailed information regarding the effect of all three is not always readily available. Most literature provides only data linking animal species and animal mass to heat production rates.

Therefore the heat production model is based on the basal metabolic rate (standard metabolic rate) of the animal. The basal metabolic rate can be expressed as a function of the mass of the animal and a constant which is animal and age specific[9],[11].

$$M = Cm^{0.75} \tag{2.34}$$

where M is the basal metabolic rate (W) determined with the animal at rest, in a post-absorptive state and in thermoneutral surroundings, m the animal mass (kg) and C (basal constant) a constant which varies accordingly to animal type and age. The constant C varies between 3 and 3.5 for adult animal species and can be as low as 2 for new-borns and as high as 7 for young animals[11].

ASHRAE[9] and CIBSE[12] provide average values of 3.5 and 3.2 respectively which is a very good estimation for heat load calculations for all species with an acceptable level of error. However if the C constant is known for the specific specie and age better accuracy will be obtained.

These basal metabolic rates only predict the heat load of animals at rest, in a post-absorptive state and in thermoneutral surroundings and are of no use for animals during normal activity in housing facilities. The active metabolic rate of an animal under normal activity can now be expressed as follows[9],[13]:

$$W = B(t)Cm^{0.75} \tag{2.35}$$

where W is the total average heat production (W), B the additional activity function of temperature (or activity constant). The active metabolic rate is primarily a function of temperature for a specific specie in housing facilities but stays almost constant in the thermal comfort zone of the animal[9]. ASHRAE prescribes a constant value of 2.5 for B for all animals, which will again be a good approximation for animal heat load estimation under normal activity in housing facilities.

There are formulas available for many animal species to obtain basal and active metabolic heat production as a function of oxygen consumption (VO_2) for the calculation of B and C values if necessary or not available. For example, the active metabolic function for horses can be obtained by the following formula at various temperatures by measuring the average VO_2[14]:

$$H_{metab} = 21{,}000(0.8)(VO_2)(m) \tag{2.36}$$

where H_{metab} is the metabolic heat produced (J/min), 21,000 is the energy equivalent of O_2 (J/ml), 0.8 is the fraction of the calorific value of oxygen released as heat, VO_2 is the oxygen consumption (ml/kg m/min) and m is the body mass (kg).

For the integration of this heat production model into the building and ventilation models, the relation between the various components of heat transfer to the inside air needs to be obtained. The latent heat production component is again primarily a function of temperature[13] but is most of the time difficult to obtain. A generalised relationship is

introduced by ASHRAE, latent heat production accounts for approximately 33% of the total heat production.

The rest of the total heat load accounts for the sensible part, which can further be broken down into a convective and a radiative component. The same ratio which is used for humans, 33% convective and 67% radiative[9], will be a good approximation for warm blooded animals.

The convective heat gain acts directly on the air node of the building model (described in chapter 1) with all the other building convective heat gains. The radiative heat gain is weighed with the other building radiative heat gains according to the surface areas and act directly on the surfaces. See the building model in Chapter 1.

The activity function can be implemented into the simulation tool as the polynomial:

$$B(t) = a_0 + a_1 T_i + a_2 T_i^2 + \ldots\ldots + a_5 T_i^5 \tag{2.37}$$

where $a_{I's}$ are the correlation coefficients and T_i is the indoor dry bulb temperature (°C). The latent to total heat gain relationship can also be implemented into the simulation tool as the polynomial:

$$W_{latent}(t) = b_0 + b_1 T_i + b_2 T_i^2 + \ldots\ldots + b_5 T_i^5 \tag{2.38}$$

where W_{latent} is the percentage latent heat gain of the total heat load, $b_{I's}$ are the correlation coefficients and T_i the indoor dry bulb temperature (°C). The accuracy of these models is validated in a passive application in Chapter 3.

2.7 CONCLUSIONS

All the models derived in this chapter are explicit and therefore no solvers are needed to calculate outlet conditions from inlet conditions. Some of the models are validated with actual measurements during integrated simulation applications in the following two chapters.

2.8 REFERENCES

[1] E van Heerden, Integrated simulation of building thermal performance, HVAC system and control, *PhD thesis,* Faculty of Engineering, University of Pretoria, Pretoria, 1997.

[2] AF Mills, Heat Transfer, Irwin, Boston, 1992.

[3] WM Rohsenow, JP Harnett, EN Ganic, editors, Handbook of Heat Transfer Applications, Heat Exchangers, McGraw-Hill Book Company, 2ed edition, New York, 1985.

[4] C Lombard, Two-Port Simulation of HVAC Systems and Object Oriented Approach, *PhD thesis,* Faculty of Engineering, University of Pretoria, Pretoria, 1996.

[5] JS Caldwell, WP Bahnfleth, Identification of mixing effects in stratified chilled water storage tanks by analysis of time series temperature data, ASHRAE Transactions, Tullie Circle, Atlanta, 1998.

[6] JCR Truman and MW Wildin, Finite difference model for heat transfer in a stratified thermal energy storage tank with throughflow, Numerical heat transfer with personal computers and supercomputing, ASME HDT 110, pp. 45-55, 1989.

[7] MA Hussain, Experimental and numerical investigation of the mixing processes on the inlet side of the thermocline in a thermally stratified storage tank, Master's thesis, Department of Mechanical Engineering, University of New Mexico, Albuquerque,1989.

[8] WP Bahnfleth, A Musser, Thermal performance of a full scale stratified chilled water thermal storage tank, ASHRAE Transactions, Tullie Circle, Atlanta, 1998.

[9] ASHRAE Fundamentals Handbook, America Society of Heating, Refrigeration and Air-conditioning Engineers, Inc, Tullie Circle, NE Atlanta, GAZ 30329, 1997.

[10] S Weggelaar, Verification, Application and Extension of a novel thermal simulation model, M Eng thesis, Faculty of Engineering, University of Pretoria, Pretoria, 1996.

[11] JA Clark, Environmental aspects of housing for animal production, First edition, Butterworths, London, 1998.

[12] CIBSE Guide Volume A, Chartered Institution of Building Services Engineers, Delta House, 222, Balham High Road, London SW12 9BS, Staples Printers, 1986.

[13] LD Albright, Environmental Control for Animals and Plants, ASAE Textbook, The America Society of Agricultural Engineers, Technical Publications, 1990.

[14] HJ Mostert, RJ Lund, AJ Guthrie and PJ Cilliers, Integrated model for predicting thermal balance in exercising horses, Equine Veterinary Journal, Vol. 22, pp. 7-15, 1996.

CHAPTER 3

APPLICATION 1: ANIMAL HOUSING FACILITIES

Environmental control in horse housing facilities has become an important aspect in the construction of these facilities. Poorly designed stables may effect the animals' health (environmental diseases) and so reduce their performance. In many cases natural ventilation is used to ensure an acceptable stable environment due to considerable energy and cost savings. However it is difficult to design a stable for acceptable ventilation rates and indoor comfort without the proper tools or guidelines. The easiest and most accurate way will be to use a dynamic thermal performance and ventilation simulation tool for the prediction of the ventilation rates and indoor conditions. The passive building model described in chapter 1 was extended with natural ventilation and animal heat generation models for the design of animal housing facilities. The simulation tool was verified with actual measurements during five case studies to ensure its integrity and to illustrate its applicability in this field. The predicted indoor air temperatures of all the studies were within 1 °C for 80% of the time. The predicted indoor air relative humidities were within 8% RH for 100% of the time

3.1 INTRODUCTION

The effect of poor stable environment on the welfare and respiratory health of horses has long been appreciated in Europe and North America[1]. The concentration of potential respiratory pathogens and allergens can become unacceptably high in poorly designed stables[2]. As many horses are routinely stabled for at least 22 h a day, deficiencies in stable design may adversely affect their health, and thus may reduce their performance.

In order to provide an acceptable stable environment, guidelines have been proposed describing appropriate building designs and sizes of ventilation openings[3],[4]. Static calculation methods, which incorporate the heat load produced by animals, have also been prescribed to ascertain whether the ventilation of horse stables is adequate[5],[6]. Unfortunately, as these methods do adequately provide for the integration of all environmental components, they are generally of limited use in environments with differing climatic conditions[6].

Models for the simulation and thermal analysis of naturally ventilated buildings have received considerable attention recently[7],[8],[9]. Some of these thermal analysis models have been used in association with static ventilation analyses to describe the thermal and ventilation characteristics of selected horse stables in South Africa previously[6]. Systems for the simulation and analysis of natural ventilation in buildings have also been described[10],[11] and these have been integrated into a commercially available computer software package, QUICK II.

As this system was designed for use in domestic and industrial buildings it unfortunately did not include models for the heat production of animals housed within the buildings. In order to make the simulation system more generally applicable it was decided to develop a new program, which incorporates models that describe the heat produced by domestic animals.

The aim of this study was to validate all the new components of the simulation program. This was accomplished by simultaneously measuring the environmental conditions (temperature, humidity, solar radiation, wind speed and direction) and indoor temperature and humidity of a

stable barn under differing conditions. Using the data describing the environmental conditions as input, the simulation models were run and the output compared with measured indoor temperatures and humidities.

The specific studies allowed validation of the model of the thermal characteristics of the building envelope alone, simultaneous validation of the building envelope and animal heat production models, simultaneous validation of the building envelope and natural ventilation models and validation of all three models combined.

3.2 SIMULATION MODEL

The electrical analogy used to model the heat transfer processes in a building has been described in detail previously in chapter 1. The effects of natural ventilation were included within the building model. This included predicted unintentional flow through openings under doors and between window frames (infiltration) and deliberate flow through purpose provided openings such as open windows and ventilators (ventilation).

The empirical relationship described by the US National Bureau of Standards was used to calculate infiltration rates[12]. In order to predict ventilation a model developed by Rousseau and Mathews[10] was used in which the building is represented by a flow network of pressure nodes coupled by non-linear flow resistances.

In order to apply the building and ventilation models to naturally ventilated animal houses it was essential to incorporate the effects of heat produced by animals occupying the buildings into the model. These models are described in chapter 2.

3.3 VALIDATION OF MODELS

The facilities of the Equine Research Centre of the faculty of Veterinary Science of the University of Pretoria at Onderstepoort were used for this study. The models were evaluated by comparing the simulated predictions to measured indoor air temperatures and relative humidities in one of their horse stables. Five studies were conducted for five different building and ventilation scenarios.

Building description

The stable used, provided mechanical ventilation and evaporative cooling facilities. The building had a double layer brick construction with an air cavity between the layers. The stable roof was elevated with a 27° angle in a north and south direction and made of corrugated iron with a plaster board ceiling. The building wall surfaces faced either north or south. Figure 3.1 displays a schematic drawing of the stable.

The facility can house a maximum of twelve horses, each in its own open box with a sliding window shutter and ventilation louvers to the outside. There were two wooden doors to the outside on both sides of the building. Each window had a openable area of 1 m^2 with five of them on the north side and 7 on the south side.

The building had a floor area of 250m^2 and an internal volume of 874m^3. An important aspect of the facility is that the stables were situated in rural terrain and were unsheltered for winds from the north and south with stronger shelter from east and west winds.

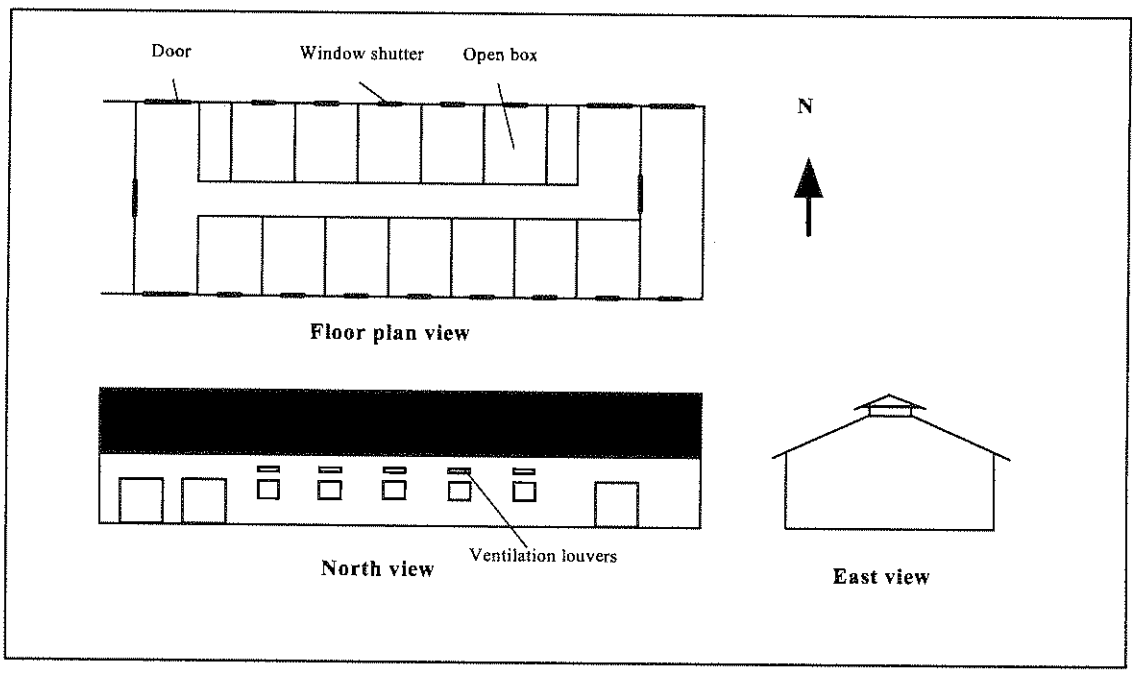

Figure 3.1: Schematic drawing of the stable

Procedure

The following five studies were conducted for 24 hour cycles on the same stable to obtain the validity and integrity of all the models in an integrated fashion:

- Case study 1: all the window shutters and doors were closed; the building was mechanically ventilated with outside air; the building space was empty (no horses).
- Case study 2: all the window shutters and doors were closed; the building was mechanically ventilated with outside air; the building space was filled with twelve horses from 09:00 to 15:00.
- Case study 3: the window shutters were open and the doors still closed; the mechanical ventilation was off; the building space was empty (no horses).
- Case study 4: the window shutters were open and the doors still closed; the mechanical ventilation was off; the building space was filled with twelve horses from 09:00 to 24:00.
- Case study 5: the window shutters were open and the doors still closed; the building was mechanically ventilated with outside air from 09:00 to 24:00; the building space was filled with twelve horses from 00:00 to 24:00.

The first study was done to verify the thermal performance of the building envelope on its own (building model). The best way to achieve this was to ventilate the building with a known rate of outside air. By doing this we simultaneously pressurised the building space to eliminate any natural ventilation or infiltration.

The second study conducted, was to evaluate the accuracy of the building model integrated with the animal heat production model. It will now be possible to obtain any inaccuracy's in the animal heat production model since the performance of the building envelope is known.

The third study was performed to obtain the accuracy of the building model and the ventilation model (wind and thermal effects) integrated. Again we are sure of the envelope performance which makes evaluating the ventilation model possible.

In the fourth study we combined the building, ventilation and heat production model in one and in the last study we also added the integration of mechanical ventilation. These last two

studies were conducted to ensure accuracy of any combination available in the simulation tool.

Measurements

Measurements were taken over a period of one week during June 1998. The measurements included indoor air temperatures and relative humidities, outdoor air temperatures and relative humidities, the radiation of the sun, wind speed and wind direction and mechanical driven air flow rates.

From this data a single representative day for each study was extracted to be compared with the 24-hour day predictions provided by the simulation tool. The building was left in its passive state with the window shutters open for 24-hours to stabilise after the first two studies, which involved mechanical ventilation.

The indoor air temperatures were measured with six shielded thermistors evenly spaced in the building at a height of 1.8 meters from the floor. The relative humidity sensors were placed at the same six locations. This was done to ensure realistic average indoor air condition measurements to be compared to the predicted simulation values. All twelve horses used in the studies were weighed before entering the stable.

Simulations

Five 24-hour day simulations, one for each study were executed to compare the predicted results to their respective measurements. The building structure was read into the simulation program as accurately as possible including shading devices like overhangs and nearby buildings. The building envelope in the simulation program stayed obviously exactly the same for all the studies except for when the window shutters were opened or closed.

The simulation program makes only provision for hourly climate data, so the average hourly measured data (dry bulb temperature, relative humidity, global and diffuse radiation, wind speed and direction) were used. For the first two studies the measured mechanical air change rate of 9.3 was used for simulation purposes.

For the studies which involved horses, the average weighed horse mass, a basal constant of 2.9, an activity constant of 3 and a constant latent percentage of 33% were the necessary inputs[13]. These constants were used since no functions of temperature were available and the horses were in their thermal comfort zone during all 5 studies.

Small time steps (the same as the measurement interval) were used during the executions of the simulations to ensure accuracy, 12 time steps per hour (Δt = 300s). These results were then compared to the actual time values of the measurements. This implies that the predicted value at a specific time was compared to the measured value at exactly that same time.

Results

Only the indoor air temperatures and relative humidities were used for evaluating the accuracy of the simulation tool. Each study's results are presented separately with the number of the case study on the graph. Figure 3.2 to Figure 3.11 display the predicted and actual measured indoor air temperatures and relative humidities for each study, as well as the outdoor air conditions for the applicable period.

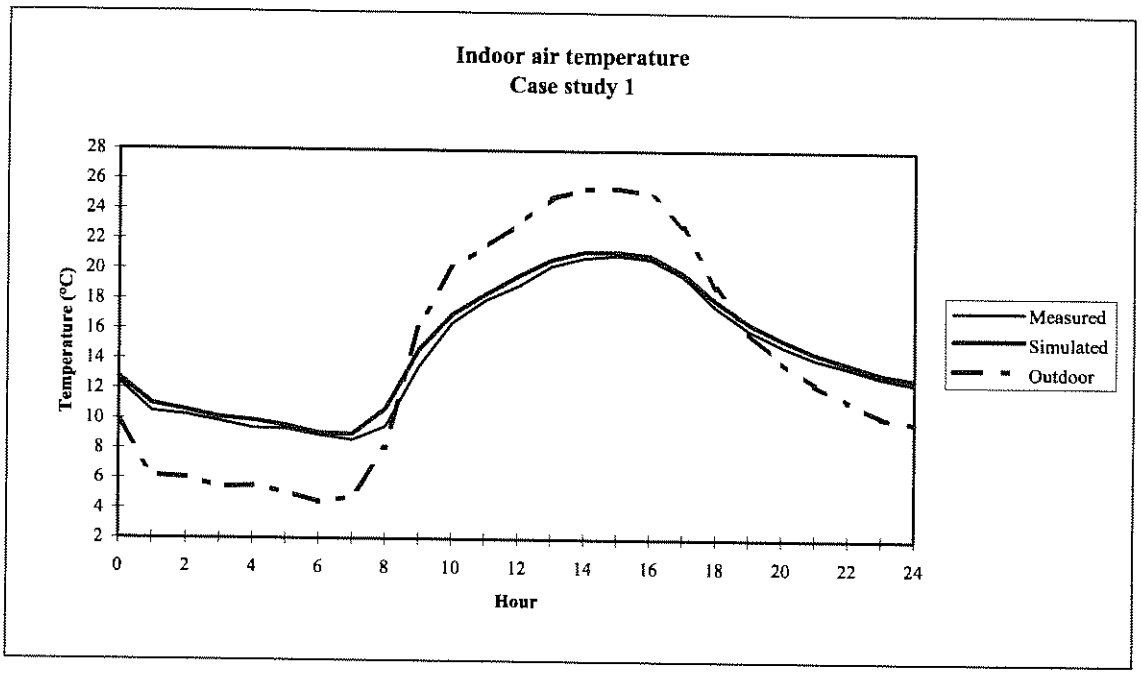

Figure 3.2: Temperature verification results

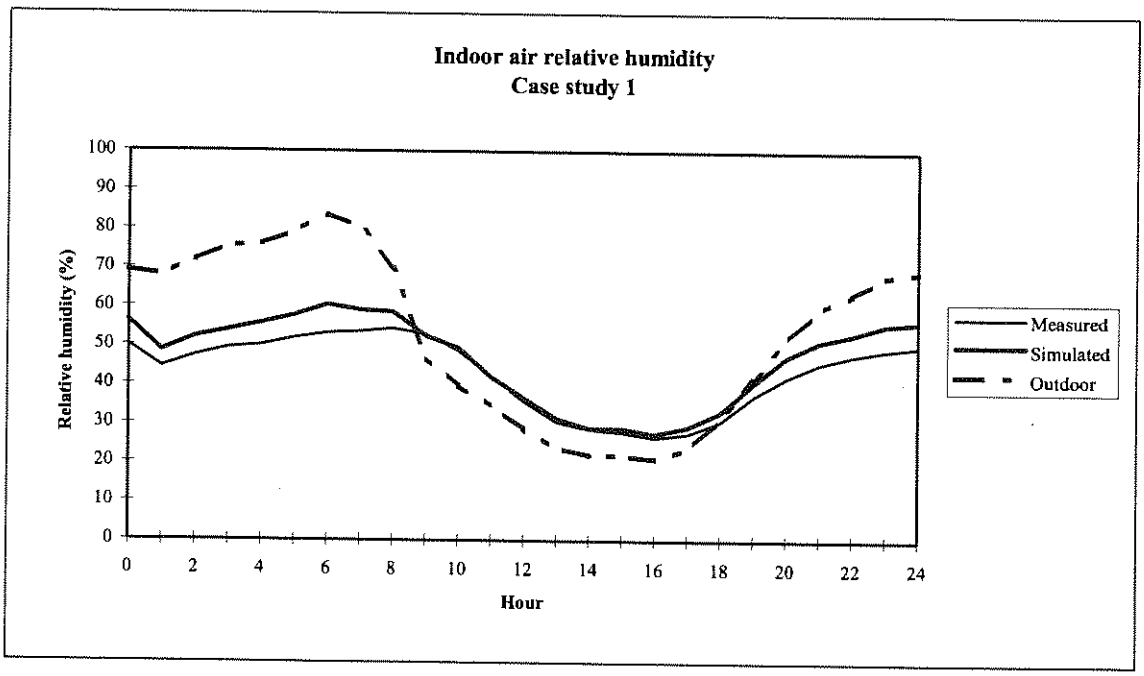

Figure 3.3: Relative humidity verification results

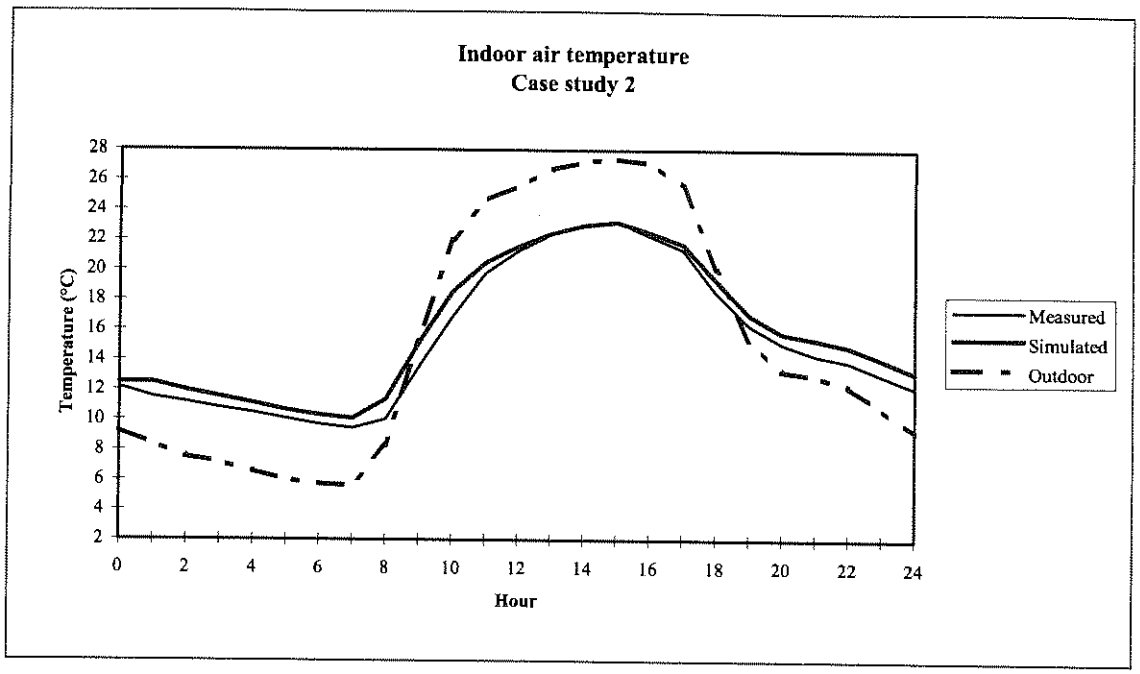

Figure 3.4: Temperature verification results

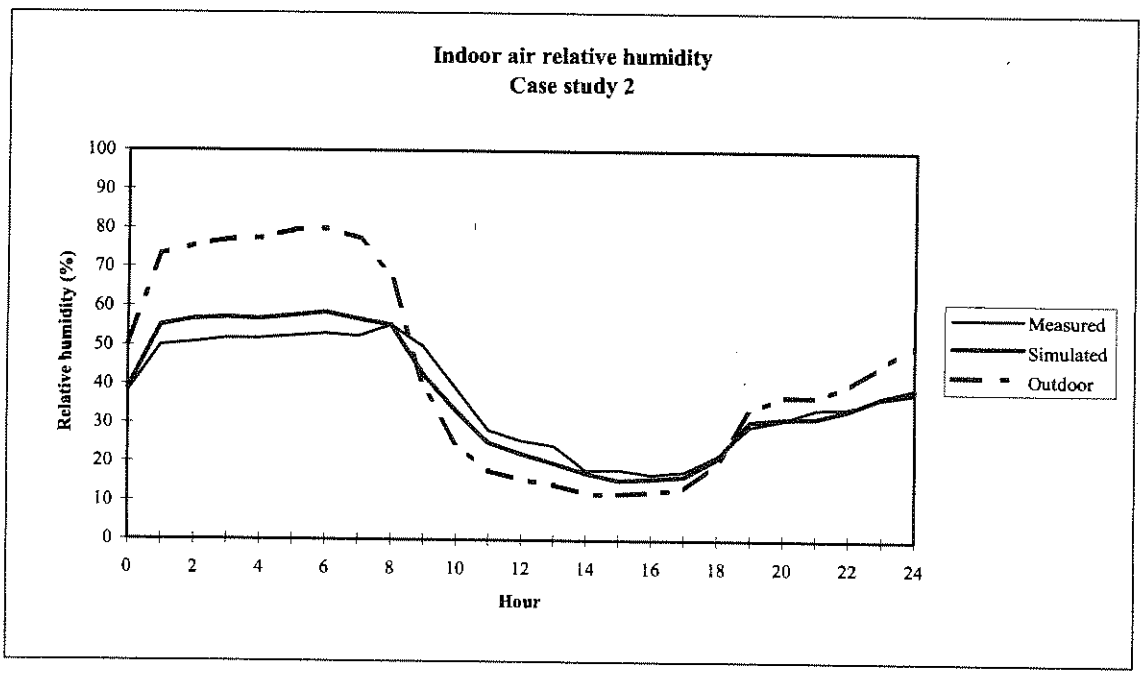

Figure 3.5: Relative humidity verification results

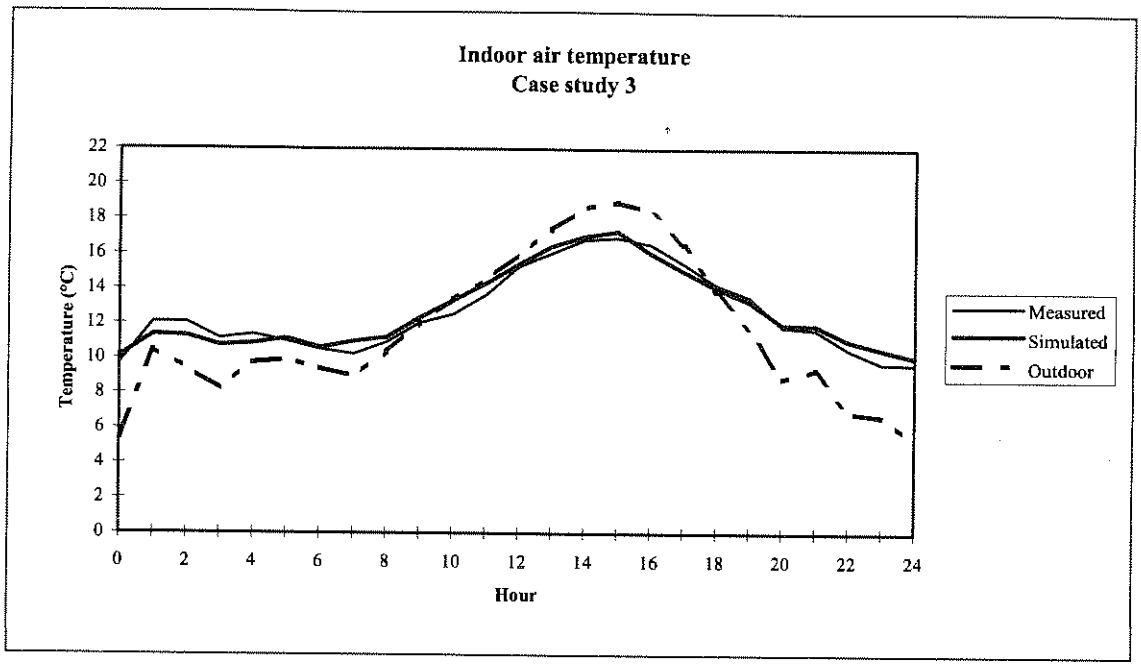

Figure 3.6: Temperature verification results

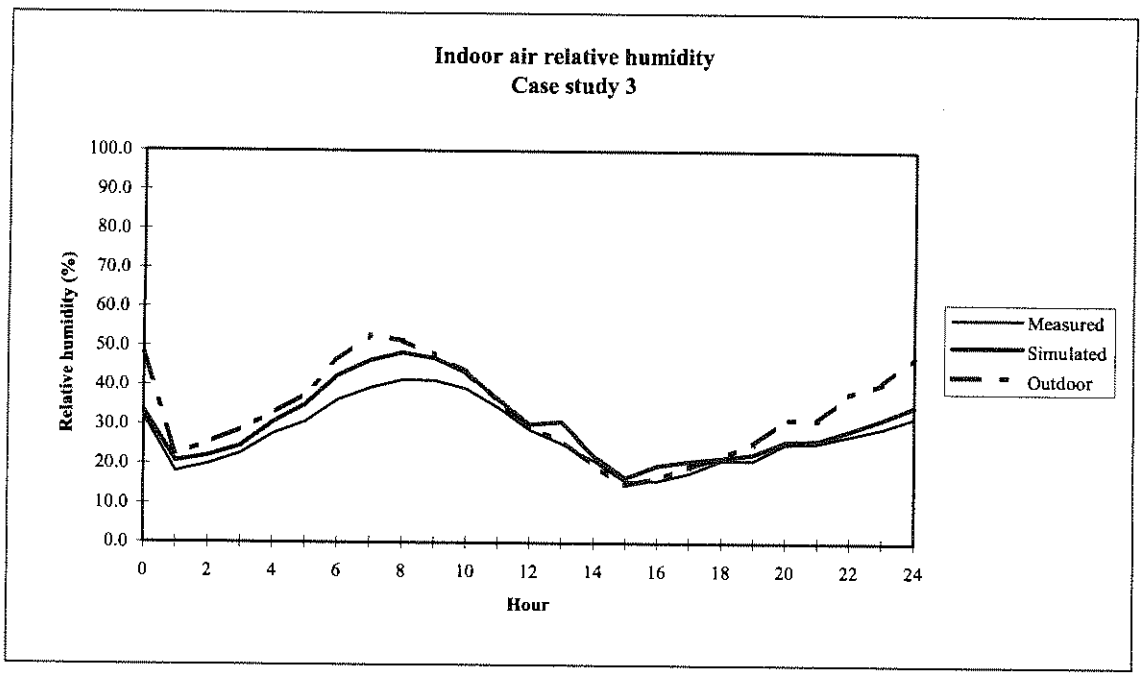

Figure 3.7: Relative humidity verification results

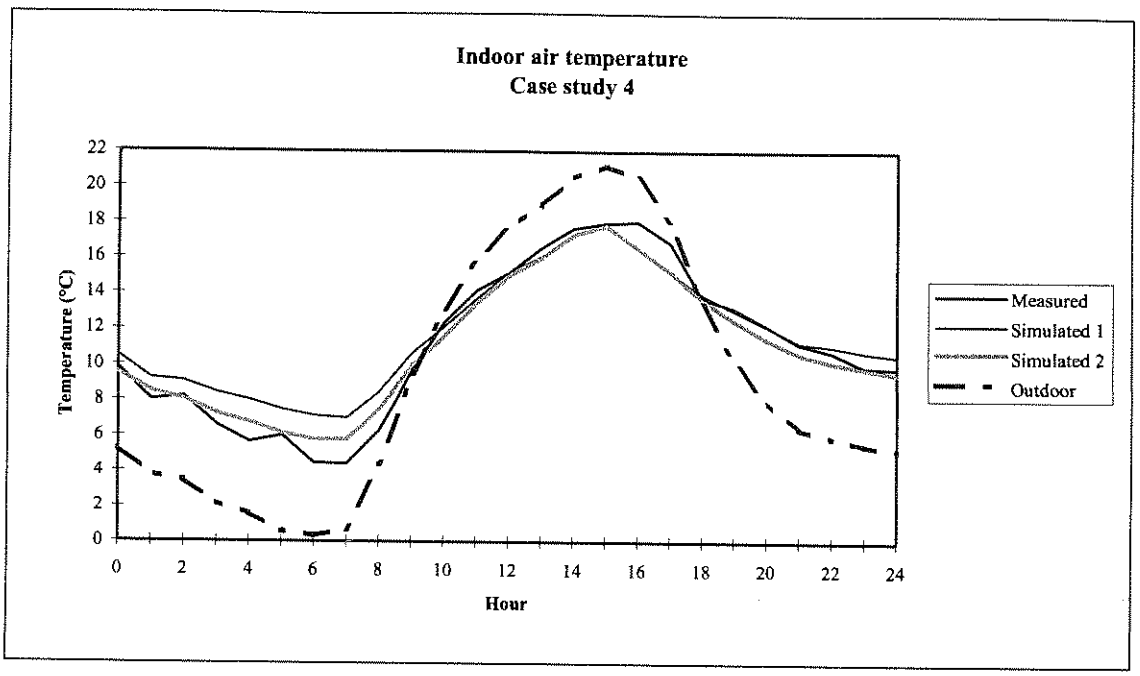

Figure 3.8: Temperature verification results

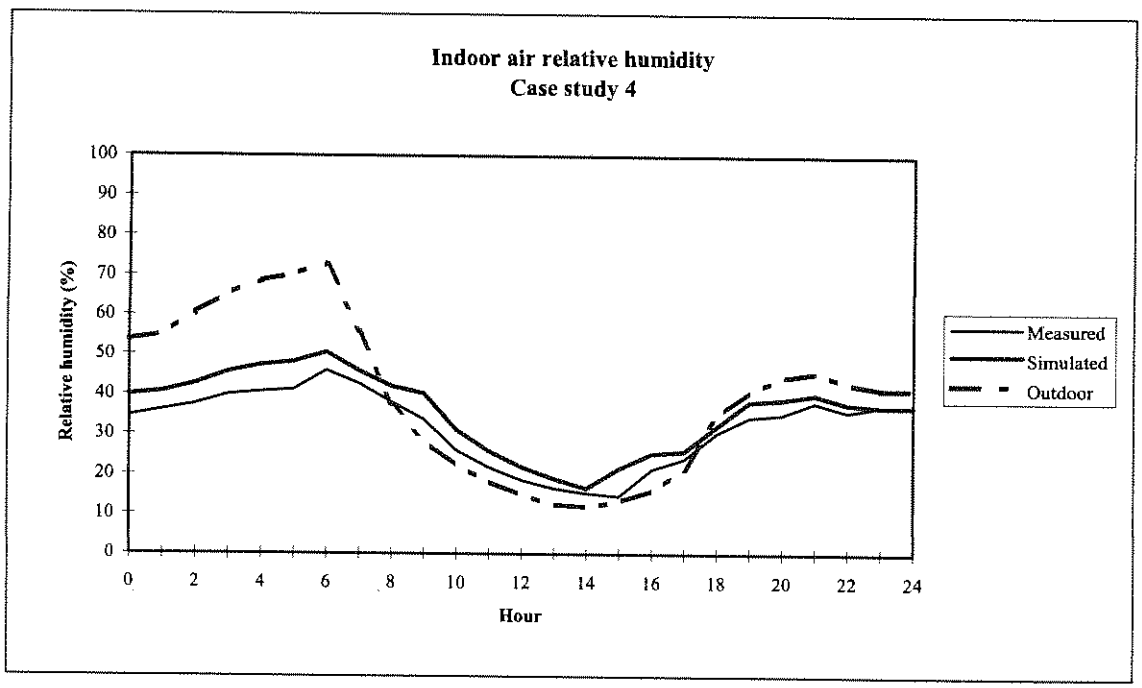

Figure 3.9: Relative humidity verification results

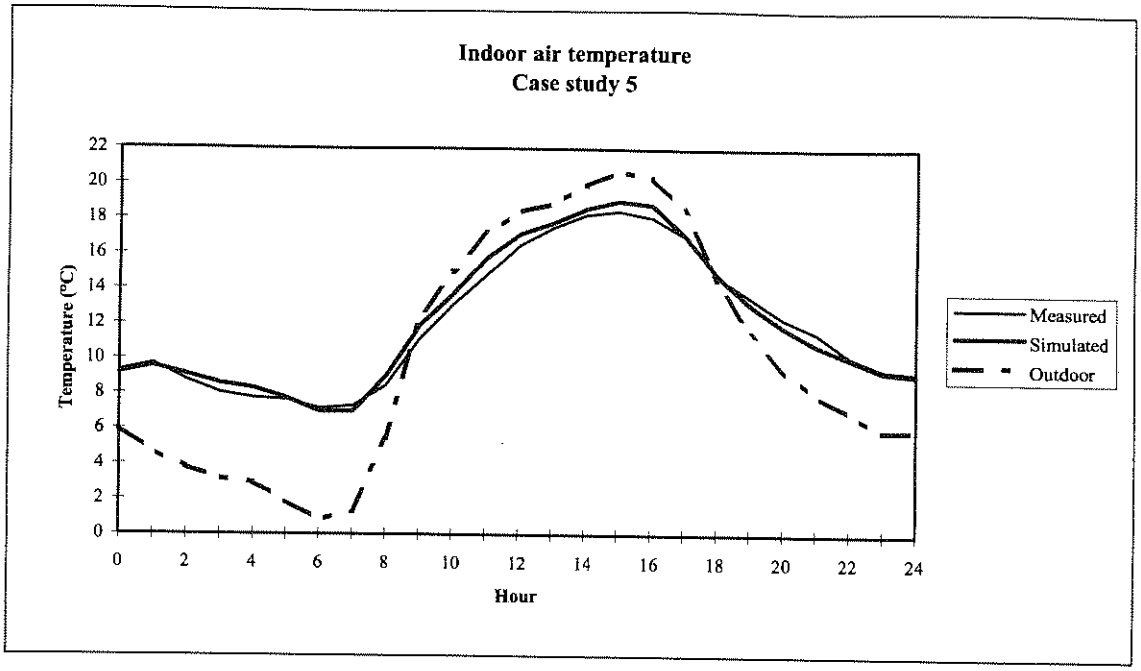

Figure 3.10: Temperature verification results

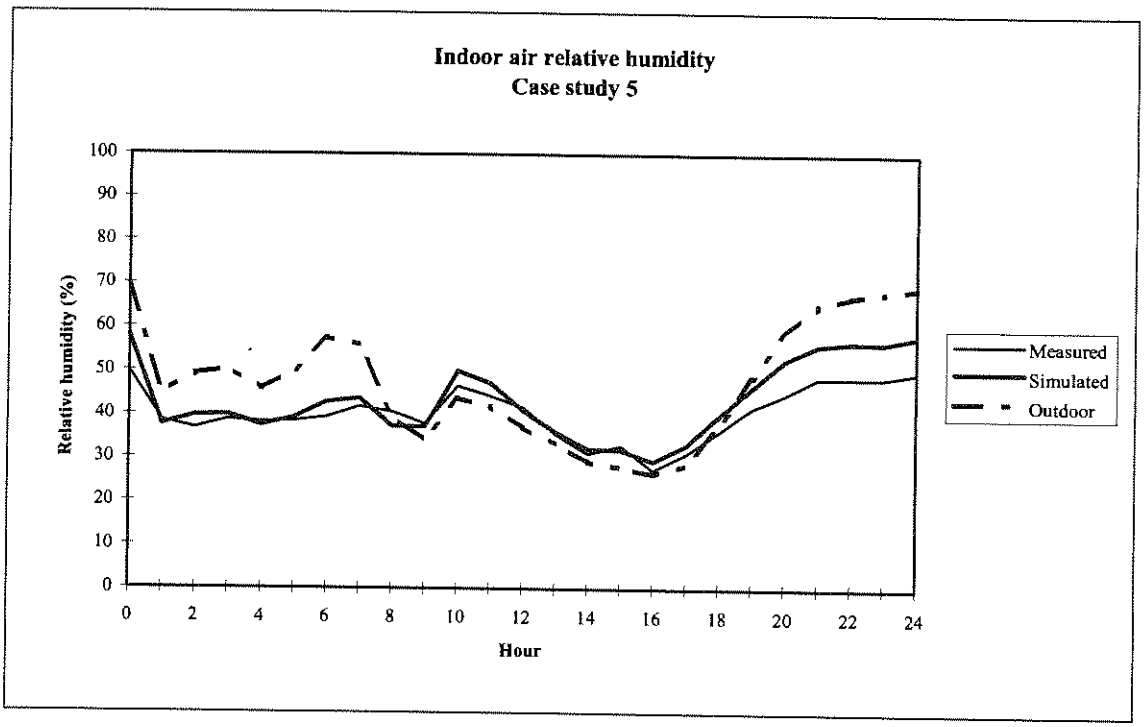

Figure 3.11: Relative humidity verification results

The results of study 1 and 2 are summarised in Table 3.1 and of studies 3 to 5 in Table 3.2. $T_{average}$ is simply the mean of the 24-hourly indoor air temperatures. The temperature swing is determined by taking the difference between the maximum and minimum indoor air temperatures of that 24 hour cycle.

The maximum error is the maximum discrepancy between the measured and predicted condition at the same moment in time. Within a specified temperature or relative humidity is the percentage of the predicted values inside that specification from that measured condition.

Study	Case study 1		Case study 2	
Type	Measured	Predicted	Measured	Predicted
T_{ave} (°C)	14.4	14.8	15.3	16
Swing (°C)	12.4	12.3	13.8	13.1
Max. error (°C)	1.2		1.7	
Within 1°C (%)	92		84	
Within 2°C (%)	100		100	
Max. error (RH%)	7.3		7.3	
Within 5 % RH (%)	70		76	
Within 10 % RH (%)	100		100	

Table 3.1: Summary of verification results

Study	Case study 3		Case study 4		Case study 5	
Type	Measured	Predicted	Measured	Predicted	Measured	Predicted
T_{ave} (°C)	12.6	12.7	11	11.1	12	12.2
Swing (°C)	7.2	7.2	13.6	12	11.3	12.1
Max. error (°C)	0.8		1.6		0.9	
Within 1°C (%)	100		80		100	
Within 2°C (%)	100		100		100	
Max. error (RH%)	7		7		8.3	
Within 5 % RH (%)	84		72		80	
Within 10 % RH (%)	100		100		100	

Table 3.2: Summary of verification results

It is clear from the results of case study 1 that the dynamic modelling of the building envelope is satisfactory with no phase shift between the measured and predicted conditions. With the outdoor air temperature and ventilation known variables, we can be sure that any discrepancies in studies 2 to 5 are caused by the animal heat production or natural ventilation modelling.

The results of case study 2 illustrate the accuracy of the animal load model integrated with the building envelope. The result is satisfactory with again no phase shift between the measured and predicted conditions with a very good correlation between 09:00 and 15:00. This does not only reflect a good total animal heat load estimation but also a good convective, radiative and latent ratio.

A moderate average wind of 1.6 m/s from a north west direction was measured during the 24 hours of case study 3. Therefore the dominant force behind the natural ventilation was wind and not the temperature difference. Natural ventilation driven by wind through vertical openings are therefore well accounted for in the simulation model. The wind velocity (direction and speed) for this study was almost consistent on an hourly basis, which made our average hourly wind inputs into the simulation tool realistic.

The results obtained from the first simulation (simulation 1, Figure 3.8) during case study 4 showed large discrepancies during the morning and late night. This result can be attributed to the inaccurate prediction of temperature induced ventilation since windless conditions existed during the time. Each window opening was treated as one opening at one specific stack height (at geometric area centre) which only made provision for one directional flow driven by the ventilation openings at a higher vertical location.

If an opening's vertical dimension is large enough to create a temperature difference due to the stack effect, two directional flow can occur through the same opening[14]. To make provision for this effect, each window opening was treated as two openings (simulation 2) directly above each other, each with its respective relative geometric area centre height.

The results from this simulation 2 (Figure 3.8) are a big improvement on the first one with acceptable accuracy. The discrepancies can now be attributed to the inconsistency of the wind velocity since the average hourly inputs values are not a good representation of the gusty wind conditions which existed for short intervals in this case.

The morning hours (00:00 to 09:00) during case study 5 were fortunately windless, before the mechanical ventilation was switched on. This isolates natural ventilation driven by temperature differences which made the validation of this part of the model possible. The

windows were again divided into two, one directly above the other. The comparison between the measured and predicted temperatures and relative humidities are very good (Figure 3.10 and Figure 3.11).

No natural ventilation air changes were measured for verification purposes. But we know that the thermal performance of the building envelope is correct for a given ventilation rate. Therefore the predicted air changes calculated for natural ventilation must be correct since the comparison between the predicted temperatures and humidities is more than satisfying.

3.4 CONCLUSIONS

An animal heat generation model was integrated with the building envelope and ventilation models presented in this chapter to simulate the passive thermal and ventilation performance of horse housing facilities.

Five case studies were conducted to verify the simulation models' predictions over a wide range of different application combinations. The simulated indoor air temperatures of all the case studies were within 1°C for 80% of the time. The predicted indoor air relative humidities were within 8% RH for 100% of the time.

The case studies have shown that the stack effect, the driving force behind temperature induced ventilation, can be better accounted for if all the vertical openings are treated as two separate openings directly above one another. The height difference between the openings is the distance between the geometric centres of the two divided areas.

The verification results reflect on the accurate modelling of the building envelope, ventilation (wind and temperature induced) and animal heat production integrated. The results were further sufficiently accurate for the simulation models to be used with confidence in the design of forced or natural ventilated (through vertical openings) horse stables or any animal housing facilities.

3.5 REFERENCES

[1] AF Clarke, TM Madelin and RG Allpress, The relationship of air hygiene in stables to lower airway disease and pharyngeal lymphoid hyperplasia in two groups of thoroughbred horses, Equine Vet. J. 19, pp. 524-530, 1987.

[2] AF Clarke, A review of environmental and host factors in relation to equine respiratory disease, Equine Vet. J. 19, pp. 435-441, 1987.

[3] AJF Webster, AF Clarke, TM Madelin and CM Wathes, Air hygiene in stables I: Effects of stable design, ventilation and management on the concentration of respirable dust, Equine Vet. J. 19, pp. 448-453, 1987.

[4] DWB Sainsbury, Housing the horse, In: Horse management Ed: J Hickman, CBAH, London, pp. 63-92, 1984.

[5] AF Clarke, Stable environment in relation to the control of respiratory diseases, In: Horse Management Ed: J Hickman, Academic Press, London, pp. 125-174, 1987.

[6] RJ Lund, AJ Guthrie and VM Killeen, Survey of selected design and ventilation characteristics of racehorse stables in the Pretoria, Witwatersrand, Vereeniging area of South Africa, JS Afr. Vet. Assoc. 64, pp. 149-153, 1993.

[7] PH Joubert and EH Mathews, QuickTEMP – A thermal analysis program for designers of naturally ventilated buildings, Building and Environment, pp. 24, 155-162, 1989.

[8] EH Mathews, Thermal analysis of naturally ventilated buildings, Building and Environment, pp. 21, 35-39, 1986.

[9] EH Mathews, Empiricism in the thermal analysis of naturally ventilated buildings, Building and Environment, pp. 23,57-61, 1988.

[10] PG Rousseau and EH Mathews, A new integrated design tool for naturally ventilated buildings, Energy and Buildings, 23, pp. 231-236, 1996.

[11] E Van Heerden and EH Mathews, A new simulation model for passive and low energy architecture, PLEA '96: Building and Urban Renewal, pp. 223-228, (Abstract), 1996.

[12] C Park, DR Clark and GE Kelley, HVACSIM Building and Equipment Program: Building Loads Calculation, Gaithersburg, 1986.

[13] LD Albright, Environmental Control for Animals and Plants, ASAE Textbook, The America Society of Agricultural Engineers, Technical Publications, 1990.

[14] ASHRAE Fundamentals Handbook, America Society of Heating, Refrigeration and Air-conditioning Engineers, Inc. Tullie Circle, NE Atlanta, GAZ 30329, 1997.

CHAPTER 4

APPLICATION 2: CONFERENCE FACILITIES

Efficient HVAC control is often the most cost-effective option to improve the energy efficiency of a building. However, the effect of changing the control strategy (i.e. on indoor comfort and energy consumption) is usually difficult to predict. The new tool described in chapter 1 was used to investigate the energy savings potential in a Conference Centre. The influences of fan scheduling, setpoint setback, economiser cycle, new setpoints, fan control, heating plant control, and various combinations thereof was investigated. The simulation models were firstly verified with measurements obtained from the existing system to confirm their accuracy for realistic new control strategy simulations. With the aid of the integrated simulation tool it was possible to predict savings of 744 MWh per year (32% building energy saving and 58% HVAC system energy saving) by implementing these control strategies. These control strategies can be implemented in the building with a direct payback period of less than 6 months.

4.1 INTRODUCTION

Heating, ventilation and air-conditioning (HVAC) system energy efficiency in buildings means monetary savings for the owner and less greenhouse gasses being released into the atmosphere. Although very important, energy saving measures must never compromise indoor air quality (IAQ). The reason is that IAQ has a direct effect on the productivity of the occupants[1]. The cost associated with poor IAQ far outweighs savings due to reduced energy consumption[2].

Popular belief in the past was that good IAQ and energy efficiency were in direct conflict[3], it is now agreed that energy savings of around 30% may be realised through retrofit projects of existing buildings without compromising indoor comfort[4]. In South Africa, studies done by TEMM International (Pty) Ltd. have shown that in the commercial sector approximately 50% of energy is used for air-conditioning[5]. This statistic clearly indicates that the area which offers the most potential for energy saving is the HVAC system.

A cost-effective way to improve the energy efficiency of a HVAC system, without compromising indoor comfort, is by implementing better control. However, when changing the control strategy of a system it is often difficult to predict the resulting changes in system energy consumption and indoor comfort.

To achieve these predictions a simulation tool, which can efficiently and accurately simulate the building with its HVAC system and controls in an integrated fashion, is required. There are many system simulation programs available. However they do not satisfy the requirements of integrated, efficient and accurate simulation by the typical consulting engineer [6],[7],[8]. QUICKcontrol was therefore extended to satisfy these requirements.

A study was conducted to investigate the potential for energy cost savings in the Conference Centre of the CSIR without compromising indoor comfort.

4.2 BUILDING AND HVAC SYSTEM DESCRIPTION

4.2.1 Building description

The Conference Centre of the CSIR is located in the eastern suburbs of Pretoria. The building consists of 3 levels and has a total air-conditioned floor area of approximately 2900 m^2. The venues make provision for a total of 1570 people. The air-conditioned areas include a restaurant on the lower floor, 3 conference halls, a restaurant and a foyer on the second floor and 3 conference halls on the first floor. The building has north, south, east and west facing windows.

4.2.2 HVAC system description

Air distribution system:

The HVAC system is a constant volume, variable air temperature system. It consists of a central cooling and heating plant, and air handling units (AHUs) for the conference halls, restaurants and reception areas. In addition to the 8 AHUs, which form part of the central system, there is a package unit that serves 4 smaller venues and an office on the ground floor. This unit is not included in the investigation. The entire system is located in a plantroom on the lower level.

The air is conditioned by cooling and heating coils located inside the AHUs. Air is supplied to the venues via ducting. It is returned from the lecture halls via grills and ducts back to the plantroom where it mixes with outdoor air before returning to the AHUs.

Fresh air is supplied to the building via grilles located on the north and south sides of the building. Dampers are responsible for the fresh/ return air mixing ratio. A schematic drawing of the system layout is depicted in Figure 4.1.

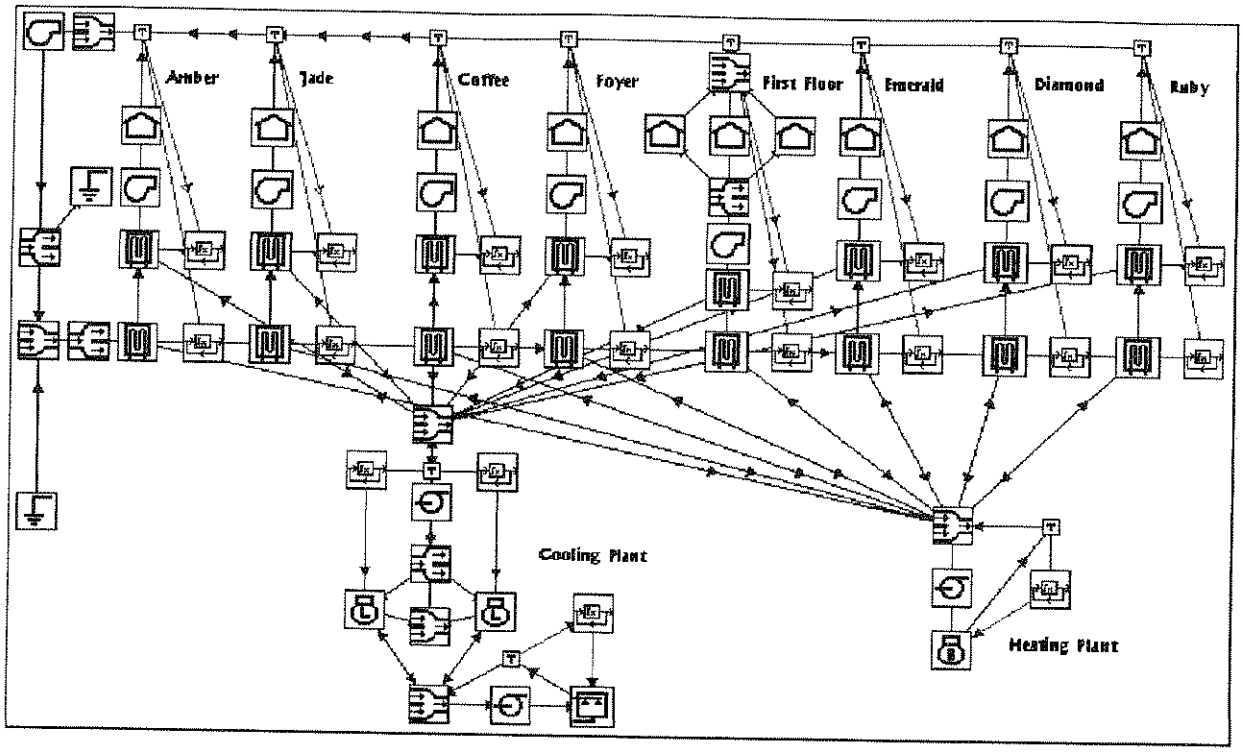

Figure 4.1: Layout of the simulation model

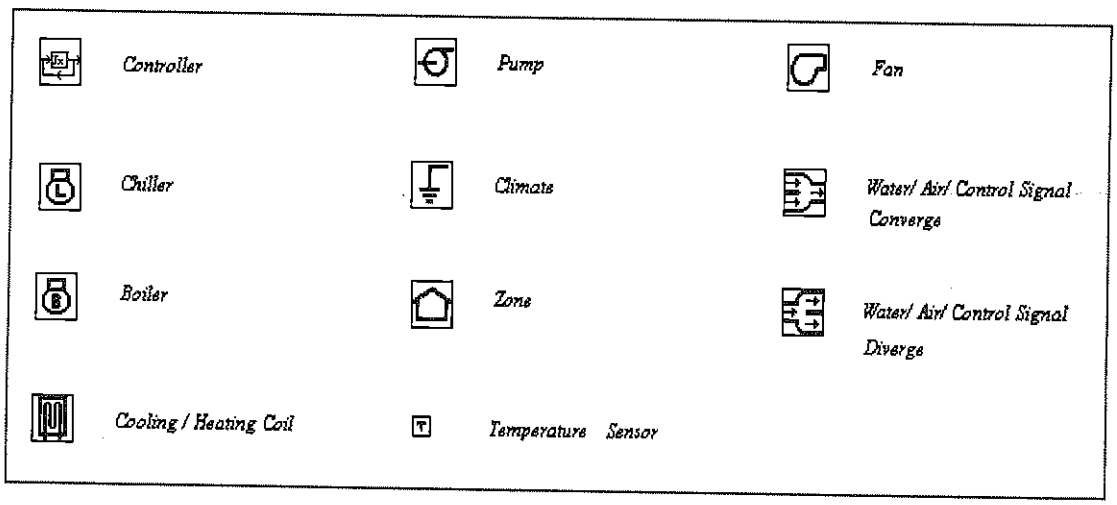

Cooling plant:

Cooling coils located inside each AHU do the cooling of the air. Digital PID controllers control the water flow through the coils to maintain a set temperature at sensors located in the venues or the return air ducts of the venues.

Two parallel, reciprocating water-cooled chillers supply chilled water to all the cooling coils in the AHU. Loading and unloading of the chiller compressors maintain a set return water temperature. Each has two compressors with a rating of 37 kW per compressor and a cooling capacity of 340 kW per chiller. Two condensing units located on the roof of the building are responsible for cooling the chiller condensing water. Chilled and condenser water pumps are responsible for water flow through the two circuits respectively.

Heating plant:

Heating coils inside the AHUs are used when heat is required in the venues. Like the cooling coils, digital PID controllers are used to control the water flow through them to maintain a set temperature inside the air-conditioned areas.

A boiler, located in the plant room, supplies the hot water to these coils. The boiler is loaded and unloaded by a step controller in 6 phases to keep the water inside at a set temperature. The boiler has a total heating capacity of 246 kW and a storage volume of 10 m^3. A hot water pump is responsible for the flow through the hot water circuit.

4.3 COMFORT AND ENERGY AUDIT

It was necessary to determine the current indoor air conditions of the Conference Centre to assess if it was up to standard, and also to be used for the verification of the simulation model. Measurements were taken to determine these conditions. If these indoor conditions were satisfactory they could be used as standards for the retrofit evaluations. A "walk through" audit was also conducted to determine any particular problem areas in the building.

An energy audit was done to determine the end-user breakdown of the energy consumption in the Conference Centre. This could be used to find the largest energy consumers, which are usually also the areas with the largest energy savings potential. The measuring of the energy consumption of the Conference Centre was a very labour intensive process. A "walk through" audit was conducted to identify the energy usage of lights and other diverse equipment. In this way it could be seen whether the energy consumption could be improved upon in other systems than the HVAC system.

HVAC, lights and other equipment were the categories used in the end-user breakdown (Figure 4.2). The "other equipment" category includes the lifts, computers, overhead projectors etc. The HVAC energy consumption was then divided into the chillers, boiler, fans and pumps (Figure 4.3).

The HVAC system in the Conference Centre had the greatest potential for energy saving as it consumed approximately 57% of the total building energy. The reason for this is the large internal load in the form of people in the auditoriums, which can accommodate as many as 750 people.

The system control strategy of the Conference Centre was investigated to determine the system's energy savings potential. The energy audit identified the major energy consumers as well as areas where retrofits could be made to obtain energy savings.

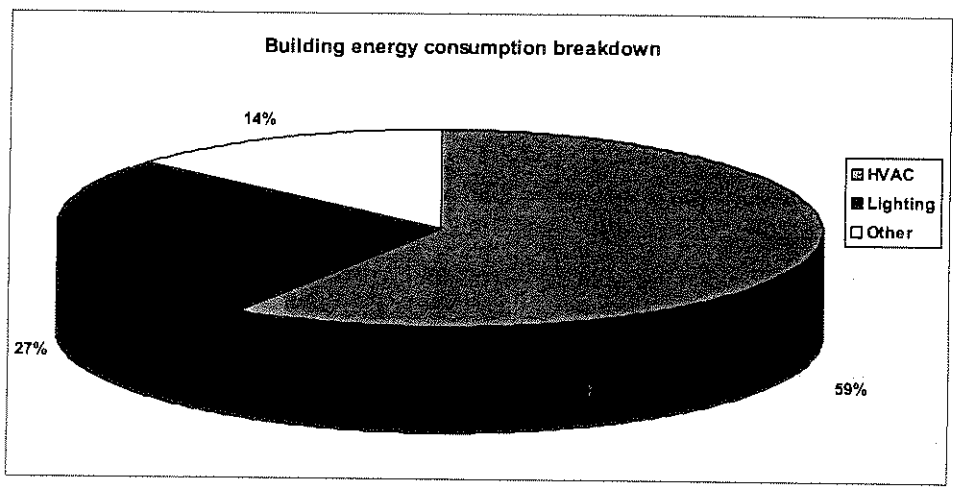

Figure 4.2: Current building energy consumption breakdown

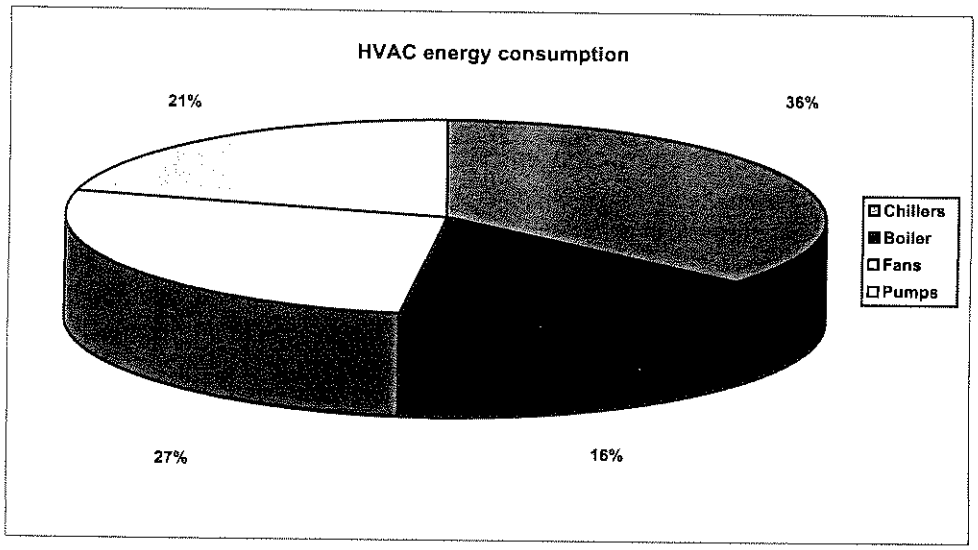

Figure 4.3 : Current HVAC system energy consumption

4.4 VERIFICATION STUDY

A verification study was performed to verify and confirm the accuracy of the simulation models (including control parameters) to calculate realistic energy savings with the retrofit simulation. The main purpose of the verification study was not so much to verify the building model and the HVAC models individually, but to verify the "real life" dynamic interaction between the building model and the HVAC system models with the influence of the controllers, in an integrated fashion.

The building model has already been empirically verified over a wide range of different building structures and climates in 140 case studies with great accuracy as seen in references[9]. The building model can therefore be used with confidence if it is properly constructed without verifying it again.

Simulation model:

For the verification study it was necessary to take measurements, set up the simulation tool, execute the simulations and compare the measurements with the predicted values. The measurements include temperatures, relative humidities, air flow rates, water flow rates and electrical power required by each HVAC system component. From the measured data a single representative day was extracted to be compared to the 24-hour day predictions provided by the simulation tool.

The integrated simulation tool requires a large number of inputs. These inputs comprise building structural data, outdoor climatic data, internal loads, occupancy data, all the HVAC component data and the control parameters. Some of these inputs vary with time, namely in our case, outdoor climate data, occupancy and internal loads. Most of the input data or if possible all of it should be available to perform a verification study with integrity.

The building was divided into 10 zones. Each venue supplied by an AHU was taken as a zone. These include the Amber restaurant, Jade restaurant, Diamond hall, Ruby hall, Emerald hall, the foyer, coffee area and the 3 first floor conference halls. Figure 4.1 depicts the simulation model layout. The building structure data with the zone dimensions were obtained from building drawings and a database. All of this was read into the simulation program. The internal loads in the form of occupants were available from the building booking system.

Regressions for the HVAC components were set up from measured and catalogue data. The control strategy, including operating times and control parameters for most system components, was obtained from measurements and read into the simulation program.

Results:

The verification results of the indoor air temperatures, AHU supply air temperatures, the chiller power, and the boiler power are summarised in this section. In the case of the first floor the measured indoor air temperature of the zone is the average temperature of all the conference halls in that zone.

The figures in Appendix B display the simulated and actual measured indoor air and supply temperatures of each zone. It is clear from the figures that satisfactory results were obtained from all 10 zones. The indoor and supply air temperature results are respectively summarised in Table 4.1 and Table 4.2.

Zone	Average error (°C)	% Within 2°C of the time
Diamond	0.9	100
Ruby	1	100
First floor	0.6	100
Foyer	0.2	100
Coffee	0.4	100
Amber	0.6	100
Jade	0.4	100
Emerald	1.1	100

Table 4.1: Summary of indoor air verification

Zone	Average error (°C)	% Within 2°C of the time
Diamond	1.5	75
Ruby	3.1	32
Emerald	2.8	27
First floor	1.4	81
Foyer	3.4	72
Coffee	0.6	99
Jade	1.1	89
Amber	1.6	74

Table 4.2: Summary of supply air verification

The simulated and measured chiller power is compared in Figure 4.4. The simulation tool successfully simulated the loading and unloading of the chiller capacity steps. There is not a large phase difference between the predicted and simulated values. This verifies the time constants of the building structure and the HVAC system components. The difference between the measured and simulated energy consumption over 24 hours is only 13%.

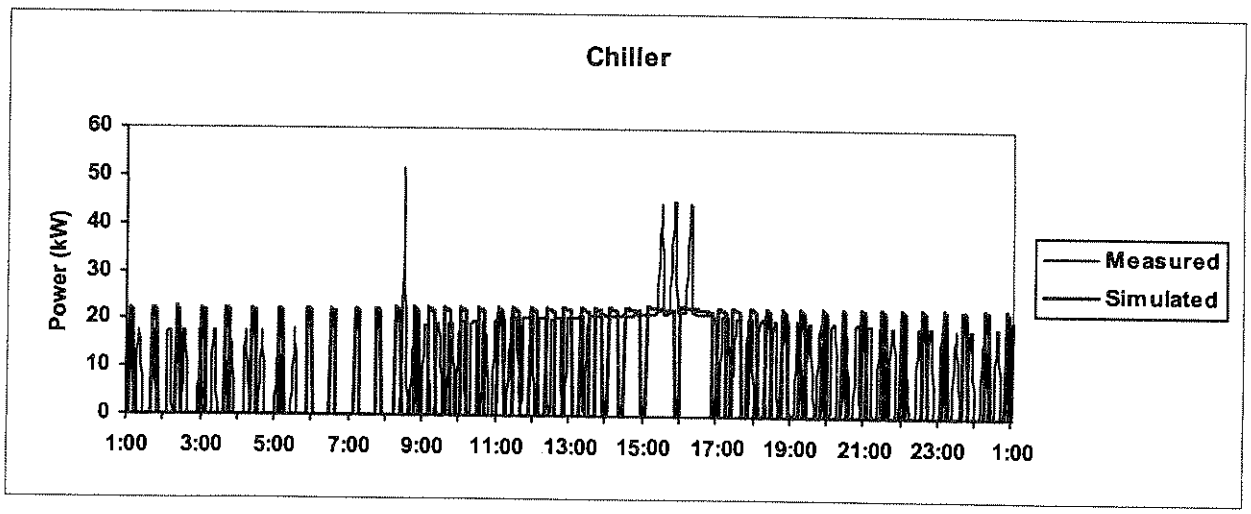

Figure 4.4: Chiller power verification result

Figure 4.5 displays the boiler power verification results. The simulated values do not follow the measured values exactly but the total energy consumed over 24 hours compares well. There is a difference of 3% between the measured and simulated boiler energy consumption over the 24-hour day. Thirty time steps per hour were needed to simulate the dynamics of the building zones and the HVAC system with its controls to this degree of accuracy.

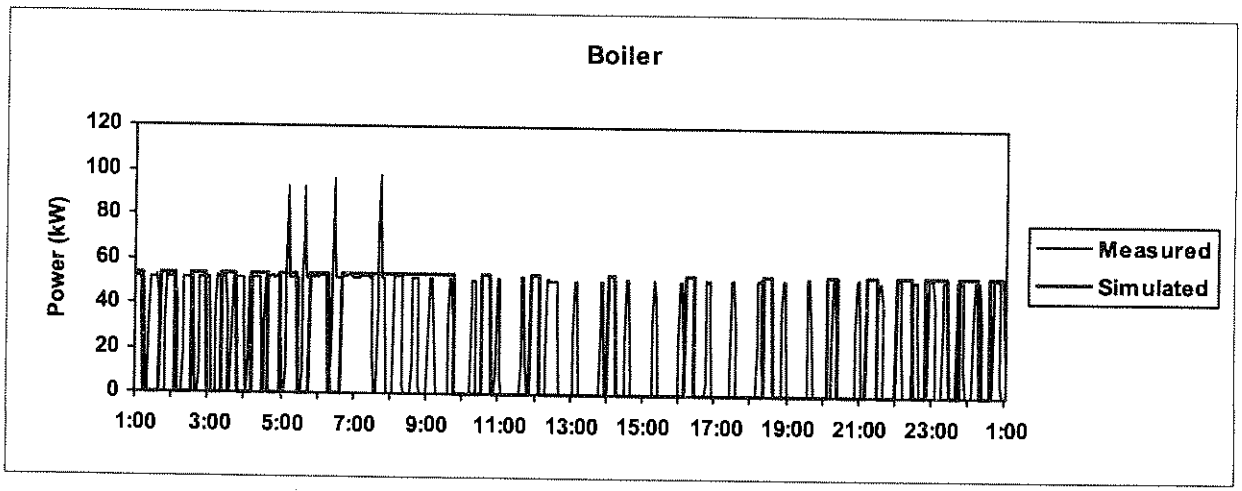

Figure 4.5: Boiler power verification result

One may look at the simulation results and feel that the accuracy of the integrated modelling is perhaps not that good. In some instances the predicted and measured values are out of phase and the graphs do not always have exactly the same profiles. Just remember the idea was not to simulate the dynamics of the system 100 % correctly but to predict accurate realistic daily (and yearly) system energy consumption and accurate average indoor air temperatures to ensure indoor comfort.

4.5 NEW CONTROL STRATEGIES

4.5.1 Introduction

This section describes numerous control and scheduling options, which will result in possible monetary savings. The potential of these options will be obtained by simulation and can be seen in the following section, Retrofit Simulation Results.

All the options, except the one on lighting, were done on the HVAC system of the building, since 59% of the total building energy is consumed by it. This means the biggest potential for building energy saving lies in HVAC system retrofit. In the following sections a brief overview of each retrofit option is given.

4.5.2 Fan scheduling

The present HVAC system should be operating with fan scheduling, where the fans are turned off during the night and early mornings. This corresponds to the time when the building is not in use, and therefore does not need any air-conditioning. However, from the temperature and electrical measurements it was clear that this was in fact not the case.

For this option we propose the following fan operating time schedules. The operating times differ for each zone, according to the times of use by the occupants. An hour was allowed in the mornings to get the zones on temperature before occupied by the people. This resulted in the use of 100 % return air during winter and no internal heat during summer to save on maximum system demand. These times can be seen in Table 4.3.

Zone	Day	Operating time
First Floor	Weekday	6:00-24:00
	Saturday	6:00-24:00
	Sunday	7:00-8:00
Amber, Jade	Weekday	6:00-22:00
	Saturday	6:00-22:00
	Sunday	7:00-8:00
Foyer, Coffee	Weekday	6:00-24:00
	Saturday	6:00-24:00
	Sunday	7:00-8:00
Diamond, Emerald, Ruby	Weekday	6:00-20:00
	Saturday	6:00-20:00
	Sunday	7:00-8:00

Table 4.3: HVAC fan scheduling times

The return air fans, that work in tandem with their relevant supply air fans, can therefore be switched off according to Table 4.3.

4.5.3 Economiser

The economiser control manages the fresh air intake into the building. With this control the air intake can be controlled to let in as much as 100% fresh air, and as little as 40% during occupied times and 0% during unoccupied times.

The outside air can therefore be used for cooling if required when the outdoor temperature is lower than the return air temperature. If the outside air is at a higher temperature than the return air, it will be cut down as much as possible.

In the case of the Conference Centre there are two separate sets of fresh and return air dampers. One set on the North side and the other on the South side. Each damper set will be controlled from a temperature sensor located in the relevant return air plenum and one just inside the fresh air dampers for monitoring the outdoor air temperature.

This strategy can be divided in two parts, an occupied strategy and an unoccupied strategy. Infrared motion detectors located in the venues will be responsible for selecting the relevant strategy. The occupied strategy will be active for 15 minutes after movement was detected by any of the sensors in the venue. This implies that the timer will reset itself if new movement is detected during this period and the 15-minute countdown will start all over again. The unoccupied strategy will therefore only be activated when all the sensors in the venue are passive for a period of 15 minutes.

For this option all the relevant motion detectors of the venues which return air to the same set of dampers must be passive for 15 minutes to activate the unoccupied economiser control strategy.

Occupied strategy:

If the return air temperature is higher than the outdoor air temperature the following strategy will be followed:

- If the return air temperature exceeds 22°C the fresh air damper will open proportionally from its minimum setting (40% fresh air of total supply) until fully open at 23°C.
- The return air damper will for the same conditions start to close proportionally from its maximum setting (60% return air) to fully closed.
- If no cooling is required the fresh air damper will be at its minimum setting (40% fresh air) and the return air damper at its maximum (60% return air).
- If the outdoor air temperature exceeds the return air temperature the fresh air damper will close to its minimum setting (40% fresh air) and the return air to its maximum, 60% return air. The strategy is graphically presented in Figure 4.6.

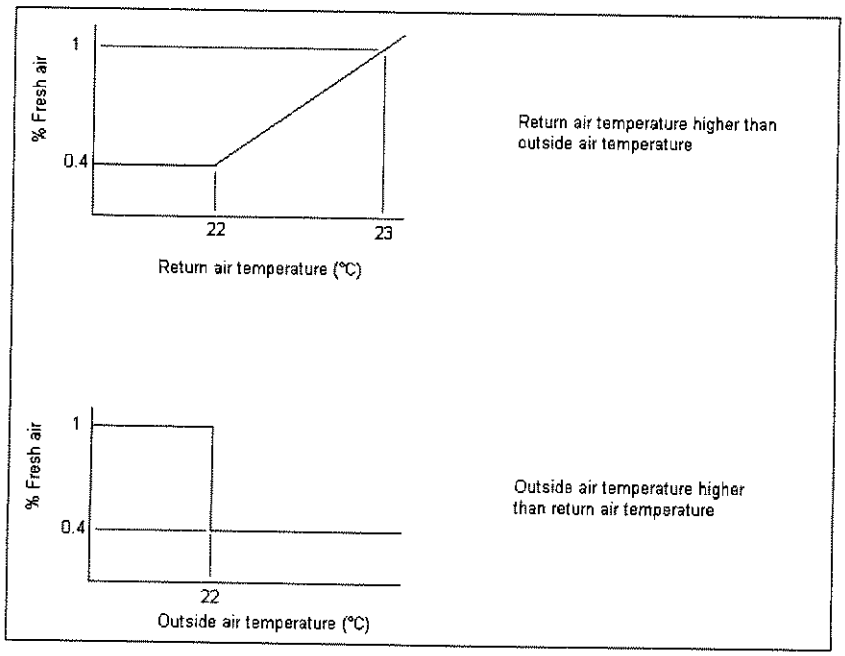

Figure 4.6: Occupied economiser control strategy

Unoccupied strategy:

If the return air temperature is higher than the outdoor air temperature the following strategy must be followed:

- If the return air temperature exceeds 22°C the fresh air damper will open proportionally from its closed position (0% fresh air of total supply) until fully open at 23°C.

- The return air damper will for the same conditions start to close proportionally from its fully open position (100% return air) to fully closed.

- If no cooling is required the fresh air damper will be closed and the return air damper fully open.

- If the outdoor air temperature exceeds the return air temperature the fresh air damper will close completely and the return air damper will be fully open. The strategy is graphically presented in Figure 4.7.

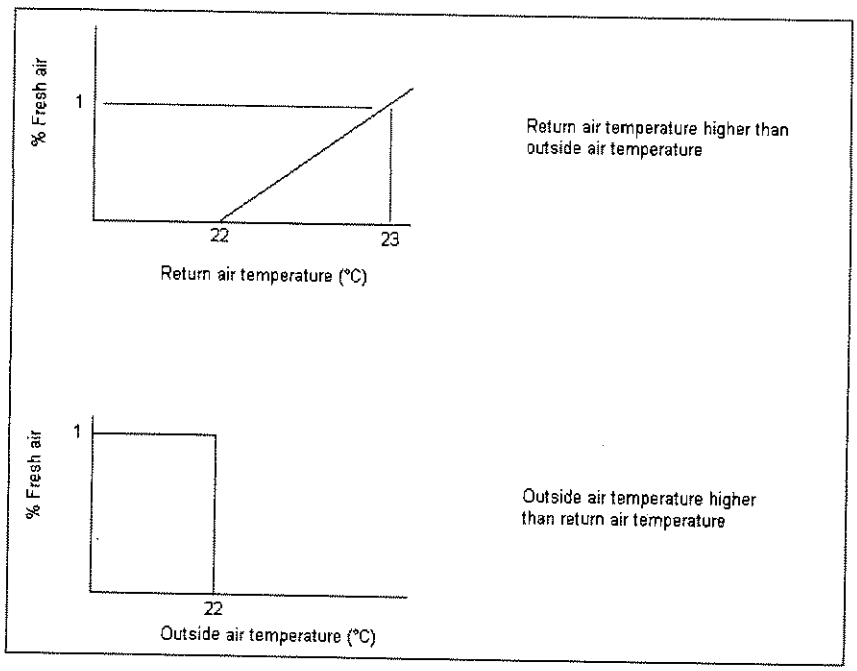

Figure 4.7: Unoccupied economiser control strategy

4.5.4 New setpoints

The setpoints of the zones were fairly low, as was seen from the temperature measurements. For this control strategy the cooling and heating setpoints were raised, but kept within the comfort band. See Figure 4.8 for this control strategy. This strategy will result in peak reduction and energy savings due to a reduction in the cooling load.

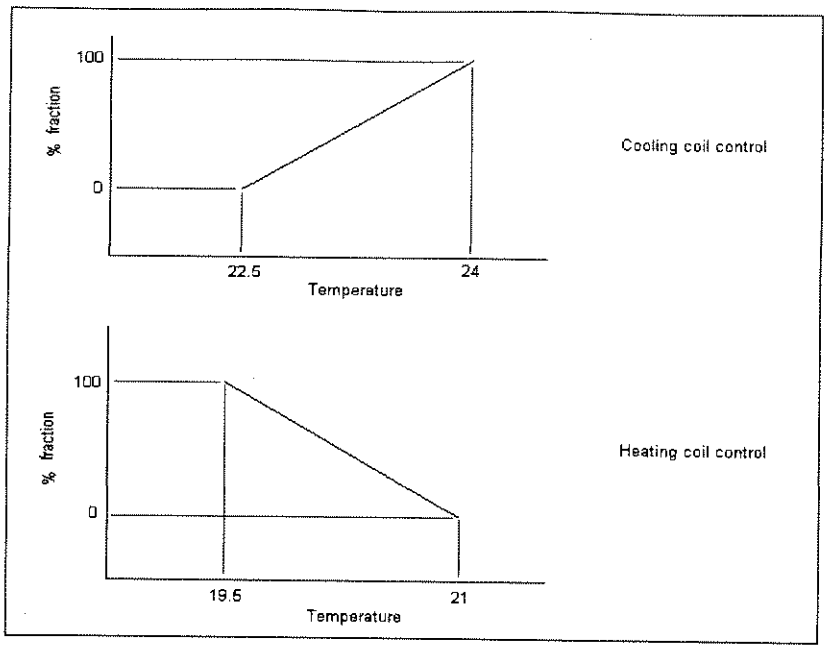

Figure 4.8: New zone setpoints

If the indoor temperature exceeds 22.5°C the cooling valve will open proportionally from its closed position until fully open at 24°C. If the indoor temperature drops below 21°C the heating valve will open proportionally from its closed position until fully open at 19.5°C.

4.5.5 Setpoint setback

This option allows setpoint drift if the venues are unoccupied. This control strategy also requires the installation of motion sensors in the venues. It operates on the assumption that a venue does not need to be kept on setpoint if it is not in use. If a venue is unoccupied, the control will let both the cooling and heating coil setpoints to drift to hotter and colder temperatures respectively. The zones will then require less cooling and heating from the HVAC system.

The unoccupied duration will be determined in the same fashion as discussed in section 4.3 - Economiser control. New temperature sensors will need to be located inside the venues for this option. For the unoccupied conditions the cooling coil will be fully open at 26 °C and fully closed at 24.5 °C. The heating coil will be fully open at 16.5 °C and fully closed at 18 °C. The strategy can be viewed in Figure 4.9.

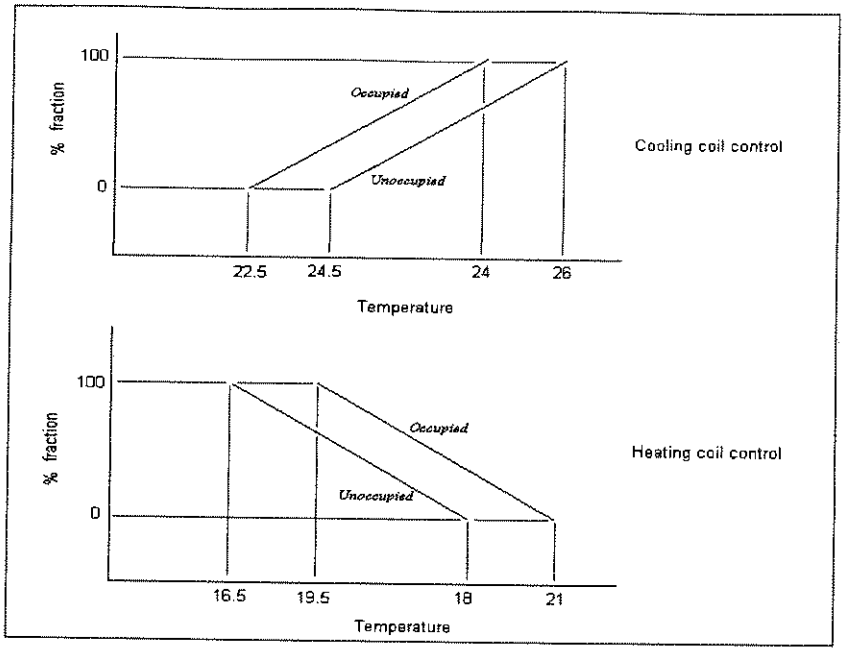

Figure 4.9: Setpoint setback control strategy

4.5.6 Fan control

This retrofit works on the assumption that the supply fan of a venue need not operate if the cooling and heating coil valves are closed during unoccupied times. See Figure 4.10 for the control strategy of fan control.

This control strategy can therefore only be used during unoccupied venue times. This control has a strategy for both cooling and heating sides. For the cooling side, the fan is switched on when the cooling valve opens at 24.5 °C. The fan will then stay on until the temperature drops 1 °C below the opening temperature before it switches off. For the heating side the fan will switch on at 18 °C. It will then switch off 1 °C above the valve opening temperature.

The supply fans must run at all times if the venue is occupied. The return fans will operate in tandem with their correlating supply fans.

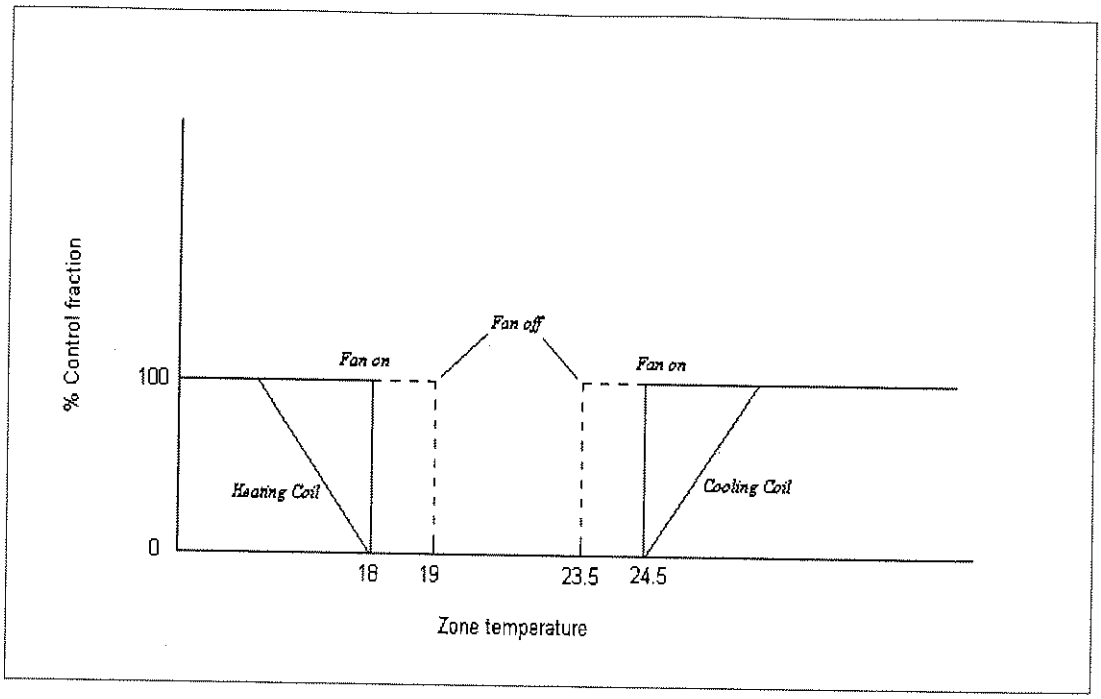

Figure 4.10: Fan control strategy

4.5.7 Heating plant control

The current heating plant control strives to keep the boiler water on 75 °C throughout the year. The pump also runs right through the year. This wastes energy, as no heating is required during the hot summer months of the year.

Propose boiler control strategy:

The boiler setpoint will be a second order function of the average outdoor air temperature of the previous 24 hours. The outdoor air temperature will therefore be monitored and locked at half hour intervals. A new average outdoor air temperature will be calculated for each new half hour by taking the previous 48 locked temperature points. A new setpoint will then be calculated for each half-hour of the day by the following function:

$$setp = 0.162t^2 - 8.857t + 139.18$$

where setp is the boiler in °C and t is the average outdoor air temperature in °C. This function was obtained by calculating the maximum needed boiler supply water temperature of a typical day for each month of the year. These temperatures were then plotted over the

average ambient air temperature of the respective days. A curve was thereafter fitted through the points to calculate the equation of the function. A safety factor was included to make provision for extreme days.

Propose hot water pump control strategy:

The pump will only start to run when one of the heating coils requires hot water, in other words, when one of the heating coils control valves open. If no heat is required the pump will shut down. To keep the pump from cycling, a time delay of 30 minutes can be incorporated before pump shut down can happen.

4.6 SIMULATION RESULTS

4.6.1 Introduction

The options discussed in the previous section and various combinations thereof were simulated to obtain the potential for energy and peak demand savings. In this section the new control strategy simulation results are compared to a base year simulation.

This base year simulation was done with the present building, system and control configuration. According to our power and temperature measurements the fans were operational 24 hours per day, 7 days per week. This assumption was incorporated into the base year simulation. Average yearly occupancy and average monthly climate data were used during the execution of the simulations. The average monthly climate data is based on the past 20 years.

4.6.2 Base year

Figure 4.11 and Figure 4.12 show the measured and simulated energy consumption (MWh) and the peak demand (kVA) of the HVAC system of a typical year.

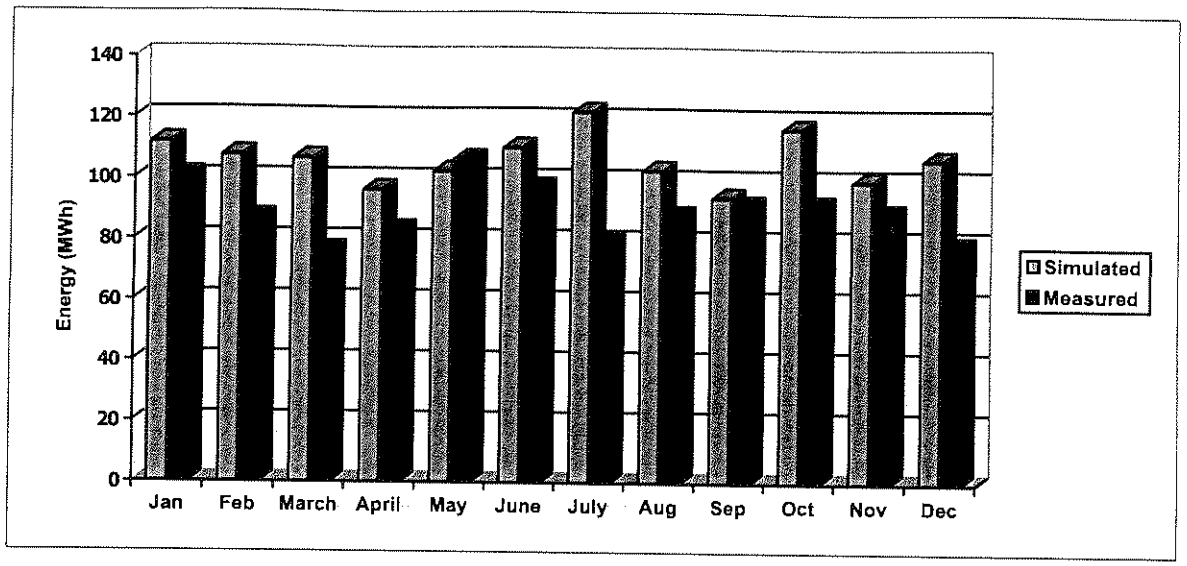

Figure 4.11: HVAC system energy consumption

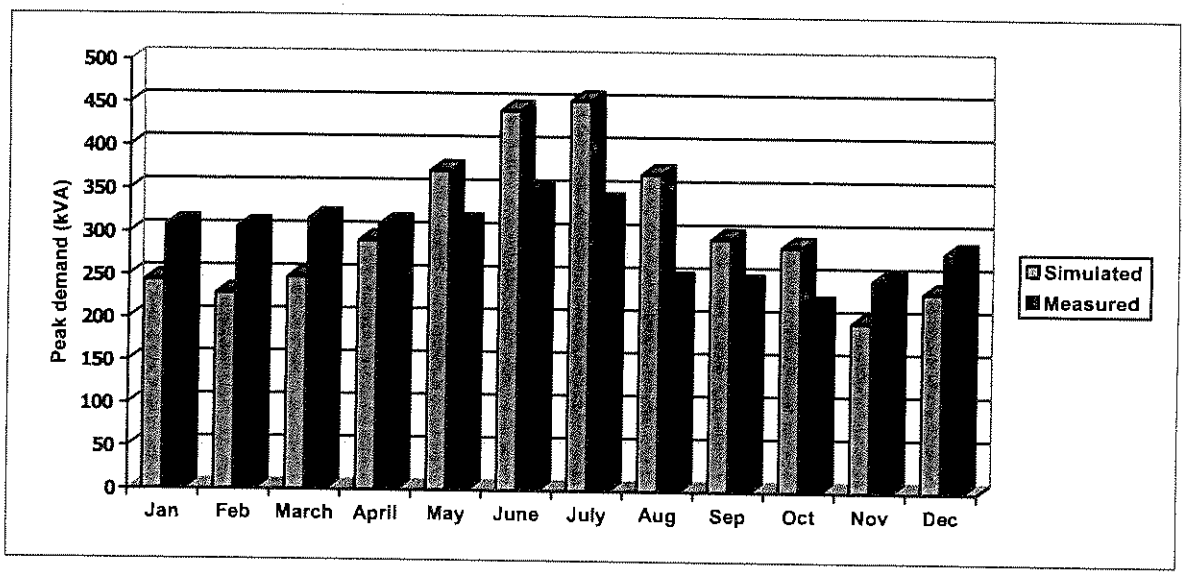

Figure 4.12: HVAC system peak demand

The yearly energy consumption of the simulation differs only by 15% from the measured data. The difference between the predicted and measured peak demand is somewhat bigger and differs by 24% on average. This could be due to the fact that it only takes one extreme half hour per month to produce a high peak demand. The monthly simulations were base on average occupancy and average climate data.

4.6.3 Summary

This section summarises the results. Figure 4.13 displays the energy consumption of all the retrofit options. Figure 4.14 shows the average monthly peak demand of all the options. Detailed results can be seen in Appendix B. Options 2 to 7 include Fan Scheduling.

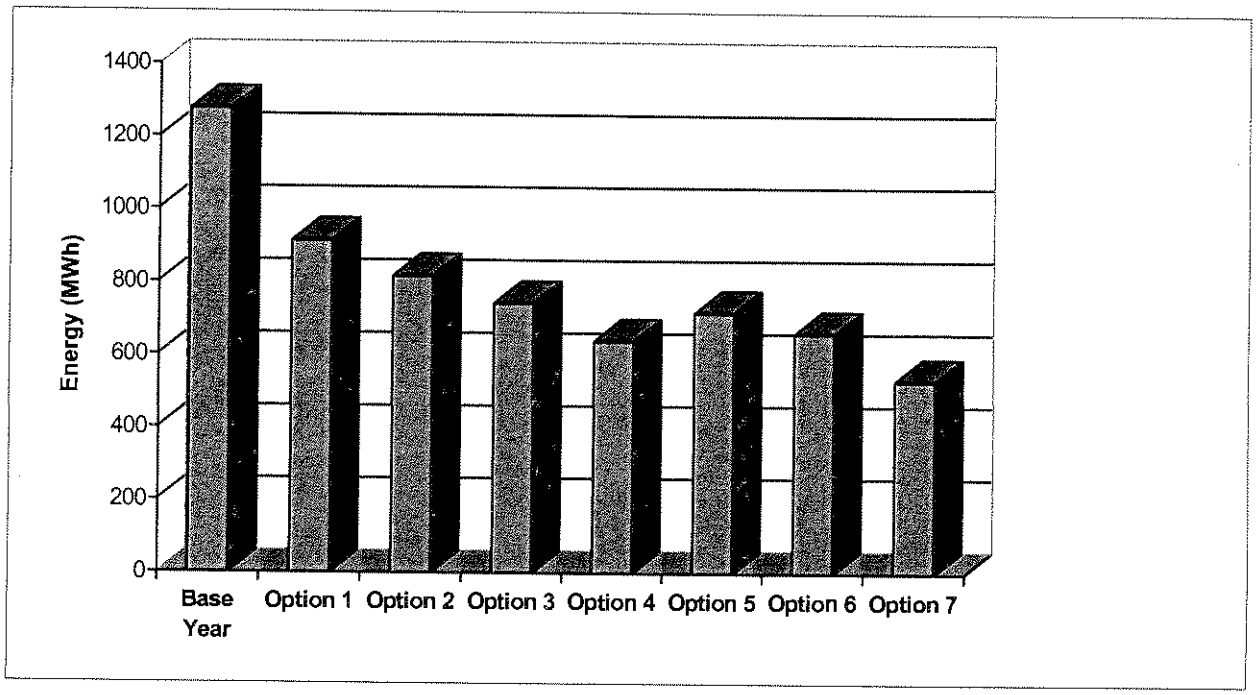

Figure 4.13: System retrofit total energy simulation comparison

Option 1 - Fan Scheduling

Option 2 - Economiser control and new setpoints

Option 3 - Economiser control and setpoint setback

Option 4 - Economiser control, setpoint setback and fan control

Option 5 - Economiser control, new setpoints and heating plant control

Option 6 - Economiser control, setpoint setback and heating plant control

Option 7 - Economiser control, setpoint setback, fan and heating plant control

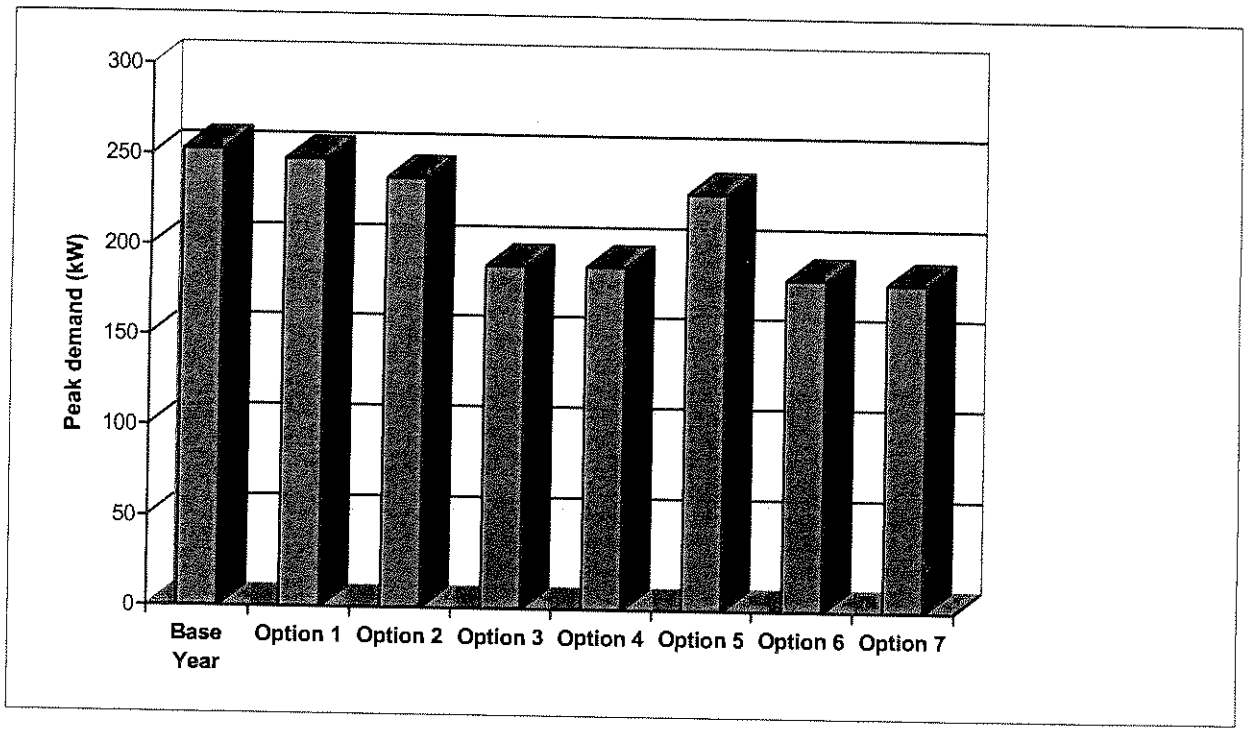

Figure 4.14: System retrofit total power consumption comparison`

Table 4.4 displays the percentage savings on the building and system energy with the relevant direct payback periods for implementation. The building did have a building management system already in place, thus setpoint and scheduling changes can be implemented at no extra cost. The only costly changes were the implementation of temperature sensors and motion detectors. The payback period of the first option is zero since no additional costs were necessary to change the scheduling of the fans.

Options	% Saving on HVAC energy	% Saving on building energy	Payback period (months)
Option 1	28.4	17.4	0
Option 2	36.0	21.6	0.5
Option 3	41.8	25.1	5.6
Option 4	49.9	30.0	5.7
Option 5	43.8	26.9	1.1
Option 6	48.2	29.0	5.4
Option 7	58.3	31.0.	5.3

Table 4.4: Economic analysis

4.7 CLOSURE

A verification study was conducted to ensure realistic and accurate retrofit energy savings and indoor comfort. The predicted indoor air temperatures of all the venues were within 2° C of the actual measurements for 100% of the time. The predicted energy consumption of all the components were within 13% of the measurements for a 24-hour verification day.

The verification study showed satisfactory results for the use of the simulation model with confidence during the new control strategy simulations. The combinations of the new proposed control strategies resulted in building energy savings of up to 32% and 58% on the HVAC system energy consumption per year. These strategies can be implemented into the building with payback periods of less than 6 months.

This study was performed with the simplified building input philosophy introduced in chapter 1 and the results were satisfactory. With this method it was possible to construct the building model on site with only dimensions shown on plan view drawings. All the other information was entered into the model during visits to each of the building zones. The entire building model was entered in one day on site.

It took some time to configure the HVAC system model since the one operating point philosophy was not yet introduced before the completion of the study. The simulation model was further very sensitive for the control parameters and it took some time by experienced users to perform stable efficient simulations.

It takes an experience user 6 weeks to perform an energy study on a typical building with the existing simulation tools available in the world today. The author beliefs by using the approach discussed in chapter 1, such an investigations can be conducted in less than 2 weeks. However this will have to be verified in the future.

4.8 REFERENCES

[1] J.E. Woods, Cost avoidance and productivity in owning and operating buildings, Occupational Medicine, State of the art reviews, vol. 4, no. 4, January 1989.

[2] E. Sterling, C. Collett, S. Turner and C. Downing, Commissioning to avoid indoor air quality problems, Proc. ASHRAE Transactions: Symposia, pg. 867, January 1994.

[3] E.H. Mathews, C.B. Piani, Establishing the energy savings potential in South African office buildings, Refrigeration and Air-conditioning, Vol.12, No. 4, pp. 59-65, July 1996.

[4] R. Bevington, and A.H. Rosenfield, Energy for buildings and homes, Scientific American, pp. 207-215, September 1990.

[5] TEMM International (Pty) Ltd., Energy savings potential and guidelines for effective energy use in buildings. Project report compiled for the Department of Mineral and Energy Affairs: Energy branch, Pretoria, 0002, March 1997.

[6] P.G. Rousseau, E.H. Mathews, Needs and trends in integrated building and HVAC thermal design tools, Building and Environment, Vol. 28, No. 4, pp. 439-452, 1993.

[7] J.J. Hirsch, F.C. Winkelmann, W.F. Buhl, K.L. Ellington, POWERDOE, a windows-based visually oriented analysis tool. In J.W. Mitchell and W.A. Beckman, editors, Building Simulation '95 Fourth International Conference Proceedings, Madison, Wisconsin, USA, August 1995, IBPSA.

[8] L. Lebrun, Simulation of HVAC system, Renewable Energy, Vol. 5, No. 5, pp. 1151-1158, August 1994.

[9] E. van Heerden, E.H. Mathews, A new simulation model for passive and low energy, In Proceedings of the 1996 PLEA Building and Urban Renewal conference, Louvain-la-Neuve, Belgium, 1996.

CHAPTER 5

CLOSURE

In this chapter a brief summary of the most important results and recommendations for future work are given.

5.1 SUMMARY OF THIS STUDY

User requirements for the efficient use of system simulation by the energy service contractor were identified in this part of the study. The most important requirement identified was fast efficient building and system configuration to decrease simulation input time. Another very important requirement is the simulation of the building, HVAC system and controls in an integrated fashion. Integrated simulation is of no use to the energy service contractor if the solutions are unstable.

To satisfy these requirements methods and procedures were proposed by the author. The integrated simulation tool QUICKcontrol was extended with some of these philosophies and evaluated in integrated applications.

New explicit building and system component models were derived to extend the existing tool with models of equipment commonly used in the building sector. Explicit models will always produce answers since they are exact. They will further decrease simulation time due to the absence of numerical iterations. This philosophy will therefore have a positive influence on the stability of the solutions of any integrated simulation tool.

The accuracy and applicability of integrated building and natural ventilation modelling was illustrated in animal housing facilities. The predicted results obtained during this study were satisfactory to use these models with confidence in this type of building applications.

The applicability of building, HVAC system and control simulations was illustrated in conference facilities. The results obtained show the value of integrated building and system simulation in the evaluation of energy cost saving inventions in commercial buildings. Integrated simulation should be part of the daily standard procedures of the energy service contractor in practice.

5.2 RECOMMENDATIONS FOR FUTURE WORK

During this part of the study a number of problems were encountered. These will be discussed here as a basis for future work. During the duration of the case study conducted in chapter 4 the following two major problems were encountered. Firstly, finding the performance curves of the system component models and secondly, obtaining stable solutions with QUICKcontrol during the investigation.

The one operating point curve fit philosophy proposed in chapter 1 was not utilised during the investigation performed in chapter 4. This implied that a number of system operating points for all the components were needed to obtain the simulation models. Most of the equipment's manufacture performance data was not available since the system was old. It was very difficult and time consuming to obtain performance data at a number of operating points for all the component models. A large percentage of the study's time was therefore utilised for system model input.

Expert QUICKcontrol users found it very difficult and time consuming to obtain stable simulation solutions during the investigation. The program was very sensitive to control parameters and certain system configurations. It was therefore necessary to increase the control ranges and simplify the configuration of the system until stable simulations were obtained.

Based on the previous discussion the following is suggested for future work:

- The one point operating curve fit philosophy introduced in this study must be developed for all commonly used HVAC equipment and implemented into the simulation program. This will reduce the time of system input considerably and make the tool more user-friendly.

- There are still many component models, which are implicit and do not always produce answers. All these models must be replaced by explicit equations to improve the stability of the simulation tool and reduce simulation time.

- The presently used mass flow calculation procedure of QUICKcontrol does not always find a solution for any given network with more than one closed-loop. The flow network must sometimes be simplified to produce an answer. A new algorithm must therefore be developed and implemented to calculate the mass flow rates in any given complex network.

- A new stable simulation procedure must be developed to solve the conditions of any complex system with a large number of closed-loops.

5.3 CONCLUSIONS

Any new integrated system simulation tool must be developed taking the following requirements into account. They are given here in the order from most important to least important for the development of an efficient simulation tool:

- Model set-up must be fast and easy.
- Solutions must be stable for any given model
- Answers must be accurate for realistic predictions
- Simulation time must be fast.

The heart of any integrated component-based simulation program is the simulation engine. This consists of the mass flow simulation procedure and the algorithm responsible for solving the system conditions in an integrated fashion.

The biggest shortage in QUICKcontrol is the presence of a robust simulation engine to produce stable solutions. The tool is at present only useful to experienced users and even for them it takes some effort to produce stable solutions. This implies the development and implementation of a complete new simulation platform to perform efficient integrated simulations.

CHAPTER 6

INTRODUCTION

The mining and industrial sectors in South Africa consume about 40% of ESKOM's total electrical energy production. Mines alone uses nearly 20% of the electricity provided by ESKOM. Ventilation and cooling (VC) are responsible for approximately 25% or R750 million of this energy. It will therefore be beneficial if the mines can be more energy clever to reduce their VC operating costs. The use of an extended integrated building and system simulation tool was therefore realised to investigate the potential for energy cost savings in mine VC applications. The integrated building and system simulation tool QUICKcontrol was extended and utilised during two case studies to illustrate its applicability in mine applications.

6.1 THE NEED FOR AN INTEGRATED TOOL

Mining is one of South Africa's biggest industries, along with manufacturing, trade and agriculture[1]. It forms almost 20% of the gross domestic product of South Africa, with sales of R76.5 billion for 1999[2]. Of this, gold sales were 33% of the total sales, or R24.99 billion for 1999. Platinum sales were 19.5% of the total sales, or R14.92 billion for 1999.

These prices vary with time and influence the profit margin of the mines. With the varying economy and mineral prices, the need for retrieving the maximum amount of ore in the most energy efficient way has become very important. One of the techniques employed to achieve this goal is deep level mining with typical depths of between 3 - 5 kilometres.

For platinum mining below 1400 m will alter operations radically with the need for a lot more refrigeration and changes to the support systems[3]. For a gold mine, this crucial level is typically 3000 m below the surface. At these depths the virgin rock temperature rises above the acceptable human endurance levels and special ventilation and cooling is needed[4].

This presents a difficult and potentially dangerous situation concerning the comfort and health of the workers. Satisfactory ventilation is needed, as well as a means to investigate the impact of machines, in the ventilation cycle, breaking or performing at lower efficiency[5].

Most mines use relatively standard ventilation and cooling layouts (Figure 6.1). A conventional way of cooling the intake air is by placing the heat exchangers at the mine intake or down shaft. This is satisfactory for mines that are not too deep. When the mine gets deep, the air speed needed to convey the cold air to the stopes becomes too fast and uncomfortable. The airspeed is also dangerous at this point as it can propagate fires or dangerous gas.

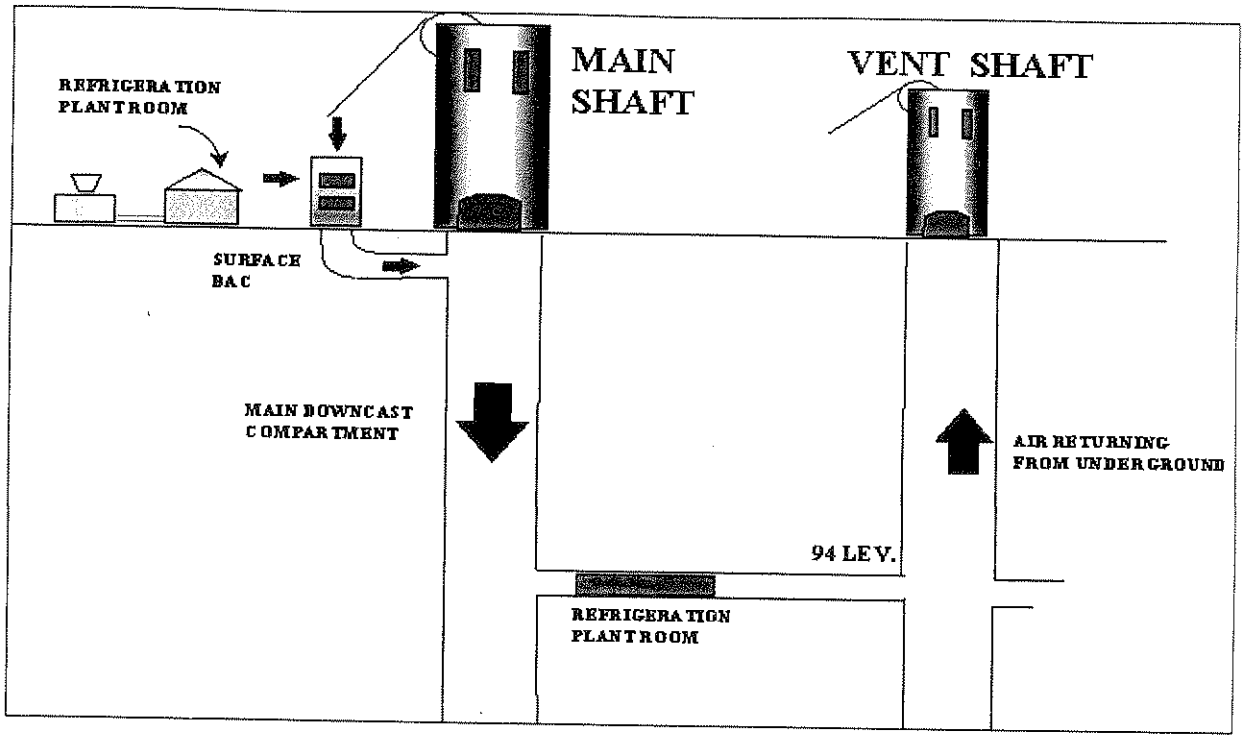

Figure 6.1: Typical layout of mine's ventilation and cooling system

For most mines these layouts consist of a surface cooling plant and an underground plant. This underground plant is typically between 1000 m and 2000 m below the surface. The surface plant contains the chillers or icemakers, water storage dams and cooling towers. The underground plant consists of a thermal storage dam and cooling coils or spray-chambers.

If extra cooling is needed a further cooling plant or mobile plant can be installed below the surface. The warm intake air, heated by internal loads and the virgin rock, passes through the cooling coils or the chambers. Extraction fans, placed in the return airways, then suck the warm air out. Producing satisfactory cooling and ventilation for deep mines is a precise and necessary task.

Large and expensive equipment is needed for satisfactory ventilation and cooling. Along with the capital cost, the energy usage of this equipment is very high. The mining and industrial sector consumes about 40% of ESKOM's (South Africa's electricity utility) total energy production. Mines alone use nearly 20% of the electricity provided by ESKOM[6]. This amounts to approximately R3 000 million of electricity per annum just for the gold mines.

Ventilation and cooling (VC) uses approximately 25% or R750 million of this energy. The gold mines had recently financial problems and some were threatening to close down (ERPM did close down in 1999). Every time the gold price drops, ESKOM can lose some of their biggest clients.

It will therefore be beneficial if the mines can be more energy clever to reduce their operating cost. Secondly, it will provide ESKOM with more DSM (Demand Side Management) opportunities, e.g. spot pricing, load shedding, etc. A further benefit would be that with more efficient mining systems, the use of virtual power stations could be implemented[7].

ESKOM is moving towards a price structure for electricity that reflects the real cost of generation, namely real time pricing (RTP). ESKOM developed various cost structures to coax customers to manage their electricity demand (DSM) to use more energy in off-peak periods (low cost of generation) and less energy in peak periods (high generation costs). However, many industries do not effectively use these price offerings from ESKOM.

The best, if not the only way, to effectively use the ESKOM price structures without affecting operation is the better control of the VC system for optimal use or for load shifting. However, this is difficult to predict, as a comprehensive, fully integrated, component-based, dynamic simulation is needed to ensure that the safety of the miners is not compromised by any new DSM control strategy.

A comprehensive international survey showed that no integrated dynamic mine VC simulation software is available in the world today. The only thermal mine simulation software found was ENVIRON[8], developed by CSIR in South Africa for the design of VC systems of deep mines. However this software is static and does not solve the mine in an integrated fashion over the duration of time.

The potential to extend QUICKcontrol for the use in applications other than building applications was realised since it is dynamic, fully component-based and solves all the components in an integrated fashion. The only big difference in thermal systems is the equipment and processes on the demand side. The heating and cooling equipment used in the different types of industries are more or less the same.

The major difference between buildings and mines is the modelling of stopes (haulages and shafts) rather than building zones on the demand side. This also applies to other industrial thermal applications where the demand side is normally thermal processes. Since QUICKcontrol is component-based it will be possible to develop and integrate new demand side models for any thermal industrial simulation application.

The requirements for a general integrated thermal simulation tool will be the same as discussed in chapter 1. The proposed tool in chapter 1 can be extended with thermal models found in the mining and industrial sectors to investigate the potential for energy cost savings. Two case studies were performed and discussed in this part of the study to illustrate the applicability of system simulation in these sectors.

6.2 CONTRIBUTIONS OF THIS STUDY

The following contributions were made in this study:

- The use of an extended integrated building and system simulation program in other thermal applications was realised.

- The derivation of new explicit component models not available in QUICKcontrol and commonly used in mining and industrial applications.

- The development of a new mass flow simulation procedure to calculate flows in any complex open and closed-loop networks.

- The practical applicability of a mine system simulation is illustrated in a cooling plant case study.

- The practical applicability of a mine system simulation is illustrated in a pumping system case study.

6.3 OUTLINE OF THIS STUDY

The needs and trends of an efficient integrated thermal simulation tool for industrial and mining applications are discussed in chapter 6. Extensions to QUICKcontrol are identified to satisfy the requirements of industrial or mine thermal system applications.

There are many shortages in system component models in QUICKcontrol of equipment commonly used in mining and industrial applications. New explicit models for variable thermal storage, pipes, wet surface heat exchangers are therefore derived in chapter 7. A new mass flow simulation procedure was developed to simulate flow in any open or closed-loop network.

The applicability of dynamic system simulation is illustrated in chapter 8. A case study was conducted on a mine cooling plant to investigate the use of simulation in these applications. A second applicability of dynamic system simulation is illustrated in chapter 9. A case study was conducted on a mine pumping system to obtain the potential for load shifting in the deep mines of South Africa.

Chapter 10 briefly summarises this part of the study and proposes recommendations for future work.

6.4 REFERENCES

[1] I, Goldberg, South Africa's Mineral Industry, pp. 1-12, 1992.

[2] Mining: production and sales, Statistical release P2041, Statistics South Africa, http://www.statssa.gov.za/Statistical_releases/, Contact numbers: +27 12 310 8095/8390/8351, Postal address: Private Bag X44, Pretoria, 0001, South Africa, 6 June 2000.

[3] B, Ryan, Impala Platinum: Jewel of the Bush, Financial Mail: Corporate report, 21-22, September 1999.

[4] RDC Shone and TJ Sheer, An overview of research into the use of ice for cooling

deep mines, Fourth International Mine Ventilation Congress, July 1988.

[5] RP Viljoen, Deep-Level Mining - A Geological Perspective, Technical Challenges in Deep-Level Mining, pp. 411-427, 1990.

[6] DME, Energy balances, http://www.dme.gov.za/energy/, Energy balance for 1997, Private Bag X59, PRETORIA, 0001, South Africa.

[7] IA Lane and J Delport, Load Audits and Simulations to develop DSM Potential in the Mining Sector, 1996.

[8] ENVIRON 2.5, Mining Technology (MiningTek), CSIR, PO Box 91230, Auckland Park, Johannesburg, 2006, South Africa.

CHAPTER 7

NEW THERMAL MODELS

To extend QUICKcontrol for the simulation of other large thermal systems found in mining and industrial applications, new component models and simulations procedures were developed. These new models include variable thermal storage, water pipes and wet surface heat exchangers. A new flow simulation procedure to calculate flow in any open or closed-loop network was also developed.

NOMENCLATURE

A	Area (m^2)
cp	Specific heat capacity (J/kg.K)
d	Depth under ground (m)
Gt	Direct solar radiation (W/m^2)
h	Enthalpy (J/kg)
hc	Convection coefficient ($W/m^2.K$)
ho	Outside heat transfer coefficient ($W/m^2.K$)
k	Conductivity (W/m.K)
L	Length (m)
m	Mass flow rate (kg/s)
P	Perimeter (m)
r	Radius (m)
t	Time (s)
T	Temperature (°C)
U	Overall heat transfer coefficient ($W/m^2.K$)
Vol	Volume (m^3)
α	Solar absorptance
ΔR	Surface radiation to atmosphere (W/m^2)
ε	Hemispherical emittance
ρ	Density (kg/m^3)

Subscripts

a	Air
d	Dam
i	Inlet
o	Outlet/Outside
p	Pipe
s	Solar air
w	Water

7.1 INTRODUCTION

To extend QUICKcontrol for the simulation of other large thermal systems found in mining and industrial applications, new component models and simulations procedures need to be developed. The same philosophy and requirements discussed in chapter two for system component models are utilised in this section.

New system component models commonly used in the mining and other industrial applications, variable thermal storage, water pipes and wet surface heat exchangers are derived in this section. A new flow simulation procedure to calculate flow in any open or closed-loop network is also developed and discussed in this section.

7.2 VARIABLE THERMAL STORAGE

7.2.1 Description

Variable thermal storage in the form of dams is not commonly found in Building HVAC applications. However this method of storage is often used in industrial and mining applications where the demand for thermal energy in the form of water varies considerably throughout the day. The load on heating and cooling plants can be kept constant at full capacity while the dams absorb the demand load fluctuations.

Dams can therefore reduce the size of heating and cooling equipment and energy cost when time of use energy tariffs are in place. Dams are also used as pressure breaks in mining applications when systems pressures become to high. Since dams are part of open loop systems it can be utilised in gravity fed systems where a constant pressure is required.

It is therefore important to include a variable thermal storage or dam model into the thermal system simulation program due to its wide range of industrial and mining applications. An explicit dam model is derived in the next section.

7.2.2 Mathematical model

It can be assumed that the thermal storage in dams reacts like an electrical capacitor[1]. It is assumed that 100% mixing occurs and that no stratification takes place. This is a good assumption since in these applications the dam inlet water temperature is approximately at the same water temperature of the water already inside the dam. Dams are not used like stratified storage tanks where hot and cold water are stored in the same volume and blending must be minimised.

A schematic drawing of a dam as a variable control volume can be viewed in Figure 7.1.

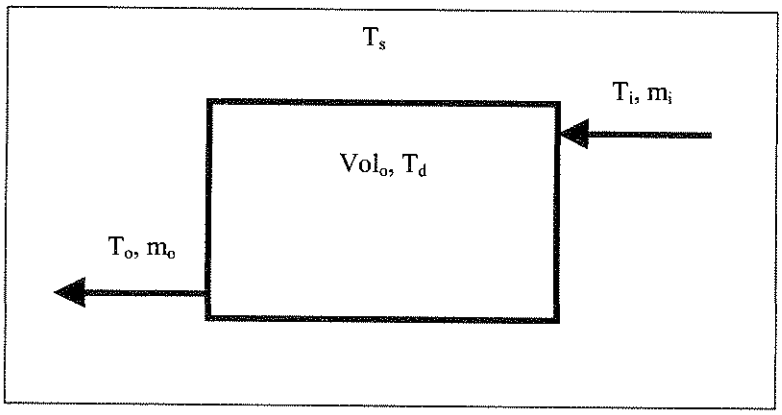

Figure 7.1: Schematic drawing of a thermal storage dam

The temperature within the tank is a function of initial temperature, initial volume, solar air temperature, which includes solar radiation on the horizontal dam surfaces, and the convection coefficient on all the surfaces. Taking convection, emittance and absorptance into account, an energy balance on the volume of the dam gives:

$$C\frac{dT}{dt} = m_i c_p (T_i - T_d) + UA(T_s - T_d) \tag{7.1}$$

where T_d is the water temperature in the dam, $C = \rho_d c_{pd} Vol_d$ and T_s is the solar air temperature given by[2]:

$$T_s = T_a + \alpha\frac{G_t}{h_0} - \frac{\varepsilon\Delta R}{h_0} \tag{7.2}$$

This formula incorporates the atmospheric, dry bulb temperature (T_a) and the effects of solar absorption ($\alpha G/h_0$) and emittance ($\epsilon \Delta R/h_0$). Multiplying the terms of Eq. (7.1) and separating the variables give the following results:

$$C\frac{dT}{dt} = -T_d a + b$$

$$a = m_i c_p + UA$$

$$b = m_i c_p T_i + UAT_s$$

$$C = C^o + (m_i - m_o)c_p \Delta t$$

$$C^o = Vol^o c_p \rho_w$$

Separating the terms and rearranging the results gives:

$$\int_{T_d^o}^{T_d} \frac{1}{T_d a - b} dT = \int_0^1 \frac{-1}{C} dt$$

Using exponential rules after integration, the equation becomes:

$$\frac{1}{a}\ln\left(\frac{T_d a - b}{T_d^o a - b}\right) = \frac{-\Delta t}{C}$$

$$T_d = \frac{1}{a}\left((T_d^o a - b)e^{\frac{-a\Delta t}{C}} + b\right) \qquad (7.3)$$

The conditions for Eq. (7.3) is, if $C > c_p \rho Vol_{dam}$ (dam overflowing) then $C = c_p \rho Vol_{dam}$, and if $C < 0$ (dam empty), then $C = 0$ and $m_o = 0$.

Due to variation in flow rates of the inlet and outlet water of a dam, the water volume or level of the dam will change over time. This change in level is also calculated at each time step. For the simulation model, the change in level is dependent on the flows in and out during the time interval Δt. A mass balance no the volume of the dam gives:

$$Vol = Vol^{t-\Delta t} + \frac{(m_i - m_o)\Delta t}{\rho_w} \qquad (7.4)$$

The conditions for Eq. (7.4) are if $Vol^{t-\Delta t} = 0$ then $m_o = 0$ and if $Vol > Vol_{max}$ then $Vol = Vol_{max}$. Again the volume of water in the dam cannot exceed the maximum dam capacity and no water can leave the dam if it is empty. This model is validated with actual measurements and the applicablity thereof illustrated in the following two chapters.

7.3 WATER PIPES

7.3.1 Description

Water pipes or conduits are used in large thermal systems to transport thermal energy for heating and cooling purposes. In building HVAC applications the modelling of thermal losses and time lags in water distribution networks are less important since these networks are relatively small and well insulated. Most of these building systems can therefore be simulated without thermal pipe models with relatively good accuracy.

However for large chilled and hot water distribution systems in industrial, mining and district heating and cooling applications, thermal loss and time lags are important and must be modelled in energy simulations. It is important to include losses to ambient air and the ground when in ground contact.

The effect of burial depth, fluid temperatures and insulation thickness can be investigated during life cycle analyses[3] with an accurate efficient pipe model. An explicit dynamic model is derived in the next section to satisfy the requirements mentioned here.

7.3.2 Mathematical model

The single stream heat transfer equation[1] can be used for each pipe segment with the same outside condition, ambient air or ground. The equation is:

$$\frac{(T_{wi} - T_{wo})}{(T_{wi} - T_e)} = \varepsilon \tag{7.5}$$

where $$\varepsilon = 1 - \exp(\frac{-U_p P_p L_p}{m_w cp_w})$$

and T_e is the effective outside wall surface temperature of either air or soil if the pipe is in ground contact. To take flow time into account each pipe segment can be broken into further smaller segments *(j)* and the pipe temperatures can be calculated over time with the following algorithm:

$$\delta t = \frac{A_w L_{wj} \rho_w}{m_w}$$

δt is therefore the time it takes the water to flow through one of the segments (*j*).

for j = 1 to n do (n = number of smaller segments)

$$T_{wjss} = T_e + (T_{wj-1}^{t-\delta t} - T_e)\exp\left(\frac{-U_{pj} P_{pj} L_{pj}}{m_w c_{pw}}\right)$$

$$\tau = \frac{C_{wallj}}{mc_p + U_{pj} P_{pj} L_{pj}}$$

$$T_{wj} = T_{wjss} + (T_{wj}^{t-\delta t} - T_{wjss})\exp\left(\frac{-\delta t}{\tau}\right)$$

(7.6)

In this algorithm a time constant approached is used to calculate the dynamic effects from the steady state single steam heat exchanger equation. When the pipe segment is in air contact[1]:

$$T_e = T_{ambient}$$

$$\frac{1}{U_p P_p} = \frac{1}{hc_o P_{po}} + \frac{\ln(r_o / r_i)}{2\pi k_p}$$

(7.7)

The inside convection coefficient will be very large compared to the natural outside convection coefficient and can be left out when calculating the total heat transfer coefficient. The k_p value will be the property value of the insulation material if the pipe is insulated. If not insulated k_p will be the property value of the pipe wall material.

For a single pipe buried under ground the soil resistance[3] can be calculated with:

$$R_s = \frac{\ln\{(d/r_o)+[(d/r_o)^2-1]^{1/2}\}}{2\pi k_s} \; for, d/r_o > 1$$

$$R_s = \frac{\ln(2d/r_o)}{2\pi k_s} \; for, d/r_o > 4 \qquad (7.8)$$

The effective temperature and the total resistance can now be calculated as follows:

$$T_e = T_{soil}$$

$$\frac{1}{U_p P_p} = \frac{\ln(r_o/r_i)}{2\pi k_p} + R_s \qquad (7.9)$$

The temperature T_{soil} is the soil temperature at a distance from the pipe where the heat transferred from the pipe does not have an influence on this temperature. The effective pipe and soil resistances for other buried pipe configurations, two pipes buried in common conduit with an air space, two buried pipes close to each other and pipes buried in trenches can be calculated by methods introduced in ASHRAE[3].

7.4 WET SURFACE HEAT EXCHANGERS

7.4.1 Description

When the heat exchanger surface in contact with moist air, is at a temperature below the dewpoint temperature of the air, condensation of vapour will occur. The dry bulb temperature and the humidity ratio both decrease as the air flows through the exchanger. Therefore, sensible and latent heat transfer occur simultaneously.

This described process happens in building chilled water cooling coils which is the most common process to cool air in these applications. Rousseau[4] introduced a method to calculate the outlet conditions for a coil from the inlet conditions which is currently used in the simulation software QUICKcontrol. This method makes use of the straight-line law[5] to solve for the outlet conditions.

The problem with this method is that six non-linear equations must be solved simultaneously to obtain the outlet conditions. This method is therefore not explicit and is an intensive calculation procedure. In building applications the number of cooling coils can be minimised to the number of zones, thus this method is satisfactory here.

In industrial and mining applications where the cooling systems are large and complex an explicit method would result in more efficient simulations. An explicit model for heat exchangers where heat and mass transfer occurs is derived in the next section.

7.4.2 Mathematical model

In mine cooling one of the most common methods to cool air is to make use of bulk air coolers or spray chambers. These heat exchangers are counter-flow or single pass cross flow configurations. For the counter flow type the explicit equation derived in section 2.3.2 combined with the heat and mass transfer analogy introduced by Lombard[6] in section 2.4.2, the following equation can be written:

$$\frac{h_{ai} - \phi T_{wo}}{h_{ao} - \phi T_{wi}} = \exp\left[-U_e A \left(\frac{\phi}{c_{pw} m_w} - \frac{1}{m_a} \right) \right] \tag{7.10}$$

and the heat balance equation as:

$$\begin{aligned} C_a (h_{ai} - h_{aa}) &= C_w (\phi T_{wo} - \phi T_{wi}) \\ C_a &= m_a \\ C_w &= \frac{c_{pw} m_w}{\phi} \end{aligned} \tag{7.11}$$

If this is substituted in Eq. (7.10) and the result is solved it is found that:

$$h_{ao} = \frac{(1-r)}{(\Gamma - r)} h_{ai} + \frac{(\Gamma - 1)}{(\Gamma - r)} \phi T_{wi}$$

$$T_{wo} = \left(\frac{(\Gamma - 1) r}{(\Gamma - r)} h_{ai} \right) / \phi + \frac{(1-r)\Gamma}{(\Gamma - r)} T_{wi}$$

$$r = \frac{C_a}{C_w}$$

$$\Gamma = \exp\left[-UA \left(\frac{1}{C_w} - \frac{1}{C_a} \right) \right]$$

(7.12)

With Eq. (7.12) the air leaving enthalpy h_{ao} and the water leaving temperature T_{wo} can be calculated explicitly from the inlet conditions. The air outlet temperature can now be calculated by obtaining the equation of the straight line (see section 2.4.2) through (T_{ai}, h_{ai}) and (T_{wi}, h_{si}), substituting h_{ao} into it and calculating T_{ao}. The enthalpy h_{si} is the saturated enthalpy at the temperature T_{wi}.

This analogy can now be used to obtain the outlet conditions of any heat and mass exchanger configuration by using the explicit method introduced in section 2.3.2. For example the equation for single pass cross-flow both streams unmixed heat and mass exchanger yields (see section 2.3.2):

$$\frac{h_{ao} - h_{ai}}{\phi T_{wi} - h_{hi}} = [-0.00187 r^5 - 0.320757 r^{1.1} + 1.070107][\exp(-0.880466\Gamma)]$$
$$- [0.03961 \ln(\Gamma) - 0.088206] + 0.088206$$

$$\Gamma = \frac{C_a}{UA}, 0.3 \le \Gamma \le 2$$

$$r = \frac{C_a}{C_w}, 0.3 \le r \le 2$$

(7.13)

By using Mueller charts[7] explicit equations for most direct and indirect wet air coolers commonly used in the industry today can be obtained. The method introduced here allows for fast efficient simulation of complex systems with a large number of wet surface air cooling heat exchangers. The same time constant approach used in the previous section can be used for the simulation of dynamic effects.

7.5 MASS FLOW SIMULATION

7.5.1 Description

It is quite a formidable task to set-up a complex theoretical flow network with the correct variable flow resistances and solve it to predict the correct flows in all the branches for each time step in a dynamic system simulation tool. Therefore many system simulation tools[8] utilise the approach where flow is specified in the branches by the system elements and not calculated for each time step.

In constant flow networks the mass flow rate can be specified for each element in the thermal network by that element. However for a dynamic system where flow changes over time due to control on certain elements like valves, pumps and fans, a different approach must be used. These elements must therefore be utilised to set up flow in the different network branches for all the other components.

The procedure previously utilised by QUICKcontrol did not allow for open loop systems and was limited to typical flow networks found in building systems. Thus there is a need for a mass flow simulation procedure, which can set-up flow for any complex open and closed-loop network in mining and industrial applications.

A mass flow simulation procedure, which sets-up flow in all the components by only specifying flow in certain flow control elements for each time step, is discussed in the following section.

7.5.2 Simulation procedure

The following components are used to set-up flow in the network: Pumps, valves, fans converges and diverges. These elements will be referred to as flow elements. Pumps, valves and fans are the only components that can specify mass flow and only one of them is needed per open and closed-loop. Converges and diverges are used to add up flows or to specify flow fractions.

To set-up a given configuration, a graphical interface is used. The various components (elements), including the flow elements that make up the system, can be dragged and dropped into position.

The components can now be connected to each other in the direction of the flow by pipe elements (Figure 7.2). Pipe elements connect the outlet conditions (temperature of water; enthalpy and humidity of air) and the flow of the previous element to the inlet of the following element. This implies that an element receives its inputs for each time step from the pipe element connected to its inlet port. The conditions and flow are therefore stored in the pipe elements.

The system conditions, flow and control values must be solved for each time step in the following sequence:

- Obtain all the control output signals according to the conditions of the previous time step and store it in the control pipe elements.
- Use the flow simulation procedure discussed later to set the flow of all the pipe elements for the time step.
- Now utilise an energy solver to solve all the elements to obtain the system conditions.

The flow in the network can be set for each time step in the following sequence:

Pumps (Set flow): Search for all the pumps set as flow elements in the system. Pumps can either be flow elements or just elements for energy calculation purposes. Now set the flows of the pumps to the respective control element flows. Now search forward and backwards from each pump until the search finds another flow element or a system break (example dam, source) and set the flow of all the pipe elements found to the flow specified by that pump.

Valves and fans: Follow the same procedure used by the pumps to specify the flows of the pipe elements.

Converge (Set fractions): Get the mass flow value from the pipe element connected to the outlet and calculate the inlet mass flows according to the specified control element fractions. Search backwards from the pipe elements connected to the inlet fractions of the converge until the search finds a flow element or a system break (dam, source, climate), and set the flow of all the pipe elements found to the respective flow fractions of the converge.

Diverge (Set fractions): Get the mass flow value from the pipe element connected to the inlet and calculate the outlet mass flows according to the specified control element fractions. Search forward from the pipe elements connected to the outlet fractions of the diverge until the search finds a flow element or a system break (dam, source, climate), and set the flow of all the pipe elements found to the respective flow fractions of the diverge.

Converge (add flow): Get the mass flow values from the 2 pipe elements connected to the inlets and add them up. Search forward from the pipe element connected to the outlet of the converge until the search finds a flow element or a system break (dam, source, climate) and set the flow of all the pipe elements found to the added flows of the converge.

Diverge (add flow): Get the mass flow values from the 2 pipe elements connected to the outlets and add them up. Search backwards from the pipe element connected to the inlet of the diverge until the search finds a flow element or a system break (dam, source, climate) and set the flow of all the pipes found to the added flows of the diverge.

The user must decide on the following depending on the flow network and flow control strategy:

- Pumps and fans can either be used as flow elements or just elements.
- Diverges and converges can either be used to add flows or to set fractions.

The converges and diverges must either be solved in the correct sequence to eliminate iterations or the procedure must be run a number of times to solve all the pipe elements. An illustrative example is discussed in the following section.

7.5.3 An illustrative example

To illustrate the procedure introduced above, consider the following example. Figure 7.2 shows a diagrammatic presentation of a simple mine surface cooling plant. Applying the flow simulation procedure to this example gives the following list of flow elements shown in Figure 7.3. Flows are set to the pipe elements by the flow elements in the sequence of the list.

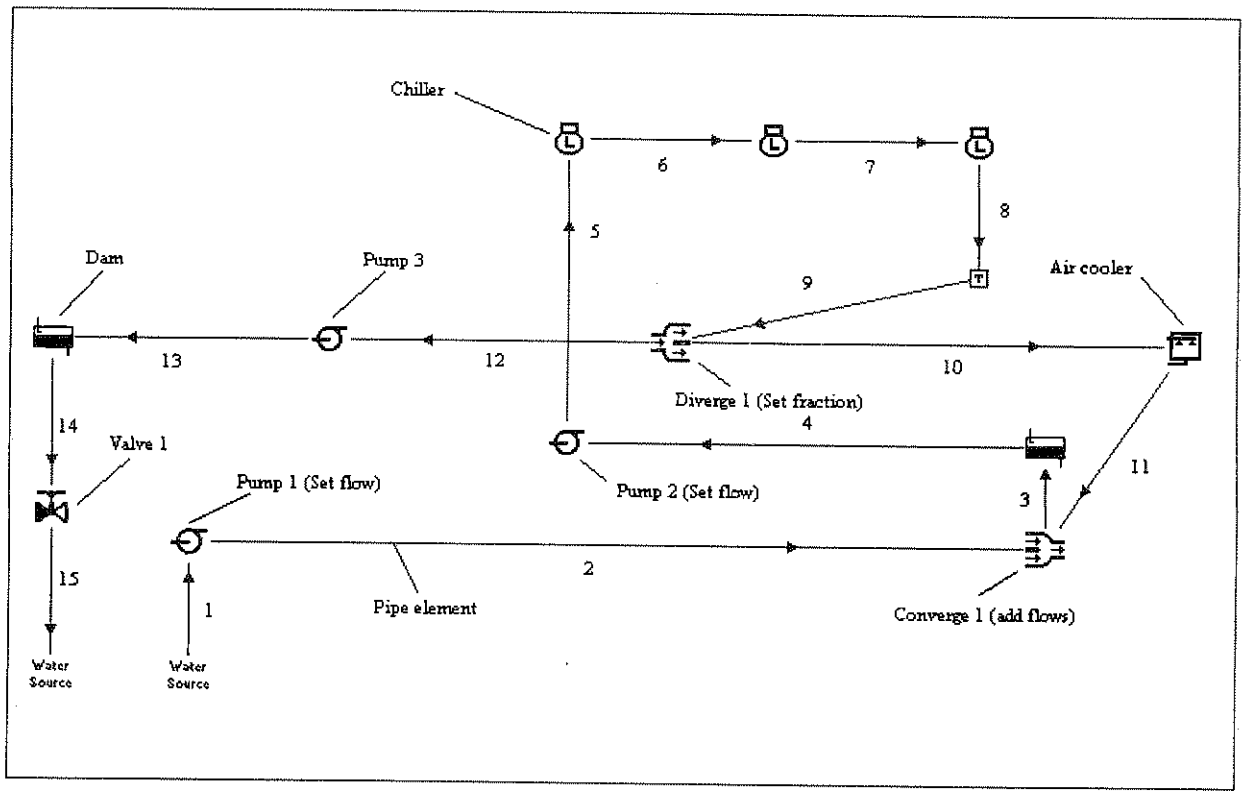

Figure 7.2: Diagram of a mine surface cooling plant

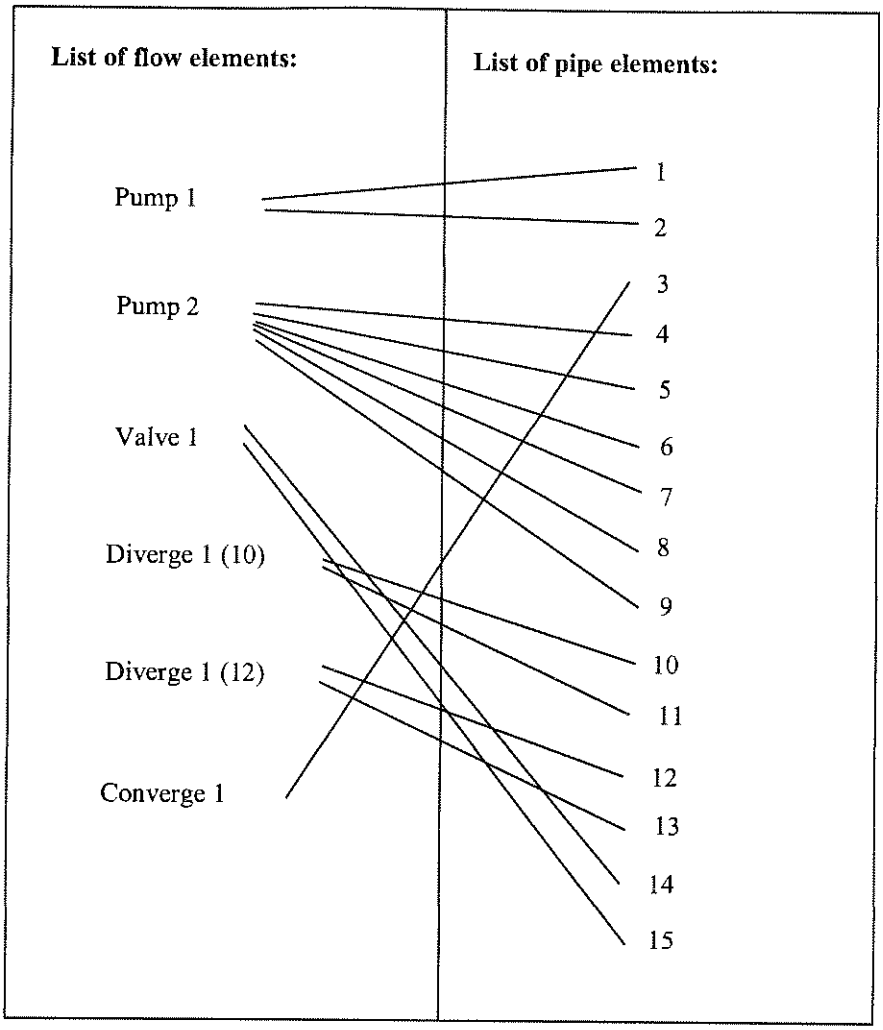

Figure 7.3: Procedure to simulate flow

The flow values of the flow elements can either be set constant over time as in this example, or the flow values can change due to changing control outputs. The mass flow rates of pumps, valves and fans can be controlled from system conditions. Diverges and converges which are set on set fraction can also be controlled from system conditions. Pump 3 in the figure is utilised as an element and not a flow element to include the thermal performance of heat pump in the simulation.

7.6 CONCLUSIONS

New thermal component models not often used in building applications, dams, water pipes and wet surface heat exchangers were derived in this section to extend the applicability of QUICKcontrol. All these models satisfy the philosophy and requirements discussed in chapter 2.

A new flow simulation procedure to calculate flow in any flow network was developed to make provision for more complex systems found in mining and industrial applications. The new models developed in this section are validated with actual measurements during integrated mining applications in the following two chapters.

7.7 REFERENCES

[1] AF Mills, Heat Transfer, Irwin, Boston, 1992.

[2] FC McQuiston and JD Parker, Heating, Ventilating and Air Conditioning *Analysis and Design*, Fourth edition, John Wiley & Sons Inc, New York, 1994.

[3] ASHRAE HVAC Systems and Equipment Handbook, America Society of Heating, Refrigeration and Air-conditioning Engineers, Inc. Tullie Circle, NE Atlanta, GAZ 30329, 1996.

[4] PG Rousseau, Integrated building and HVAC thermal simulation, *PhD thesis,* Faculty of Engineering, University of Pretoria, Pretoria, 1993.

[5] WF Stoecker and JW Jones, Refrigeration and Air Conditioning, McGraw-Hill, 1982.

[6] C Lombard, Two-Port Simulation of HVAC Systems and Object Oriented Approach. *PhD thesis,* Faculty of Engineering, University of Pretoria, Pretoria, 1996.

[7] WM Rohsenow, JP Harnett, EN Ganic, editors, Handbook of Heat Transfer Applications, Heat Exchangers. McGraw-Hill Book Company, 2^{ed} edition, New York, 1985.

[8] E van Heerden, Integrated simulation of building thermal performance, HVAC system and control, *PhD thesis,* Faculty of Engineering, University of Pretoria, Pretoria, 1996.

CHAPTER 8

APPLICATION 1: THE POTENTIAL FOR DSM ON MINE COOLING SYSTEMS

A study was conducted on a typical deep gold mine to investigate the potential for Demand Side Management (DSM) on its cooling system. This was done to obtain the feasibility of RTP or any other time of use price structures on mine cooling systems. To implement DSM on a cooling system the potential for load shifting has to be investigated for various time periods of the day. The only means to predict these load shifts efficiently without effecting the supply of chilled water is by using an integrated thermal system simulation tool. The tool used was successfully verified with actual measurements to ensure its integrity during the investigation. With the aid of an integrated system simulation tool it was possible to shift a cooling system load of 4 MW over a maximum time period of 5 hours per 24-hour cycle. This was accomplished without compromising the demand of chilled water. This load can also be shifted in a number of smaller time intervals with a total time period of 5 hours per 24-hour cycle to fit any specific time of use tariff for a maximum cost benefit.

GRAPHICAL SYMBOLS

System symbols

Thermal storage dam

Centrifugal Pump

Control Valve

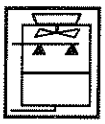

Cooling Tower

Controller

Simulation symbols

Valve

Thermal storage dam

Climate

Cooling Tower

Pump

Controller

Water cooled chiller / Ammonia chiller

Water source at specific temperature

8.1 INTRODUCTION

This study was conducted for ESKOM in close collaboration with R Els[1] and only a summary of the study is therefore given in this chapter. Some of the detail results obtained during the study are given in Appendix C.

Real Time Pricing (RTP) is a methodology, which sets the selling price of electricity equal to marginal and transmission cost plus profit. The marginal cost of electricity however includes a component which reflects the marginal outage cost. The marginal cost of electricity is defined as the hourly market price by which electricity is generated and transferred from the transmission system to the distribution system.

RTP offers a clear economic signal, motivating customers to adjust patterns of use to match ESKOM's (South Africa's electricity Utility) marginal costs. The RTP structure includes a mechanism to ensure that the revenue requirements of ESKOM are met. RTP will likely become the dominant foundation of electricity transactions in South Africa.

The objectives of the RTP product are[2]:

- The promotion of economic efficiency through appropriate marginal cost based price signals.
- To stimulate optimal behaviour through dynamic price signalling. This includes:
- Energy conservation when the system is constrained, as signalled by high prices.
- Increased energy sales when the system is unconstrained, as shown by low prices.
- Reduced system peaks implying deferred capital expenditure.
- Reduced operating cost resulting from not having to start up more expensive units to supply short peak loads.
- Improved customer service, through lower overall average prices and more customer choice.

It is important to note that the consumer may not respond favourably to RTP or any other pricing system if the cost of the response is greater than the potential savings. This may also happen if the consumer does not have sufficient information about the present and expected price levels to enable decision-making concerning the level of consumption[3].

This study forms part of an ESKOM investigation to obtain the potential of RTP or any other time of use price structures on the deep mining industry of South Africa. The feasibility of RTP and other time of use tariffs, depends greatly on the ability of the mines to shift load during certain time periods of the day. The main objectives of the study were therefore to answer the following questions:

- Does their exist a potential for load shifting in the deep mining industry?
- Where can this load be shifted without compromising the operations of the mine (which systems)?
- What is the size of the load that can be shifted?
- During what times of the day and for what length of time periods can this load be shifted?

The South Deep gold mine west of Johannesburg was used as pilot mine during the investigation. The cooling system of this mine was identified as a potential candidate where load can be shifted without compromising the operations of the mine. The only means to predict these shifts efficiently without effecting the supply of chilled water to the mine is with the aid of an integrated thermal system simulation tool.

The extended system simulation tool QUICKcontrol discussed previously was therefore used during the investigation. The tool was firstly verified with actual measurements to ensure its integrity during the investigation.

8.2 SIMULATION AND VERIFICATION

8.2.1 Introduction

The cooling system of a mine is an integrated, dynamic process. To thoroughly investigate the performance of such a system, it is necessary to use integrated software that can model the different components and their interaction relevant to each other. Such software is only usable for investigations if it is properly verified, using the proper verification procedures.

To verify the model properly, it is necessary to use actual system measurements. These measurements include temperatures, flows, dam levels and electricity consumption measured over a period, at specified time intervals. Different measuring equipment is needed, either installed in the system, or additionally provided.

By using the simulation software, the system can be modelled by building the system using the different component models in the software. Taking the measured data of the system for a typical day and then comparing it to the simulated data from the simulation software, the verification is achieved.

8.2.2 System description

The mine's cooling plant is well maintained with an extensively installed monitoring system on the cooling plant. The mine has an installed cooling capacity of 30 MW in their surface plant, provided by four York R12 chillers and one Howden ammonia chiller. The Yorks provide 20MW of cooling and the Howden provides the remaining 10 MW of cooling. The system furthermore includes the use of various dams to serve as thermal capacitors for the system and cooling towers. A detailed layout is seen in Figure 8.2.

The surface system starts with warm water pumped from under the ground into the mine water dam. A pump station pumps the water to a hot water dam from where it is gravity fed to the pre-cooling towers. The water is pumped through filters to the refrigeration plant with the chillers.

The path the water follows through the refrigeration plant varies according to need. The operators can use different schemes to route the path.

Chilled water dams connect the chillers and serve as thermal storage of the chilled water as well as emergency reserve storage. From the chilled water dams the water is gravity fed to and down the shaft at a controlled temperature and flow rate. This is largely determined by the demand (Load) from the underground processes.

The water going down the shaft in the pipes builds up pressure. To break this pressure, dams are placed at certain depths that serve as pressure breakers. These dams also serve as distribution centres of the chilled water to the different working points and cooling processes. The chilled water is used in the various processes, including air-cooling, spot cooling and equipment cooling.

8.2.3 Measurement and simulation procedures

Measurements were taken over a period of four weeks to get familiar with the typical operation of the plant and to get a good average day depicting the most common profiles of the equipment. From the downloaded data, a single representative day was selected to be compared to the 24-hour day predictions provided by the simulation software.

The following measurements were taken at different points by the already installed measuring equipment:

Temperatures

1. The water from the mine water dam to the hot water dam,
2. The water being fed into the pre-cool towers and leaving the tower,
3. Water entering the cool water dam,
4. Water entering the York chillers before the pipe diverges,
5. After the converge of the York chillers and before the Howden chiller,

6. After the chilled water dams that is the same as the water going down the shaft.

Flows

1. From the hot water dam to the pre-cooling towers,
2. Through the York chillers (all four flows combined),
3. Through the Howden chiller,
4. Chilled water to the shaft.

Levels

1. All the dams above ground.

The additional equipment was used on one of the Yorks and the Howden to ensure the accuracy of the installed measuring equipment and to build a model for the simulation software. The temperatures were measured at the in- and outlets of the evaporator and condenser of the chillers. The electricity usage of the compressors and pumps of the chillers was measured. All the other pumps' electricity was measured as well.

The climate conditions were also used in the simulation software, along with a large number of inputs needed to set up the integrated simulations. These inputs comprise mainly of all the design and performance data of various cooling and pumping equipment. The electrical power consumption that was measured was also used to set up the chiller models.

The current control strategies, including operating times and control parameters, were obtained from the system operating manuals, operators and measurements, where needed. The layout of the simulation model is presented in Figure 8.1.

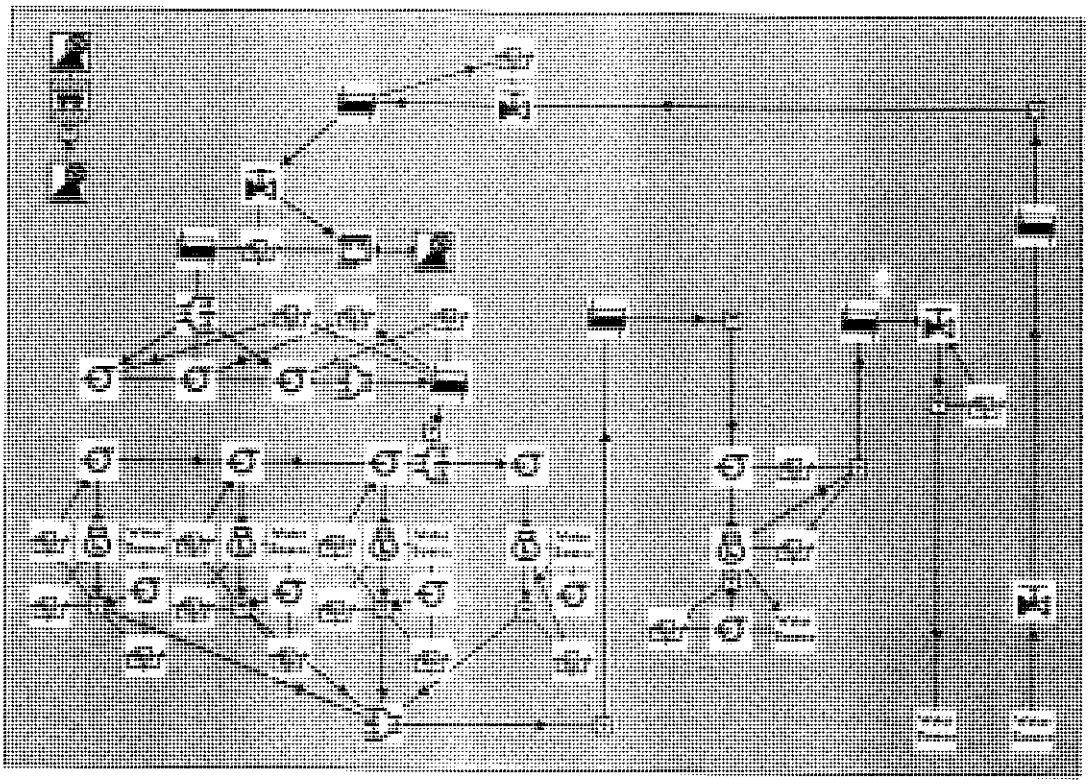

Figure 8.1: Layout of the surface plant simulation model

8.2.4 Verification results

The measured data was used to verify the integrated simulation tool's predictions. For the Surface plant, temperatures were mostly verified. This was done to ensure the accuracy of the power verifications to come. From Table 8.1 it is clear that the verification results are satisfactory. Detail results can be seen in Appendix C. If the power consumed by the components corresponds well to the measured data the simulation model can be used with confidence during the load shifting investigation.

The power consumed by the different components was determined by measuring the electrical current flowing through the equipment, taking the voltage as fixed and using the power-factor and efficiency as given by the manufacturers.

A summary of the results can be seen in Table 8.2. All the results of the verification study are satisfactory and the simulation model can now be used with confidence during the investigation of load shifting.

Component	Within 2°C (%)	Within 3°C (%)
Pre-cool tower in	100	100
Pre-cool tower out	64.18	77.61
Yorks in	79.10	98.51
Yorks out	83.58	86.57
Chill-dam 1	100	100
Howden out	85.07	85.07
Chill dam 2	91.04	98.51

Table 8.1: Summary of component temperature verification results

Component	Within 10% (%)	KWh Error over 24 hours (%)
Pre-cool tower fan	62.5	34.26
Filter pumps	88.1	1.92
York evaporator pumps	84.72	0.83
York condenser pumps	88.89	5.92
York compressor	68.66	6.96
Howden evaporator pump	85.28	4.44
Howden condenser pump	85.28	6.99
Howden compressor	72.22	1.95
Total power	62.5	0.05

Table 8.2: Summary of power consumption

8.3 OPERATING STRATEGIES FOR LOAD SHIFTING

8.3.1 Introduction

Nearly 25% of the electricity used by the mining sector goes to the VC system of the mine to maintain the comfort and safety of the workers. Of this percentage certain equipment is responsible for a big part of the demand load. To investigate the potential for load shifting it is important to establish the representative impact of each of these larger equipment components.

Once the energy usage contributions of the different equipment have been established it is only necessary to focus on the big power users. The current operation also needs to be established for better understanding of the system. This information can then be used to optimise or control the right equipment to accomplish better power consumption and load shifting by implementing new operating strategies.

Year simulations were performed to investigate load shifting. This was done to evaluate the system's performance over a period of time, including the full variation of climatic changes. Giving the savings and load profile over a time period of a year is also more understandable. It also gives a user-friendly month-based comparison between the different new operating strategies.

8.3.2 Current operating strategy

The current system uses ultrasonic water level sensors on the dams. A signal is sent from them to the control room where operators control the system manually. The operators decide on the appropriate level for the dams, usually between 80% to 100% of the maximum volume of the dam. A detailed schematic view of the system with the currently controlled equipment can be seen in Figure 8.2.

Variable flow valves control the water flow through the pre-cooling towers according to their dam levels. The level of the cool water dam is used as input signal to control the flow from the filter pumps. The filter pumps operate in step to keep the cool dam full. The chillers are

started and stopped to keep the chilled dams full. If the chilled water dam levels drop below the set parameters the operators manually switch on the chillers.

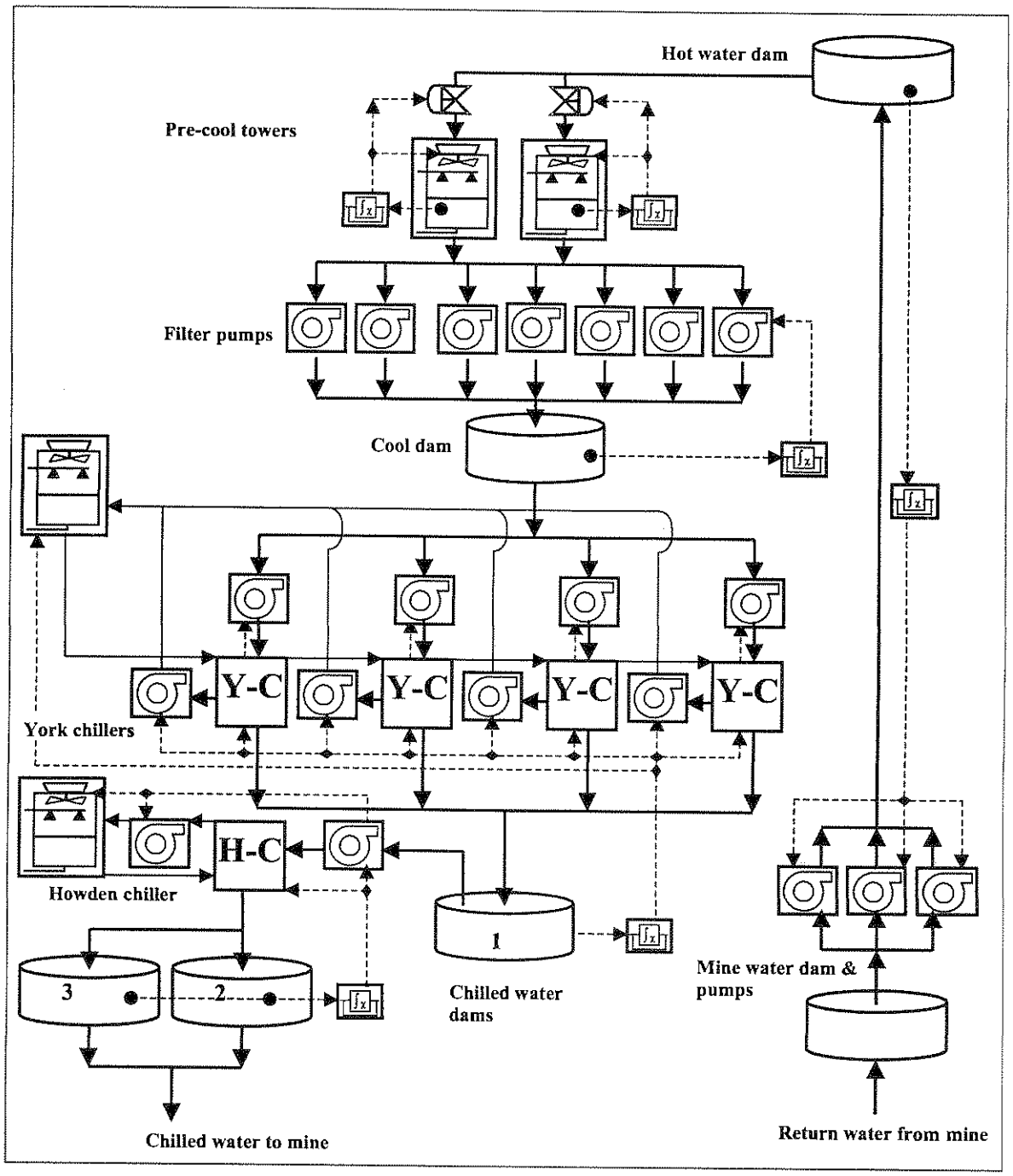

Figure 8.2: Schematic layout of surface plant with control

The current manual control parameters for chilled dam1 are seen in Figure 8.3(a) for a single York chiller. When the dam is full, there is no flow and when the level falls below 80%, the chillers are switched on. Three York chillers are used simultaneously in parallel to keep chilled dam 1 full.

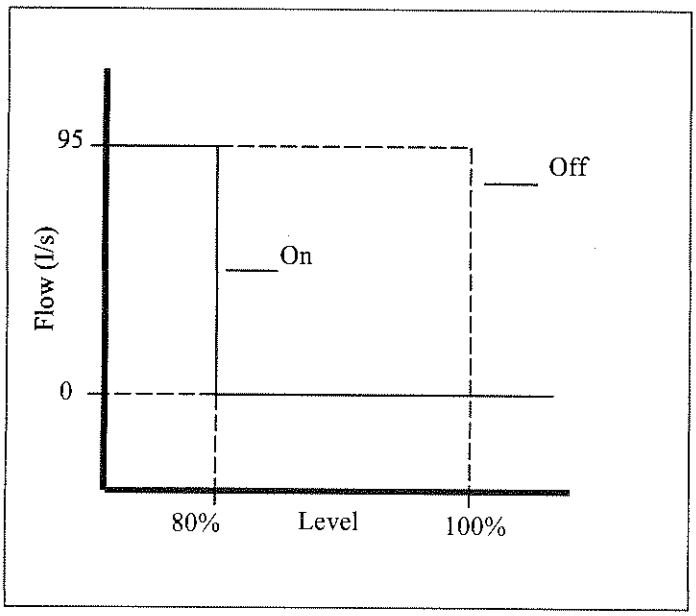

(a)

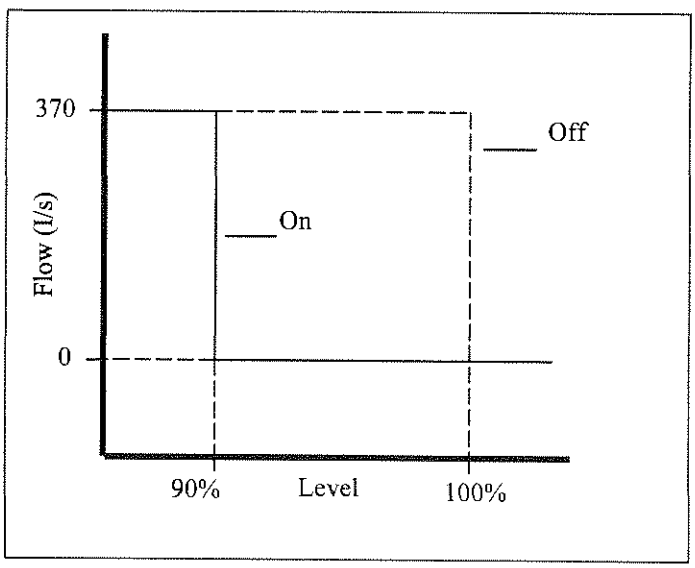

(b)

Figure 8.3: Manual control parameters on Chill Dams

The control on the chilled Dams 2 & 3 can be seen in Figure 8.3(b). The dam levels are controlled by the Howden chiller and serve as the supply storage to the mine. The water in these dams is controlled to a temperature of between 1.5 – 2°C. To maintain this exact temperature, the water is recycled to mix with the water entering the Howden, but this control is not relevant to the study.

8.3.3 New load shifting operating strategies

The first step to utilise this new operating strategy is to install PLCs on the pumps and chillers, receiving their signal from the already installed level sensors on the dams. This will allow for automatic control on the pumps and the chillers. The dam levels can be monitored more closely and the setpoints of the control can be optimised, utilising the storage capacity of the dams more effectively.

Each of the cool and chilled dams has a two-hour storage capacity, containing 2700m^3 water. To fully utilise the capacity of the dams, the three chilled dams are configured into parallel, meaning that the York and Howden operates in series without a dam in between. This is an existing scheme, Scheme A. The only difference is to use chilled dam1 in parallel with the other two dams.

The control parameters for the three dams in parallel can be seen in Figure 8.4, which will control the York and Howden chillers in series. The water flow through the 3 York chillers was inereased to 110 l/s per chiller and the flow through the Howden chiller was decreased to 330 l/s.

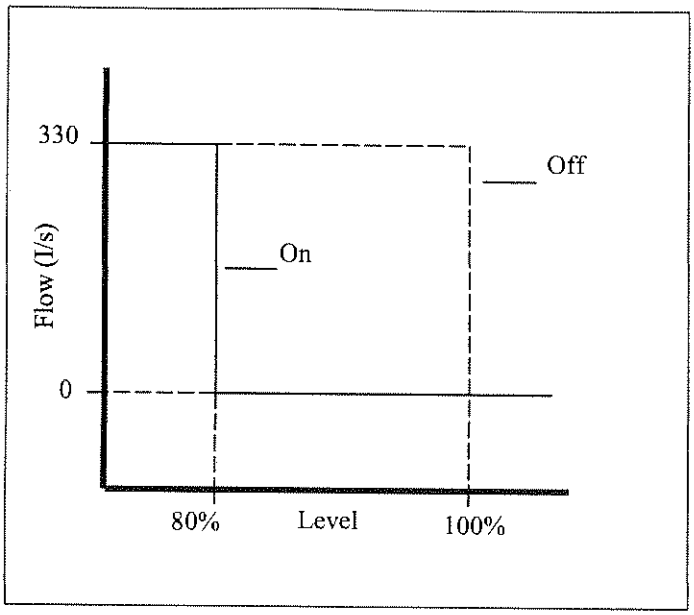

Figure 8.4: New control parameters for chillers

With the simulation tool it was possible to shift a maximum load without compromising the demand of chilled water going down the shaft. The chilled water demand profile and supply water temperature therefore stayed exactly the same as before.

Thermal storage was used to shift the demand load of the cooling plant. This can be achieved by only implementing new operation strategies on the current systems. This implies hardware changes of only new PLCs.

8.4 RESULTS AND POTENTIAL

8.4.1 Introduction

From section 8.1 it has become apparent that there is a need to find possibilities to utilise Real Time Pricing. This implies the shifting of load at certain times when electricity peaks are charged at a maximum price. This has widespread implications and benefits nationwide for the mining industry, ESKOM and consulting engineers.

One of the most effective ways to achieve this goal is to use integrated, dynamic simulation software to investigate the potential of load shifting. New operating strategies discussed in the previous section were simulated and the findings discussed in this section. Using these

findings and then extrapolating them, with a certain margin of error, the potential for load shifting of the whole South African gold mining industry can be calculated.

8.4.2 Load shifting potential for RTP

New system operating strategies were simulated and the results are compared to the current system for a typical day. Detail results can be seen in Appendix C. An average potential load shift of 4 MW for a maximum continuous period of five hours on the surface cooling plant over a 24-hour cycle was possible.

It was also important to ensure that the dam levels do not drop below their minimum levels. This was achieved and is shown in Appendix C for the three Chilled Water dams in parallel. Before load is shifted the dam is filled to capacity and during the shift the level doesn't drop below 30%. The new operating strategies did not influence the current demand for chilled water by the mine at all.

The maximum load of 4 MW can also be shifted in a number of smaller time intervals with a total time period of 5 hours per 24-hour cycle to fit any specific time of use tariff for a maximum cost benefit. This potential can now be extrapolated to the entire deep mining industry and the total potential can be calculated. Payback periods on the implementation of system changes and energy cost savings can only be obtained once RTP or time of use tariffs are in place.

8.5 CONCLUSION

The mining industry forms a big part of ESKOM's electricity sales. It is therefore important that the mining industry and ESKOM work together to find ways to optimise energy cost on a national level. One such way is to use ESKOM's time of use pricing structures available. These structures are only feasible when load is shifted during certain time periods of the day.

The purpose of this study was to investigate the potential of load shifting on the cooling system of a deep mine. This could only be done using integrated software capable of doing dynamic simulations, to investigate the effect of various load shifting options.

For the proper use of this software to achieve reliable answers, it had to be verified on an existing mine. Section 8.2 discusses the procedure and the shows the verification results for the South Deep gold mine. This mine was used as it had a typical cooling system and a reliable monitoring system.

The only way to achieve the goal of load shifting was to use automated control, for the current system is dominantly manual. Manual overrides would need to be included. Section 8.3 showed the operating strategies, current and new, to achieve load shifting. A load shift of 4 MW can be achieved during a maximum time period of 5 hours per 24-hour cycle.

It can clearly be seen that there is a potential for load shifting in the South African mining sector by only utilising their cooling systems. This can be used in the strategic planning of mines concerning their pricing structures. ESKOM can further use it to plan the implementation of new pricing structures.

8.6 REFERENCES

[1] R ELS, TEMM International (Pty) LtD, PO Box 13517, Hatfield, 0028, Pretoria, South Africa.

[2] Kern C.F., Real Time Pricing Directive, Key Customer Marketing, ESKOM, May 1998.

[3] McDonald, J.R., Whiting P.A., Lo K.L., Optimized reaction of large electrical consumers in response to spot-price tariffs, Electrical Power and Energy Systems, Vol. 16, No. 1, pp35-48, 1994.

CHAPTER 9

APPLICATION 2: POTENTIAL FOR DSM ON MINE PUMPING SYSTEMS

The underground pumping reticulation system of a gold mine was dynamically simulated and verified with actual measured data from the system. Using different operating strategies the potential for DSM was investigated by determining the maximum load that could be shifted without any of the dams reaching their full capacities. The study revealed the potential of shifting an energy load of approximately 70002 kWh from the daily operation, with a maximum demand shift of 14 MW over 5 hours.

SIMULATION SYMBOLS

Valve

Thermal storage dam

Climate

Cooling Tower

Pump

Controller

Water cooled chiller / Ammonia chiller

Water source at specific temperature

9.1 INTRODUCTION

In the previous chapter, Real Time Pricing (RTP) and other time of use tariffs were discussed as well as the fact that ESKOM are looking for opportunities to implement these structures to optimise electricity generation and distribution cost[1]. However as mentioned previously, the client must be able to shift enough load at the correct times of the day to make efficient use of these tariff structures.

In this chapter a second system was identified in the deep mining industry which has the potential for enough load shifting at certain times of the day without compromising the operations of the mine. It is important not to compromise production at any time as a loss in production can far outweigh the cost savings caused by load shifting.

Underground clear water pumping systems were identified and the potential for load shifting was investigated in this chapter. This study therefore forms part of the ESKOM investigation to find opportunities to implement RTP as mentioned in the previous chapter. These pumping systems are on their own one of the biggest energy consumers on a deep gold mine.

The pumping system of the South Deep gold mine west of Johannesburg, was used as pilot mine during the investigation. The reason for this choice was that the mine has a typical clear water pumping system used in deep gold mines and the system already has a complete monitoring system installed.

An easy and efficient way to investigate this load shifting potential on these large thermal systems is again with the aid of an integrated thermal system simulation tool. The predictions of such a tool can be used to investigate various measures to optimise load shifting without influencing mine operations.

The extended system simulation software QUICKcontrol was used during this investigation. The tool was firstly verified with actual measurements to calibrate the model and to ensure its integrity for realistic predictions during the study.

9.2 SIMULATION AND VERIFICATION

9.2.1 Introduction

The water reticulation system of a mine is an integrated, dynamic process. To thoroughly investigate the performance of such a system, it is necessary to use integrated software that can model the different components and their interaction relevant to each other. Such software is only usable for investigations if it is properly verified, using proper verification procedures.

To verify the system properly, it is necessary to physically measure the relevant information needed from the system. This information includes water flow rates, dam levels and electricity consumption measured over a certain time period, at specified time intervals. Different measuring equipment is needed, either already installed in the system, or additionally provided.

By using simulation software, the system can be modelled by building the total system using the different component models in the software. Starting with a typical day, the measured data of the system can be compared to the simulation data acquired from the simulation software. After the initial verification, a longer period (e.g. a month or year's measured system data) can be compared to the simulation data to further the verification process.

9.2.2 Verification Procedures

To be able to verify the system model it was necessary to establish a proper procedure for verification. This procedure needed to be systematic and can be broken into the following steps:

1. A detailed schematic layout of the system was needed to establish the configuration of the simulation model and to determine the various measuring points needed for the verification purposes.

2. The measurements needed for verification purposes included the measuring of all underground dam levels, water flow rate from the underground system to the surface dams, pumping status (active pumps) of all the pumps of each pumping station and the electricity usage of all the power consuming equipment.

3. Equipment that was already installed in the system as well as additional measuring equipment was used to perform all the necessary measurements. Typical equipment included ultra sonic flow meters and dam level measuring equipment.

4. A typical working day, week and month was selected along with an appropriate measuring interval to cover enough working conditions of the pumping cycle.

5. The measured data was collected and sorted into useful formats.

6. The simulations were set up for the measuring day, week and month. The simulations were run and the simulation data was compared to the actual measured data.

7. Corrections and modifications were made to the simulation models, and the simulations were repeated until the simulation data compared well to the measured data.

9.2.3 System Description

The mine's underground pumping reticulation system is well maintained with an extensive monitoring system implemented. There are clear water dams (hot water dams) on the levels with pumping stations, which serve as a buffer for the pumping chambers. For emergencies, such as power failures etc., the dams on 80 level have a much larger capacity. The details of the various dams can be seen in Table 9.1.

LEVEL	NUMBER OF DAMS	TOTAL CAPACITY
SURFACE	2	7 Ml
33	3	3 Ml
49	3	3 Ml
70_{SV1}	6	6.8 Ml
$80_{SV2\ \&\ 3}$	5	23 Ml
95_{A}	3	9 Ml

Table 9.1: Summary of the specifications of all the mine water (clear hot water) dams.

It should be noted that measurements were taken on the clear water reticulation system, as this system is the major energy consumer of the total pumping reticulation system. The clear water dams on 95A level and on 70 level SV1 receive their water from settlers on 95 and 68 level. A settler basically collects mine water (leakage refrigeration water, service water and fissure water), and separates the mud from the dirty mine water to provide clear water, which can be pumped by normal operating centrifugal pumps.

The muddy water is fed to mud dams from where the slurry is pumped to the surface via the different levels, which are fitted with slurry dams and pumps. The mine has six underground pumping chambers situated on five different levels below surface. The details of each pumping station are shown in Table 9.2.

LEVEL	DEPTH	NUMBER OF PUMPS	MANUFACTURER	CAPACITY
33	919m	5	GRIFO 10-STAGE	230 l/s
49	1337m	5	GRIFO 4-STAGE	260 l/s
70_{SV1}	2000m	3	GRIFO 8-STAGE	230 l/s
$80_{SV2\ \&\ 3}$	2305m	4	GRIFO 10-STAGE	210 l/s
95A	2794m	4	GRIFO 5-STAGE	240 l/s

Table 9.2: Summary of the specifications of all the clear water pumping stations.

The depth mentioned in Table 9.1 of each pumping station, is the depth below surface. Each pumping station pumps to it's neighbour (the next station above it's own level). The head that each pumping station must overcome can thus be calculated by determining the distance between the stations.

The clear water is pumped from 95A level to 80 level, which is divided into two stations SV2 and SV3 (SV2 and SV3 each have two pumps in their chambers). The two pumping chambers SV2 and SV3 are connected to each other. The water is pumped from 95A to SV3 from where a valve regulates the water flow to SV2. From 80 level the water is pumped to 49 level. Clear water is also pumped from 70 level SV1 to 49 level. The water is then pumped from 49 level to 33 level, from where the water is finally pumped to the surface mine water dams.

It was decided that the only water flow rate measured, would be the total water flow from 33 level to the surface mine water dams. Other flow rates could easily be calculated if needed. A detail schematic drawing of the entire pumping reticulation system can be seen in Figure 9.1.

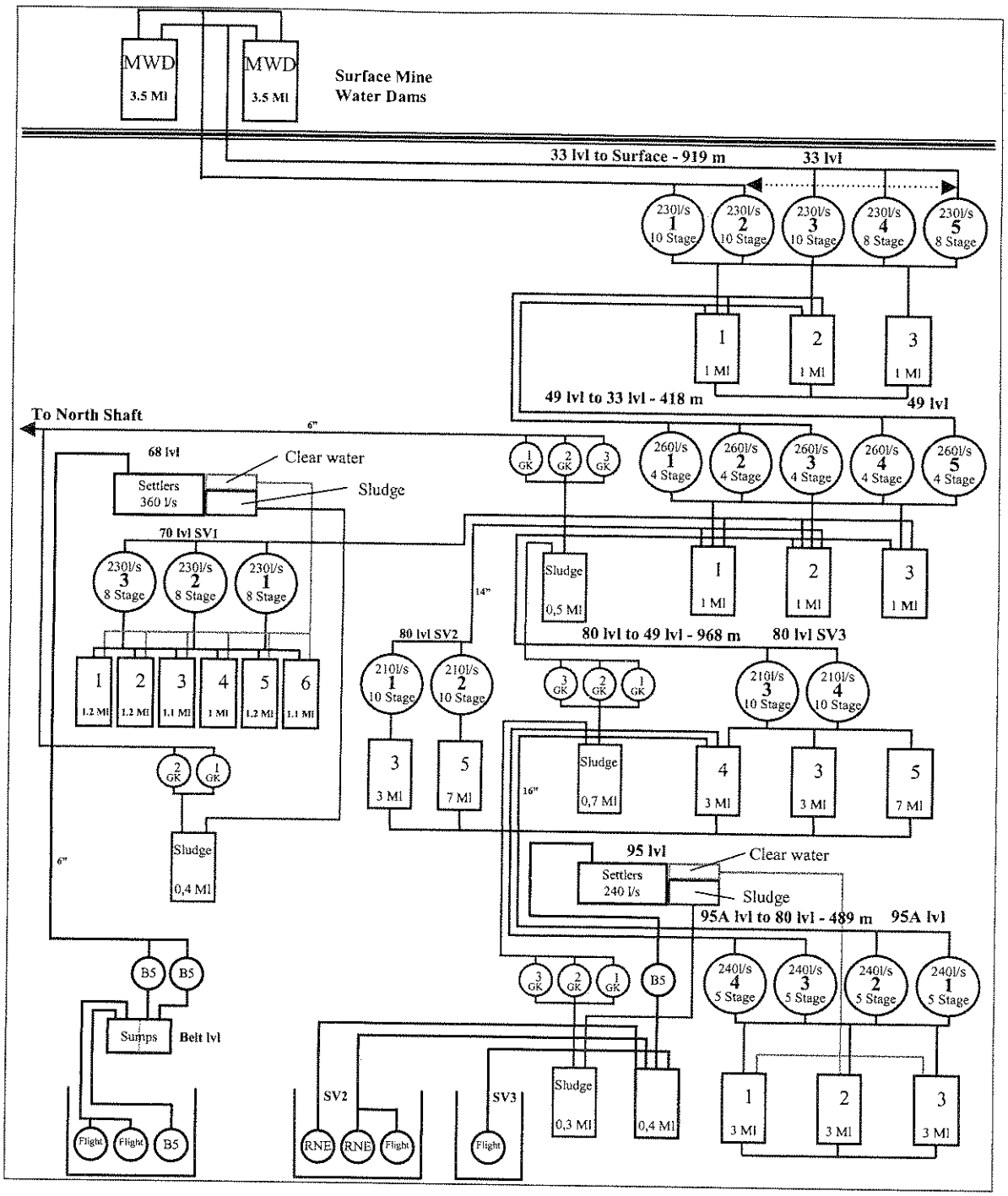

Figure 9.1: Schematic view of the underground pumping reticulation system.

9.2.4 Measurements and simulation procedures

Measurements were taken over a four-week period to get familiar with the typical operation of the system and to get a good average day depicting the most common profiles of the equipment. From the downloaded data, a single representative day was selected to be compared to the 24-hour day predictions provided by the simulation software. The installed measuring equipment monitored the following measurements:

Water flow rates:

The water flow rate from 33 level to the surface mine water dams, i.e. the total water flow leaving the underground workings.

Dam levels:

The dam levels of all the underground clear water (hot water) dams.

Pumps:

The activity of all the underground clear water pumps, i.e. specific times and durations when each pump was active.

Electricity usage:

The power consumption of each pumping station. With the measured hours of activity, the electrical units of each station could be calculated.

The current control strategies, including operating times were obtained from the system operators and measurements. The layout of the simulation model can be seen in Figure 9.2.

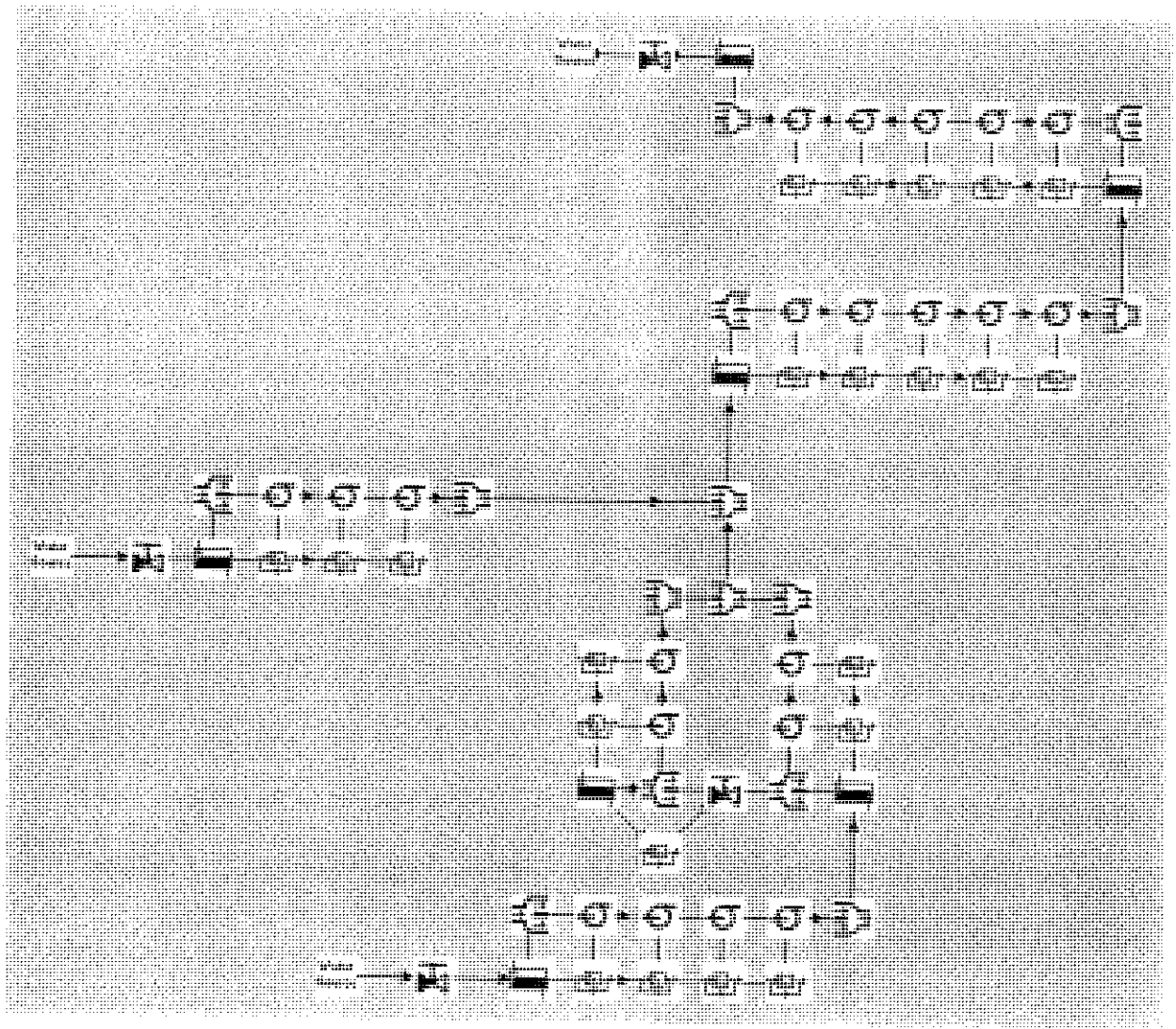

Figure 9.2: Layout of the simulation model.

9.2.5 System Operation Verification

The actual measured system data was used to verify the predictions obtained by the simulation program. A specific typical 24-hour day of system operation was chosen for verification purposes. A simulation was performed according to the exact operating schedules of the measured system. The predictions of this simulation were compared to a specific typical 24-hour day of normal operation, chosen from the measured data.

This 24-hour simulation was done to find out if it was possible to simulate the operation of the system accurately, i.e. it was necessary to simulate the "real life" operation of the system. The predictions made by the simulation program were verified against the actual measured water flow to the surface, clear water dam levels and system energy usage. These

verifications showed that the capacities of the pumps and dams were modelled correctly in the simulation program. The verification results are given graphically in this section. Figure 9.3 displays the simulated and measured water flow from 33 level to the surface.

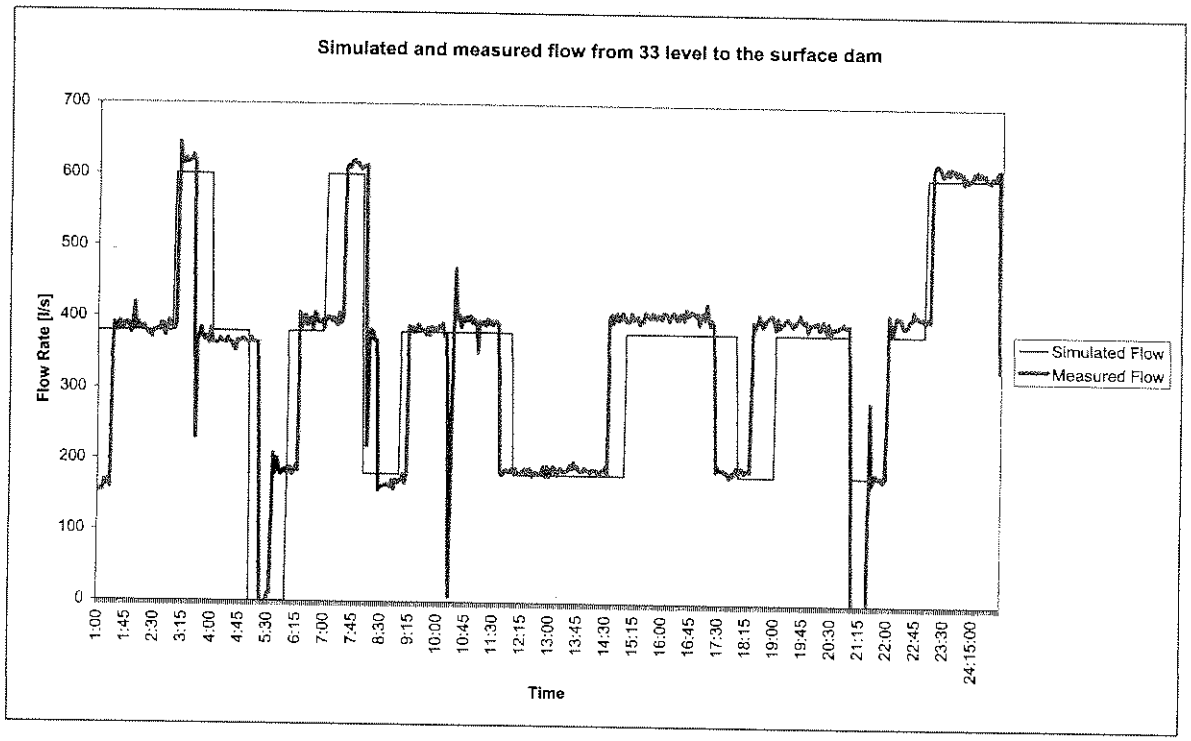

Figure 9.3: Verification results of the flow rate to the surface mine water dams

The phase shifts in Figure 9.3 is due to the hourly input interface of the simulation program. The pumps can only be manually set to be active or inactive on the hour for an hour in the tool. The verification result of the total volume of water pumped over this 24-hour period from 33 level to the surface mine water dams is shown in Table 9.3.

TOTAL VOLUME$_{SIMULATED}$	TOTAL VOLUME$_{MEASURED}$	ERROR
30204 m^3	30508 m^3	1%

Table 9.3: Summary of the total daily water volume pumped to the surface

The daily dam levels of the system were measured, and this data was used to verify the dam level predictions made by the simulation program. The following figures will show the predicted dam levels against the actual measured dam levels.

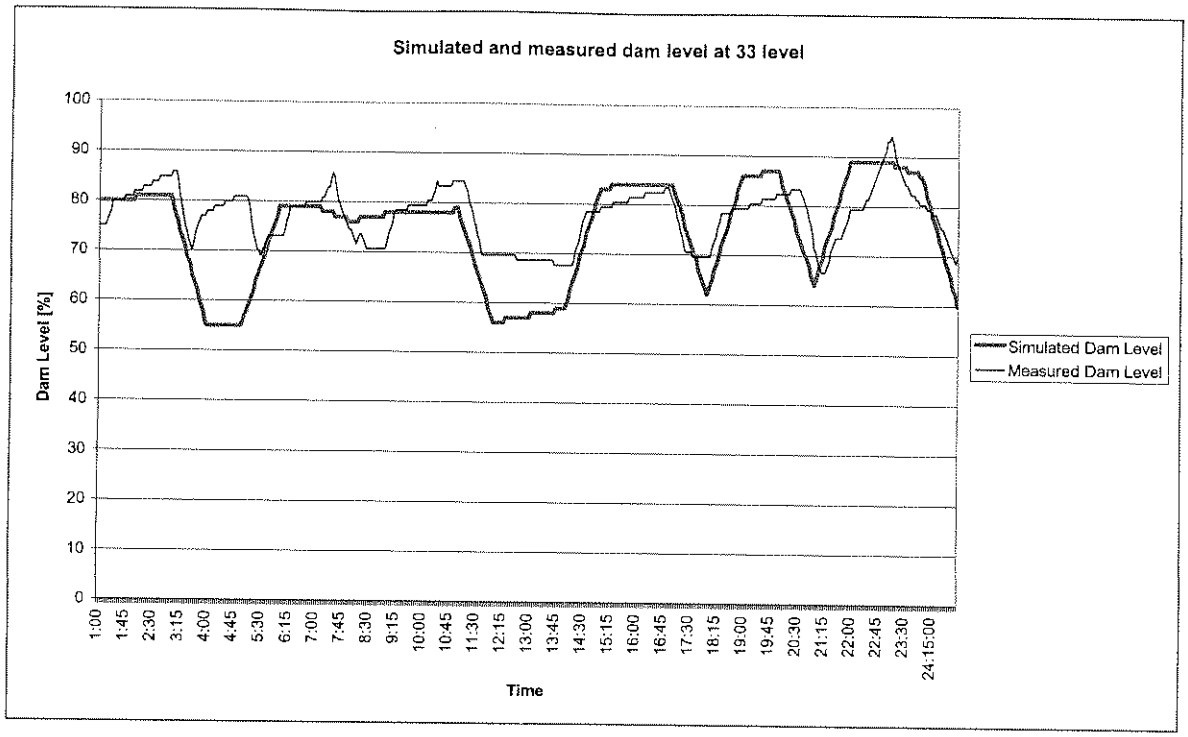

Figure 9.4: Verification results of dams at 33 level

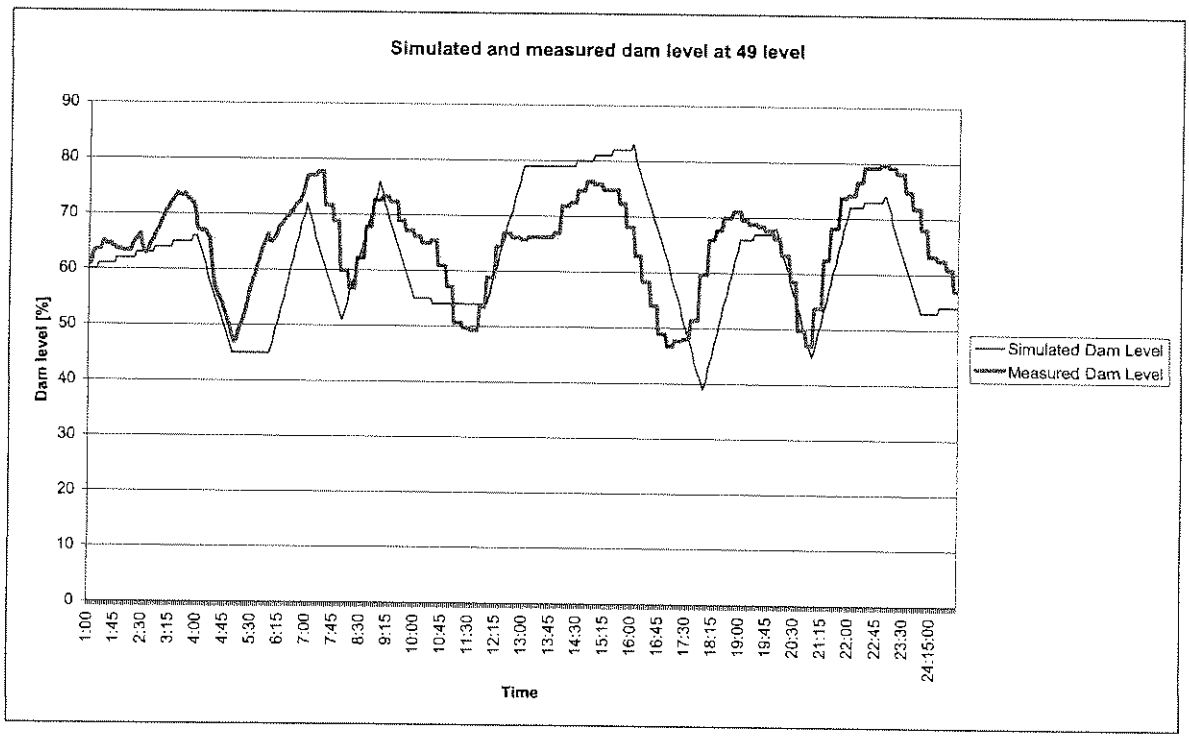

Figure 9.5: Verification results of dams at 49 level

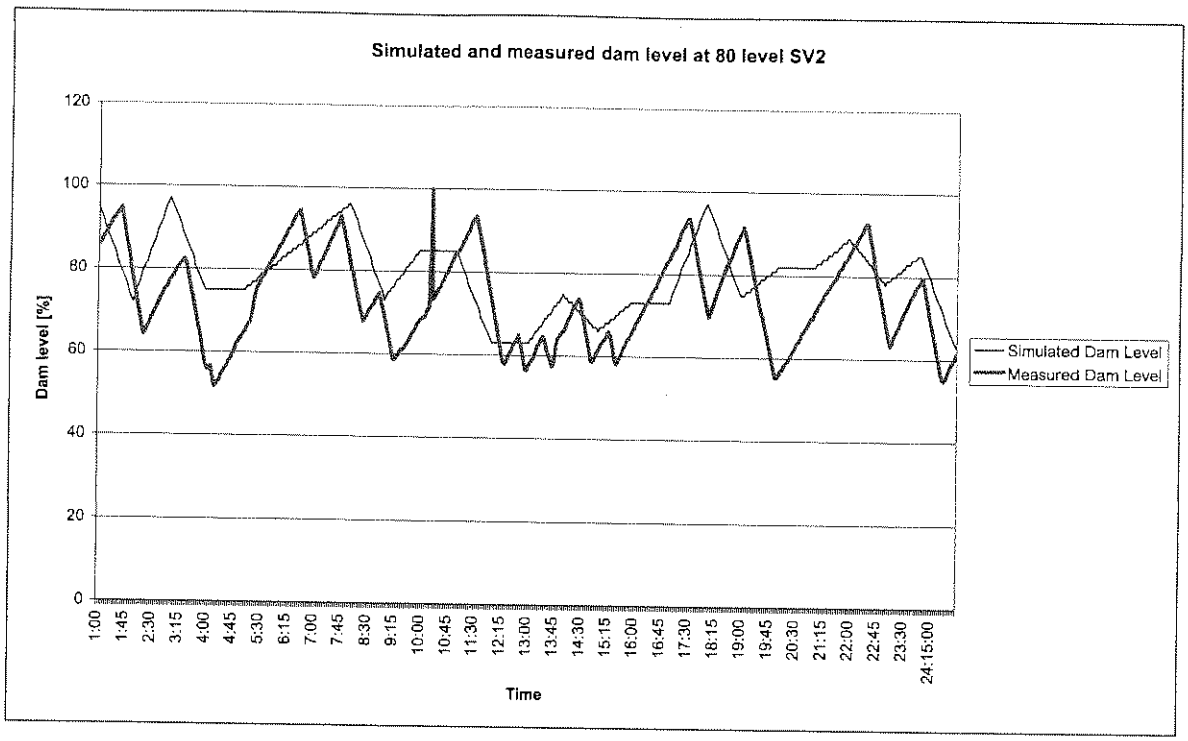

Figure 9.6: Verification results of dams at 80 level SV2

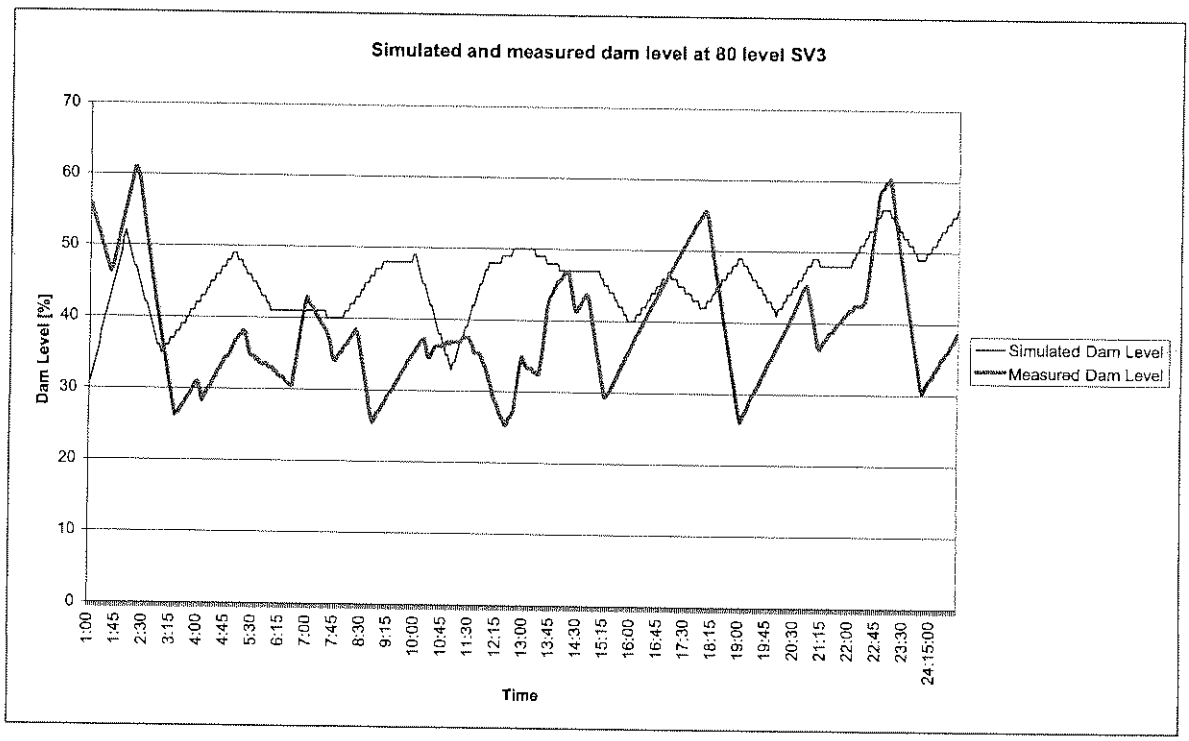

Figure 9.7: Verification results of dams at 80 level SV3

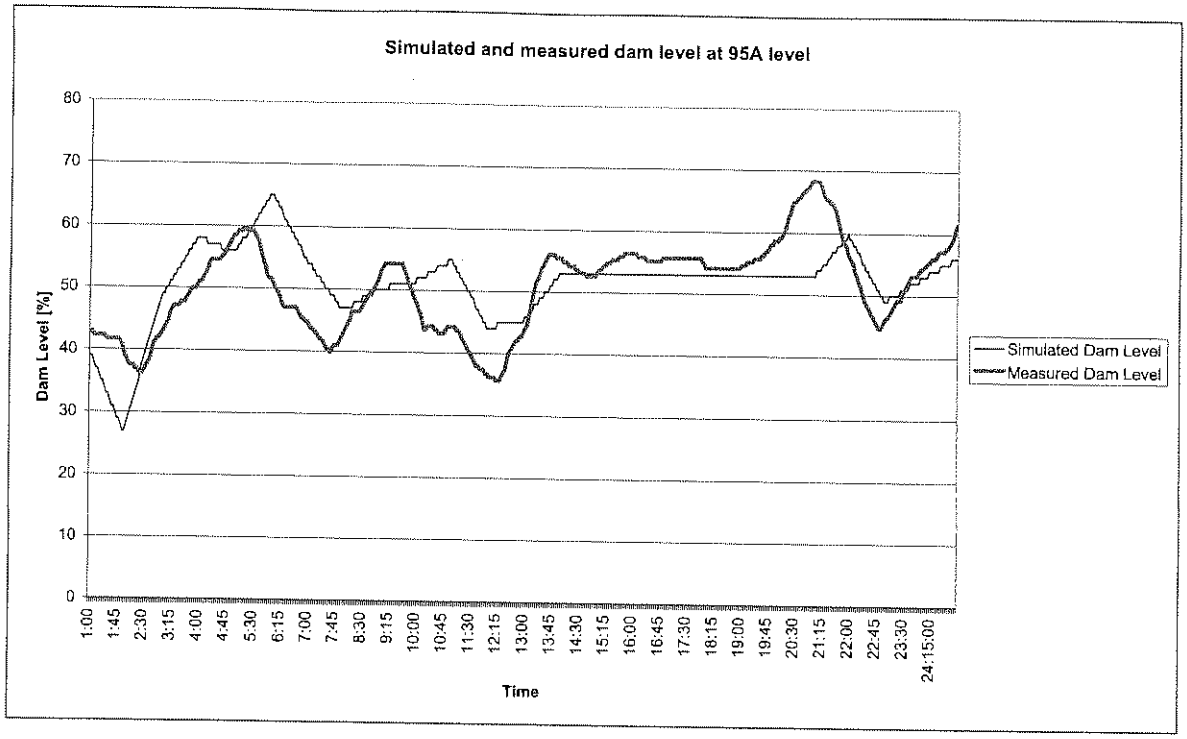

Figure 9.8: Verification results of dams at 95A level

A summary of the verification results of the dam water levels is shown in Table 9.4. The percentage error in the table is the absolute percentage level error between the measured and predicted values over 24 hours.

LEVEL	MAXIMUM ERROR	AVERAGE ERROR
33	25.9%	5.9%
49	22.9%	7.4%
80 SV2	26.6%	9.6%
80 SV3	24.7%	9.2%
95A	15.3%	4.9%

Table 9.4: Summary of the verification results of the dam levels

The graphs show that the measured profiles and the predicted profiles are not exactly the same. This is due to sludge in the dams, which decrease their capacities. Further allows the simulation program for only hourly scheduling of equipment (pumps), which means the actual and simulated operating schedules of the pumps was not exactly the same. Table 9.4 summarises the accuracy of the dam levels.

The daily energy usage of the clear water pumps of the reticulation system was measured, and these results were used to verify the predictions made by the simulation program. The total active pumps on each level are shown graphically and the total energy usage of these pumps for each level is shown in Table 9.5.

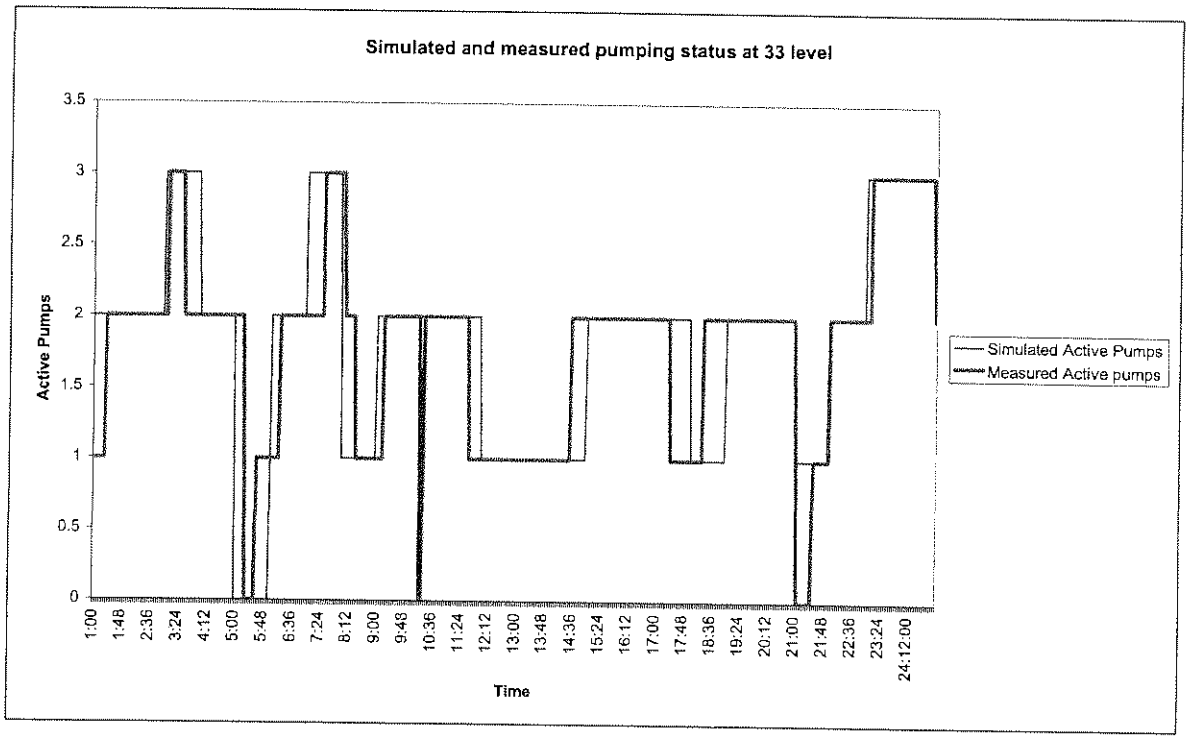

Figure 9.9: Verification results of the active pumps at 33 level

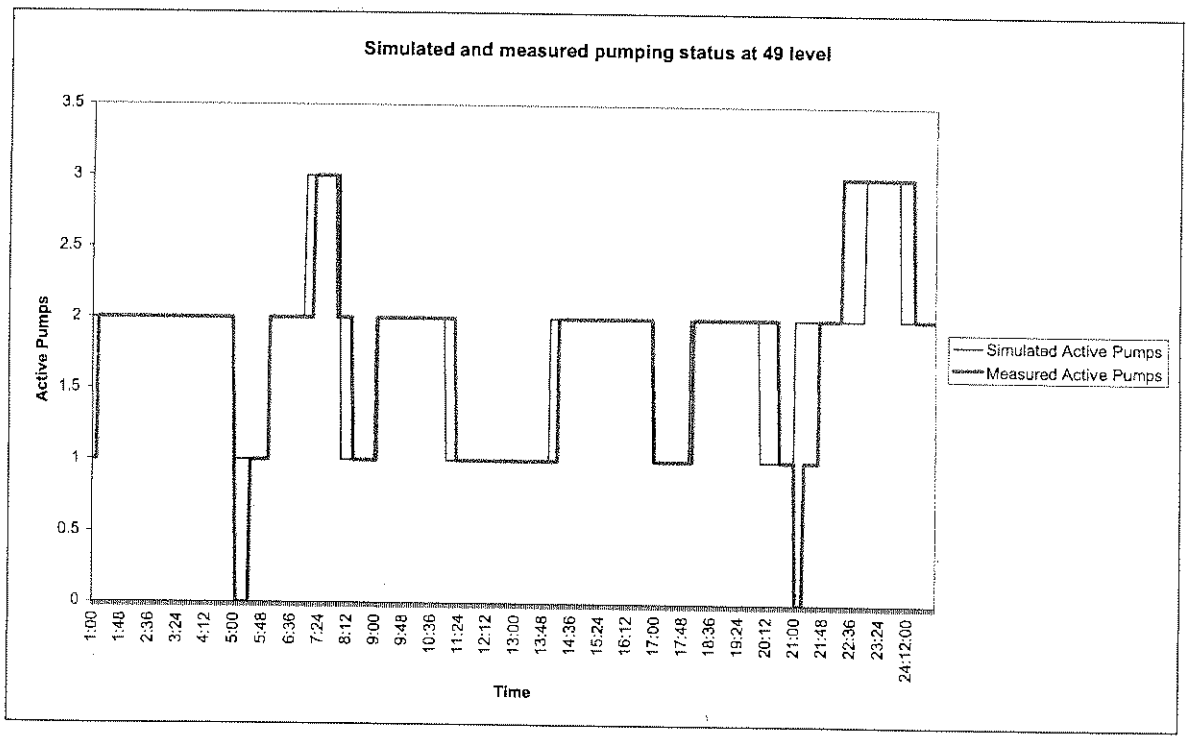

Figure 9.10: Verification results of the active pumps at 49 level

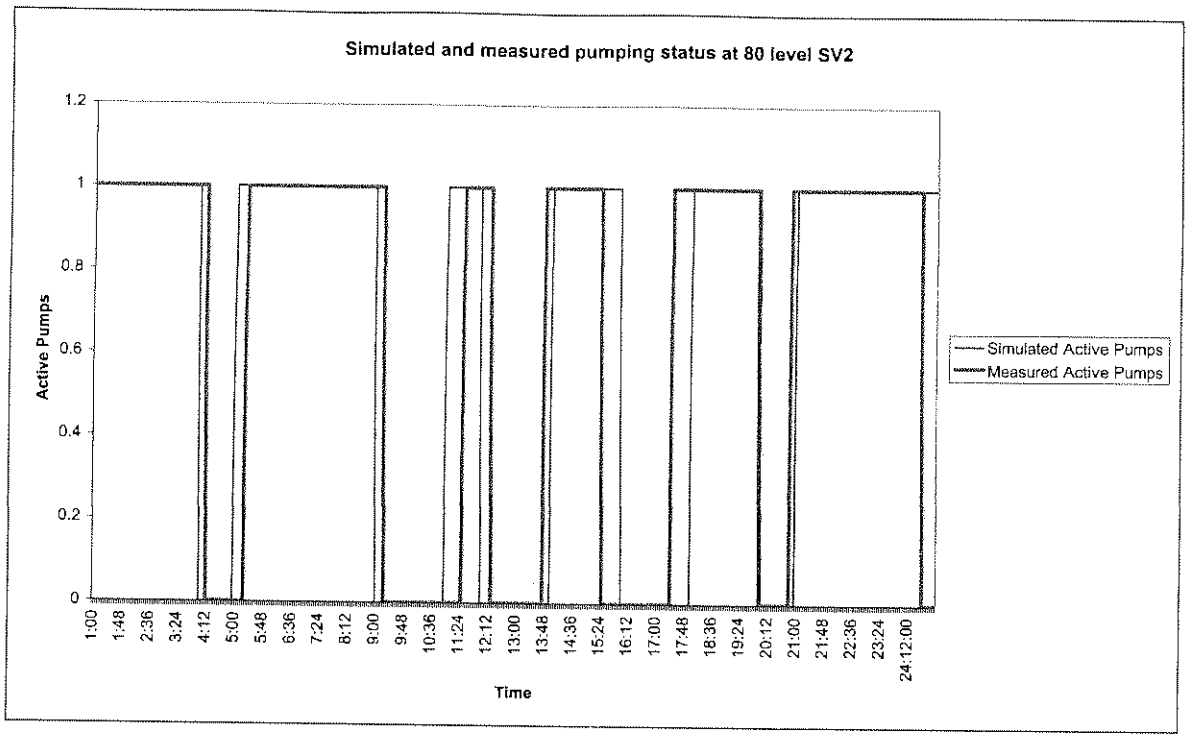

Figure 9.11: Verification results of the active pumps at 80 level SV2

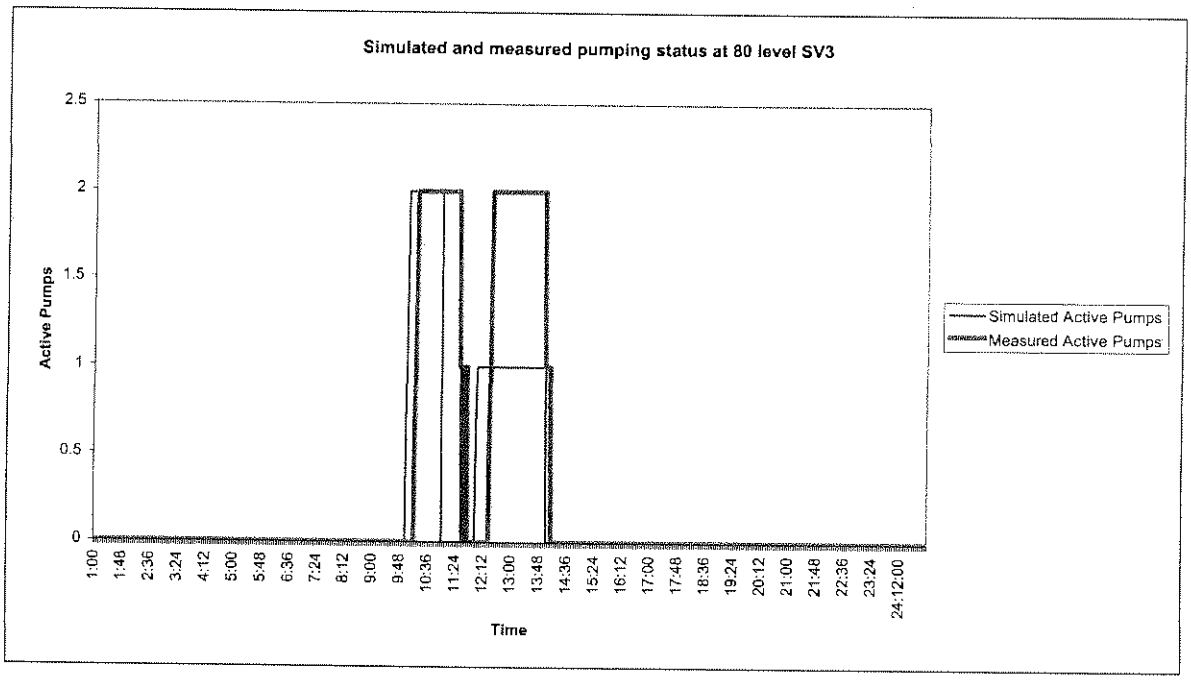

Figure 9.12: Verification results of the active pumps at 80 level SV3

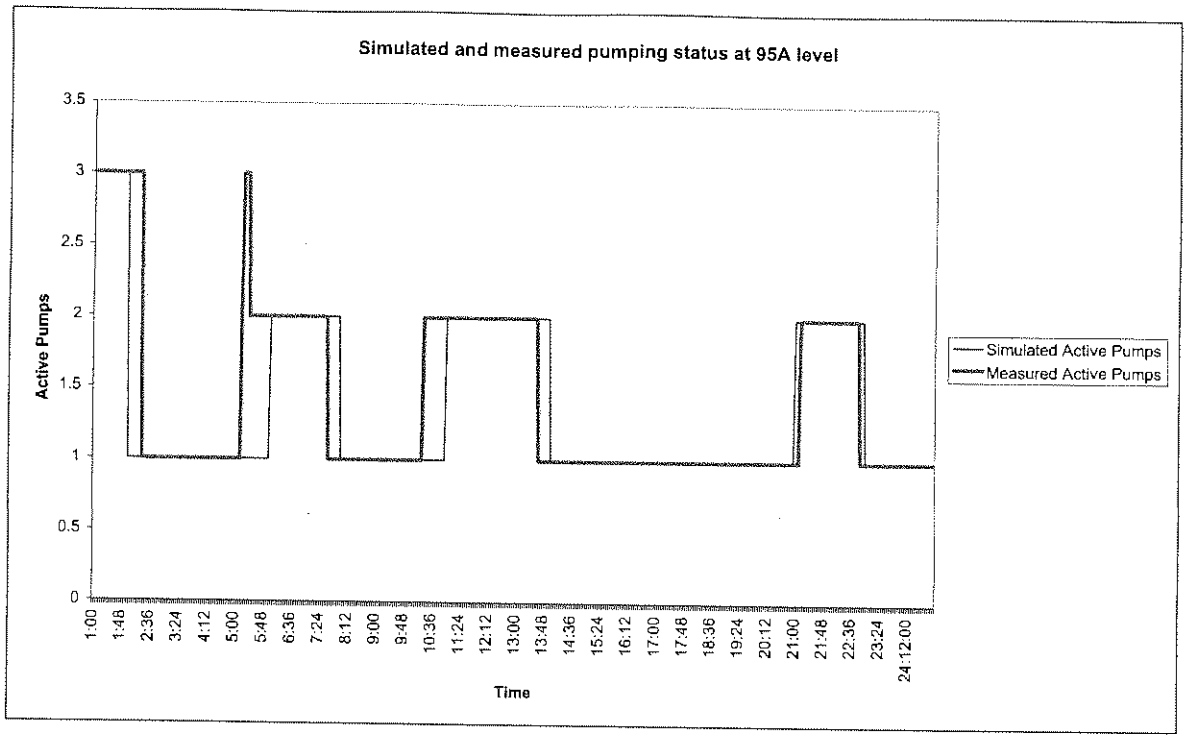

Figure 9.13: Verification results of the active pumps at 95A level

The phase shifts in the graphs were yet again caused by the hourly input of the simulation tool. The verification results of the total daily energy usage of the various levels, for the specific typical day of operation, are shown in Table 9.5.

LEVEL	$TOTAL_{MEASURED}$	$TOTAL_{SIMULATED}$	% ERROR
33	113683 kWh	120700 kWh	5.81 %
49	61894 kWh	57799 kWh	6.62 %
70	21383 kWh	48805 kWh	56.19 %
80	118923 kWh	54648 kWh	54.05 %
95_A	49970 kWh	43752 kWh	12.44 %

Table 9.5: Summary of the total energy usage of the pumps

During the energy comparisons the daily measured energy usage of each pumping station was not available, only the monthly energy consumption of each station was available. This implies that the daily measured energy consumption of each station compared in Table 9.5 is the average daily consumption of that month and not the energy consumption of the specific verification day. Therefore the error discrepancies in the results of 70 and 80 level.

Although the error values for 70 level and 80 level are quite large (it was not possible to get accurate energy measurements from these levels), the verification results of the energy usage of the various levels are satisfactory.

The total daily energy usage of the entire pumping reticulation system is given in Table 9.6.

$TOTAL_{MEASURED}$	$TOTAL_{SIMULATED}$	% ERROR
365853 kWh	325703 kWh	10.97 %

Table 9.6: Summary of the total energy usage of the pumping reticulation system

From Table 9.6 it is clear that the verification of the total daily energy usage of the entire pumping reticulation system is satisfactory. These verification results show that all the dam and pump capacities are modelled correctly for the right amount of energy input when the correct pumping schedules are used as simulation input.

9.2.6 Base Year Verification

A base year simulation was done to try and simulate the philosophy of the system's operators. It was found that the pumps of each pumping station were operated according to a certain trend of the dam levels of each pumping station's dams. Average monthly measured data of the dam levels was used to try and determine the trends used by the operators.

By using certain control parameters on the dam levels, to keep them within certain boundaries, a base year simulation was done to see if the simulation model could accurately simulate the current trends in the system's operation. An average typical 24-hour day of system operation was chosen for investigation purposes. The excellent verification result of the total volume of water flow from 33 level to the surface mine water dams is shown in Table 9.7.

$TOTAL\ FLOW_{SIMULATED}$	$TOTAL\ FLOW_{MEASURED}$	ERROR
30445 m^3	30508 m^3	0.21%

Table 9.7: Summary of the total daily water pump to the surface

Detailed results of the water flow to the surface are shown in Appendix D. The daily average dam levels of the system were used to verify the dam level predictions made by the simulation program, for the base year simulation. The verification results of the dam water levels are shown in Table 9.8.

LEVEL	MAXIMUM ERROR	AVERAGE ERROR
33	10.33%	2.68%
49	14.78%	8.08%
80 SV2	14.69%	8.71%
80 SV3	14.66%	0.19%
95_A	19.29%	4.09%

Table 9.8: Summary of the base year verification results of the dam levels

From Table 9.8 it is clear that the verification results are satisfactory. Detailed results of the dam levels can be seen in the form of graphs in Appendix D. These verification results show that the trend (dam levels) of the system's operators could be simulated accurately.

The daily average energy usage of the clear water pumps of the reticulation system was used to verify the predictions made by the simulation program. The base year verification results of the total daily energy usage of the various levels, for an average typical day of operation, are shown in Table 9.9.

LEVEL	$TOTAL_{MEASURED}$	$TOTAL_{SIMULATED}$	% ERROR
33	113683 kWh	121513 kWh	6.44 %
49	61894 kWh	58605 kWh	5.31 %
70	21383 kWh	26029 kWh	17.85 %
80	118923 kWh	85877 kWh	27.79 %
95_A	49970 kWh	54154 kWh	7.73 %

Table 9.9: Summary of the total daily energy usage of the various pumps

The error values of 70 level and 80 level are actually reduced in the base year simulation. During these simulations the average daily measured energy consumption was compared to the simulation model's predictions for a typical operational day and not to the schedules of a specific day during the previous verification study. It should be noted that although it was possible to simulate the trends of the system, there was still a human factor involved (sometimes the operators would operate their stations outside their normal trends).

The verification results of the energy usage of the various levels are quite satisfactory. The most important result for the purposes of this study is the total energy usage of the entire pumping reticulation system, i.e. the joint total energy usage of all the levels are investigated. The total daily energy usage of the entire pumping reticulation system is given in Table 9.10.

$TOTAL_{MEASURED}$	$TOTAL_{SIMULATED}$	% ERROR
365853 kWh	346178 kWh	5.38 %

Table 9.10: Summary of the total daily energy usage of the entire pumping system

From Table 9.10 it is clear that the base year verification of the total daily energy usage of the entire pumping reticulation system is satisfactory. These verification results show that the energy using equipment in the system can be simulated accurately for an average day of system operation, and that it was possible to simulate the philosophy of the system's operators accurately.

9.3 POTENTIAL FOR LOAD SHIFTING

9.3.1 Introduction

ESKOM is moving towards a price structure for electricity that reflects the real cost of generation, this structure is called real time pricing (RTP). ESKOM developed various cost structures to coax customers to manage their electricity demand (DSM), to use more energy in off-peak periods (low cost of generation) and less energy in peak periods (high generation costs). However, many industries do not effectively use these price offerings from ESKOM.

The best, if not the only way, to effectively use the ESKOM price structures without affecting normal operation, is the implementation of control strategies to optimally operate the system within the price structure boundaries, i.e. the potential for load shifting has to be investigated. The impact on the rest of the system and mine, however, has to be investigated to ensure the safety of the mineworkers. Using the simulation model verified in the previous section, the various impacts on the system can be studied.

Various simulations were executed to find the potential period of load shifting per operational day. These investigations were made possible by implementing control in the simulation model to study the DSM potential. The main impact of importance, the dam levels, had to be carefully monitored during this investigation. It was necessary to ensure that the dams have a large enough capacity, to make it possible to shift load.

9.3.2 Procedures

The following procedures were followed to ensure the successful investigation of the potential for load shifting in the pumping reticulation system of a gold mine:

1. The total period (total hours) of possible load shifting, without flooding any of the dams of the system, had to be determined. There must also still be a certain amount of emergency capacity for use during power or pump failures.

2. There is no current control on any of the system components, and the operators of the system used existing monitoring equipment (of dam levels) to determine when water should be pumped from the underground workings. Controllers were implemented into the simulation model to ensure that the pumps could be switched on, or off, at the pre-determined and specified times. By monitoring the dam levels the pumps could also be controlled to ensure that a certain level would not be exceeded. After the final implementation of the various controllers, various simulations were studied.

3. A graphical presentation of the active pumps of the entire system was then compared to the original actual measured pumping status of the system.

4. The dam levels of all the dams were graphically monitored to ensure that they never reached their maximum capacities and still allowed for emergency capacity.

9.3.3 Load Shifting Investigation

The verification study of the previous section provided us with the necessary evidence of the accuracy of the simulation model. In this section the simulation model was used to investigate various load shifting options, while the dam levels for each level were monitored to ensure that none of the dams reached their maximum capacity (emergency capacity).

Various investigations showed that it was possible to shift maximum load for a period of five hours per day, with dam levels within acceptable limits. These five hours of load shifting could either be consecutive or could be separated into two sessions for 3 hours and then again for 2 hours. It was decided to shift load for the above mentioned time periods during this study.

First operating strategy:

The first control strategy implemented into the simulation model was the de-activation of all the pumps of the entire system for the specified consecutive five hours (07H00 to 12H00), while ensuring that no dams would overflow. This was done to find the maximum load that could be shifted. The total active pumps of the entire system and the various dam levels are shown in the following figures.

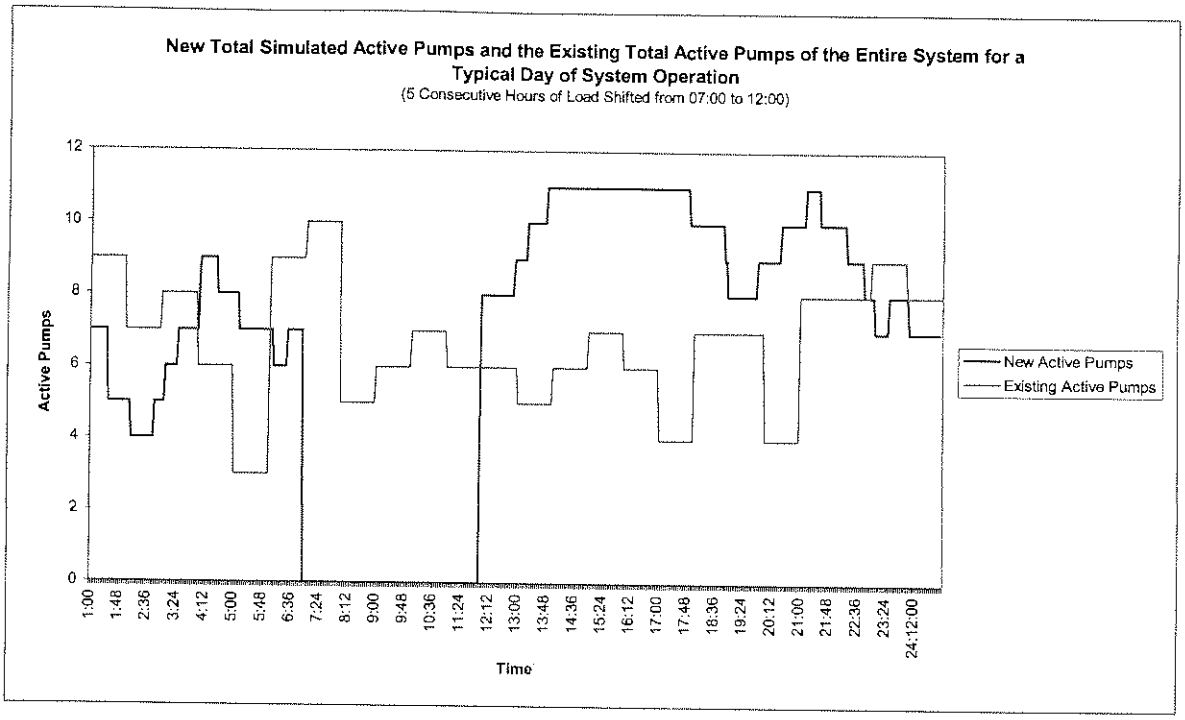

Figure 9.14: Total active pumps for the first operating strategy

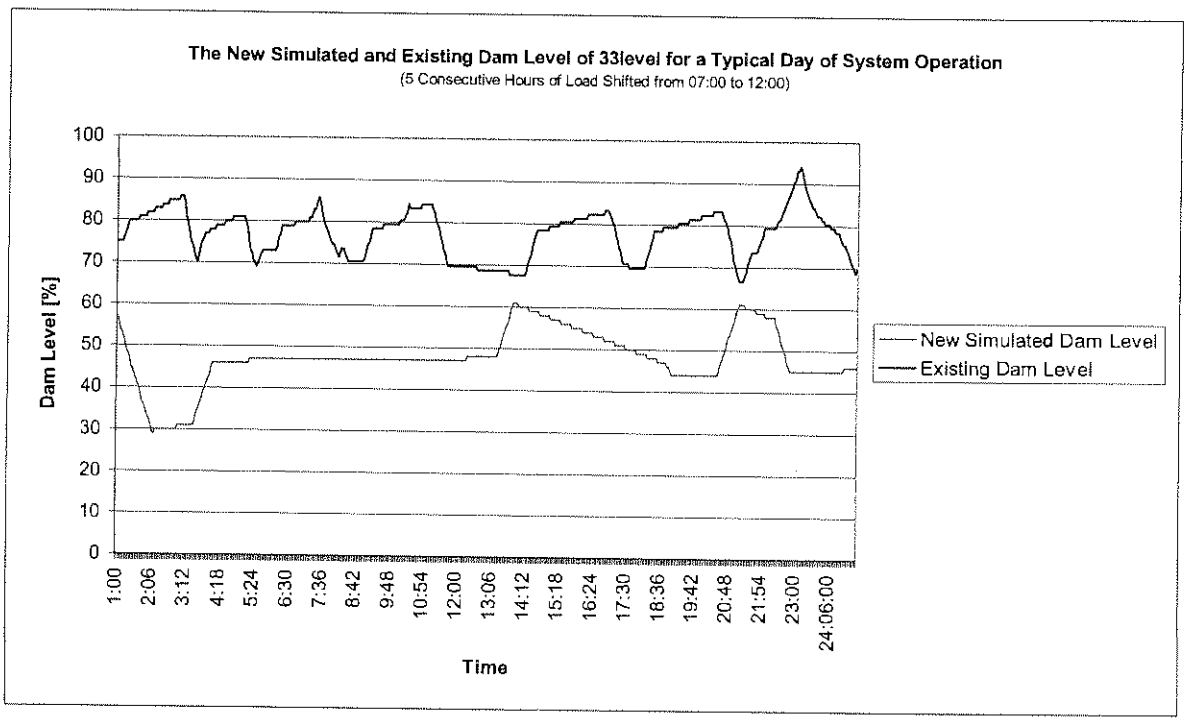

Figure 9.15: Dam levels of 33 level with the first operating strategy implemented

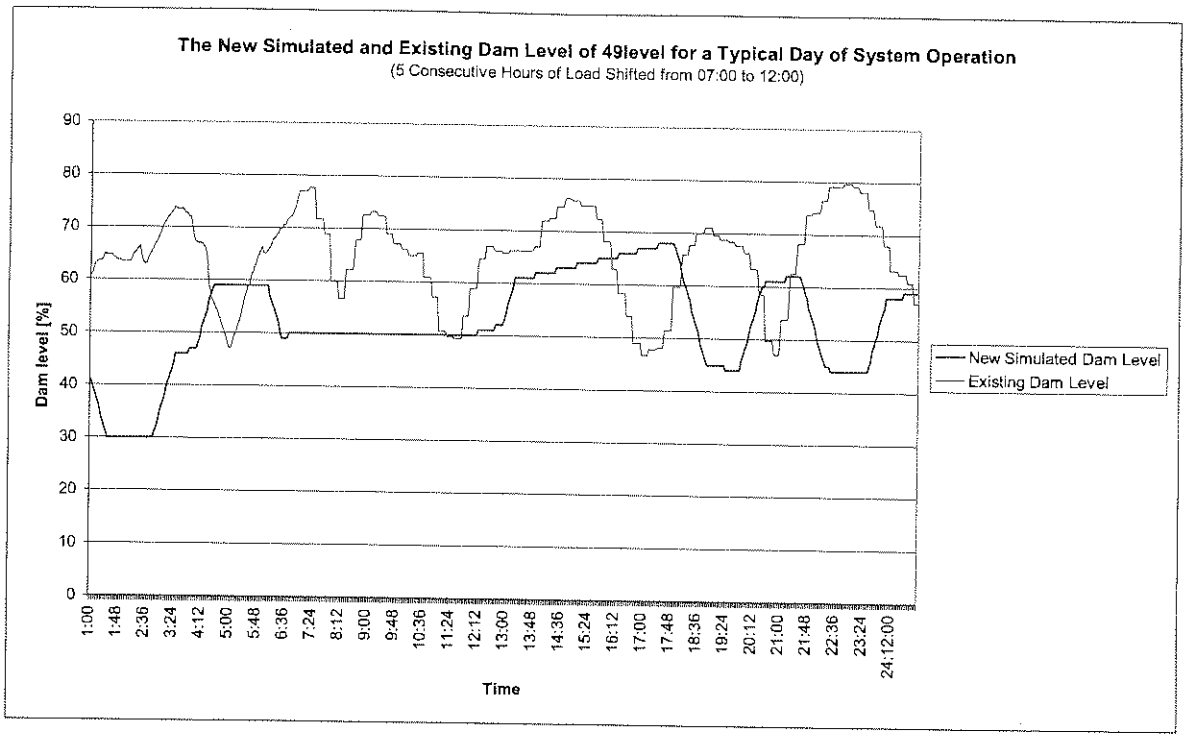

Figure 9.16: Dam levels of 49 level with the first operating strategy implemented

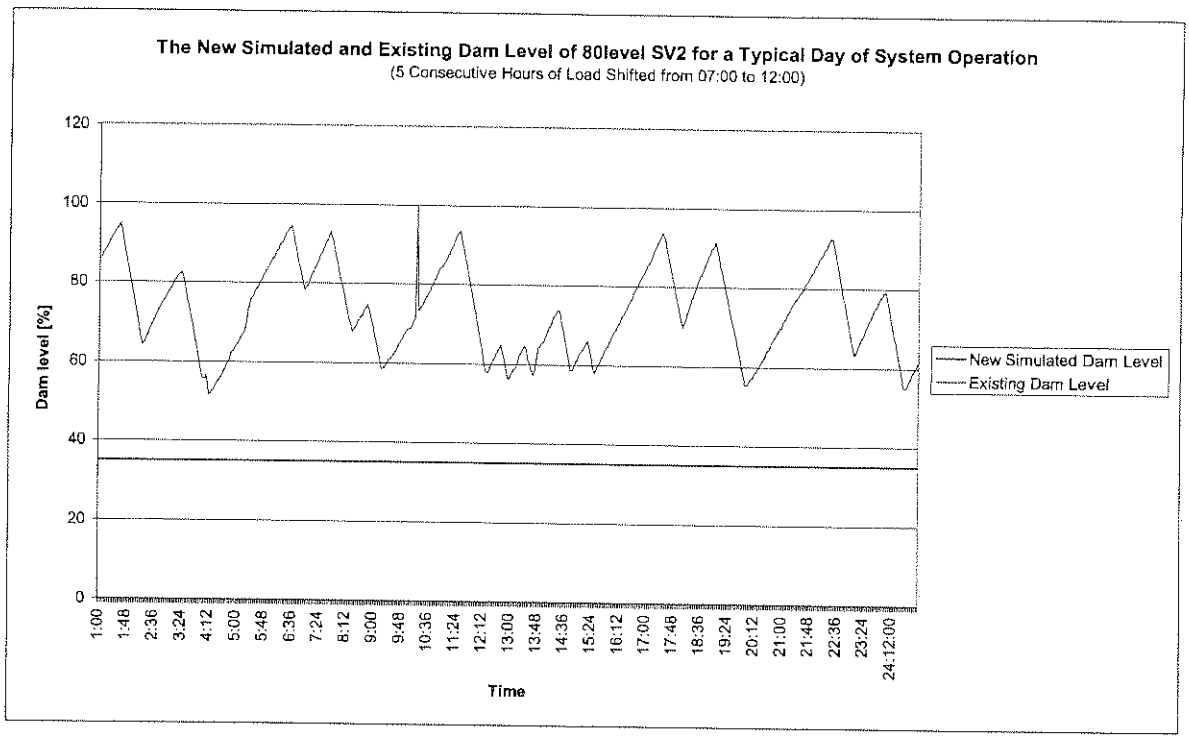

Figure 9.17: Dam levels of 80 level SV2 with the first operating strategy implemented

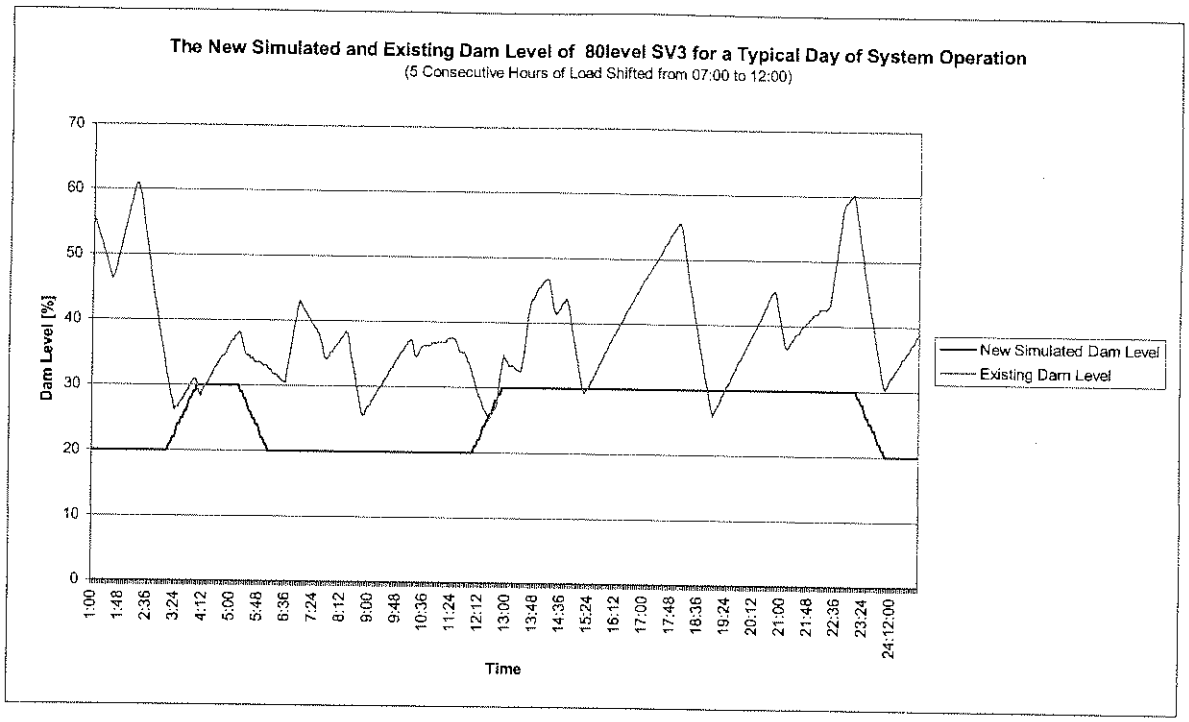

Figure 9.18: Dam levels of 80 level SV3 with the first operating strategy implemented

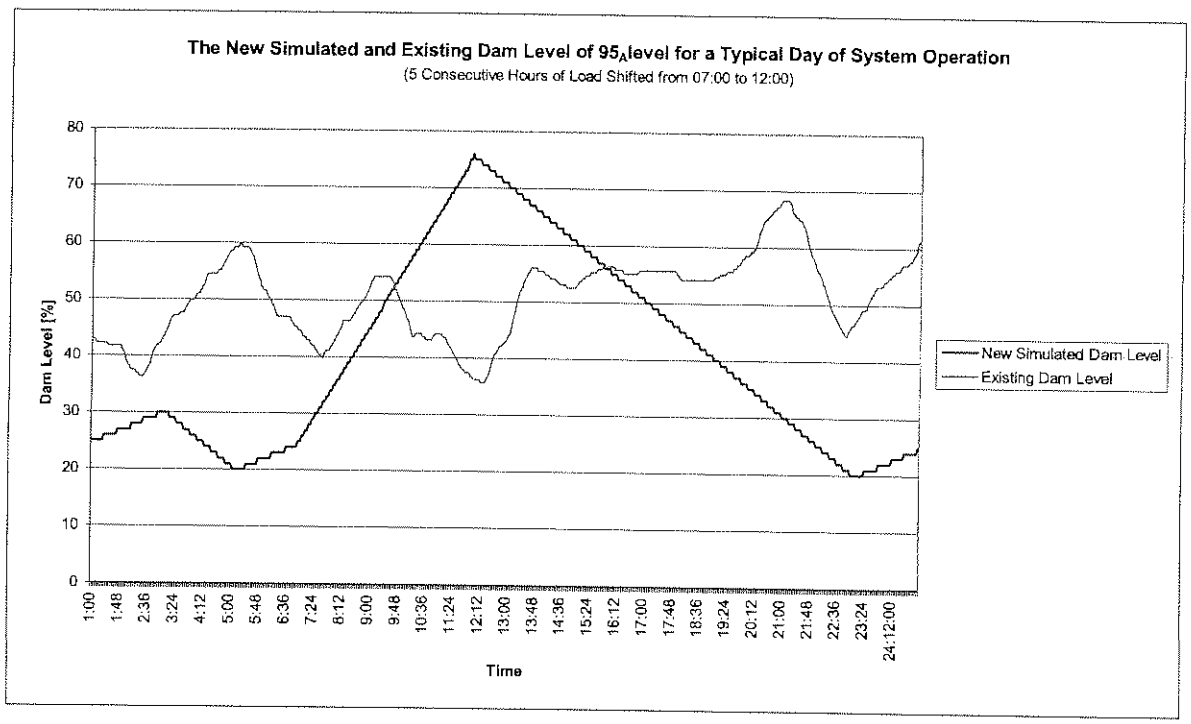

Figure 9.19: Dam levels of 95A level with the first operating strategy implemented

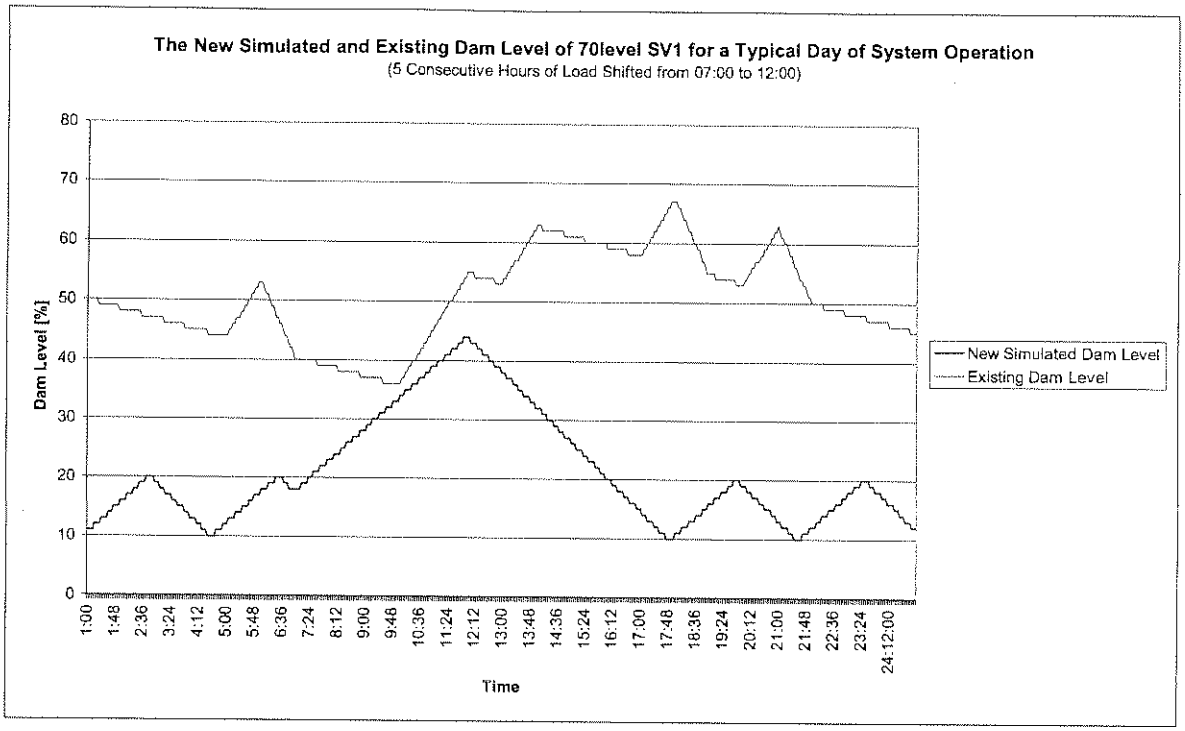

Figure 9.20: Dam levels of 70 level with the first operating strategy implemented

The simulation showed that it was possible to shift a energy load of approximately 70002 kWh while keeping all of the dam levels well within acceptable standards, with a maximum demand shift of 14 MW over five hours. The graphs show the percentage level of the full capacity of the total install dam capacity of each level, except for 80 level. It should be noted that it was decided to use 9 Ml, of the total 23 Ml installed dam capacity on 80 level, for emergency purposes. Table 9.11 shows the total energy usage of the system for a typical day of system operation.

$TOTAL_{EXISTING}$	$TOTAL_{NEW\ (SIMULATED)}$	% ERROR
365853 kWh	346955 kWh	5.45%

Table 9.11: Summary of the total pump energy usage for the first operating strategy

Second operating strategy:

The following figures display the simulated total active pumps and various dam levels for the simulation where the total 5 hours of load shifted, was divided into two periods, from 07H00 to 10H00 and from 18H00 to 20H00. This was done to illustrate the possibility of shifting maximum load at different periods of the day.

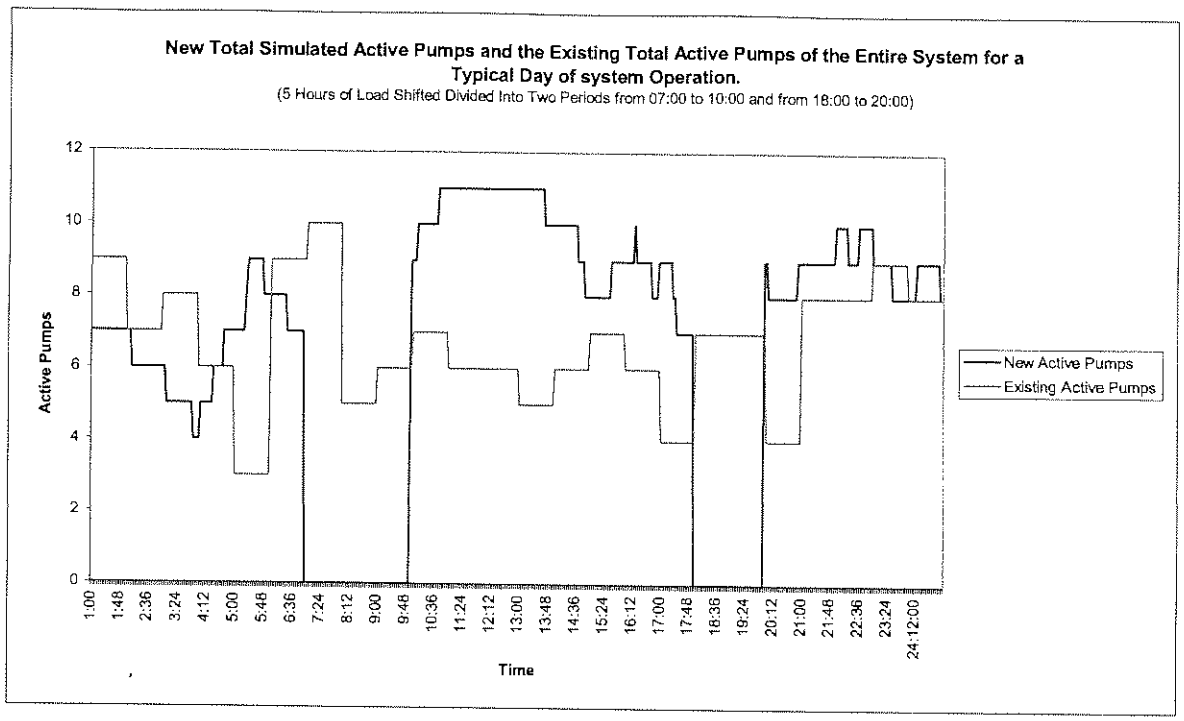

Figure 9.21: Total active pumps for the second operating strategy

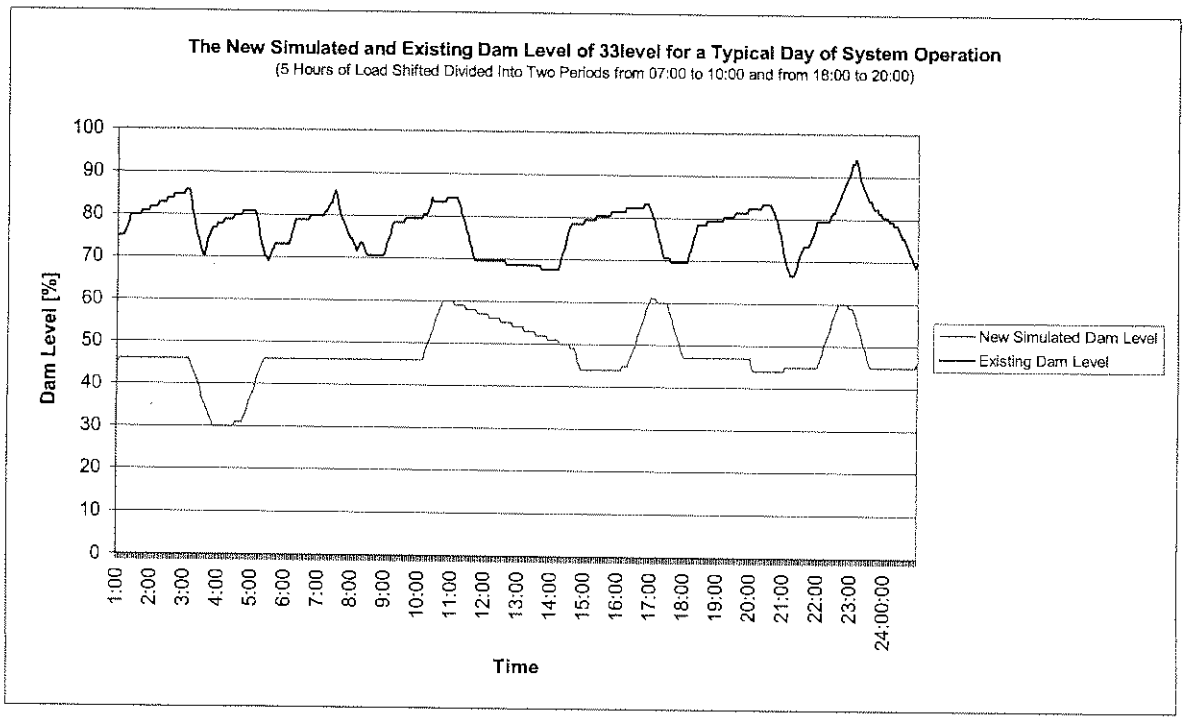

Figure 9.22: Dam levels of 33 level with the second operating strategy implemented

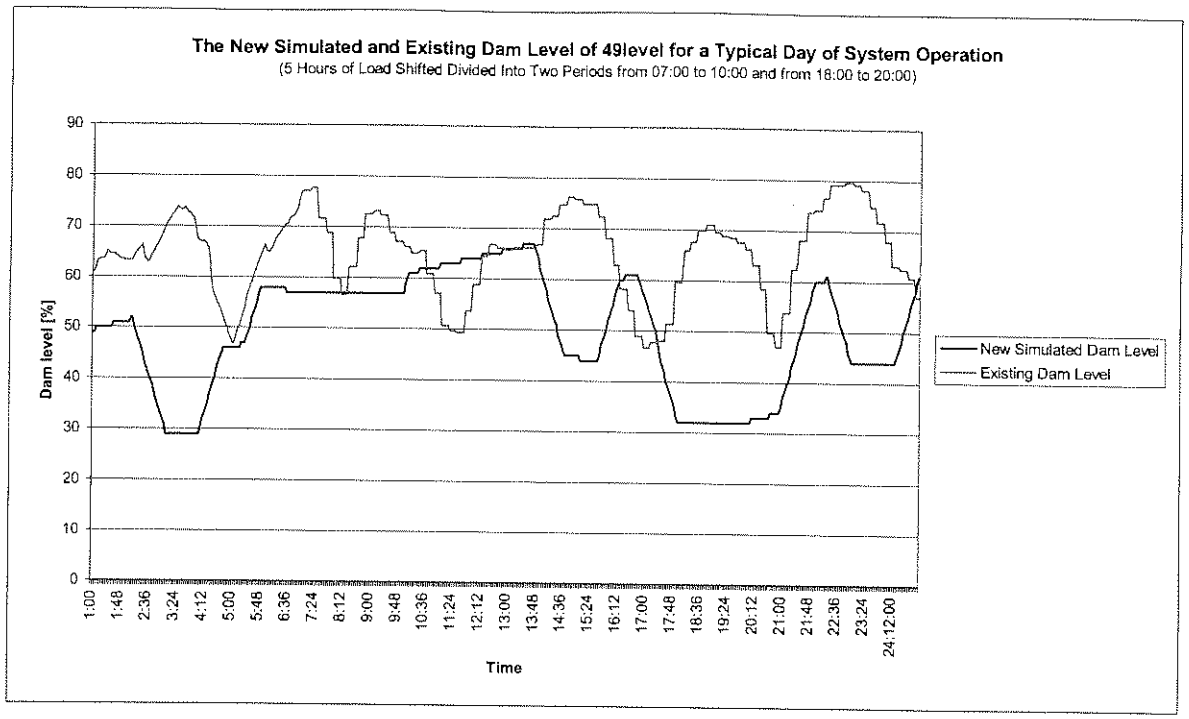

Figure 9.23: Dam levels of 49 level with the second operating strategy implemented

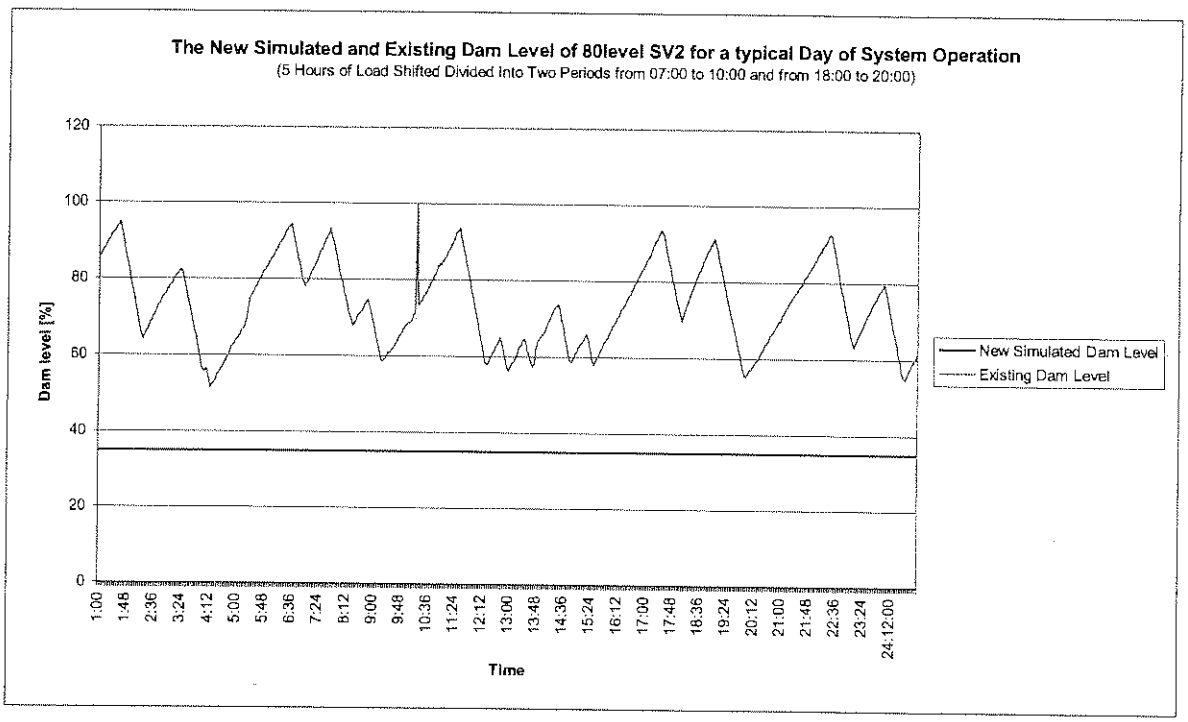

Figure 9.24: Dam levels of 80 level SV2 with the second operating strategy implemented

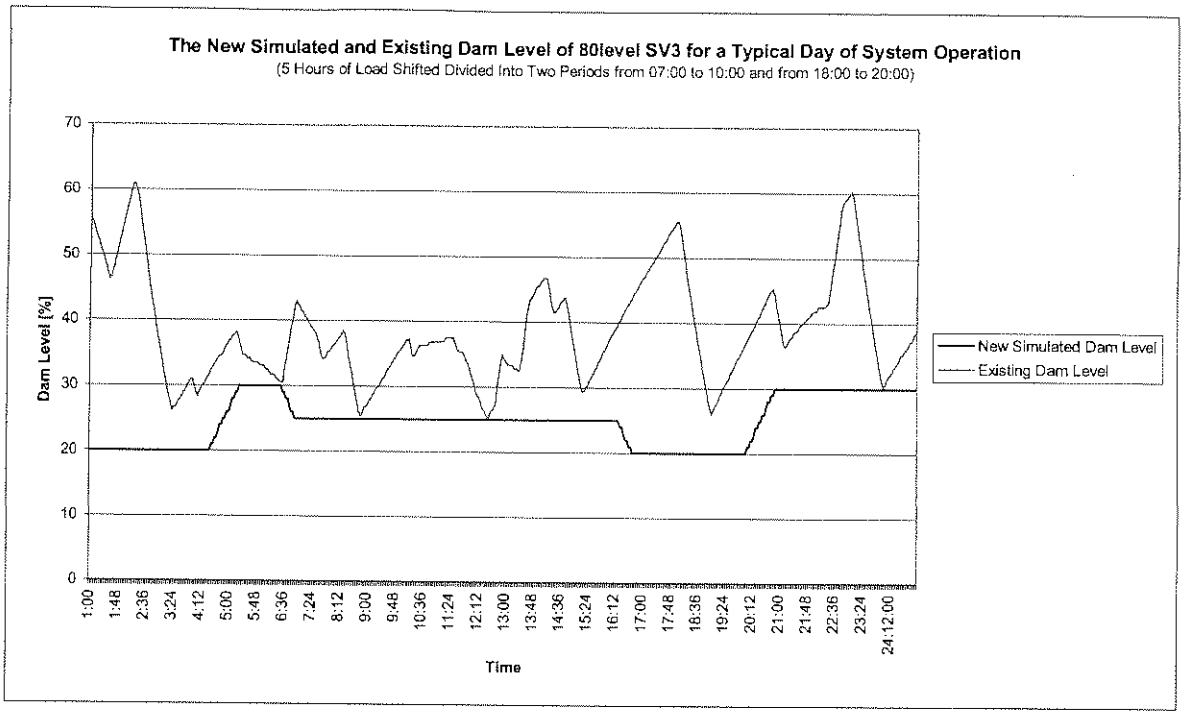

Figure 9.25: Dam levels of 80 level SV3 with the second operating strategy implemented

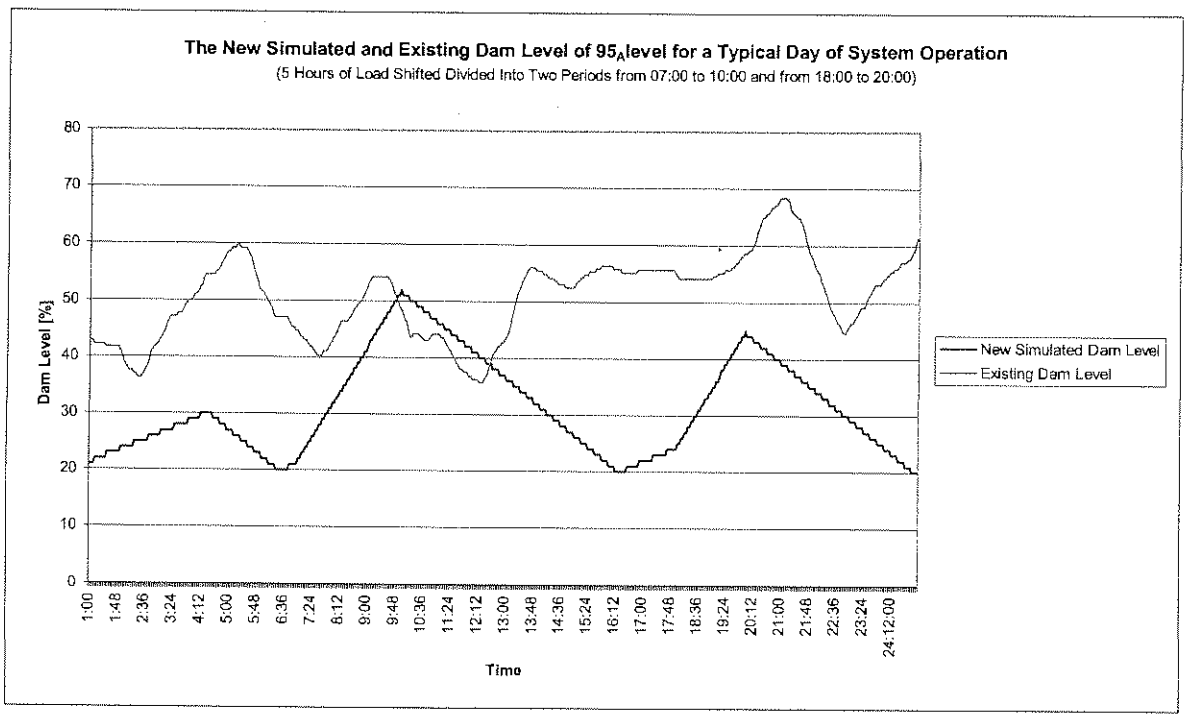

Figure 9.26: Dam levels of 95A level with the second operating strategy implemented

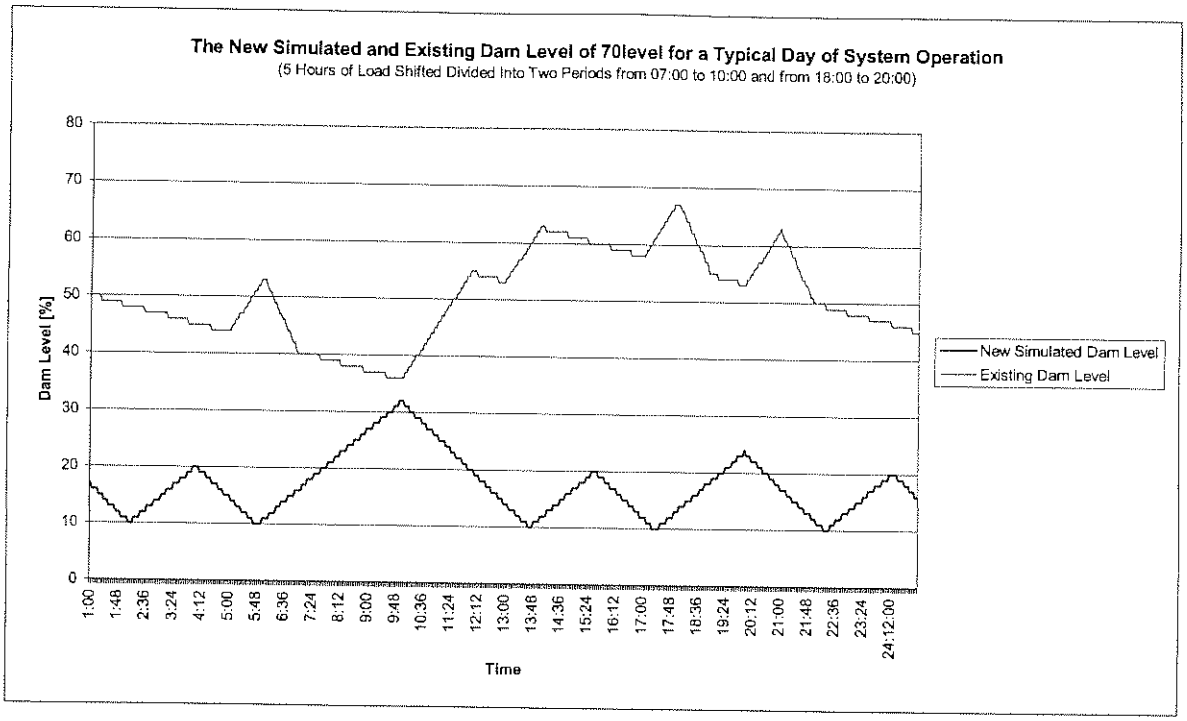

Figure 9.27: Dam levels of 70 level with the second operating strategy implemented

The simulation showed that it was possible to shift a total energy load of approximately 68884.01 kWh while keeping all of the dam levels well within acceptable standards, with a maximum demand shift of 13.77 MW over five hours (divided into two periods). Table 9.12 shows the total energy usage of the system for a typical day.

$TOTAL_{EXISTING}$	$TOTAL_{NEW\ (SIMULATED)}$	% ERROR
365853 kWh	343049 kWh	6.65%

Table 9.12: Summary of the total pump energy usage for the second operating strategy

The effect that these two operating strategies have on the daily maximum demand (MD) of the total pumping reticulation system, for a typical day of system operation, are shown in Table 9.13.

LOAD SHIFT	ORIGINAL MD	NEW MD	% INCREASE
One-period	18.49 MW	23.62 MW	21.72%
Two-periods	18.55 MW	23.84 MW	22.19%

Table 9.13: Summary of daily maximum demand (MD) of both operating options.

For the purpose of this study, the maximum possible load that could be shifted from the system was investigated (it was found to be 14 MW), and two control strategies were studied. It should be noted that other control strategies could also be studied, i.e. various load shifting options could be studied according to a specific tariff structure of ESKOM.

A specific tariff structure could for example require the shifting of load from certain peak times, but for a longer period than 5 hours. The effect that these kinds of RTP strategies would have on the rest of the system could easily be investigated. Examples of options are shown in Figure 9.28.

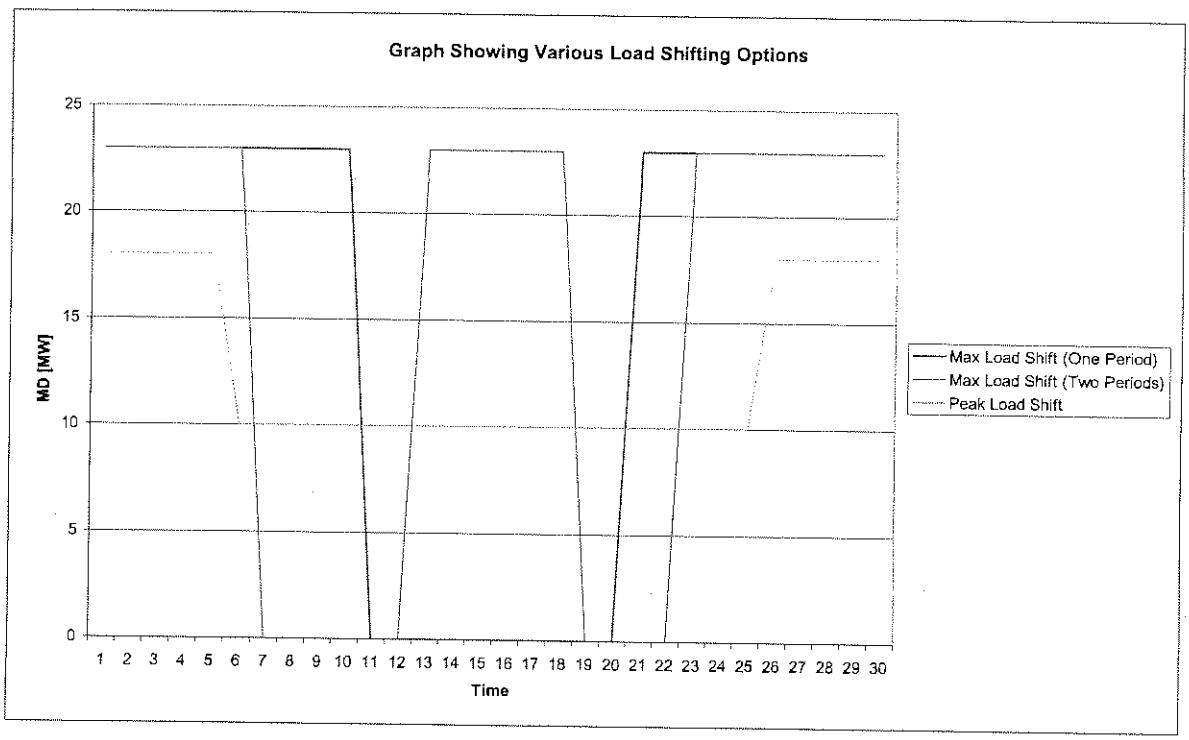

Figure 9.28: Load shifting options

9.4 CONCLUSIONS

The entire pumping reticulation system of a specific gold mine was simulated with the extended integrated simulation tool. The predictions made by the tool were verified with actual measured data from the system, such as dam levels, active pumps, water flows and energy usage.

Satisfactory results were obtained from the verification study for a typical specific day. The total daily volume of water, from the underground workings to the surface mine water dams, were verified with an error of 1%. The various dam levels of the system were verified with average errors ranging from 0.61% to 5.89% for a typical specific day of system operation. The total energy usage for a typical specific day verified with an error of 10.97% against the actual measured data.

A base year simulation was also conducted to try and determine the trend in the system's operation. By using control parameters on the dam levels, the philosophy of the system's operators was simulated. The predictions made by these simulations were verified against the actual measured data of an average typical day of system operation. The total daily volume of water, from the underground workings to the surface mine water dams, were verified with an error of 0.21%. The various dam levels of the system were verified with average errors ranging from 0.19% to 8.71% for an average typical day of operation. The total daily energy usage for this simulation of an average typical day verified with an error of 5.38% against the actual measured data.

The simulation program was also used to conduct various energy studies. Various investigations showed that it was possible to shift a energy load of approximately 70002 kWh from the daily system operation without flooding any underground workings, with a maximum demand shift of 14 MW over a period of five hours. Two operating strategies were investigated: the maximum load could be shifted for five consecutive hours, or could be divided into more than one period and applied at different times of the day.

The most important parameter during the energy studies was the dam levels. These dam levels had to be constantly monitored, to ensure that none of the dams reached their maximum capacities. It is for this reason that an extra emergency dam capacity of 14 Ml was made available on the critical 80 level. It was found that none of the dams reached their maximum capacities during the study.

There is sufficient opportunity, using the existing equipment with minor adjustments, to shift the load for a few hours. This is mainly due to the available storage capacity of the dams. This is fairly standard practice in most mines and it can therefore be concluded that most

mines will be able to shift its pumping system's load by a couple of hours, should it be needed for RTP purposes.

9.5 REFERENCES

[1] CF Kern, Real Time Pricing Directive, Key Customer Marketing, ESKOM, May 1998.

CHAPTER 10

CLOSURE

In this chapter a brief summary of the most important results and recommendations for future work are given.

10.1 SUMMARY OF THIS PART

The potential to use an integrated building and system simulation tool in thermal system applications other than building applications was realised. It seemed possible to extend a dynamic component-based building simulation tool with new demand side models to allow the simulation of mining and industrial thermal systems. The program QUICKcontrol was therefore extended with new thermal models commonly used in the mining industry.

Two case studies were performed with the extended tool to illustrate its applicability in other thermal systems than building systems. The potential for Demand Side Management (DSM) on two of the biggest thermal systems found on deep mines was investigated. This included a surface cooling plant and an underground clear water pumping system.

Satisfactory results were obtained during the two investigations to utilise this extended tool with confidence in practice. With more extension to the tool it should be possible to investigate the potential for energy cost saving in any other thermal industrial applications.

10.2 RECOMMENDATIONS FOR FUTURE WORK

During this part of the study a number of problems were encountered. These will be discussed here as a basis for future work. During the duration of the case study conducted in chapter 8 the following major problem was encountered: It was very difficult to obtain stable solutions with the tool when re-circulation of water was implemented for chilled water temperature control.

The simulation model was therefore simplified and the simulations were performed without any return loops. It did not have an influence on this specific application since water is only returned when the ambient temperature exceeds 30 °C. However, this will cause problems in other complex thermal systems with a number of return loops.

For example, when an entire mine Ventilation and Cooling system must be solved in an integrated fashion, a large number of loops will have to be solved. The simulation procedure must therefore be very stable for complex networks.

Based on the previous discussion the following is suggested for future work:

- New demand side component models (stopes, haulages, shafts, ice-makers, ice transportation, pelton wheels and industrial chemical processes) must still be developed and implemented into the program.
- A new stable simulation procedure must be developed to solve the conditions of any complex system with a large number of closed-loops in an integrated fashion.

10.3 CONCLUSIONS

In this part of the study the biggest shortcoming of the existing simulation tool QUICKcontrol was again identified. This is to perform stable simulations of large complex systems with a large number of closed-loops.

A new simulation platform will have to be developed to perform efficient stable simulations as standard procedure in practice. The success of any integrated system simulation tool depends on the easiness of use and the stability of its solutions.

With a new developed stable simulation platform, the simulation of entire mine VC systems in an integrated fashion should be possible in the feature. The investigation of energy cost savings on the demand side of the system (underground heat exchangers) and not only the supply side (cooling plants) as illustrated here in this study, will be possible.

APPENDIX A

SIMULATION MODELS

This appendix presents all the existing simulation models in QUICKcontrol and typical system curves of certain equipment.

A.1. PUMPS

A.1.1 Assumptions:

- No psychrometric property relations are needed to calculate the liquid density. The density is taken throughout as $\rho_l = 1000$ kg/m^3. Similarly the specific heat at constant pressure will be taken throughout as $c_{pl} = 4187$ J/kg°C.
- The drive motor may not be situated within the liquid flow.
- The dynamic pressure difference over the pump is assumed to be negligible.

A.1.2 Parameters:

a_j Correlation coefficients for the K_h versus K_f relation with j = 0 to 2.

b_j Correlation coefficients for the η_{pump} versus K_f relation with j = 0 to 2.

A.1.3 Inputs:

A.1.3.1Simulation:

m_l Mass flow rate of liquid at inlet [kg/s].

T_{li} Temperature of liquid entering at inlet [°C].

A.1.3.2Interface:

D Rotor diameter [m].

N Rotational speed of the pump [rpm].

η_{motor} Efficiency of the drive motor.

H Pressure head [m].

q Flow rate [kg/s].

η_{pump} Pump efficiency.

A.1.4 Outputs:

dP_l Static pressure rise [Pa].

T_{le} Temperature of liquid leaving at outlet [°C].

Pwr Pumping power required [W].

A.1.5 Internal variables:

H_1 Extra pressure head point [m].

H_2 Extra pressure head point [m].

K_f Dimensionless flow coefficient.

K_h Dimensionless pressure head coefficient.

η_{pump} Efficiency of the pump.

η_1 Extra efficiency point.

η_2 Extra efficiency point.

Q_l Rate of heat gain to the liquid [W].

A.1.6 Explicit equations:

Three different pressures and efficiencies at three different flows are needed to calculate the correlation coefficients. A flow variation of 20% above and below the interface input value is assumed. The extra points are then calculated as follow:

$$H_1 = a_h(0.8q)^2 + b_h(0.8q) + c_h$$
$$\eta_1 = a_\eta(0.8q)^2 + b_\eta(0.8q) + c_\eta$$
$$H_2 = a_h(1.2q)^2 + b_h(1.2q) + c_h$$
$$\eta_2 = a_\eta(1.2q)^2 + b_\eta(1.2q) + c_\eta$$

with

$a_h = -0.63125$

$b_h = 1.18125$

$a_\eta = -0.06188$

$b_\eta = 0.33625$ for $0 < q < 3$.

$a_h = -0.25914$

$b_h = 0.591667$

$a_\eta = -0.01816$

$b_\eta = 0.190308$ for $3 < q < 7.5$.

$a_h = -0.3248$

$b_h = 3.736$

$a_\eta = -0.00648$

$b_\eta = 0.133$ for $7.5 < q < 15$.

$a_h = -0.100$
$b_h = 2.197$
$a_\eta = -0.00507$
$b_\eta = 0.159$ for $15 < q < 20$.

$a_h = -0.02674$
$b_h = 0.639$
$a_\eta = -0.00089$
$b_\eta = 0.05089$ for $20 < q < 40$.

$a_h = -0.01505$
$b_h = 0.88875$
$a_\eta = -0.00028$
$b_\eta = 0.029263$ for $40 < q < 80$.

$a_h = -0.00164$
$b_h = 0.262$
$a_\eta = -0.000047$
$b_\eta = 0.010467$ for $80 < q < 150$.

These values were calculated as the average values of the coefficients of a wide range of centrifugal pump curves. These results are shown in figures A.1 to A.14. c_h and c_η are now calculated from the one given operating point obtained from the supplier or measurements. This implies only one operating point is needed to obtain the mathematical model of a specific pump.

And

$$c_h = H - (a_h q^2 + b_h q)$$
$$c_\eta = \eta - (a_\eta q^2 + b_\eta q)$$

For each of these three points the K_h and K_f value must be calculated as follow:

$$K_{h1} = \frac{gH_1}{N^2 D^2}$$

$$K_{f1} = \frac{m_{l1}}{\rho_1 N D^3}$$

$$K_h = \frac{gH}{N^2 D^2}$$

$$K_f = \frac{m_l}{\rho_1 N D^3}$$

$$K_{h2} = \frac{gH_2}{N^2 D^2}$$

$$K_{f2} = \frac{m_{l2}}{\rho_1 N D^3}$$

Using these values the correlation coefficients can be calculated as follow:

$$a_2 = \frac{(K_{h2} - K_{h1})(K_f - K_{f1}) - (K_{f2} - K_{f1})(K_h - K_{h1})}{(K_{f2}^2 - K_{f1}^2)(K_f - K_{f1}) - (K_{f2} - K_{f1})(K_f^2 - K_{f1}^2)}$$

$$a_1 = \frac{(K_h - K_{h1}) - (K_f^2 - K_{f1}^2)a_2}{(K_f - K_{f1})}$$

$$a_0 = K_{h1} - K_{f1}a_1 - K_{f1}^2 a_2$$

$$b_2 = \frac{(\eta_2 - \eta_1)(K_f - K_{f1}) - (K_{f2} - K_{f1})(\eta - \eta_1)}{(K_{f2}^2 - K_{f1}^2)(K_f - K_{f1}) - (K_{f2} - K_{f1})(K_f^2 - K_{f1}^2)}$$

$$b_1 = \frac{(\eta - \eta_1) - (K_f^2 - K_{f1}^2)b_2}{(K_f - K_{f1})}$$

$$b_0 = \eta_1 - K_{f1}b_1 - K_{f1}^2 b_2$$

These coefficients can now be used to calculate the necessary outputs with the following explicit equations:

$$K_f = \frac{m_l}{\rho_l N D^3}$$

$$K_h = a_0 + a_1 K_f + a_2 K_f^{\ 2}$$

$$dP_l = K_h \rho_l N^2 D^2$$

$$\eta_{pump} = b_0 + b_1 K_f + b_2 K_f^{\ 2}$$

$$Q_l = \frac{(1-\eta_{pump}) m_l dP_l}{\rho_l \eta_{pump}}$$

$$T_{le} = T_{li} + \frac{Q_l}{m_l c_{pl}}$$

$$Pwr = \frac{dP_l m_l}{\rho_l \eta_{motor} \eta_{pump}}$$

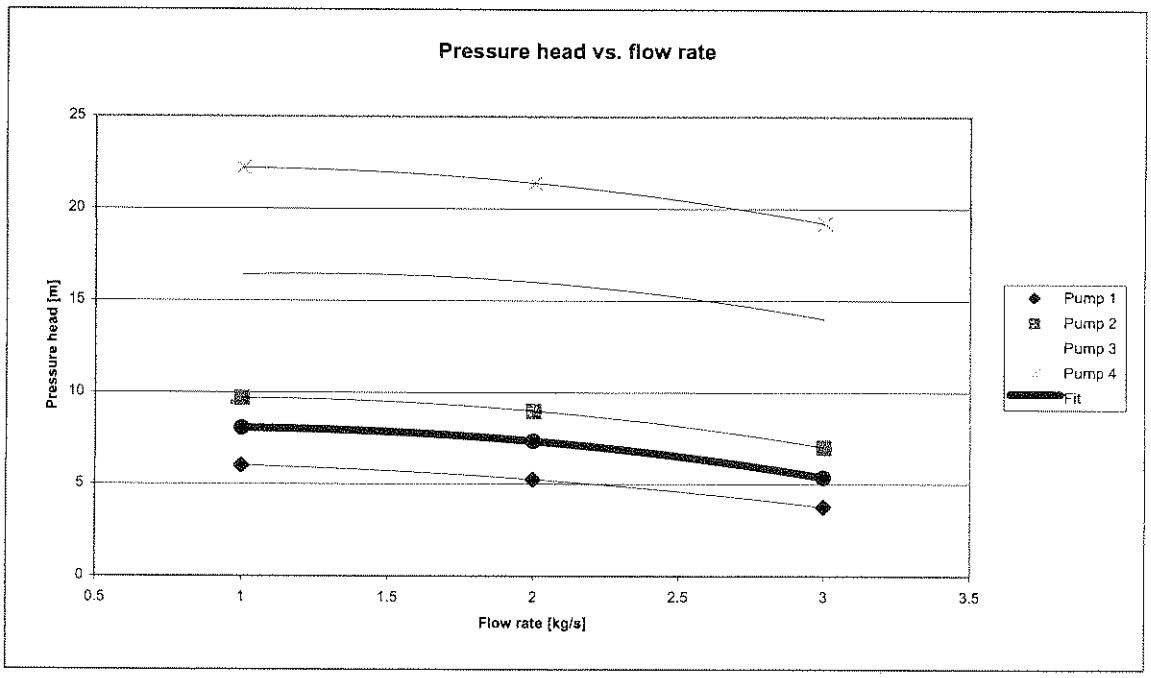

Figure A.1: Pressure head correlation for flow between 0 and 3 kg/s

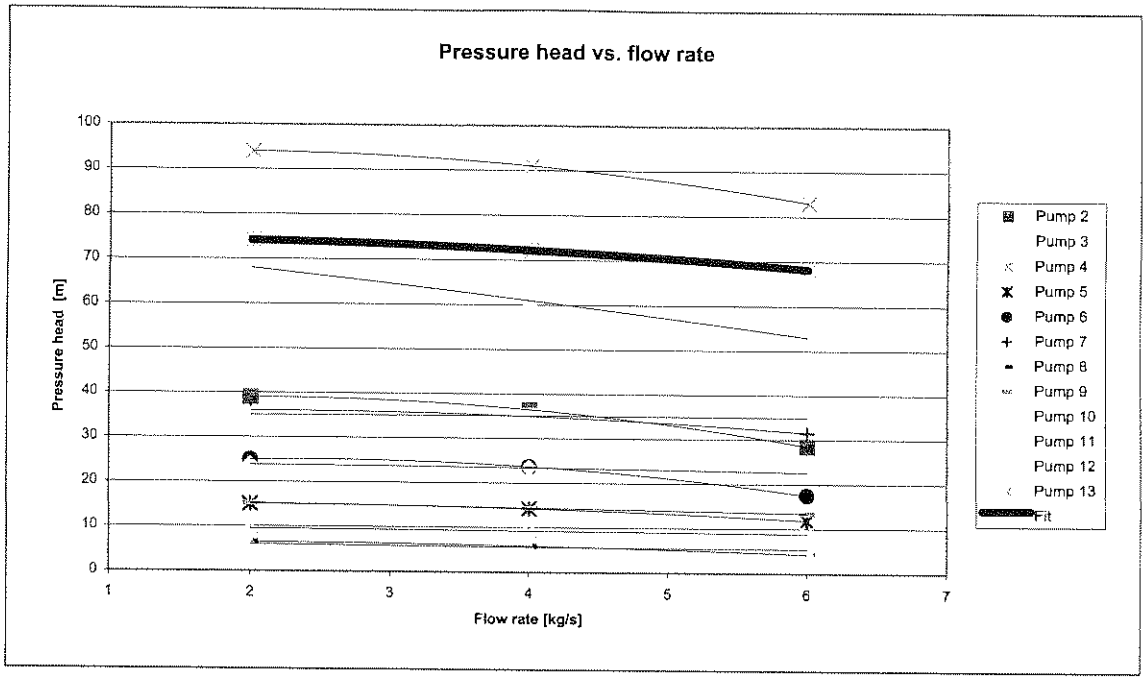

Figure A.2: Pressure head correlation for flow between 3 and 7.5 kg/s

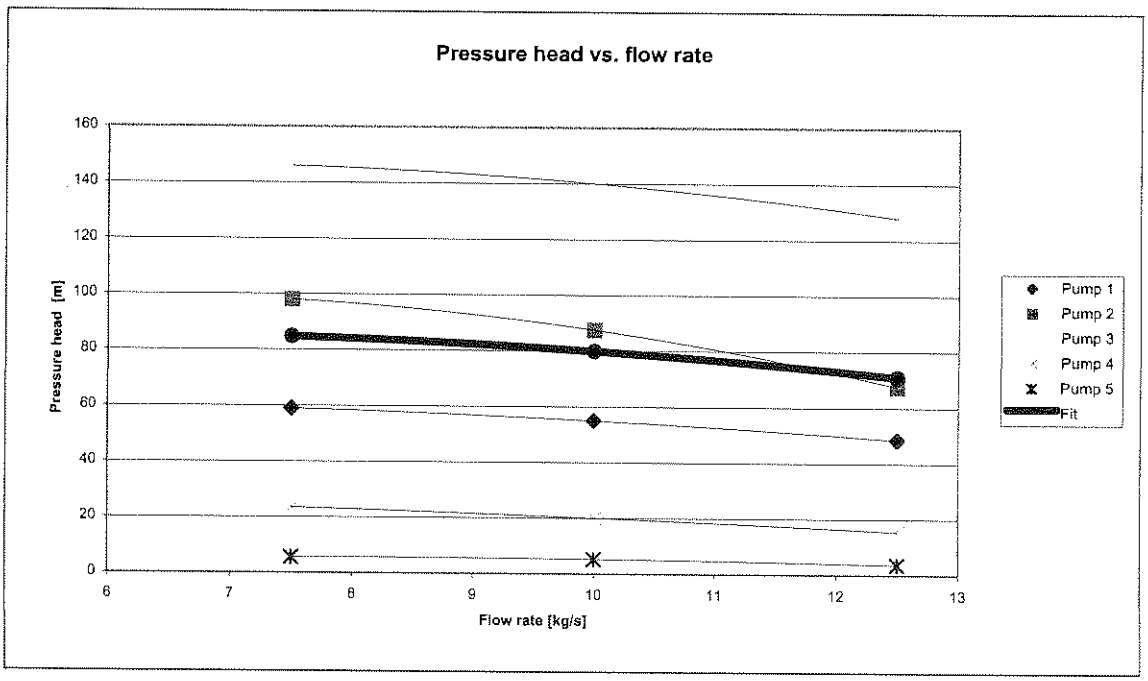

Figure A.3: Pressure head correlation for flow between 7.5 and 15 kg/s

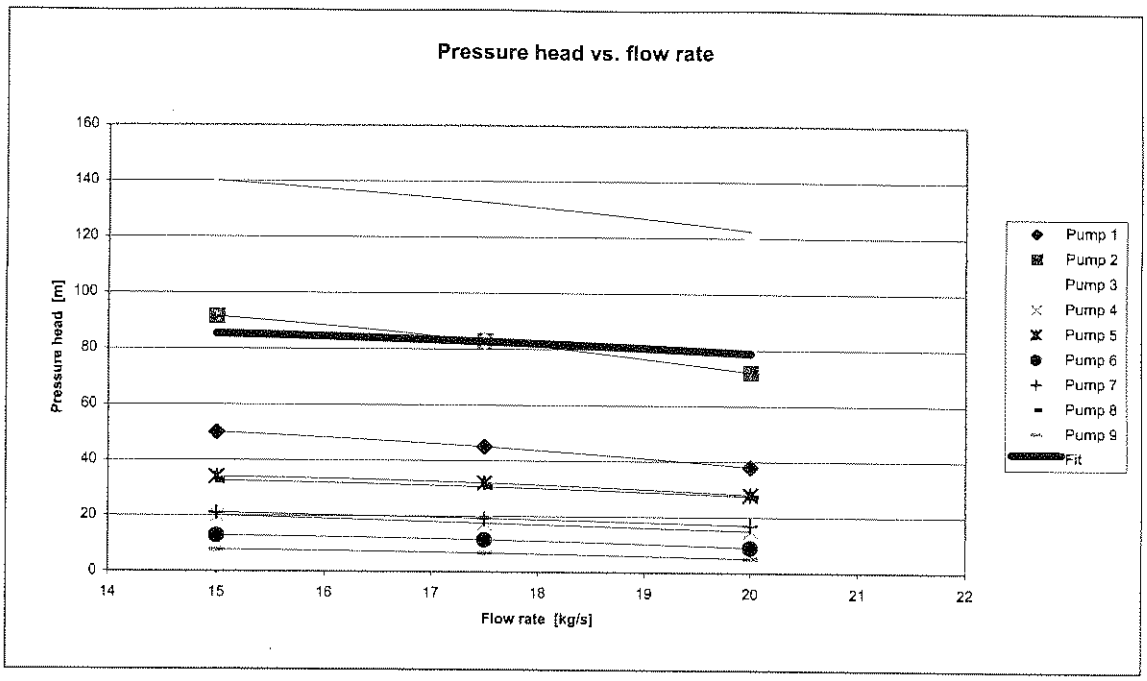

Figure A.4: Pressure head correlation for flow between 15 and 20 kg/s

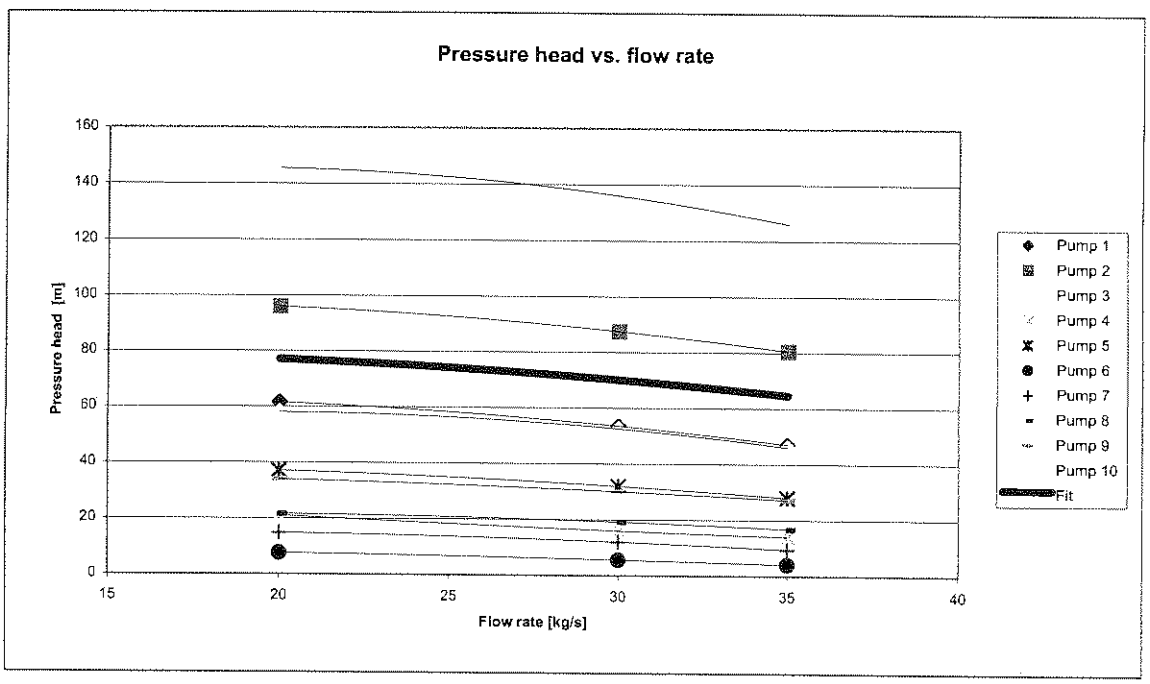

Figure A.5: Pressure head correlation for flow between 20 and 40 kg/s

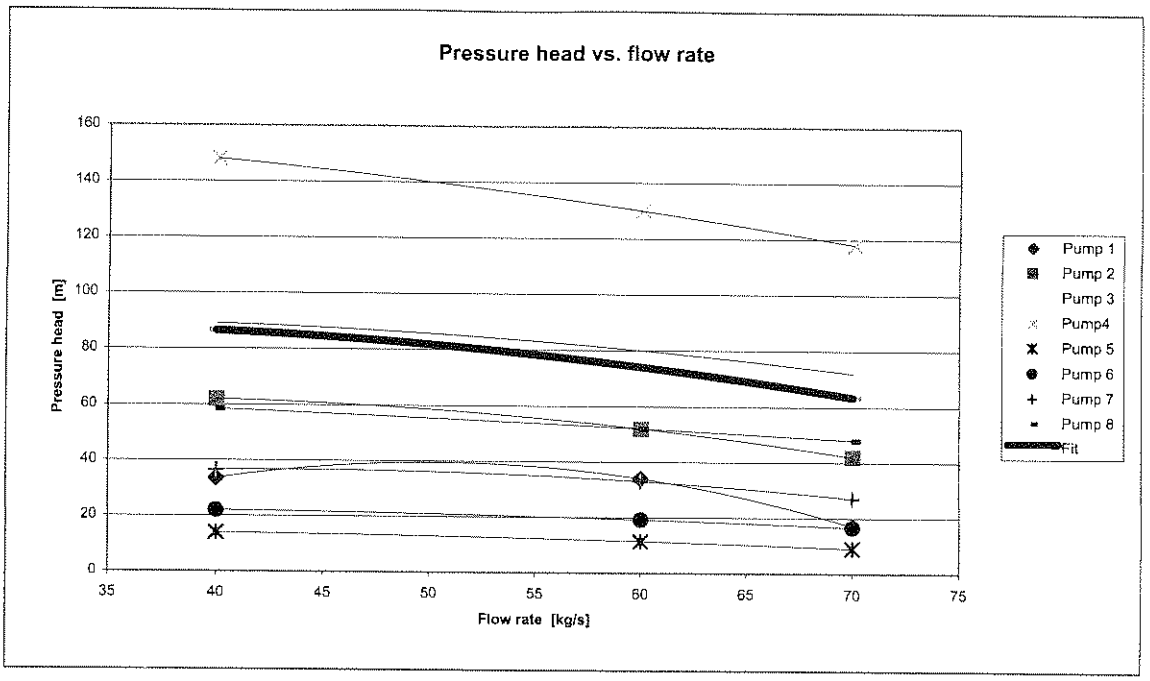

Figure A.6: Pressure head correlation for flow between 40 and 70 kg/s

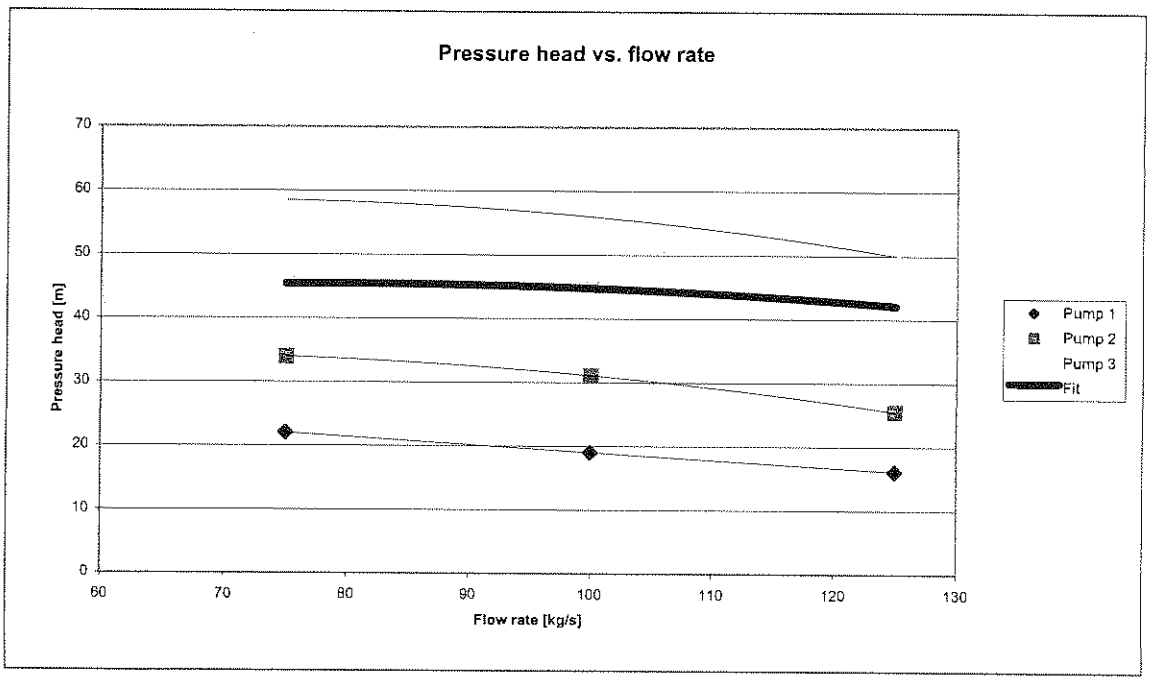

Figure A.7: Pressure head correlation for flow between 70 and 150 kg/s

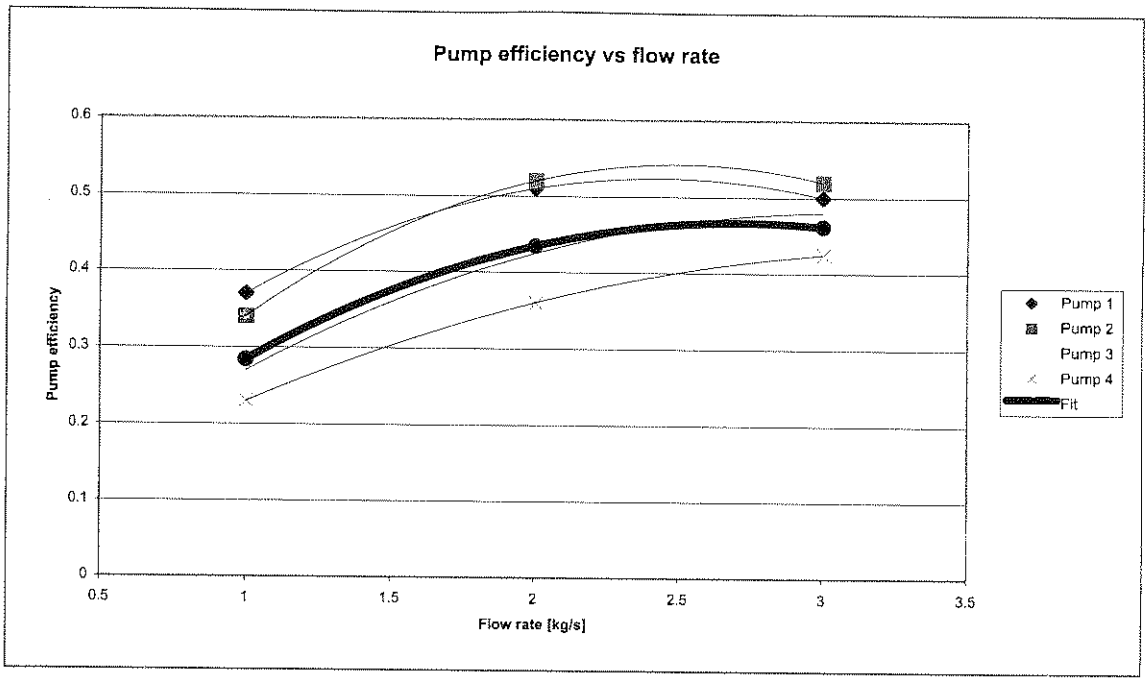

Figure A.8: Efficiency correlation for flow between 0 and 3 kg/s

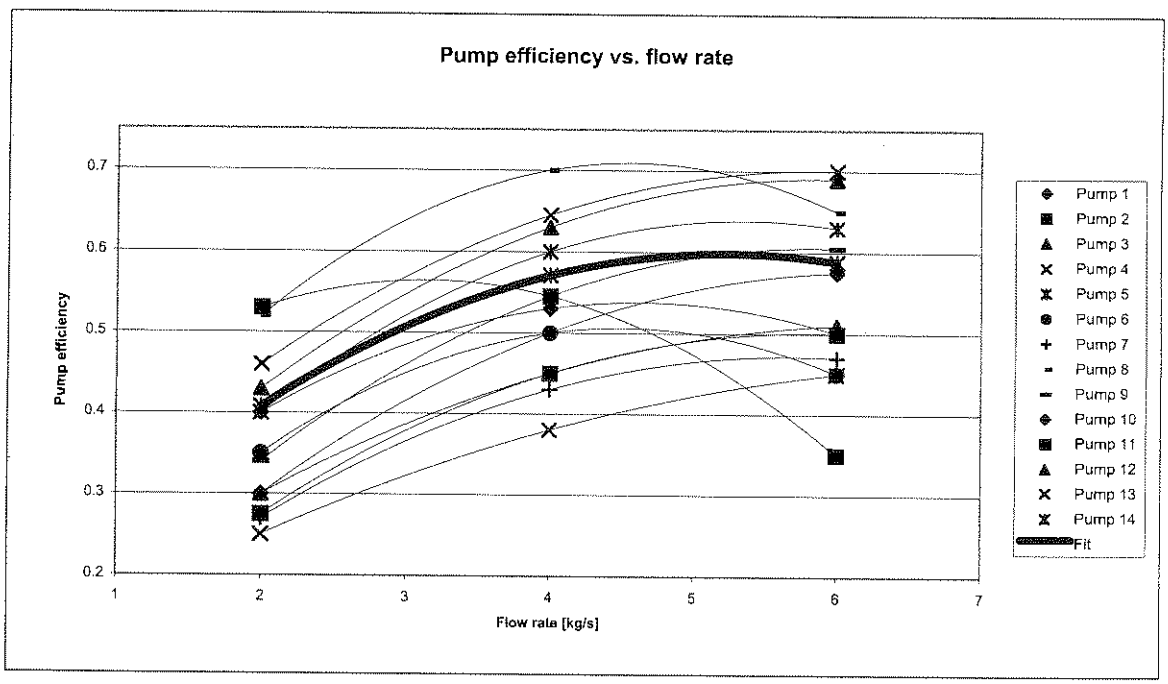

Figure A.9: Efficiency correlation for flow between 3 and 7.5 kg/s

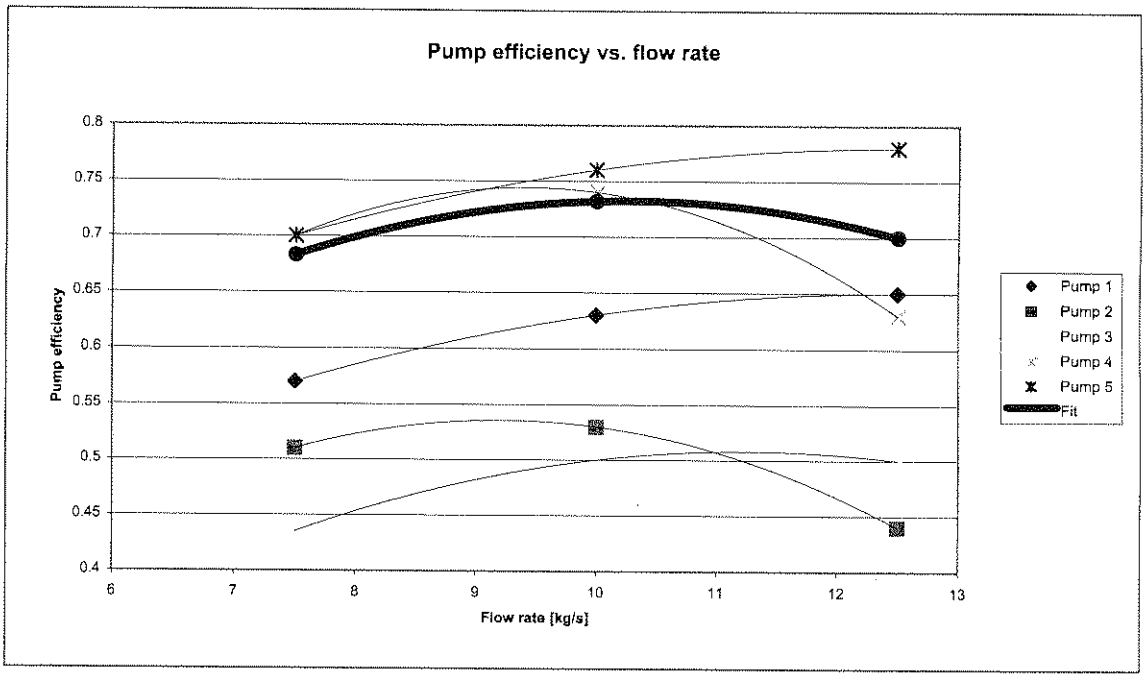

Figure A.10: Efficiency correlation for flow between 7.5 and 15 kg/s

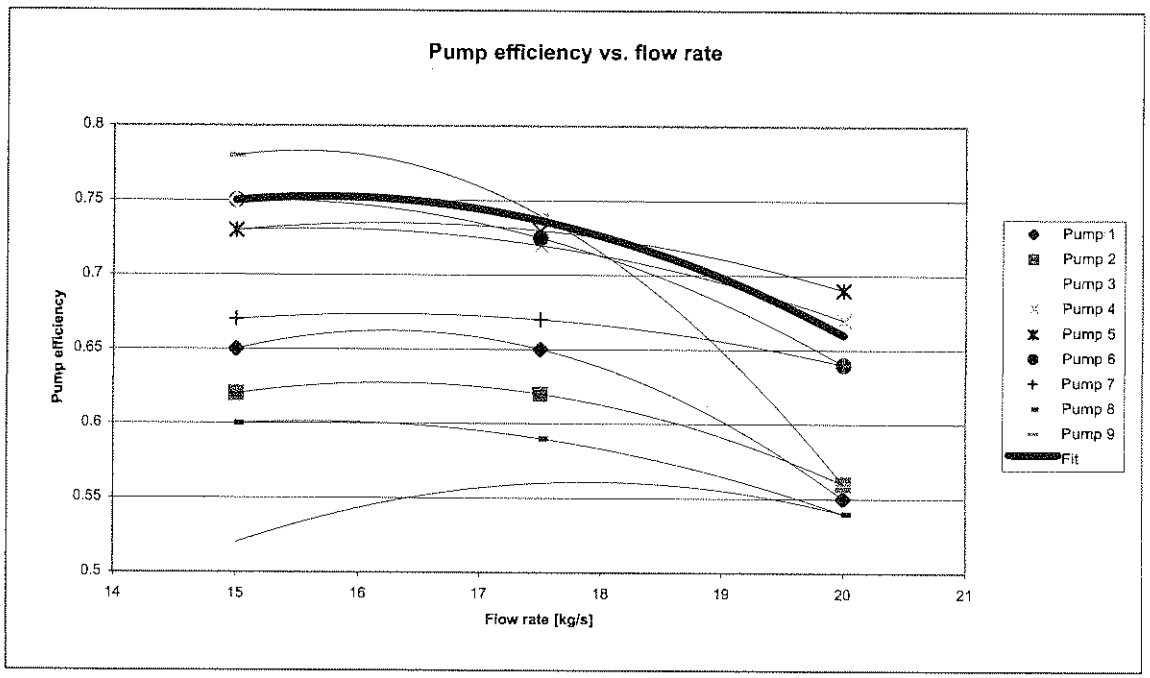

Figure A.11: Efficiency correlation for flow between 15 and 20 kg/s

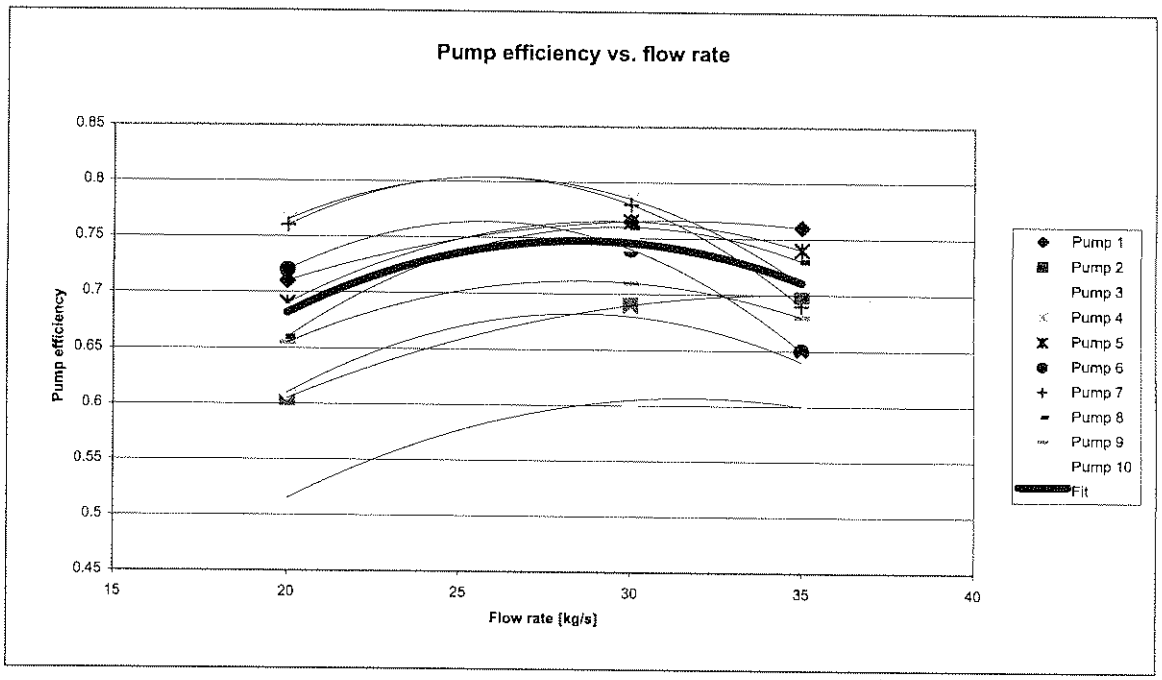

Figure A.12: Efficiency correlation for flow between 20 and 40 kg/s

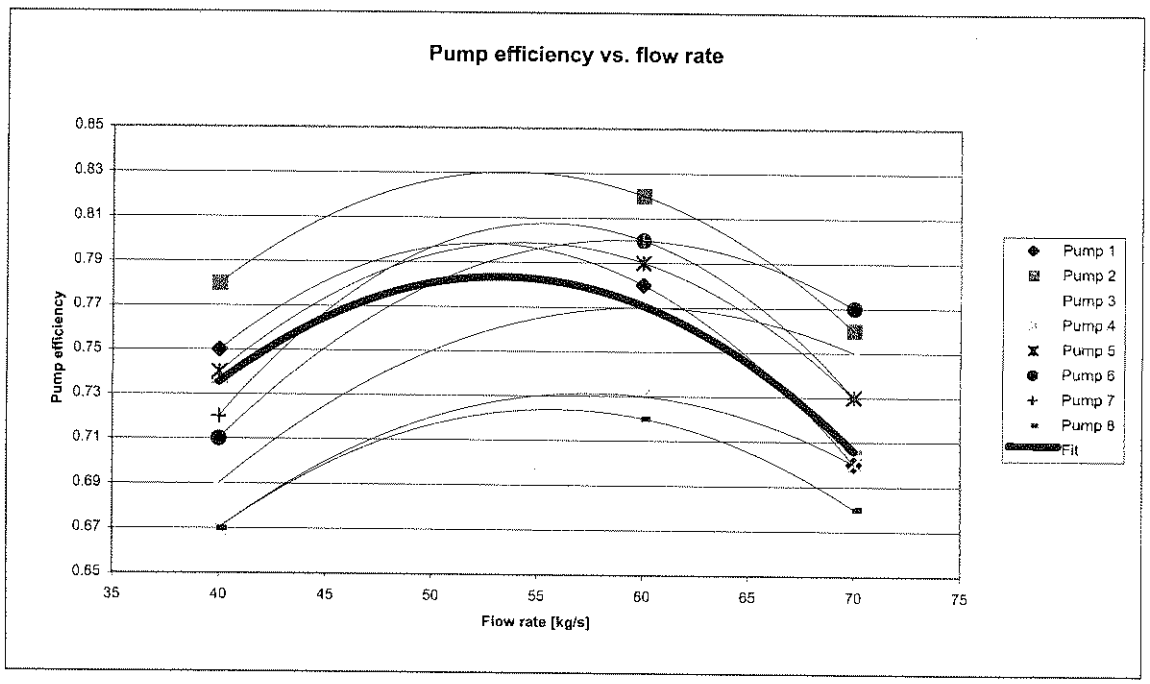

Figure A.13: Efficiency correlation for flow between 40 and 70 kg/s

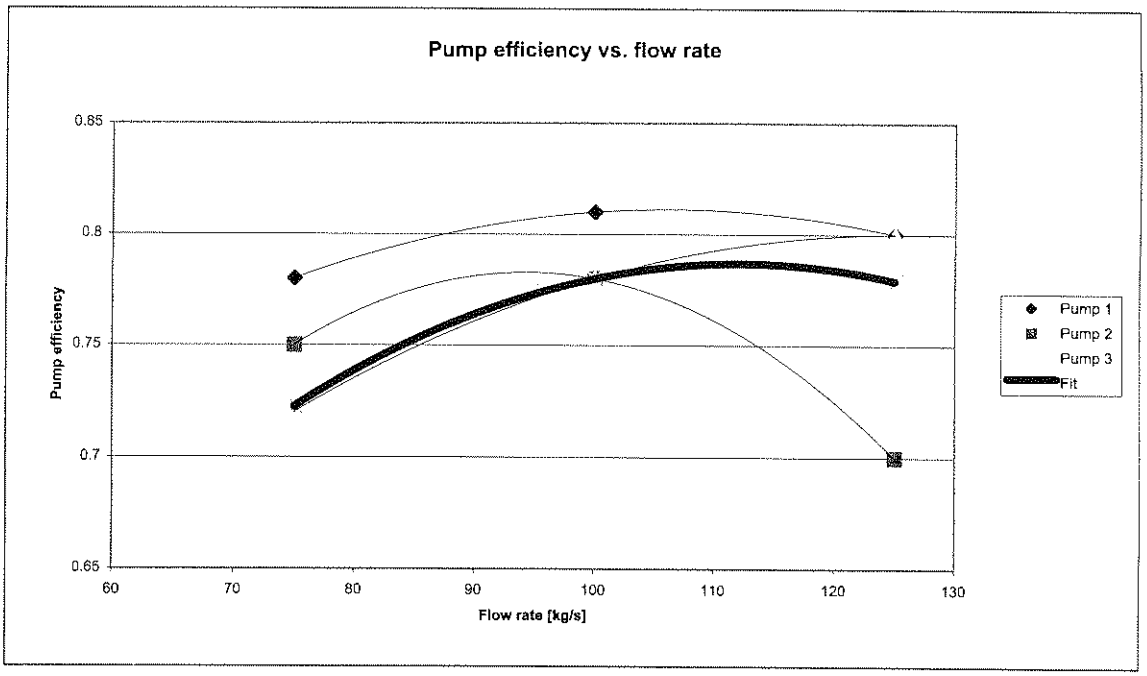

Figure A.14: Efficiency correlation for flow between 70 and 150 kg/s

A.2. FAN

A.2.1 Parameters:

a_j Correlation coefficients for the K_h versus K_f relation with j = 0 to 2.

b_j Correlation coefficients for the η_{fan} versus K_f relation with j = 0 to 2.

A.2.2 Inputs:

A.2.2.1 Simulation:

m_a Mass flow rate of dry air at inlet [kg/s].

w_{ai} Humidity ratio of air entering at the inlet [kg_{vapour} / $kg_{dry\ air}$].

h_{ai} Specific enthalpy of air entering at the inlet [J/$kg_{dry\ air}$].

A.2.2.2 Interface:

D The rotor diameter [m].

N Rotational speed of the fan [rpm].

η_{motor} Efficiency of the drive motor.

P_{total} Total pressure [Pa].

q Volume flow rate [m^3/s].

η_{fan} Fan efficiency.

A.2.3 Outputs:

dP_a	Static pressure rise [Pa].
w_{ae}	Humidity ratio of air entering at the inlet [kg_{vapour} / $kg_{dry\ air}$].
h_{ae}	Specific enthalpy of air entering at the inlet [J/$kg_{dry\ air}$].
Pwr	Power required [W].

A.2.4 Internal variables:

P_1	Extra pressure points [Pa].
P_2	Extra pressure points [Pa].
K_f	Dimensionless flow coefficient.
K_h	Dimensionless pressure head coefficient.
η_{fan}	Efficiency of the fan.
η_1	Extra efficiency point.
η_2	Extra efficiency point.
ρ_a	Air density [kg/m^3]
Q_a	Rate of heat gain to the air [W].

A.2.5 Explicit equations:

Three different pressures and efficiencies at three different flows are needed to calculate the correlation coefficients. A flow variation of 10% above and below the interface input value is assumed. The extra points are then calculated as follow:

$$P_1 = a_h(0.9q)^2 + b_h(0.9q) + c_h$$

$$\eta_1 = a_\eta(0.9q)^2 + b_\eta(0.9q) + c_\eta$$

$$P_2 = a_h(1.1q)^2 + b_h(1.1q) + c_h$$

$$\eta_2 = a_\eta(1.1q)^2 + b_\eta(1.1q) + c_\eta$$

with

$a_h = -823.114$

$b_h = 354.706$

$a_\eta = -95.3q^2 + 108.78q - 33.777$

$b_\eta = 18.281q^2 - 24q + 10.802$ for $0 < q < 1$ [m^3/s].

$a_h = -147.577$

$b_h = 378.984$

$a_\eta = -0.2432q^2 + 1.4215q - 2.176$

$b_\eta = 0.3379q^2 - 2.2688q + 4.4056$ for $1 < q < 5$ [m³/s].

$a_h = -33.262$

$b_h = 309.9086$

$a_\eta = 0.0074q - 0.0801$

$b_\eta = -0.054q + 0.7516$ for $5 < q < 15$ [m³/s].

$a_h = -5.47298$

$b_h = 158.6346$

$a_\eta = -0.00299$

$b_\eta = 0.1219$ for $15 < q < 30$ [m³/s].

$a_h = -2.14676$

$b_h = 74.34644$

$a_\eta = -0.0014$

$b_\eta = 0.081011$ for $30 < q < 60$ [m³/s].

These values were calculated as the average values of the coefficients of a wide range of backward curved centrifugal fan curves or as a function of flow. The a and b coefficients as a function of flow can be seen in figures A.15 to A.20. The accuracy of this can be seen in figures A.21 to A.30. c_h and c_η are calculated from the one given operating point obtained from the supplier or measurements. This implies that only one operating point is needed to obtain the mathematical model of a specific fan.

And

$$c_h = P - (a_h q^2 + b_h q)$$

$$c_\eta = \eta - (a_\eta q^2 + b_\eta q)$$

For each of these three points the K_h and K_f value must be calculated as follow:

$$K_{h1} = \frac{P_1}{\rho_a N^2 D^2}$$

$$K_{f1} = \frac{\rho_a (0.9q)}{\rho_a N D^3}$$

$$K_h = \frac{P}{\rho_a N^2 D^2}$$

$$K_f = \frac{\rho_a q}{\rho_a N D^3}$$

$$K_{h2} = \frac{P_2}{\rho_a N^2 D^2}$$

$$K_{f2} = \frac{\rho_a (1.1q)}{\rho_a N D^3}$$

Using these values the correlation coefficients can be calculated as follow:

$$a_2 = \frac{(K_{h2} - K_{h1})(K_f - K_{f1}) - (K_{f2} - K_{f1})(K_h - K_{h1})}{(K_{f2}^2 - K_{f1}^2)(K_f - K_{f1}) - (K_{f2} - K_{f1})(K_f^2 - K_{f1}^2)}$$

$$a_1 = \frac{(K_h - K_{h1}) - (K_f^2 - K_{f1}^2)a_2}{(K_f - K_{f1})}$$

$$a_0 = K_{h1} - K_{f1} a_1 - K_{f1}^2 a_2$$

$$b_2 = \frac{(\eta_2 - \eta_1)(K_f - K_{f1}) - (K_{f2} - K_{f1})(\eta - \eta_1)}{(K_{f2}^2 - K_{f1}^2)(K_f - K_{f1}) - (K_{f2} - K_{f1})(K_f^2 - K_{f1}^2)}$$

$$b_1 = \frac{(\eta - \eta_1) - (K_f^2 - K_{f1}^2)b_2}{(K_f - K_{f1})}$$

$$b_0 = \eta_1 - K_{f1} b_1 - K_{f1}^2 b_2$$

These coefficients can now be used to calculate the necessary outputs with the following explicit equations:

$$\rho_a = \zeta(h_{ai}, w_{ai})$$

$$K_f = \frac{\rho_a q}{\rho_a N D^3}$$

$$K_h = a_0 + a_1 K_f + a_2 K_f^{\,2}$$

$$P_{total} = K_h \rho_a N^2 D^2$$

$$\eta_{fan} = b_0 + b_1 K_f + b_2 K_f^{\,2}$$

$$Q_a = \frac{(1-\eta_{fan}) m_a P_{total}}{\rho_a \eta_{fan}}$$ motor outside airstream

$$Q_a = \frac{(1-\eta_{fan}\eta_{motor}) m_a P_{total}}{\rho_a \eta_{fan}\eta_{motor}}$$ motor inside airstream

$$w_{ae} = w_{ai}$$

$$h_{ae} = h_{ai} + \frac{Q}{m_a}$$

$$Pwr = \frac{P_{total} m_a}{\rho_a \eta_{motor}\eta_{fan}}$$

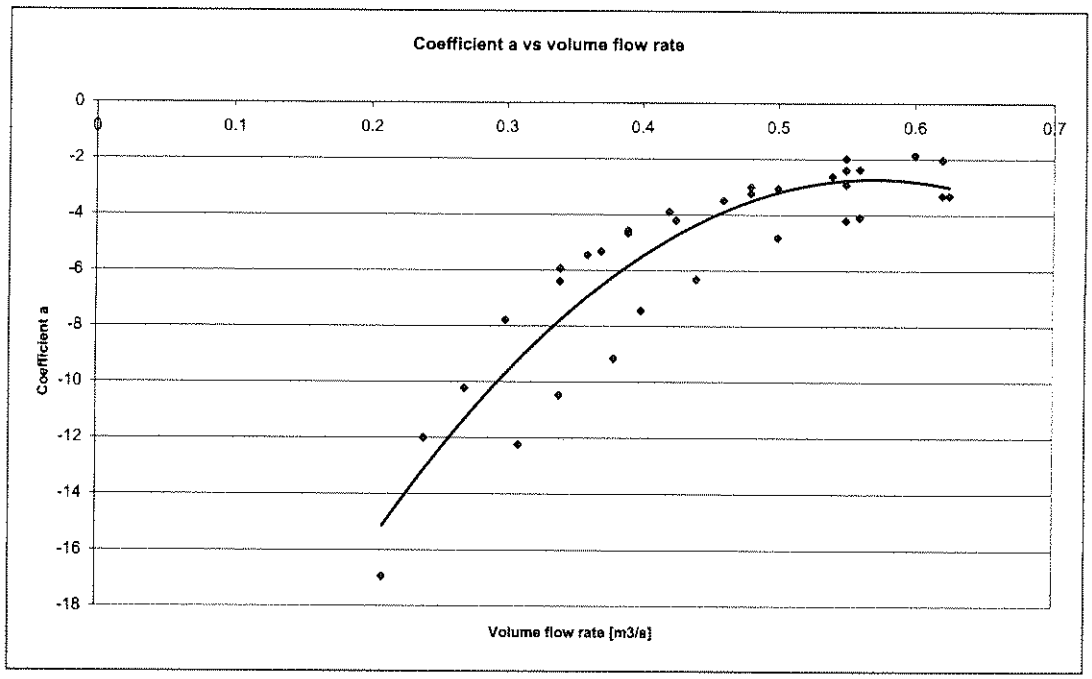

Figure A.15: Efficiency's a coefficient as a function of volume flow rate for flow between 0 and 1 m^3/s

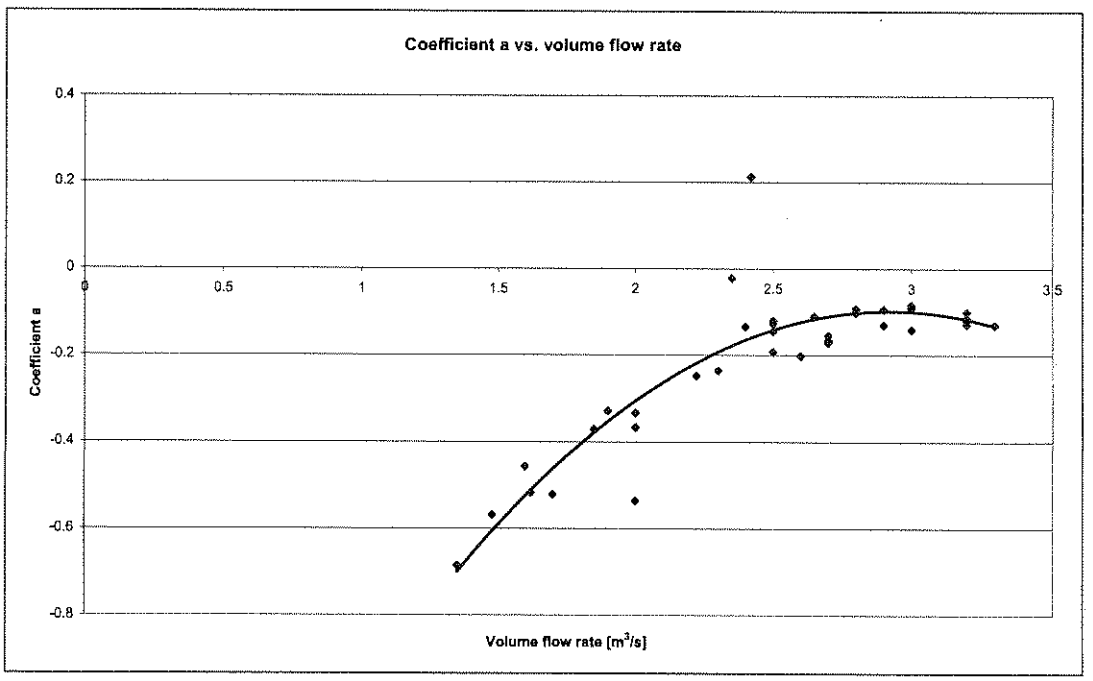

Figure A.16: Efficiency's a coefficient as a function of volume flow rate for flow between 1 and 5 m^3/s

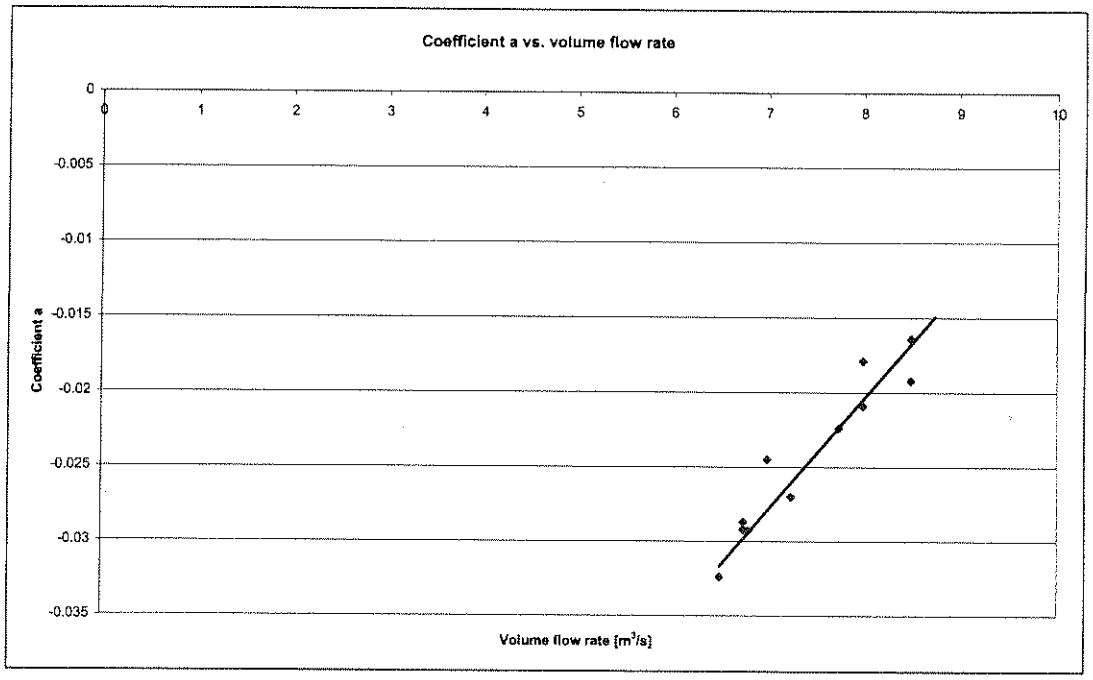

Figure A.17: Efficiency's a coefficient as a function of volume flow rate for flow between 5 and 15 m^3/s

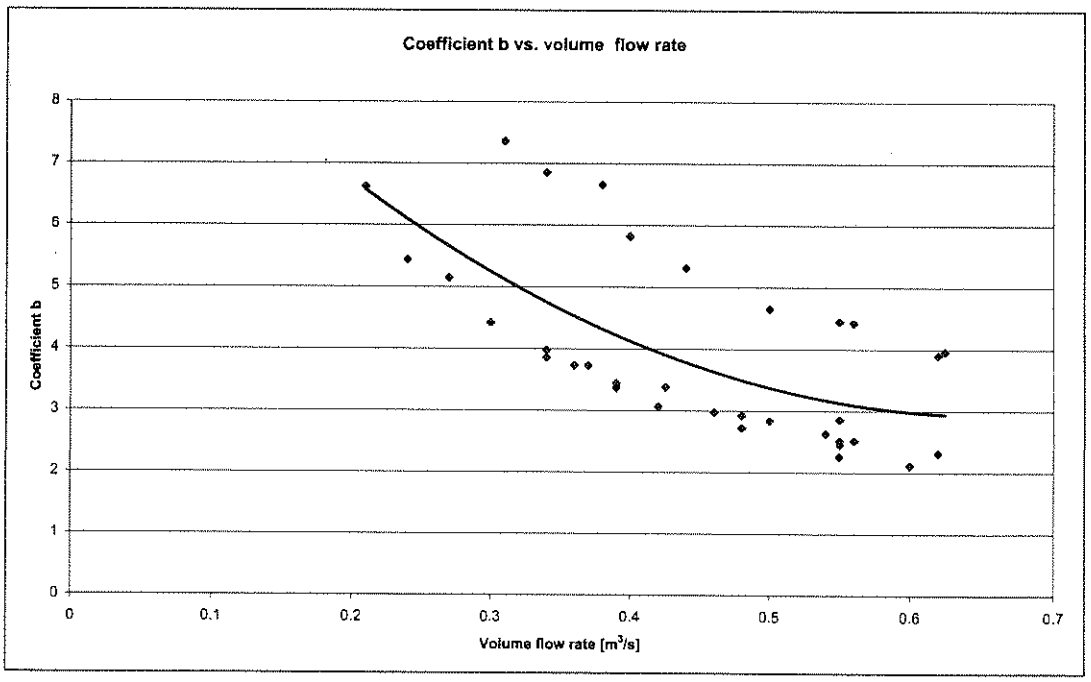

Figure A.18: Efficiency's b coefficient as a function of volume flow rate for flow between 0 and 1 m^3/s

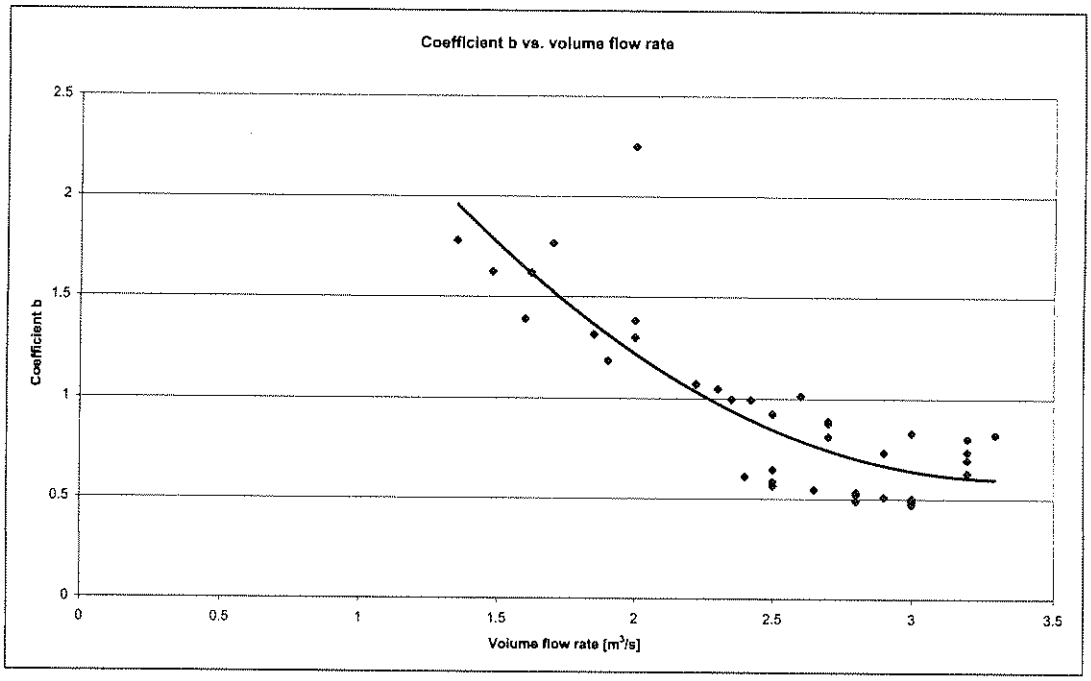

Figure A.19: Efficiency's b coefficient as a function of volume flow rate for flow between 1 and 5 m^3/s

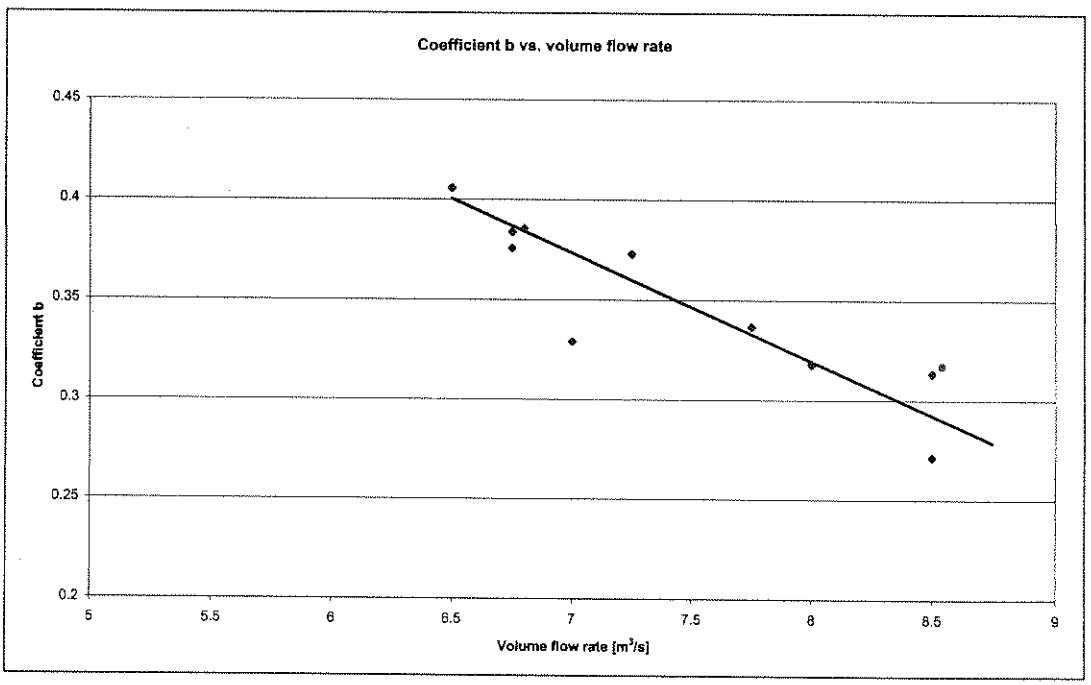

Figure A.20: Efficiency's b coefficient as a function of volume flow rate for flow between 5 and 15 m^3/s

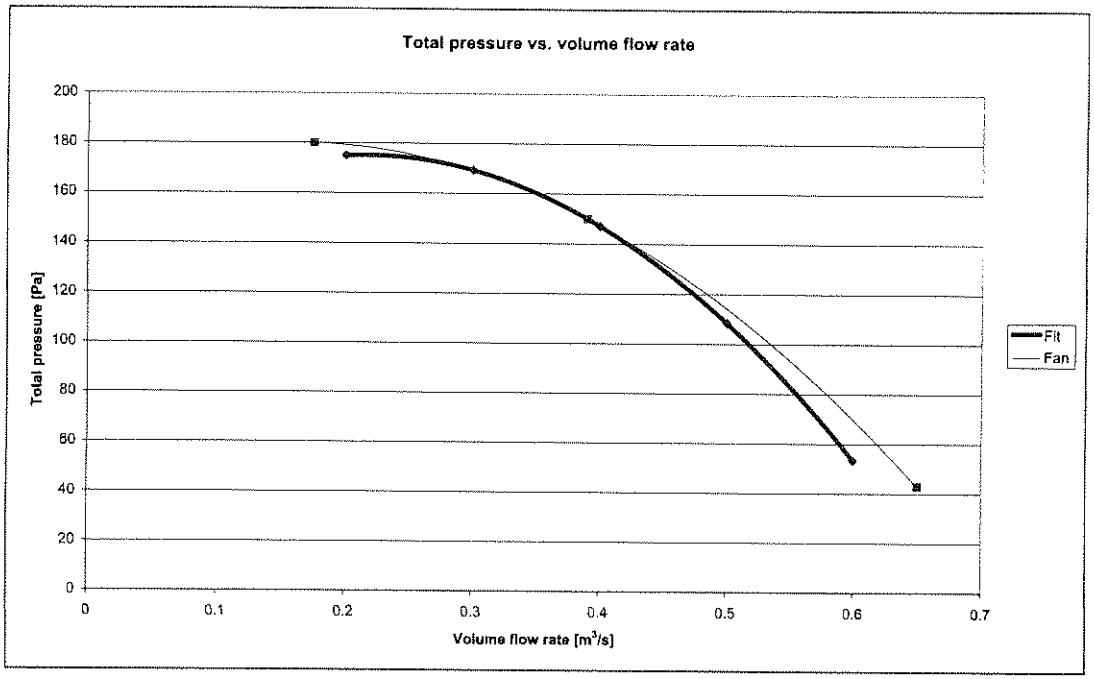

Figure A.21: Total pressure correlation for a volume flow rate between 0 and 1 m^3/s

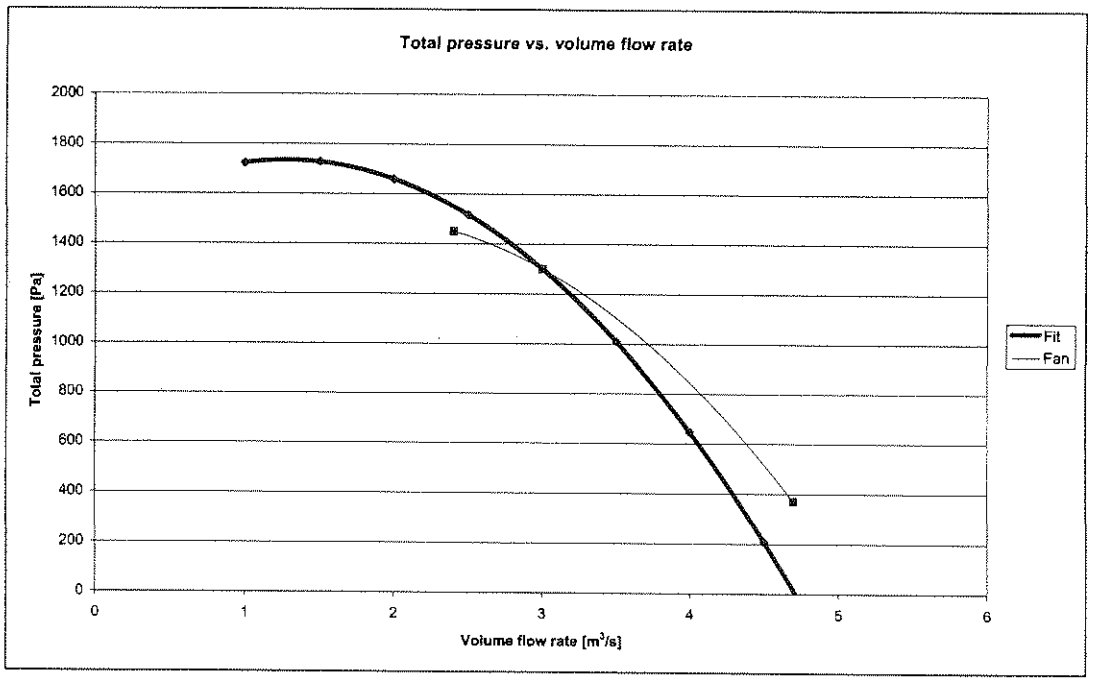

Figure A.22: Total pressure correlation for a volume flow rate between 1 and 5 m^3/s

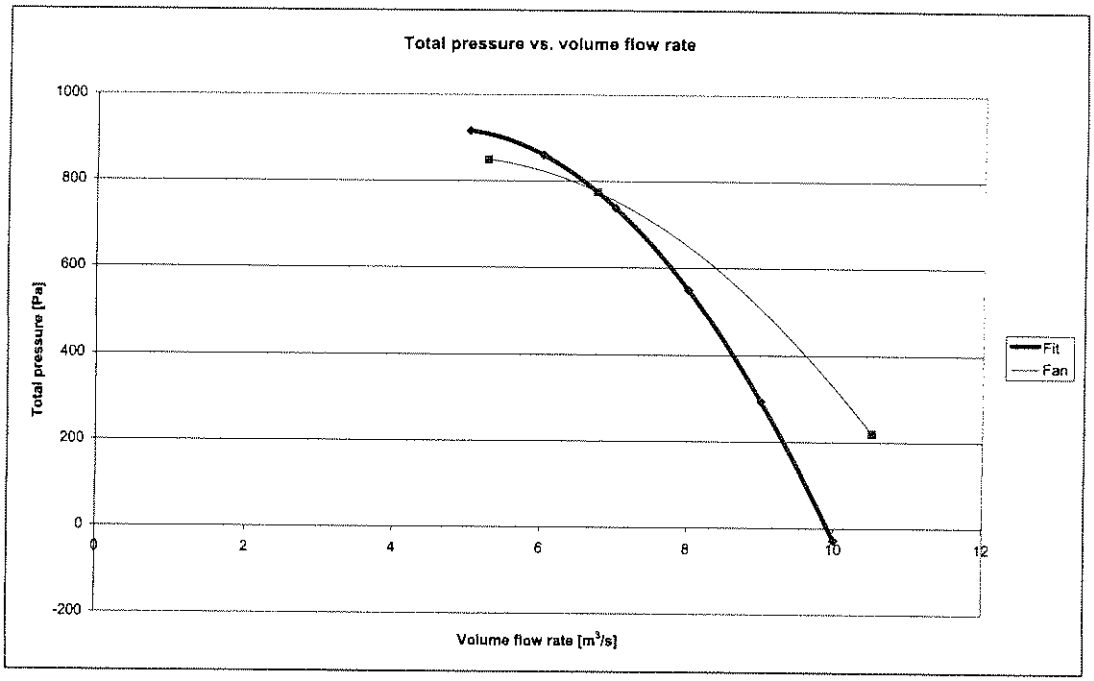

Figure A.23: Total pressure correlation for a volume flow rate between 5 and 15 m^3/s

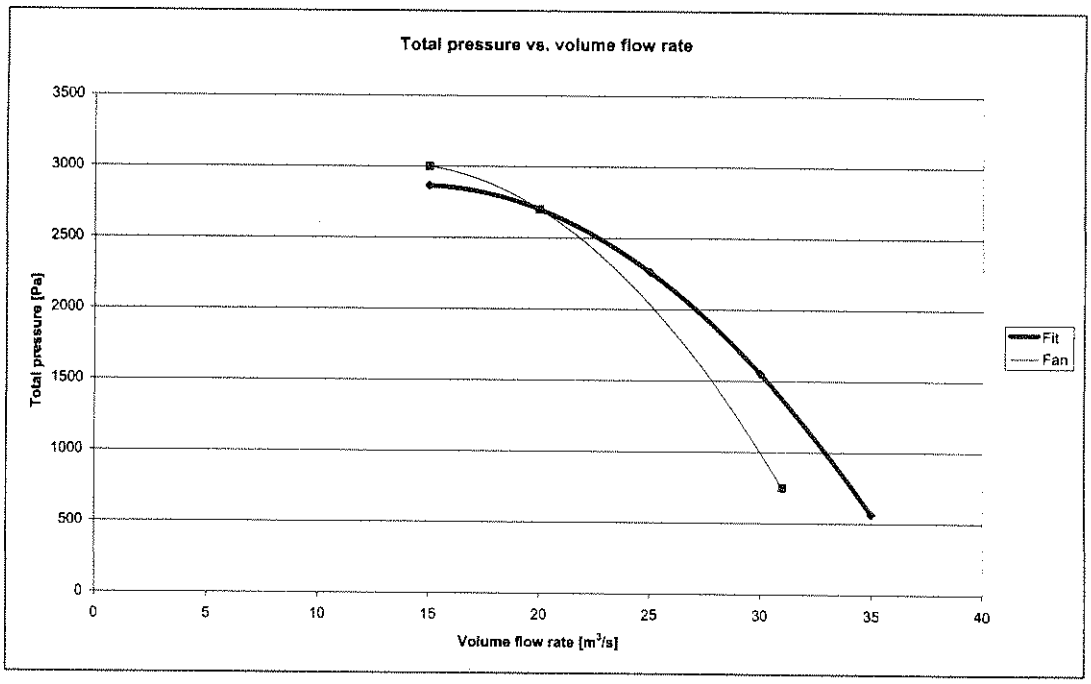

Figure A.24: Total pressure correlation for a volume flow rate between 15 and 30 m^3/s

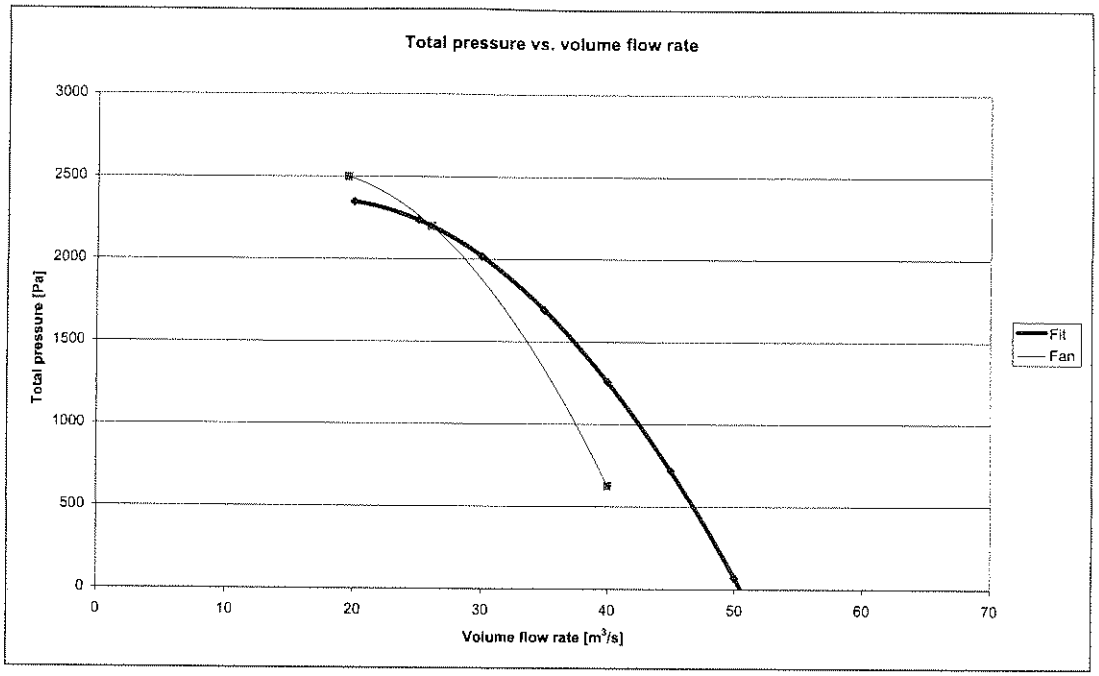

Figure A.25: Total pressure correlation for a volume flow rate between 30 and 60 m^3/s

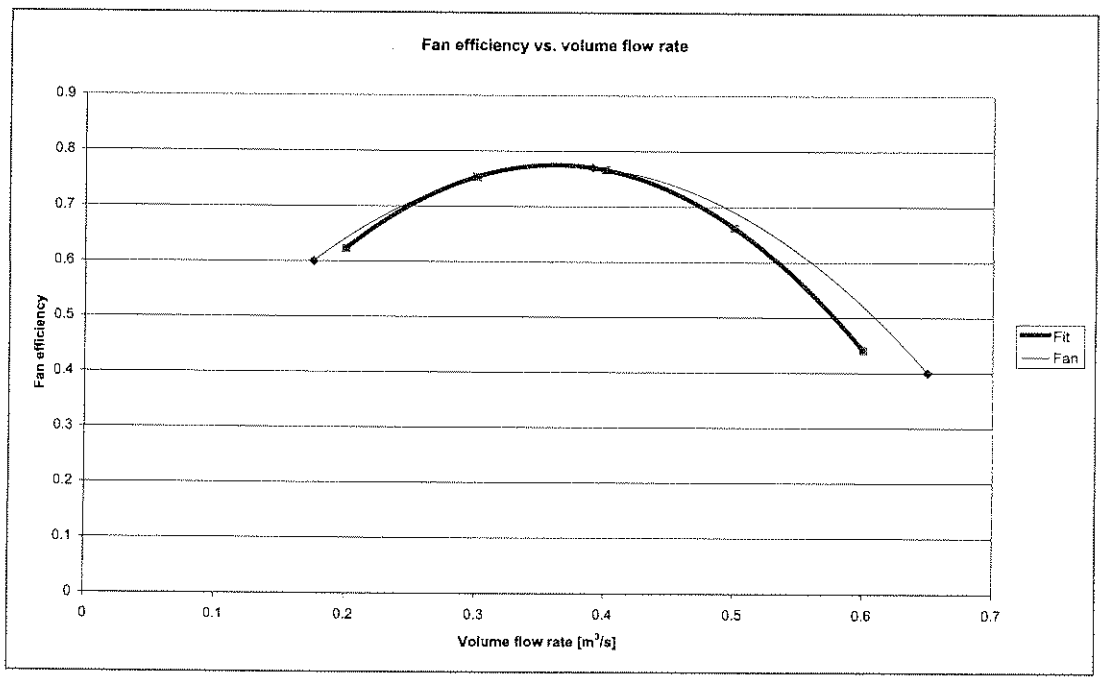

Figure A.26: Fan efficiency correlation for a volume flow rate between 0 and 1 m^3/s

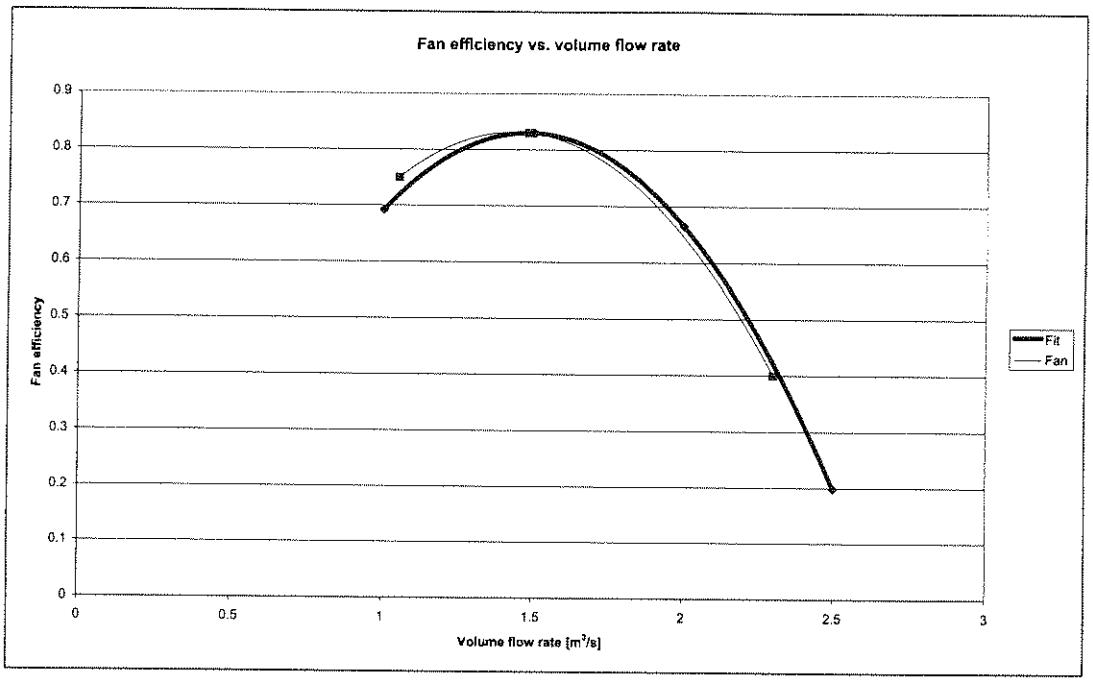

Figure A.27: Fan efficiency correlation for a volume flow rate between 1 and 5 m^3/s

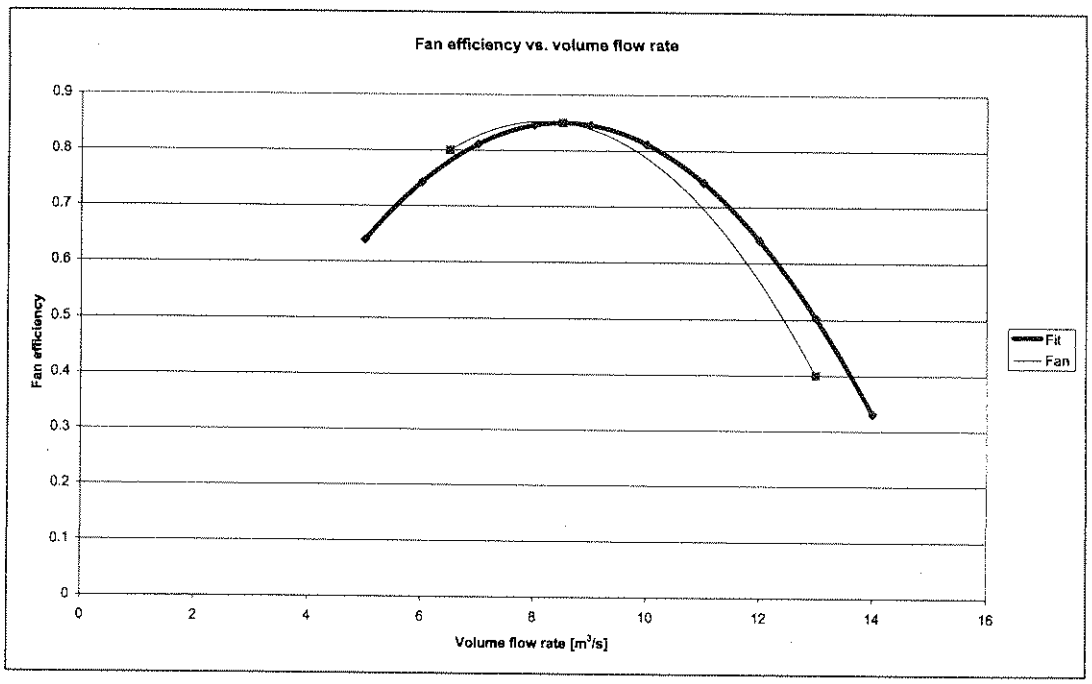

Figure A.28: Fan efficiency correlation for a volume flow rate between 5 and 15 m^3/s

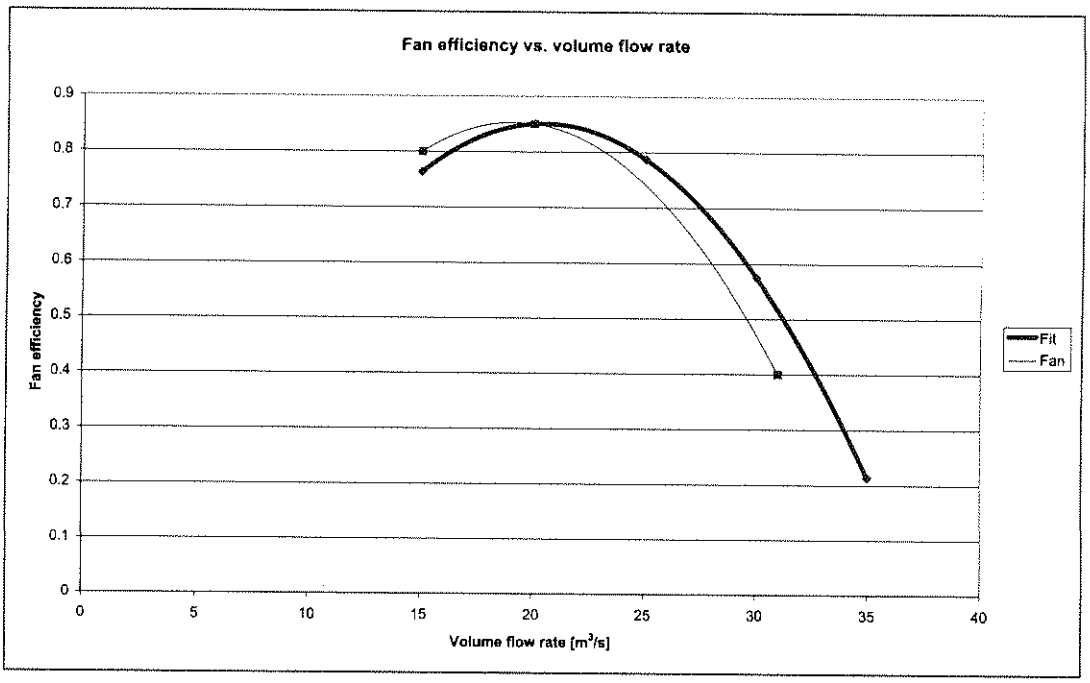

Figure A.29: Fan efficiency correlation for a volume flow rate between 15 and 30 m^3/s

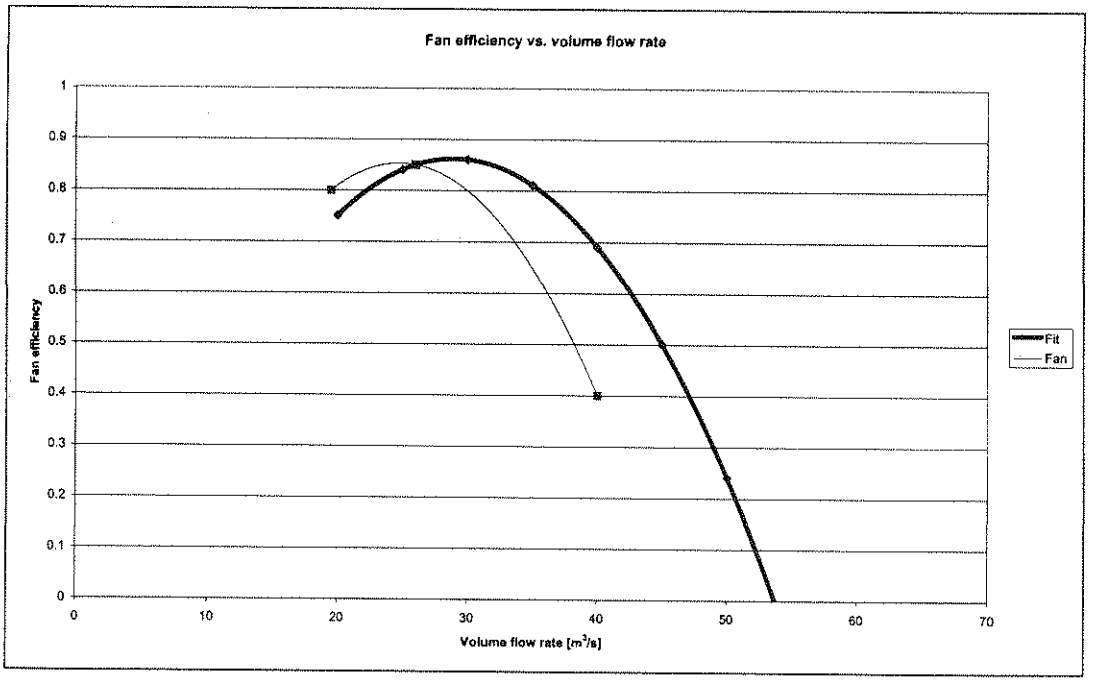

Figure A.30: Fan efficiency correlation for a volume flow rate between 30 and 60 m^3/s

A.3. AIR COOLED LIQUID CHILLER

A.3.1 Parameters:

f	Active fraction of total capacity.
a_n	Regression coefficients for cooling capacity.
b_n	Regression coefficients for power.

A.3.2 Inputs:

A.3.2.1Simulation:

$m_{l(evap)}$ Mass flow rate of water through the evaporator [kg/s].

$T_{li(evap)}$ Temperature of water entering evaporator [°C].

$w_{ai(cond)}$ Humidity ratio of air entering the condenser [kg_{vapour} / $kg_{dry\ air}$].

$h_{ai(cond)}$ Specific enthalpy of air entering the condenser [J/$kg_{dry\ air}$].

A.3.2.2Interface:

Cc Cooling capacity at the expected operational temperatures of the chiller [kW].

P Compressor power at the expected operational temperatures of the chiller [kW].

T_{aa} Expected dry bulb temperature of the air entering the condenser [°C].

T_{ee} Expected temperature of water exiting evaporator [°C].

A.3.3 Outputs:

$T_{le(evap)}$ Temperature of water leaving evaporator [°C].

Q_e Cooling capacity [kW].

Pwr Power consumed by the compressor and fan [kW].

A.3.4 Internal variables:

$T_{ai(cond)}$ Dry bulb temperature of air entering condenser[°C].

A.3.5 Explicit equations:

$$T_{ai(cond)} = \zeta\left(h_{ai(cond)}, w_{ai(cond)}\right)$$

$$Q_e = f\left(a_0 + a_1 T_{le(evap)} + a_2 T_{ai(cond)}\right)$$

With

$$a_2 = -0.0112Cc + 0.024$$

$$a_1 = 0.0265Cc - 0.2547$$

$$a_0 = Cc - \left(T_{ee}a_1 + T_{aa}a_2\right)$$

Coefficients a_2 and a_1 were found to be linear over a wide range of chillers with respect to cooling capacity as can be seen in figure A.31 and A.32. a_0 is calculated from the one given operating point obtained from the supplier or measurements. This implies that only one operating point is needed to obtain the mathematical model of a specific chiller.

$$Pwr = f\left(b_0 + b_1 T_{li(evap)} + b_2 T_{ai(cond)}\right)$$

With

$$b_2 = 0.0079P + 0.3051$$

$$b_1 = 0.0184P - 0.1403$$

$$b_0 = P - \left(T_{ee} b_1 + T_{aa} b_2\right)$$

Coefficients b_2 and b_1 were found to be linear over a wide range of chillers with respect to compressor power as can be seen in figures A.33 and A.34. b_0 is calculated from the one given operating point obtained from the supplier or measurements. This implies that only one operating point is needed to obtain the mathematical model of a specific chiller.

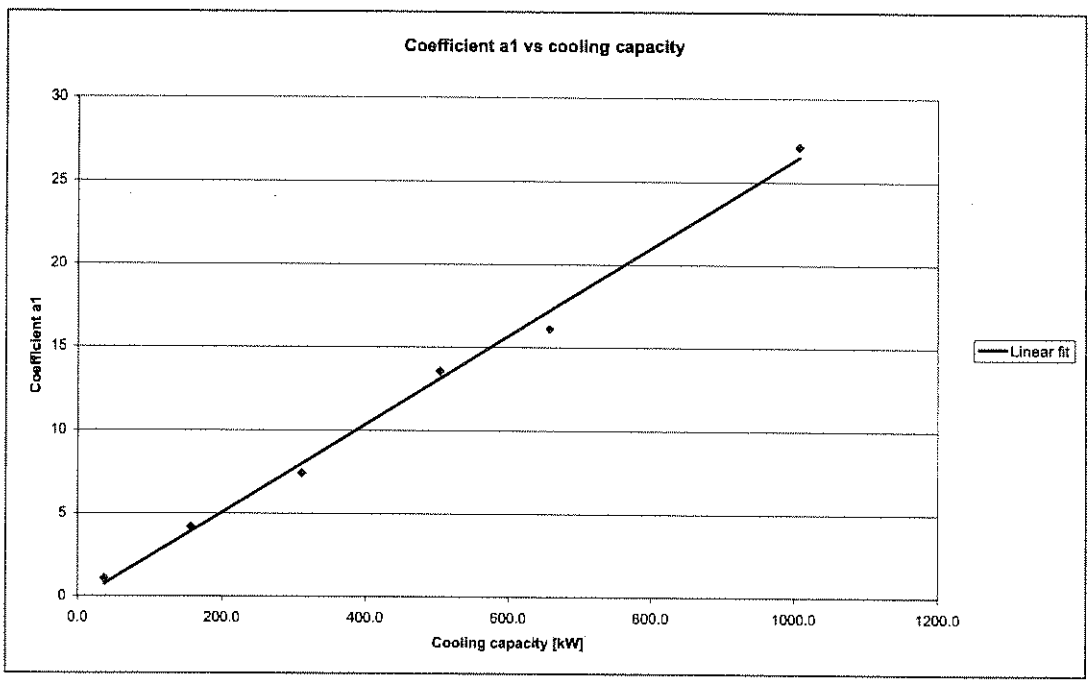

Figure A.31: Coefficient a1 as a function of cooling capacity

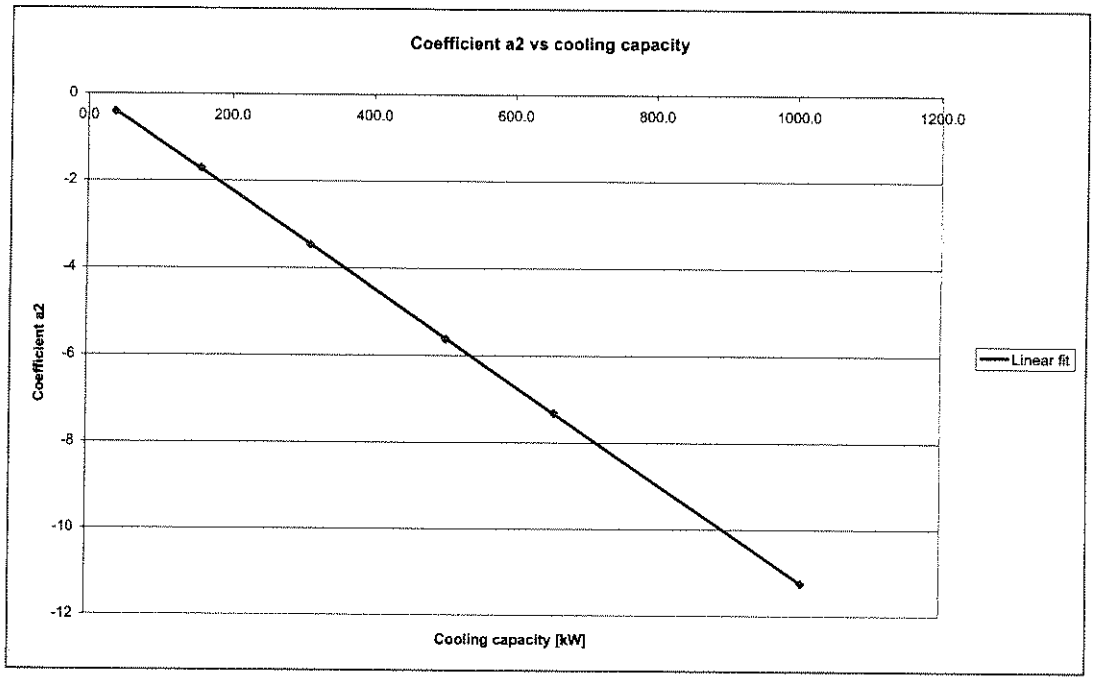

Figure A.32: Coefficient a2 as a function of cooling capacity

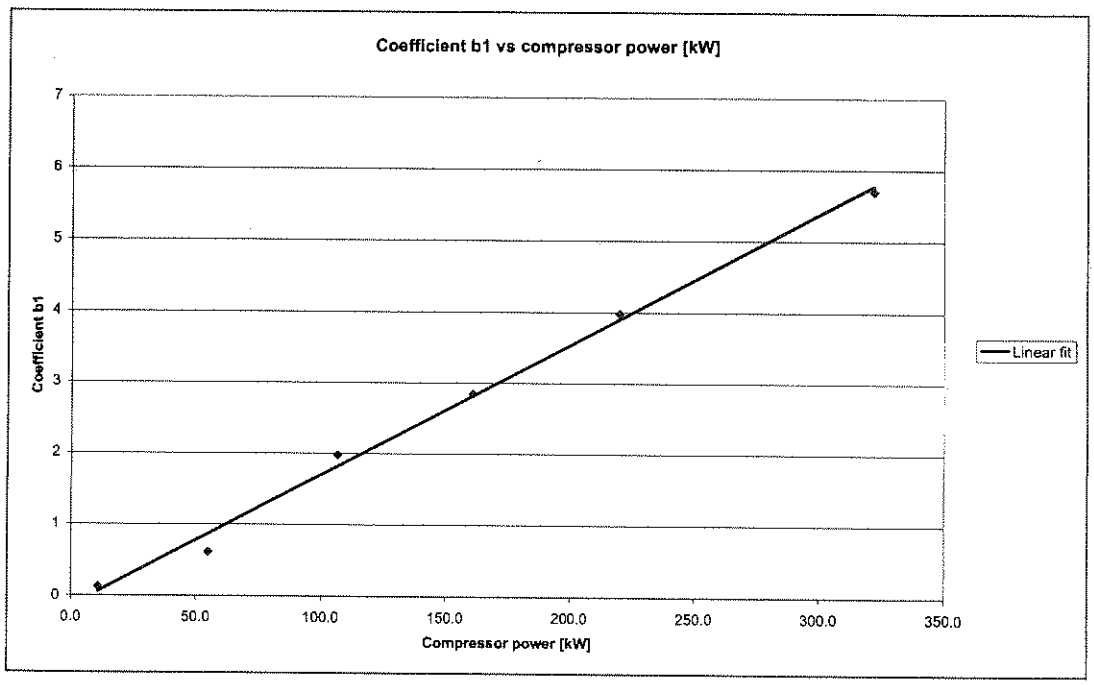

Figure A.33: Coefficient b1 as a function of compressor power

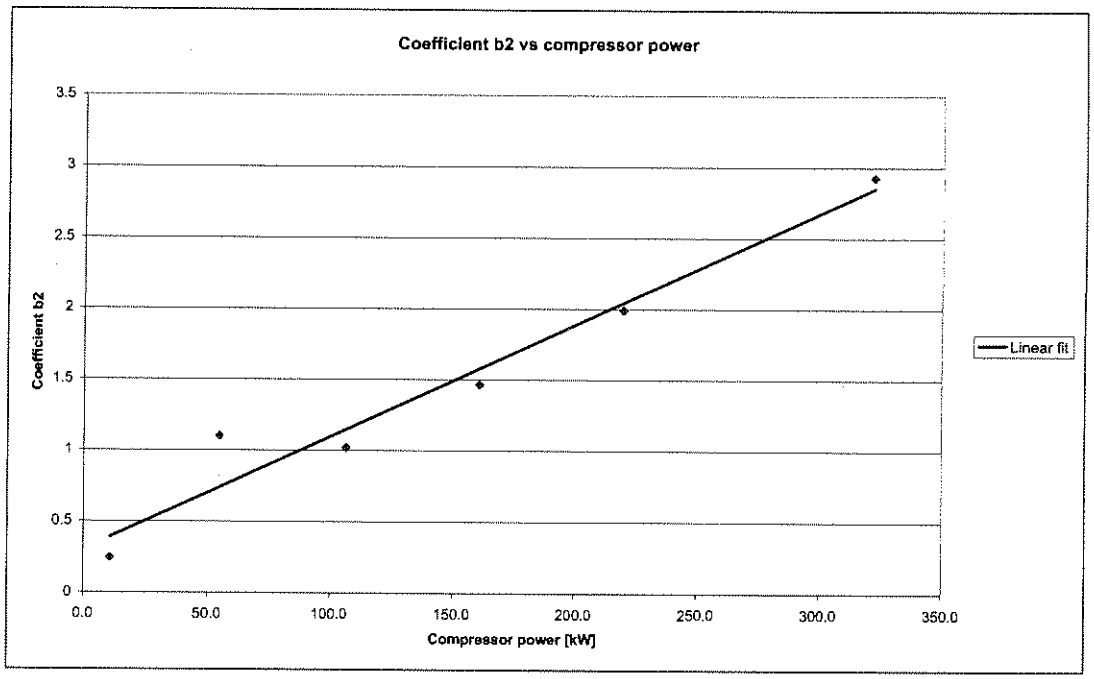

Figure A.34: Coefficient b2 as a function of compressor power

A.4. WATER COOLED LIQUID CHILLER

A.4.1 Parameters:

f	Active fraction of total capacity.
a_n	Regression coefficients for cooling capacity.
b_n	Regression coefficients for power.

A.4.2 Inputs:

A.4.2.1Simulation:

$m_{l(cond)}$	Mass flow rate of water through the condenser [kg/s].
$m_{l(evap)}$	Mass flow rate of water through the evaporator [kg/s].
$T_{li(cond)}$	Temperature of water entering condenser [°C].

$T_{li(evap)}$ Temperature of water entering evaporator [°C].

A.4.2.2Interface:

Cc Cooling capacity at the expected operational temperatures of the chiller [kW].

P Compressor power at the expected operational temperatures of the chiller [kW].

T_{ce} Expected temperature of water exiting condenser [°C].

T_{ee} Expected temperature of water exiting evaporator [°C].

A.4.3 Outputs:

$T_{le(cond)}$ Temperature of water leaving condenser [°C].

$T_{le(evap)}$ Temperature of water leaving evaporator [°C].

Q_e Cooling capacity [kW].

Pwr Power consumed by the compressor [kW].

A.4.4 Explicit equations:

$$Q_e = f\left(a_0 + a_1 T_{le(cond)} + a_2 T_{le(evap)}\right)$$

With

$$a_2 = 0.0266Cc + 2.8714$$

$$a_1 = -0.01Cc + 0.2289$$

$$a_0 = Cc - \left(T_{ce}a_1 + T_{ee}a_2\right)$$

Coefficients a_2 and a_1 were found to be linear over a wide range of chillers with respect to cooling capacity as can be seen in figure A.35 and A.36. a_0 is calculated from the one given

operating point obtained from the supplier or measurements. This implies that only one operating point is needed to obtain the mathematical model of a specific chiller.

$$Pwr = f\left(b_0 + b_1 t_{li(cond)} + b_2 t_{li(evap)}\right)$$

With

$$b_2 = 0.007P + 0.3549$$

$$b_1 = 0.0124P + 0.4207$$

$$b_0 = P - \left(t_{ce} b_1 + t_{ee} b_2\right)$$

Coefficients b_2 and b_1 were found to be linear over a wide range of chillers with respect to compressor power as can be seen in figure A.37 and A.38. b_0 is calculated from the one given operating point from the supplier or measurements. This implies that only one operating point is needed to obtain the mathematical model of a specific chiller.

$$T_{le(cond)} = T_{li(cond)} - \frac{Q_e + Pwr}{m_{l(cond)} c_{pl}}$$

$$T_{le(evap)} = T_{li(evap)} - \frac{Q_e}{m_{l(evap)} c_{pl}}$$

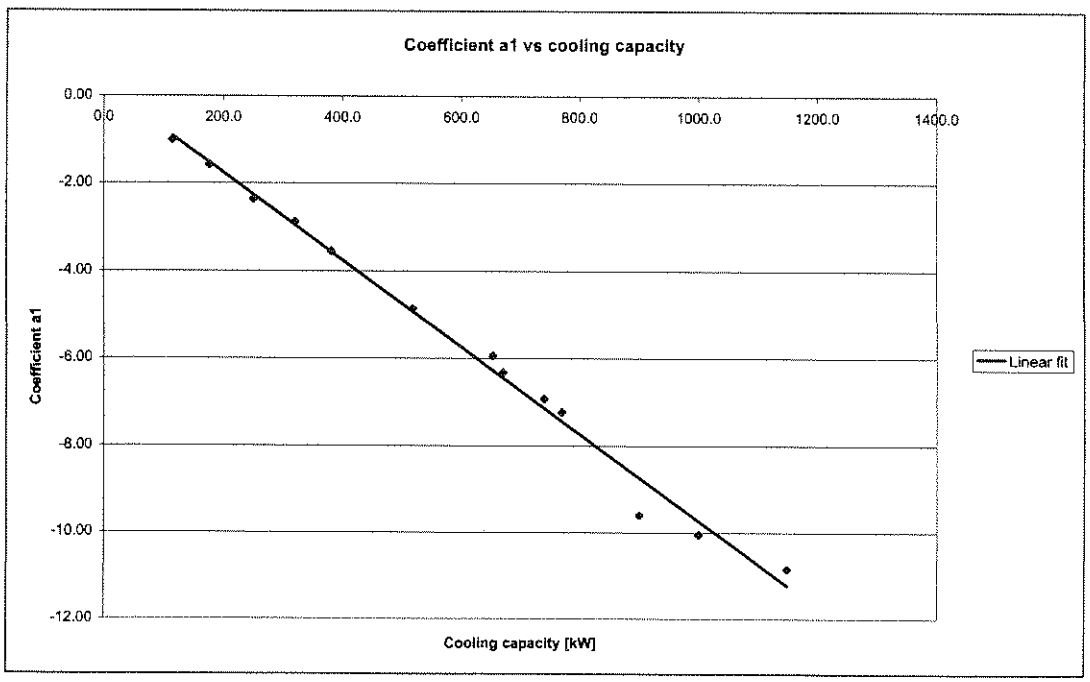

Figure A.35: Coefficient a1 as a function of cooling capacity

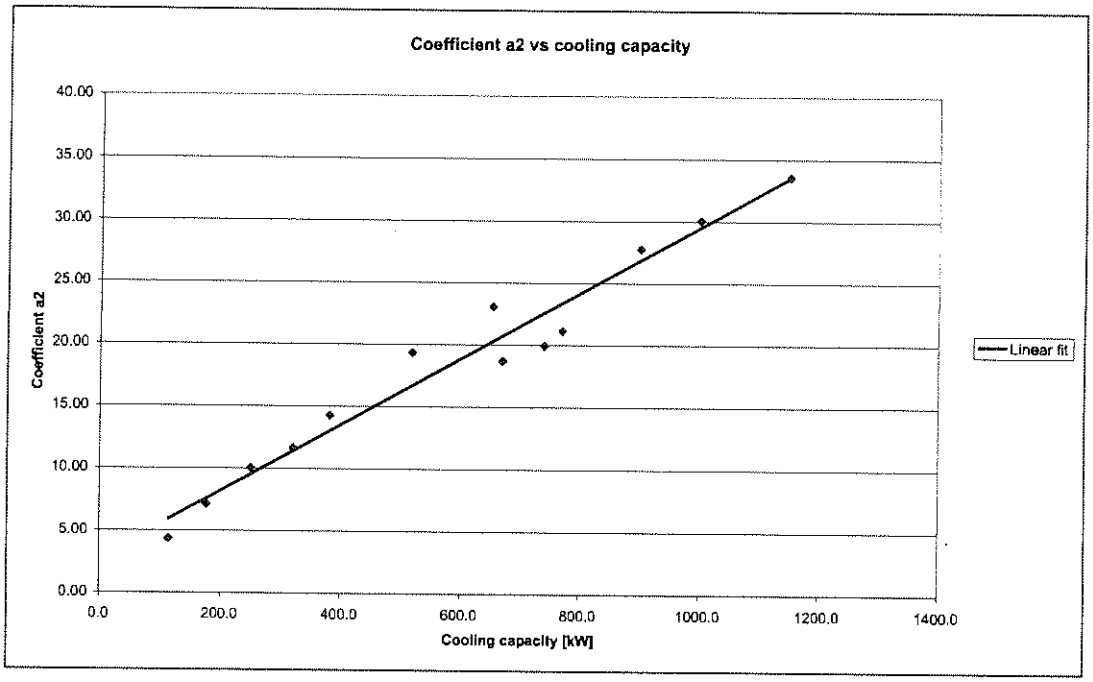

Figure A.36: Coefficient a2 as a function of cooling capacity

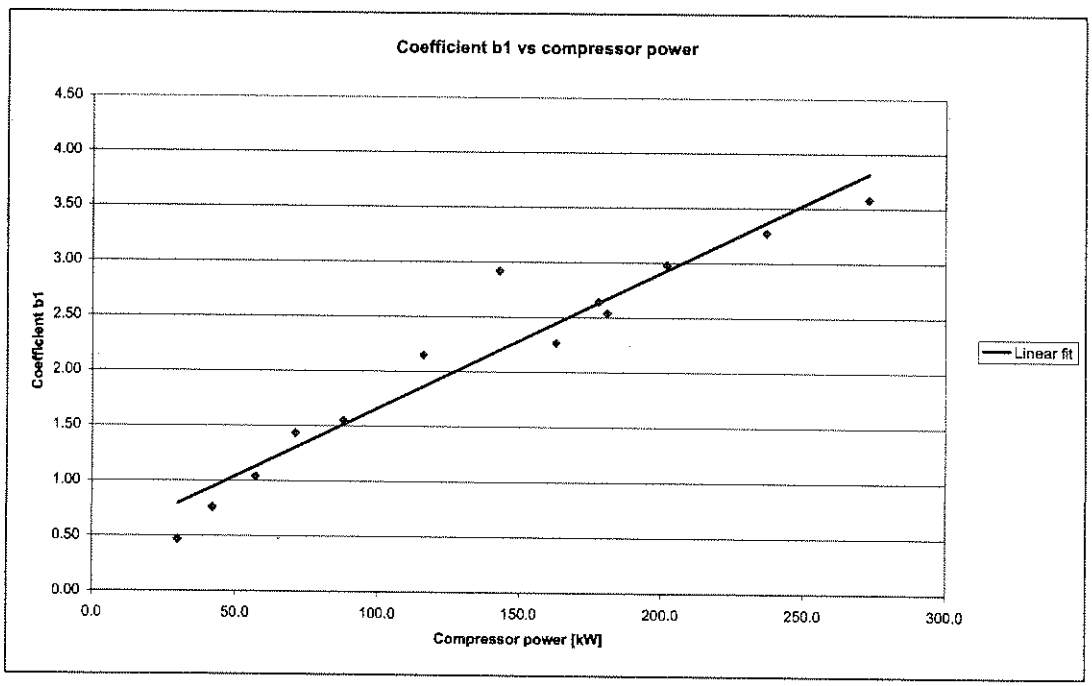

Figure A.37: Coefficient b1 as a function of compressor power

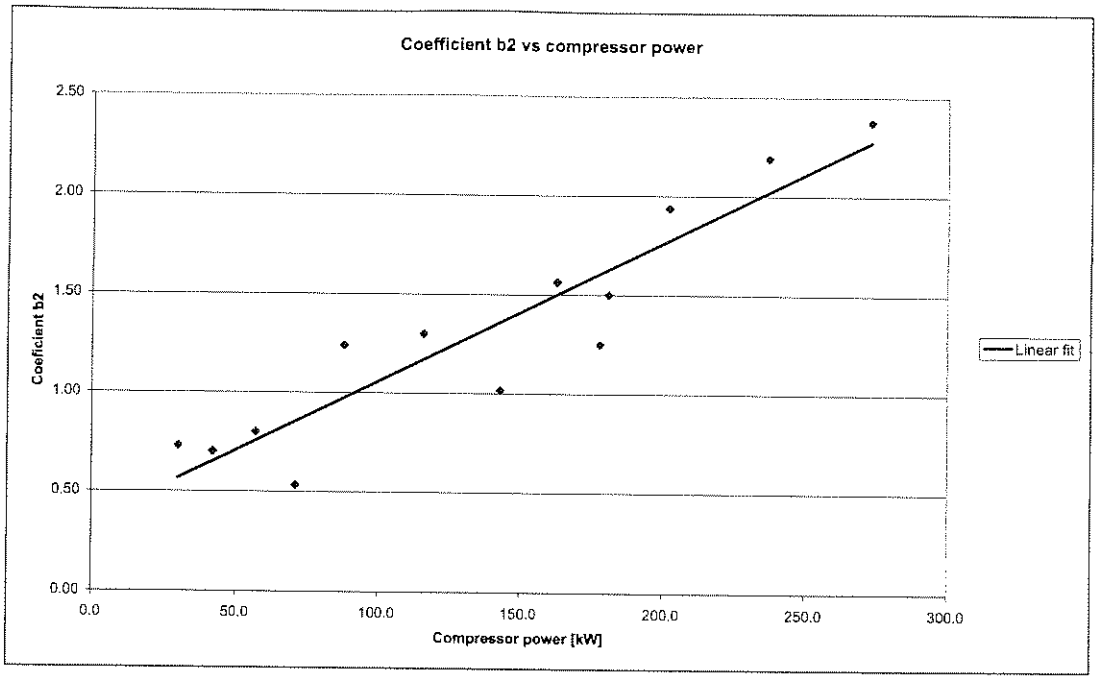

Figure A.38: Coefficient b2 as a function of compressor power

A.5. COIL

A.5.1 Parameters:

A_f Coil face area [m^2].

R Ratio A_o/A_f.

f Fraction of m_i that is not bypassed and passes through the coil.

a_j Correlation coefficients for the h_o versus V_a relation with j = 0 to 2.

A.5.2 Inputs:

m_a Mass flow rate of dry air at the inlet [kg/s].

w_{ai} Humidity ratio of air entering at the inlet [kg_{vapour}/kg_{dryair}].

h_{ai} Specific enthalpy of air entering at the inlet [J/kg_{dryair}].

m_l Mass flow rate of liquid at inlet [kg/s].

T_{li} Temperature of liquid entering at inlet [°C].

A.5.3 Outputs:

w_{ae} Humidity ratio of air leaving at the outlet [kg_{vapour}/kg_{dryair}].

h_{ae} Specific enthalpy of air leaving at the outlet [J/kg_{dryair}].

T_{le} Temperature of liquid leaving at outlet [°C].

A.5.4 Internal variables:

A_o	Total outside heat transfer area [m^2].
ρ_a	Air density [kg/m^3].
T_{ai}	Dry-bulb temperature of air at the inlet[°C].
V_a	Air face velocity [m/s].
h_o	Outside surface convection heat transfer coefficient [$W/m^2°C$].
T_{ae}	Dry-bulb temperature of air at the outlet [°C].
w_{adp}	Humidity ratio of saturated air at t_{li} [$kg_{vapour}/kg_{dry\ air}$].
h_{ad}	Specific enthalpy of air at the outlet [$J/kg_{dry\ air}$].
S	Sensible heat ratio.

A.5.5 Explicit equations:

$$m_l = fm_l$$

$$\rho_a = \zeta(h_{ai}, w_{ai})$$

$$T_{ai} = \zeta(h_{ai}, w_{ai})$$

$$V_a = \frac{m_a}{\rho_a A_f}$$

$$h_o = a_0 + a_1 V_a + a_2 {V_a}^2$$

$$A_0 = RA_f$$

If $T_{li} \geq \zeta$ (T_{ai}, saturated) the coil is dry which means that S = 1, $w_{adp} = w_{ai}$ and $h_{ad} = h_{ai}$ and the following equations apply.

$$w_{ae} = w_{ai}$$

$$T_{ae} = \frac{\left[e^{h_o A_o\left(\frac{1}{m_a c_{pa}} - \frac{1}{m_l c_{pl}}\right)} - 1\right] T_{li} - \left[\frac{m_a c_{pa}}{m_l c_{pl}} - 1\right] T_{ai}}{e^{h_o A_o\left(\frac{1}{m_a c_{pa}} - \frac{1}{m_l c_{pl}}\right)} - \frac{m_a c_{pa}}{m_l c_{pl}}}$$

$$h_{ae} = \zeta(T_{ae}, w_{ae})$$

$$T_{le} = T_{li} - \frac{m_a c_{pa}}{m_l c_{pl}}(T_{ae} - T_{ai})$$

Else the coil is wet and the following equations apply

$$w_{adp} = \xi(T_{li}, saturated)$$

A.5.6 Simultaneous equations:

$$h_{ae} = h_{ai} + \frac{h_o A_o (T_{le} - T_{ai}) - (T_{li} - T_{ae})}{m_a S \ln \frac{(T_{le} - T_{ai})}{(T_{li} - T_{ae})}}$$

$$T_{le} = T_{li} - \frac{m_a}{m_l c_{pl}} (h_{ae} - h_{ai})$$

$$T_{ae} = T_{ai} - \frac{w_{ai} - w_{ae}}{w_{ai} - w_{adp}} (T_{ai} - T_{li})$$

$$w_{ae} = \zeta(T_{ae}, h_{ae})$$

$$h_{ad} = \zeta(T_{ai}, w_{ae})$$

$$S = \frac{h_{ad} - h_{ae}}{h_{ai} - h_{ae}}$$

A.5.7 Explicit equation:

$$T_{le} = f T_{le} + (1 - f) T_{li}$$

A.6. COOLING TOWER

A.6.1 Parameters:

a_j	Correlation coefficients for the UA versus m_l and t_{li} relation with j = 0 to 5
m_a	Mass flow rate of outdoor air through the tower [kg/s]
Pwr_{fan}	Power required by the built-in fan [W]
Pwr_{pump}	Power required by the built-in pump [w]

A.6.2 Inputs:

w_{ai}	Humidity ration of air entering at inlet [kg $_{vapour}$/kg $_{dry\ air}$]
h_{ai}	Specific enthalpy of air entering at inlet [J/kg $_{dry\ air}$]

m_i Mass flow rate of liquid at inlet [kg/s]

T_{li} Temperature of liquid entering at inlet [°C]

A.6.3 Outputs:

w_{ae} Humidity ratio of air leaving at outlet [$kg_{vapour}/kg_{dry\ air}$]

h_{ae} Specific enthalpy of air leaving at outlet [$J/kg_{dry\ air}$]

T_{le} Temperature of liquid leaving at outlet [°C]

Pwr Input power required [W]

A.6.4 Internal variables:

h_{si} Specific enthalpy of saturated air entering at t_{le} [$J/kg_{dry\ air}$]

h_{se} Specific enthalpy of saturated air entering at t_{li} [$J/kg_{dry\ air}$]

A.6.5 Explicit equations:

$$UA = a_0 + a_1 m_l + a_2 T_{li} + a_3 m_l^{\ 2} + a_4 T_{li}^{\ 2} + a_5 m_{li} T_{li}$$

$$h_{se} = 10^3 (16.66326 + 4.701617 T_{li} - 0.11237 T_{li}^{\ 2} + 0.004991 T_{li}^{\ 3} - 0.17197 p_{barom} - 0.01364 p_{barom} T_{li} + 0.000493 p_{barom} T_{li}^{\ 2} - 2.9x10^{-5} p_{barom} T_{li}^{\ 3})$$

$$Pwr = Pwr_{fan} + Pwr_{pump}$$

A.6.6 Simultaneous equations:

$$h_{si} = 10^3 (16.66326 + 4.701617 T_{le} - 0.11237 T_{le}^{\ 2} + 0.004991 T_{le}^{\ 3} - 0.17197 p_{barom} - 0.01364 p_{barom} T_{le} + 0.000493 p_{barom} T_{le}^{\ 2} - 2.9x10^{-5} p_{barom} T_{le}^{\ 3})$$

$$Q_a = UA \left[\frac{(h_{si} - h_{ai}) - (h_{se} - h_{ae})}{\ln \frac{(h_{si} - h_{ai})}{(h_{se} - h_{ae})}} \right]$$

$$Q_a = m_a (h_{ae} - h_{ai})$$

$$Q_a = m_l c_{pl} (T_{li} - T_{le})$$

A.6.7 Explicit equations:

$$T_{ae} = \xi(h_{ae}, saturated)$$

A.7. HEATER

A.7.1 Parameters:

Q_a^* Heater capacity [W]

A.7.2 Inputs:

m_a Mass flow rate of air entering the heater [kg/s]

h_{ai} Specific enthalpy of air entering heater [J/kg $_{dry\ air}$]

w_{ai} Humidity ration of air entering the heater [kg $_{vapour}$/kg $_{dry\ air}$]

A.7.3 Outputs:

h_{ae} Specific enthalpy of air leaving the heater [J/kg $_{dry\ air}$]

w_{ae} Humidity ratio of air leaving the heater [kg $_{vapour}$/kg $_{dry\ air}$]

A.7.4 Explicit equations:

$$h_{ae} = h_{ai} + \frac{Q_a}{m_a}$$

$$w_{ae} = w_{ai}$$

A.8. PID CONTROLLER

A.8.1 Parameters:

t Present time

Δt Size of simulation time step

θ_{lo} Throttling range (proportional band) low of controlled variable

θ_{hi} Throttling range (proportional band) high of controlled variable

ϕ_{lo} Low potential of final control element

ϕ_{hi} High potential of final control element

k_I Integral control factor

k_D Derivative control factor

A.8.2 Inputs:

θ Value of controlled variable

A.8.3 Outputs:

ϕ	Potential of final control element

A.8.4 Internal variables:

θ_{sp}	Set-point value of controlled variable
ϕ_{sp}	Set-point potential of final control element
k_P	Proportional control factor
ε	Error function

A.8.5 Explicit equations:

$$\theta_{sp} = \frac{\theta_{lo} + \theta_{hi}}{2}$$

$$\phi_{sp} = \frac{\phi_{lo} + \phi_{hi}}{2}$$

$$k_P = \frac{\phi_{lo} - \phi_{hi}}{\theta_{lo} - \theta_{hi}}$$

$$\varepsilon_t = \theta_t - \theta_{sp}$$

$$if = \theta_{t-\Delta t} \le \theta_{lo} \quad then \quad \phi_t = \phi_{lo}$$

$$else \quad if \quad \theta_{t-\Delta t} \ge \theta_{hi} \quad then \quad \phi_t = \phi_{hi}$$

$$else \quad \phi_t = k_P \varepsilon_{t-\Delta t} + k_I \sum_{t=0}^{t=t-\Delta t} \left[\varepsilon \Delta t\right]_t + k_D \left[\frac{\varepsilon_{t-\Delta t} - \varepsilon_{t-2\Delta t}}{\Delta t}\right]$$

A.9. STEP CONTROLLER

A.9.1 Parameters:

t	Present time.
Δt	Size of simulation time steps.
n	Number of steps.
$\theta_{L,1\ldots n}$	Loading set-points of controlled variable.
$\theta_{U,1\ldots n}$	Unloading set-points of controlled variable.
$\phi_{L,1\ldots n}$	Loading potential steps of final control element.

$\phi_{U,1...n}$ Unloading potential steps of final control element.

A.9.2 Inputs:

θ Value of controlled variable.

A.9.3 Outputs:

ϕ Potential of final control element.

A.9.4 Explicit equations:

$$\text{If } \theta_{t-\Delta t} \geq \theta_{t-2\Delta t} \text{ and } \theta_{t-\Delta t} \geq \theta_{L,i} \text{ then } \phi_t = \phi_{L,i}$$

$$\text{Else if } \theta_{t-\Delta t} \prec \theta_{t-2\Delta t} \text{ and } \theta_{t-\Delta t} \prec \theta_{L,i} \text{ then } \phi_t = \phi_{U,i}$$

APPENDIX B

CONFERENCE FACILTIES

This appendix presents all the zone verification results and the new control results of application 2, chapter 4.

B.1. VERIFICATION RESULTS

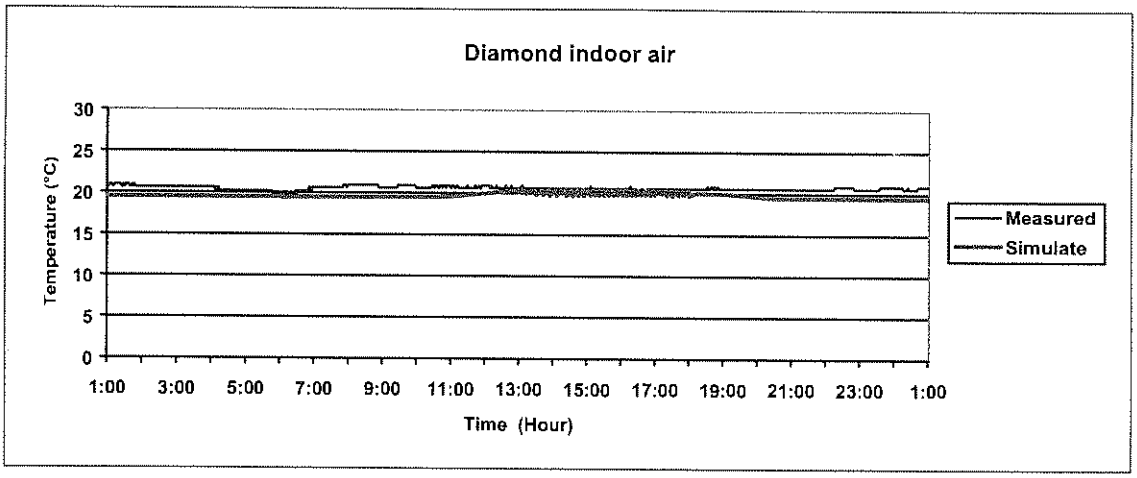

Figure B.1: Diamond indoor air verification study

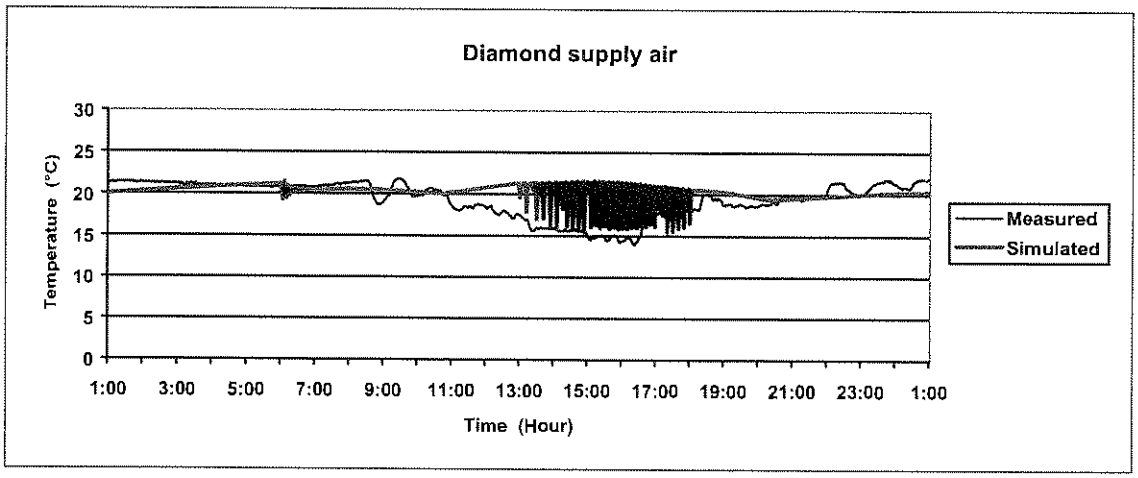

Figure B.2: Diamond supply air verification study

	MAX ERROR (°C)	AVERAGE ERROR (°C)	% OF TIME WITHIN 2 °C
SUPPLY AIR	6.8	1.5	75
INDOOR AIR	1.4	0.9	100

Table B.1: Summary of Diamond results

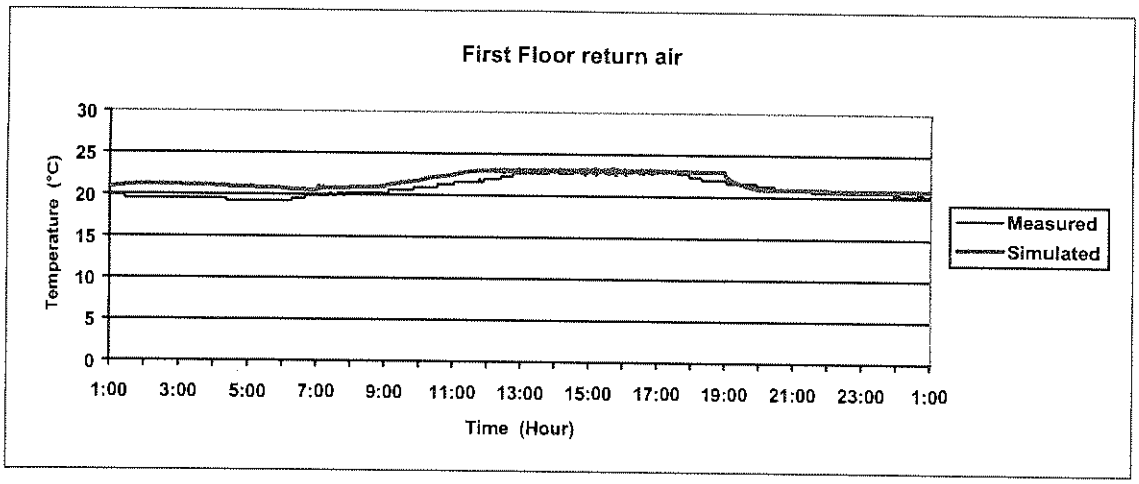

Figure B.3: First Floor return air verification study

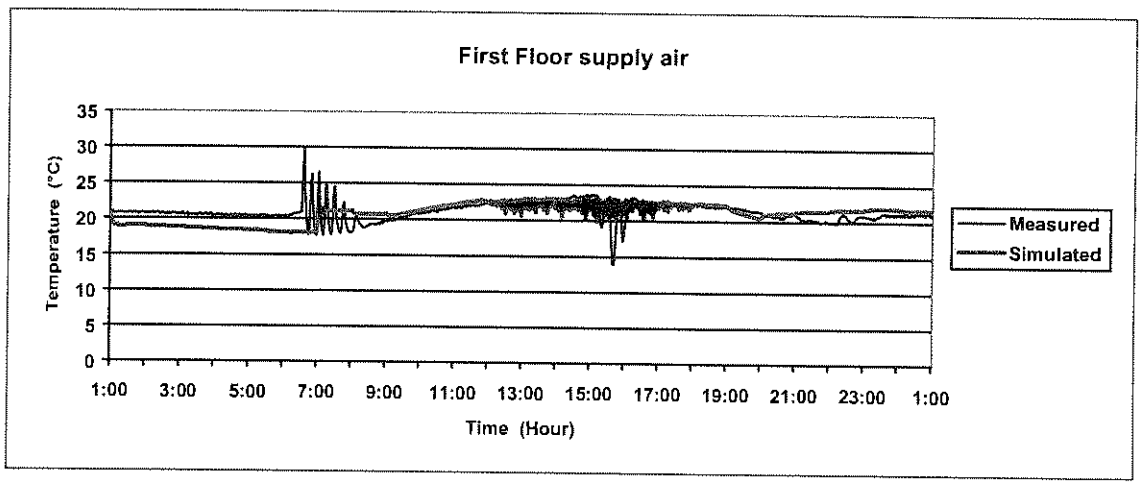

Figure B.4: First Floor supply air verification study

	Max error (°C)	Average error (°C)	% of time within 2 °C
Supply air	15	1.4	81
Return air	2.4	0.6	100

Table B.2: Summary of First Floor results

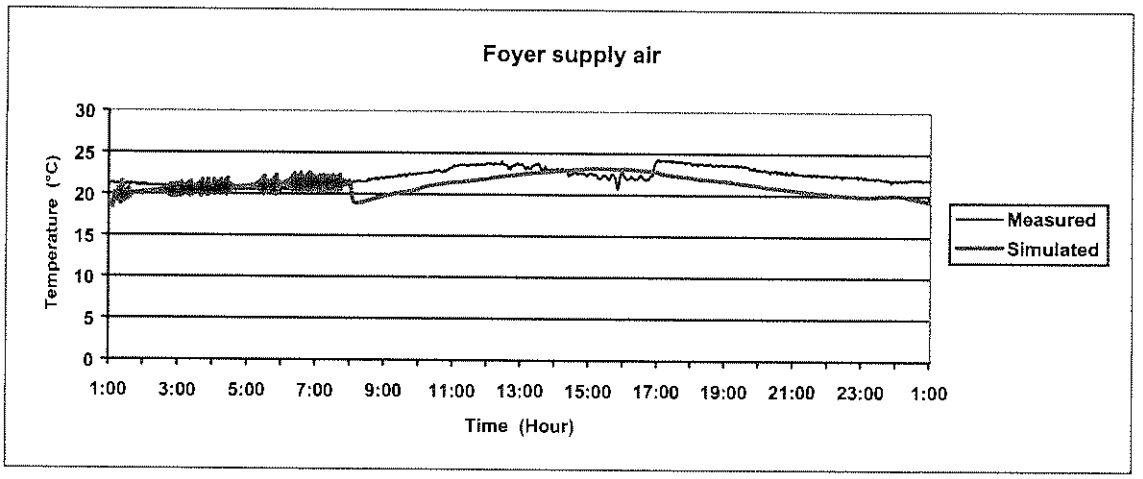

Figure B.5: Foyer supply air verification study

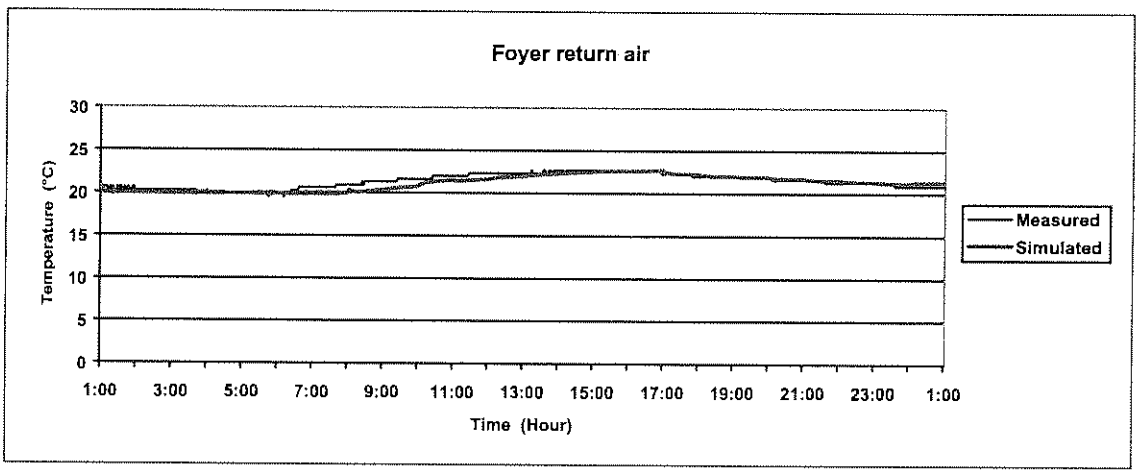

Figure B.6: Foyer return air verification study

	Max error (°C)	Average error (°C)	% of time within 2 °C
Supply air	3.4	1.3	72
Return air	4.9	0.2	100

Table B.3: Summary of Foyer results

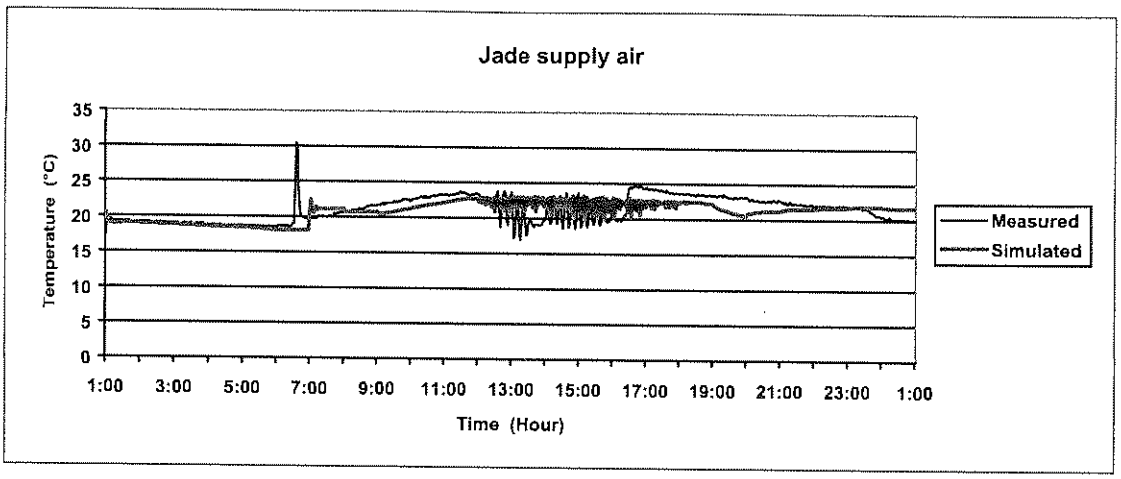

Figure B.7: Jade supply air verification study

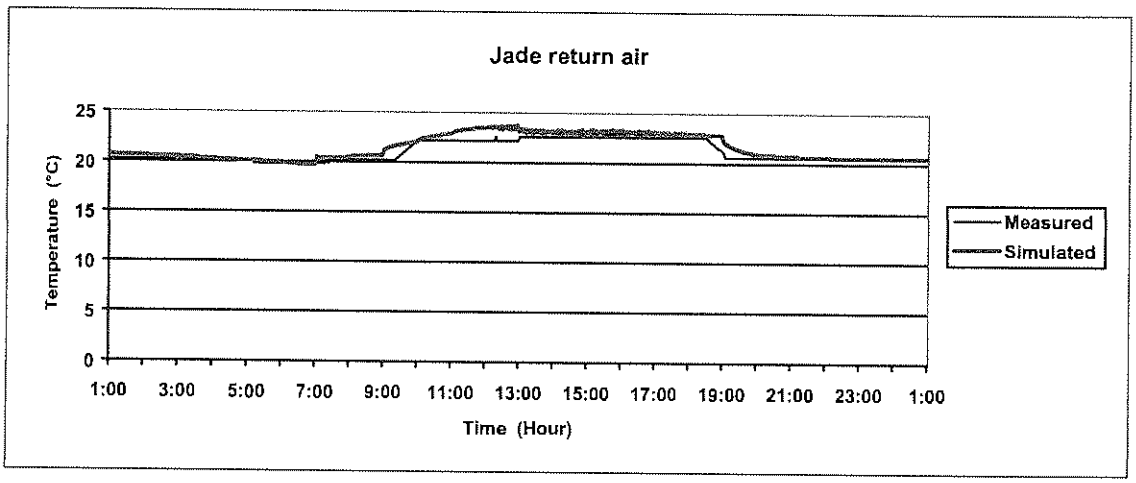

Figure B.8: Jade return air verification study

	Max error (°C)	Average error (°C)	% of time within 2 °C
Supply air	12	1.7	88
Return air	1.5	0.4	100

Table B.4: Summary of Jade results

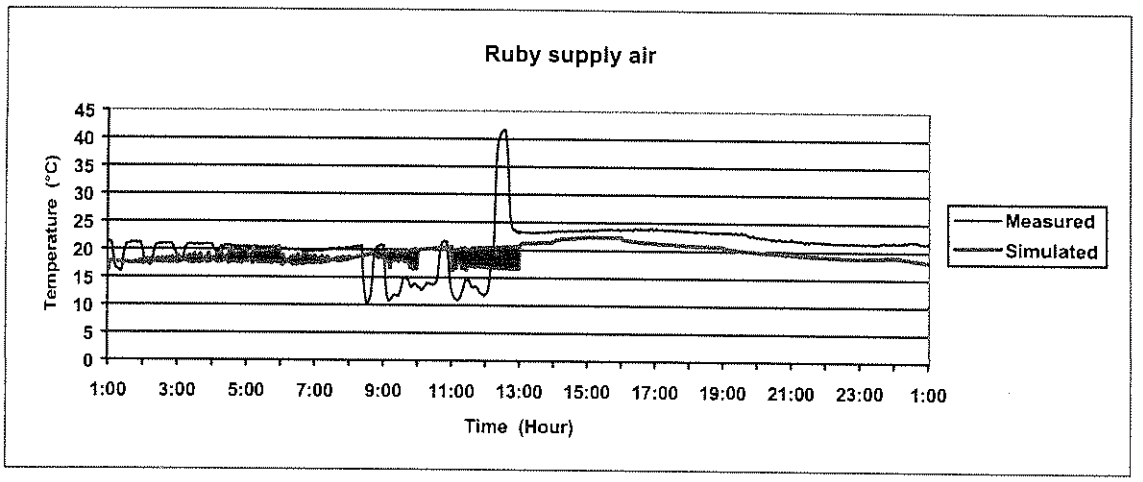

Figure B.9: Ruby supply air verification study

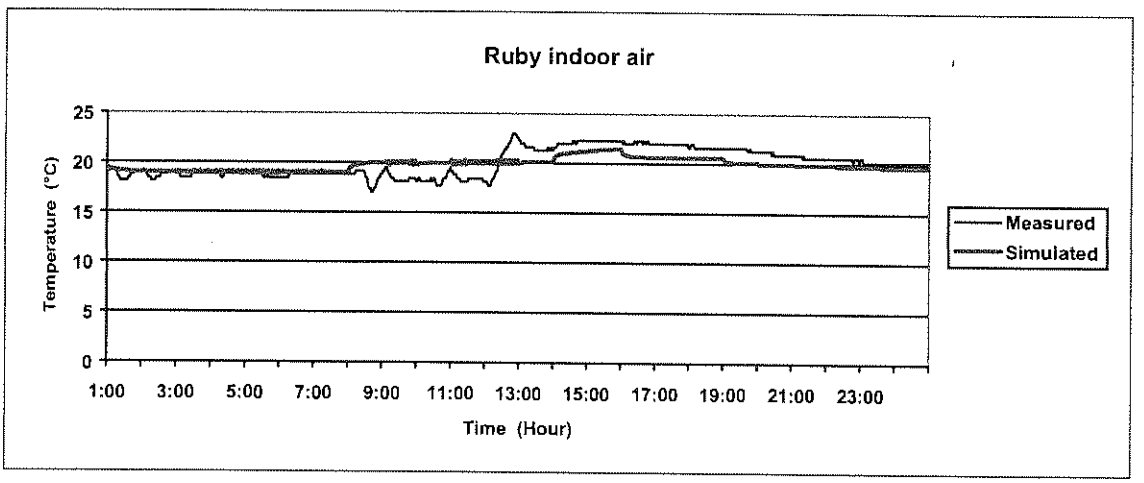

Figure B.10: Ruby indoor air verification study

	Max error (°C)	Average error (°C)	% of time within 2 °C
Supply air	20	3.1	97
Return air	3	1	100

Table B.5: Summary of Ruby results

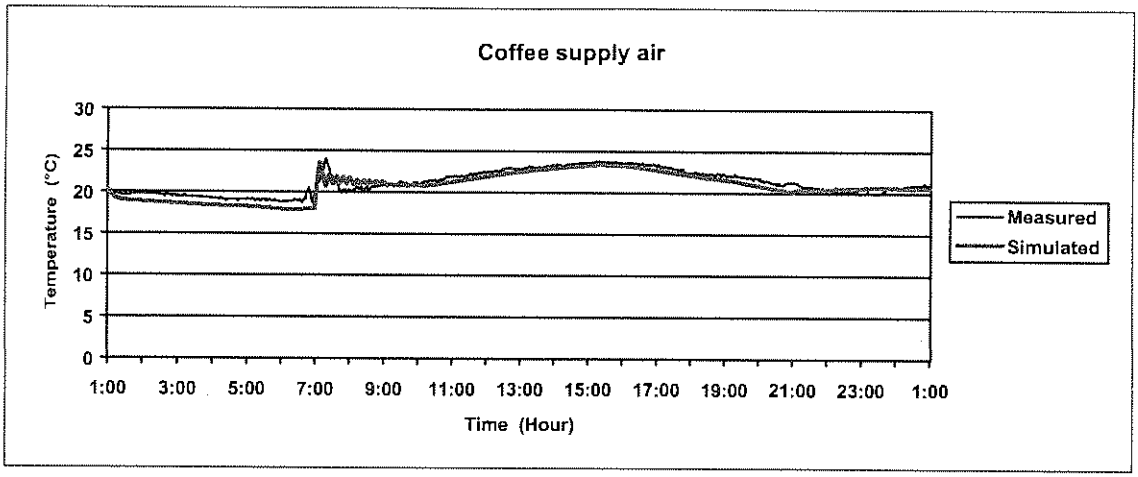

Figure B.11: Coffee supply air verification study

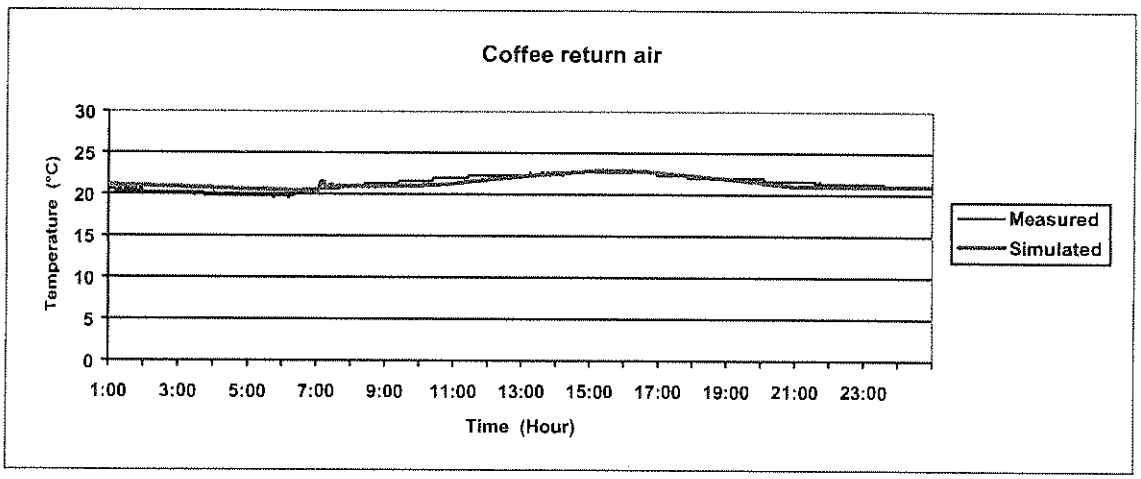

Figure B.12: Coffee return air verification study

	Max error (°C)	Average error (°C)	% of time within 2 °C
Supply air	3	0.6	99
Return air	1	0.4	100

Table B.6: Summary of Coffee results

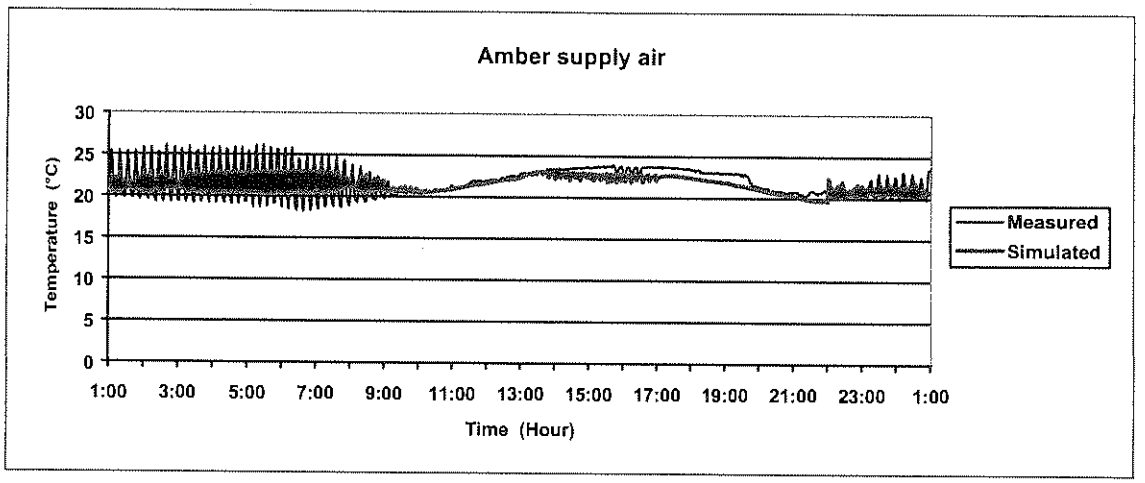

Figure B.13: Amber supply air verification study

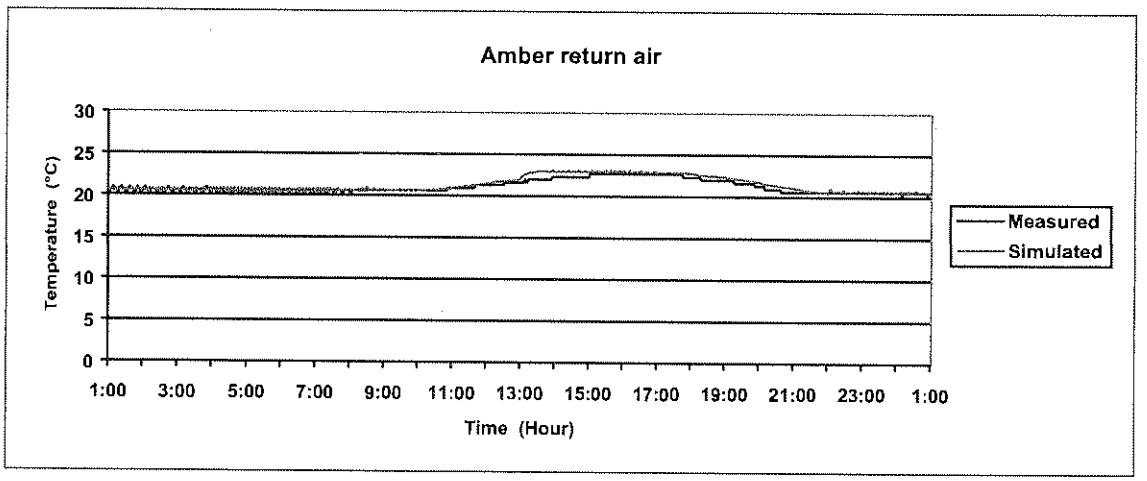

Figure B.14: Amber return air verification study

	Max error (°C)	Average error (°C)	% of time within 2 °C
Supply air	6.3	1.6	75
Return air	1.8	0.6	100

Table B.7: Summary of Amber results

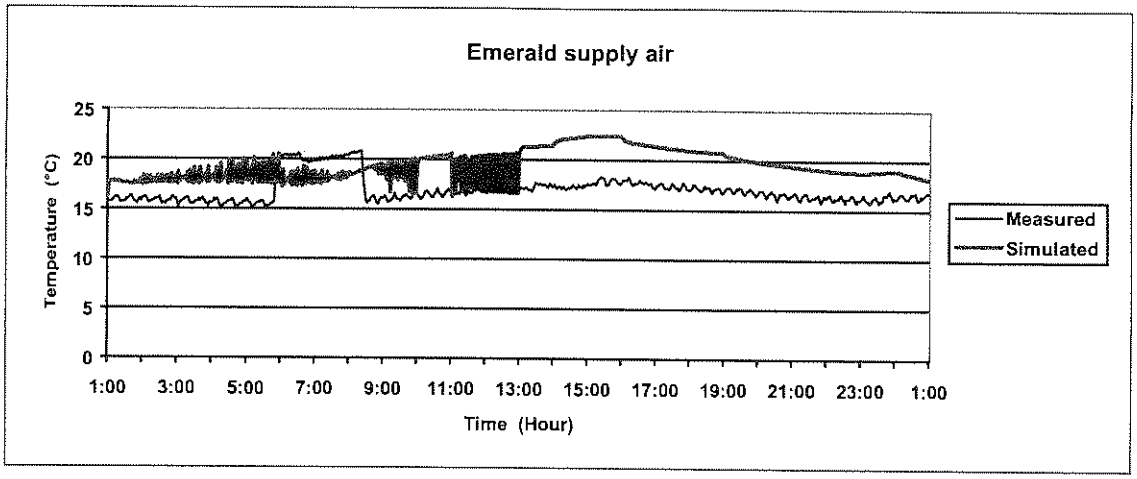

Figure B.15: Emerald supply air verification study

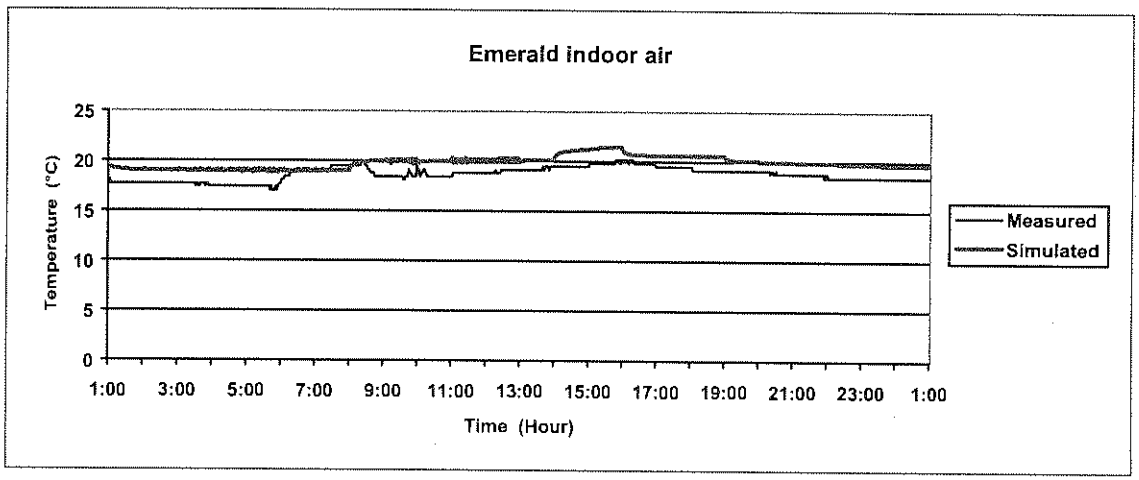

Figure B.16: Emerald indoor air verification study

	Max error (°C)	Average error (°C)	% of time within 2 °C
Supply air	5.4	2.8	27
Return air	2.1	1.1	100

Table B.8: Summary of Emerald results

B.2. ENERGY AND POWER RESULTS

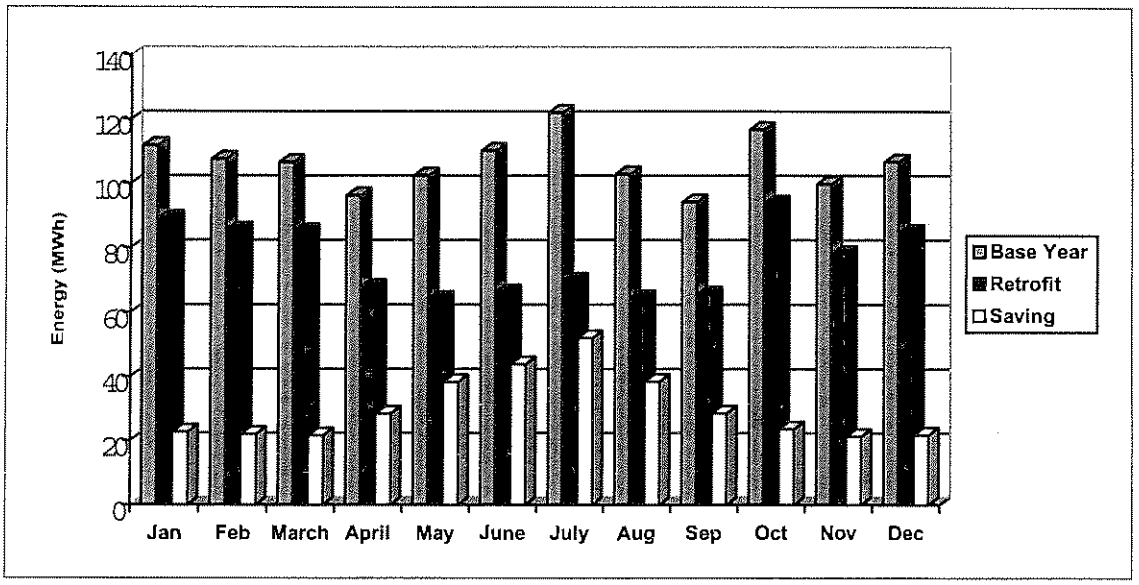

Figure B.17: Fan scheduling energy consumption result

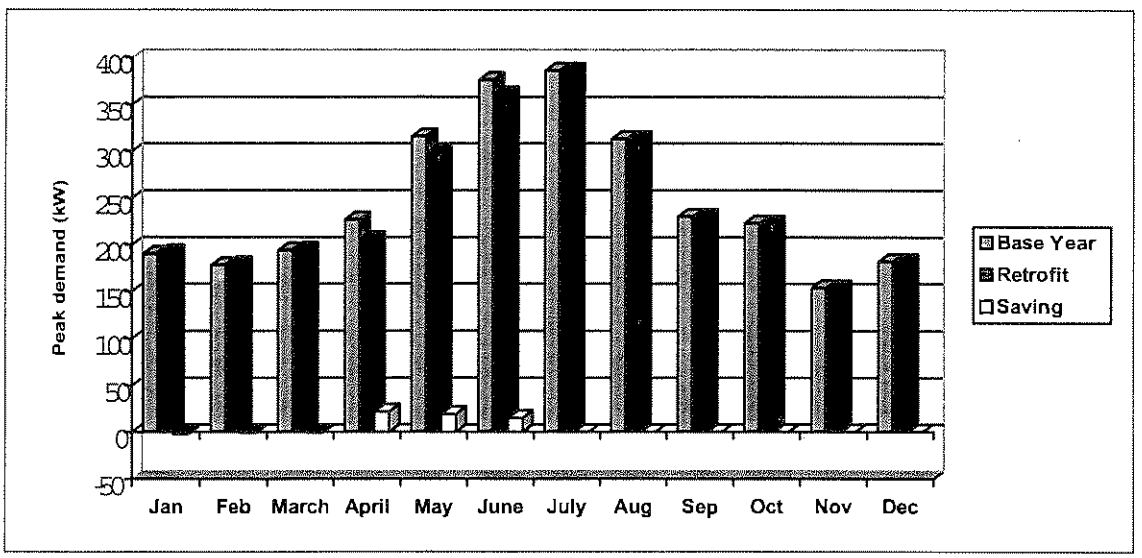

Figure B.18: Fan scheduling peak demand simulation result

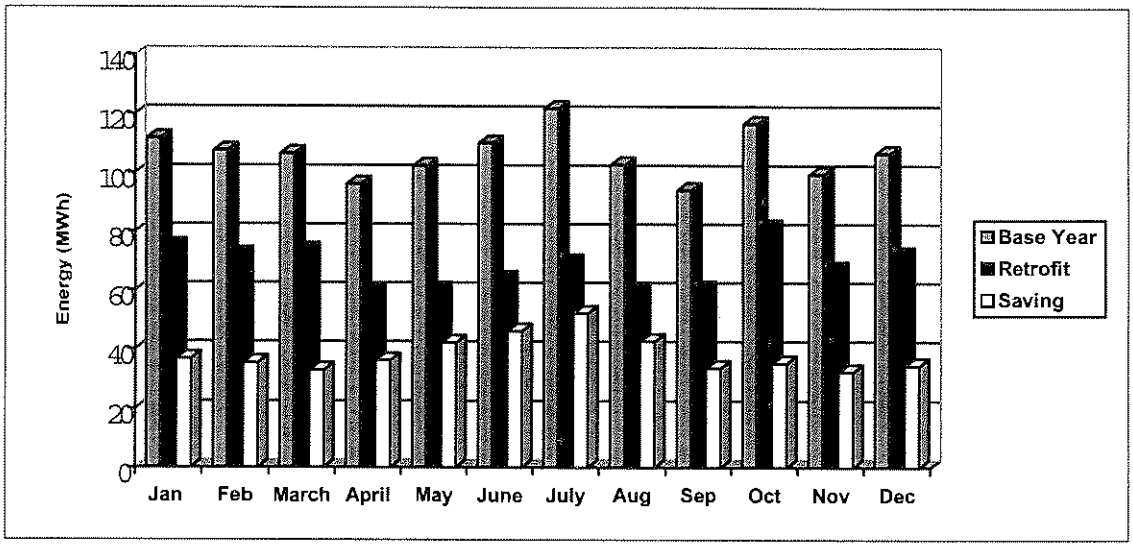

Figure B.19: Fan scheduling, economiser and setpoint energy simulation result

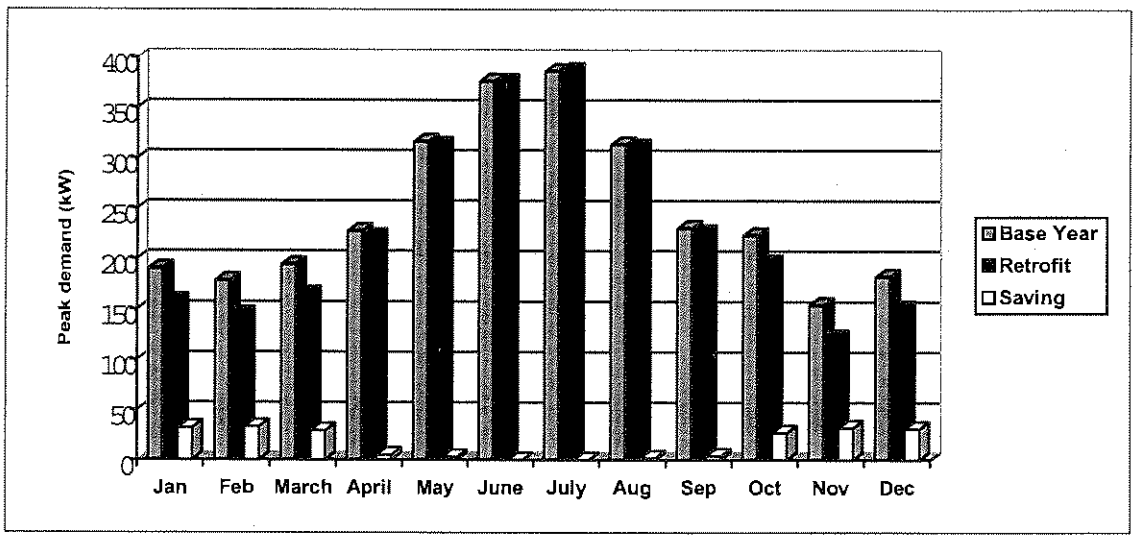

Figure B.20: Fan scheduling, economiser and setpoint peak demand simulation result

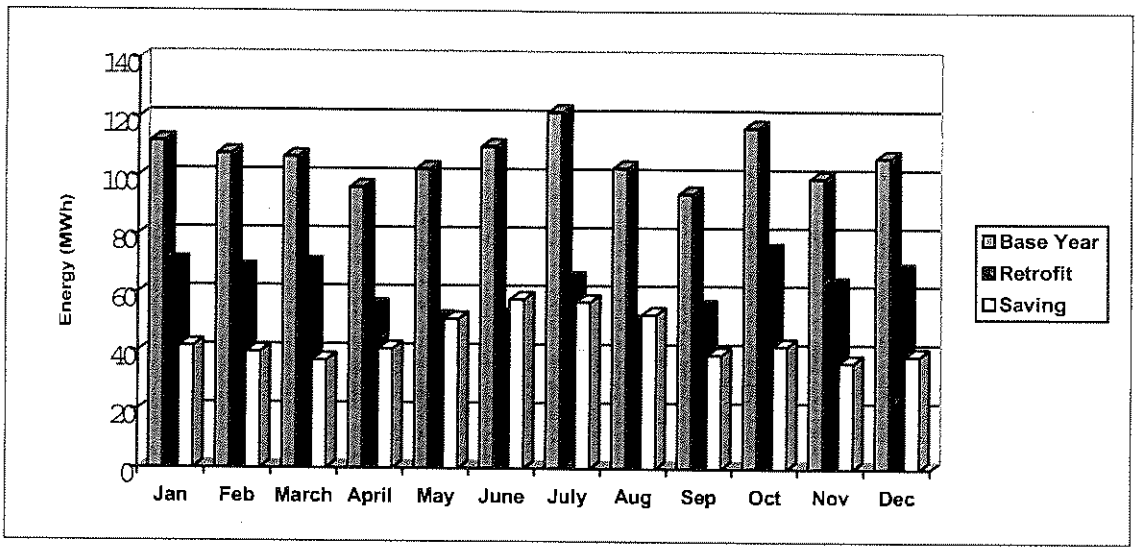

Figure B.21: Fan scheduling, economiser and setback control energy simulation result

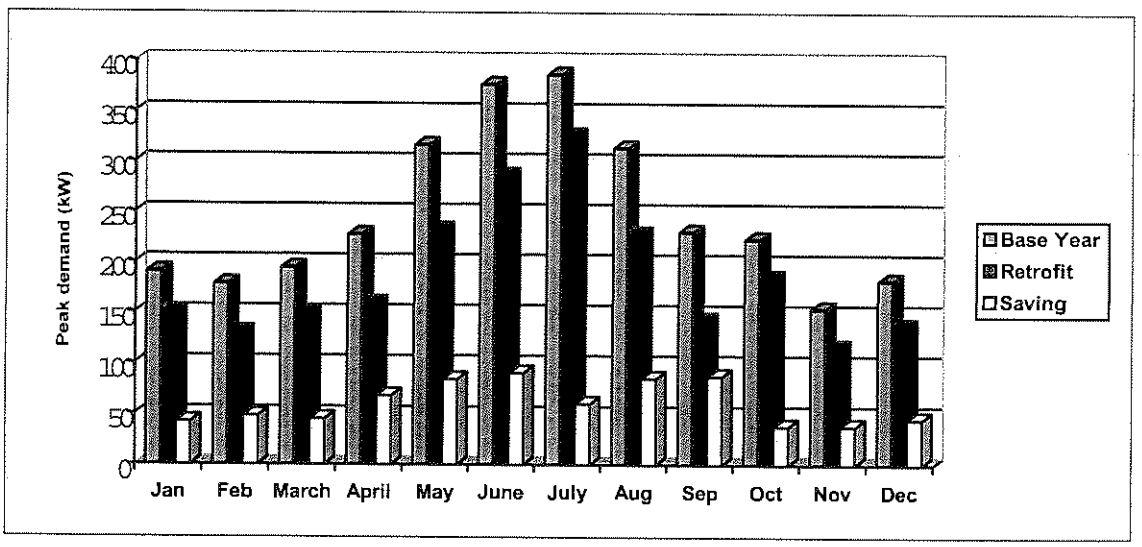

Figure B.22: Fan scheduling, economiser and setback control demand simulation result

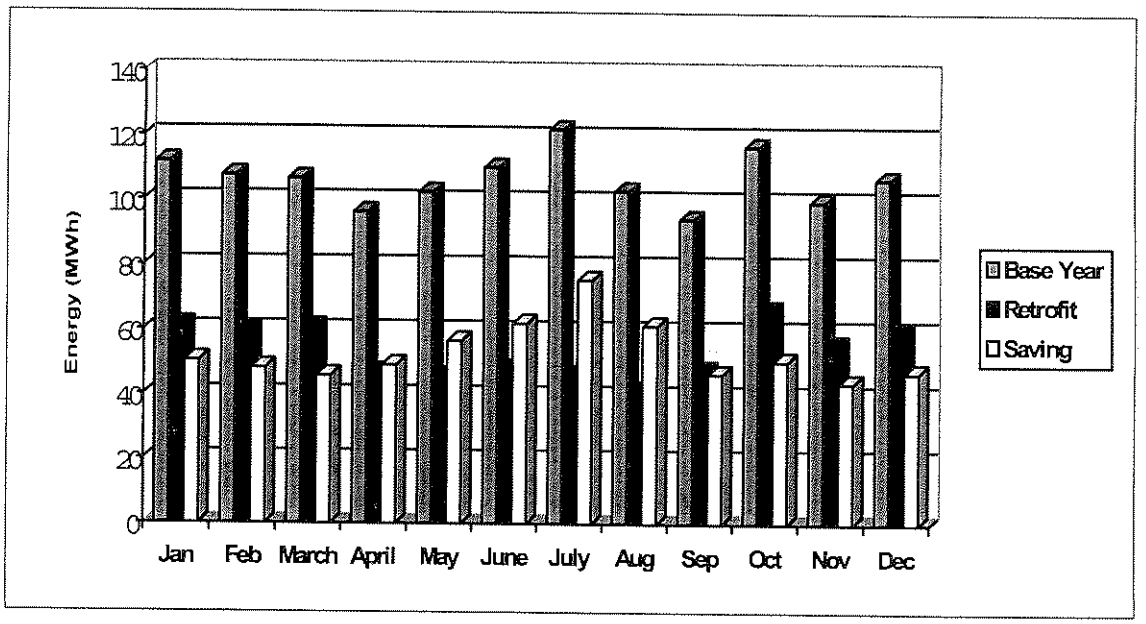

Figure B.23: Fan scheduling, economiser, setback and fan control energy simulation result

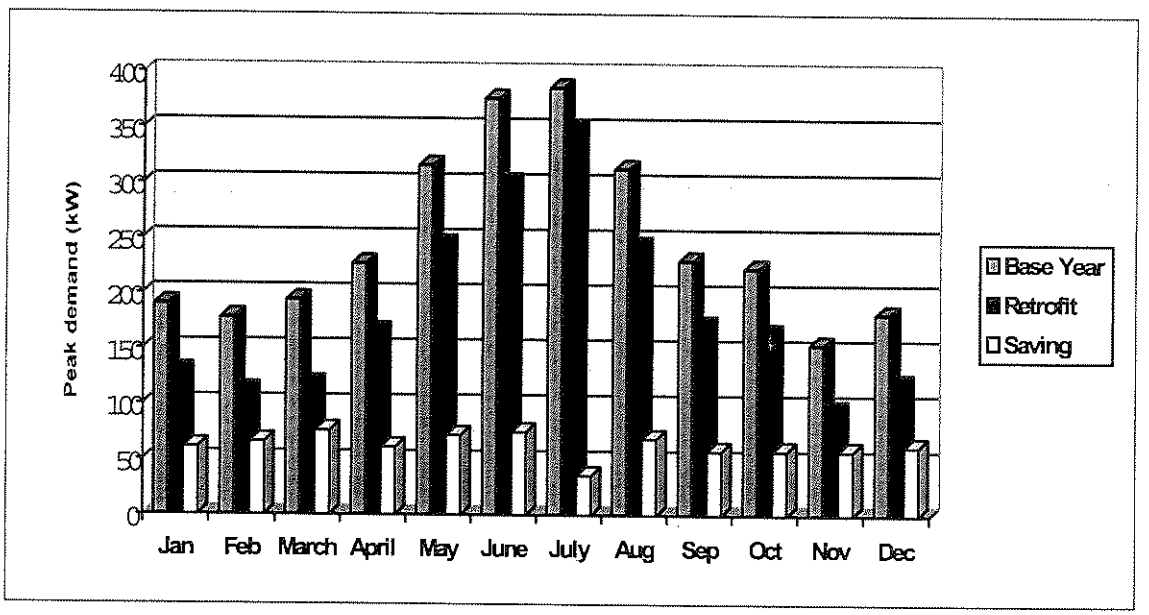

Figure B.24: Fan scheduling, economiser, setback and fan control simulation result

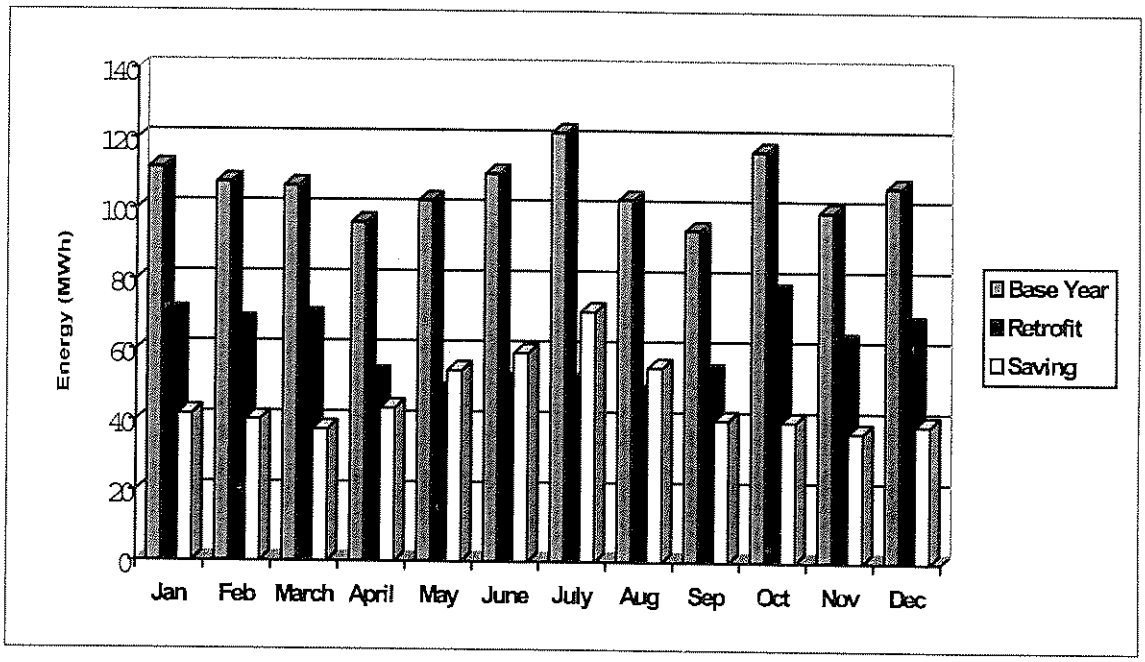

Figure B.25: Fans scheduling, economiser, setpoint and boiler control energy simulation result

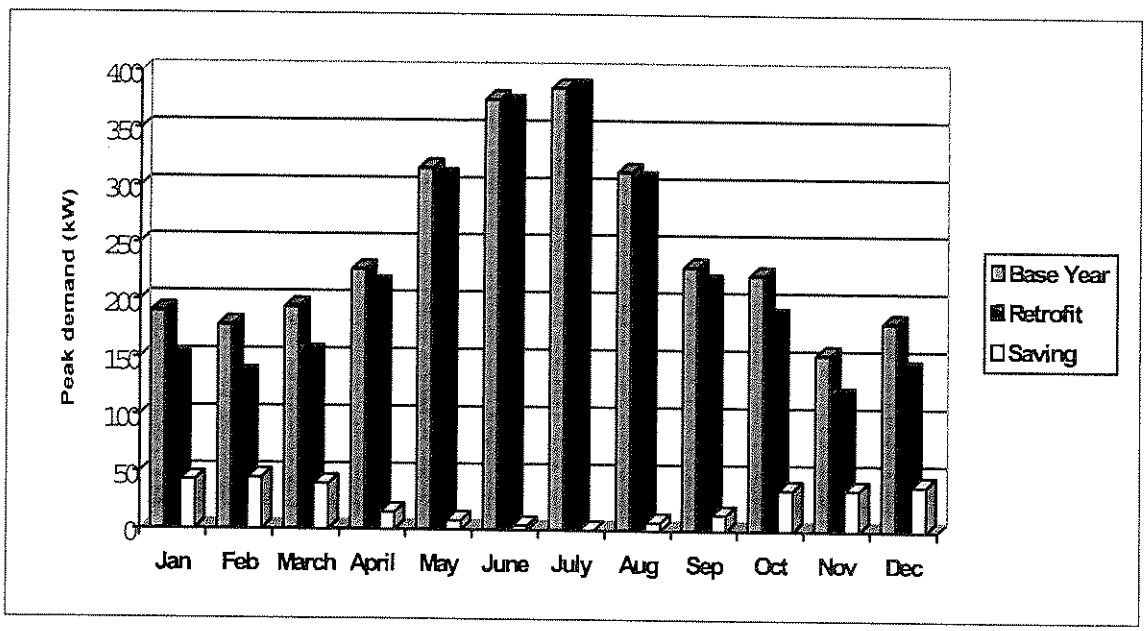

Figure B.26: Fan scheduling, economiser, setpoint and boiler control peak simulation result

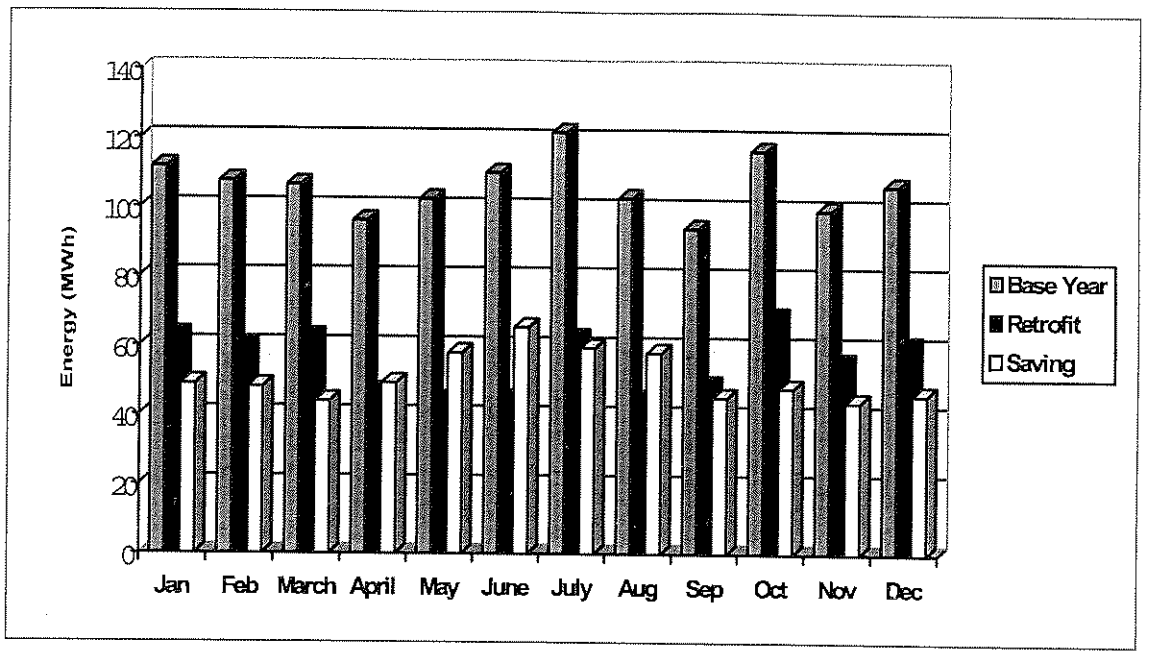

Figure B.27: Fan scheduling, economiser, setback and boiler energy simulation result

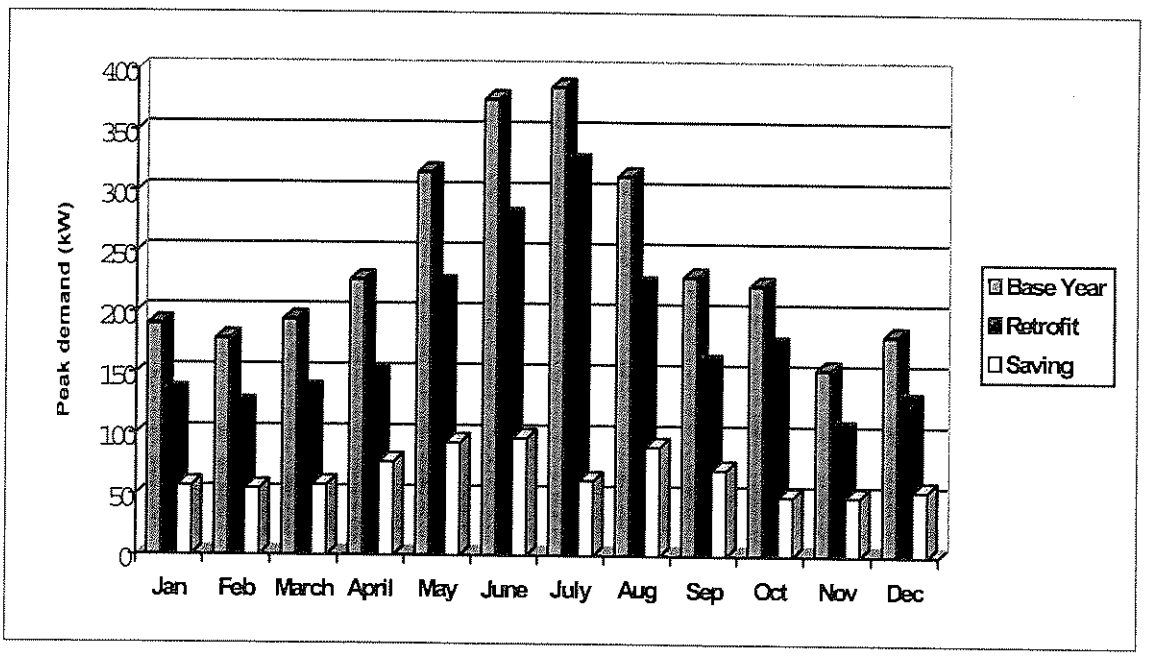

Figure B.28: Fan scheduling, economiser, setback and boiler control peak simulation result

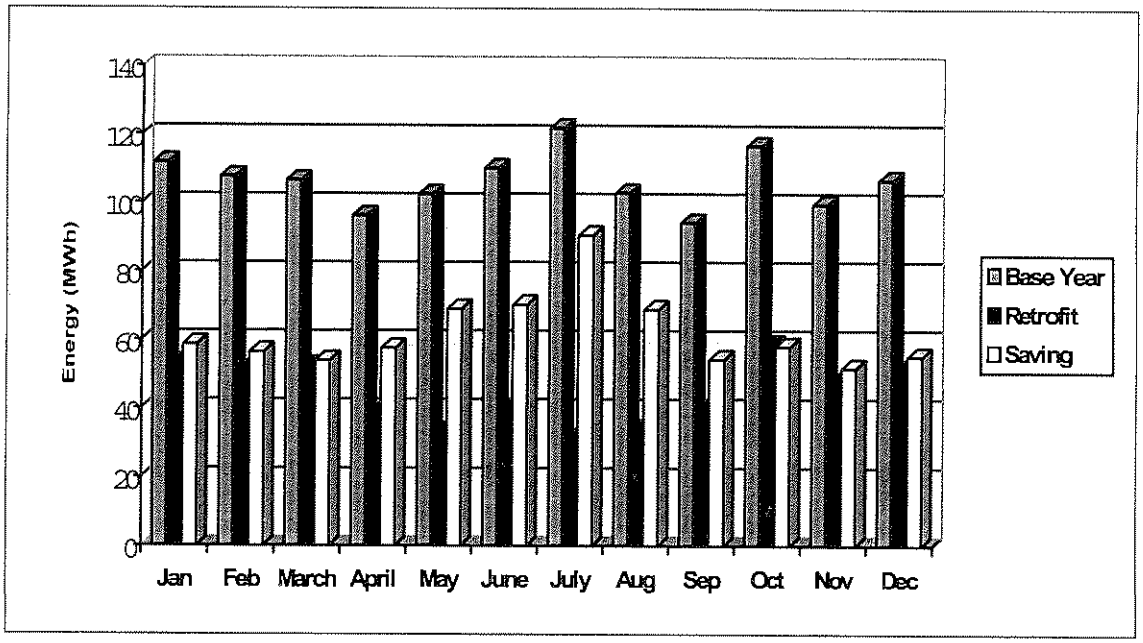

Figure B.29: Fan scheduling, economiser, setback, fan and boiler control energy simulation result

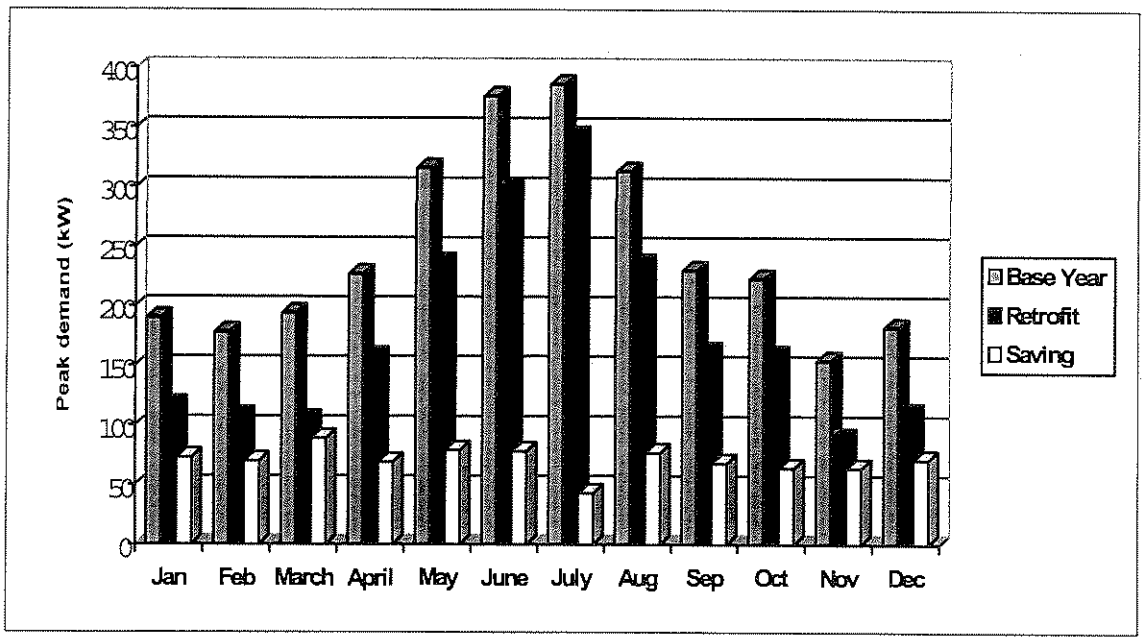

Figure B.30: Fan scheduling, economiser, setback, fan and boiler control peak simulation result

APPENDIX C

THE POTENTIAL FOR DSM ON MINE COOLING SYSTEMS

This appendix presents all the equipment specifications and the verification results of application 1, chapter 8.

C.1. EQUIPMENT SPECIFICATIONS

A more detailed look at the pre-cool towers and the surface cooling plant can be seen in Figure C.1 and Figure C.2. Scheme A is shown in Figure C.2.

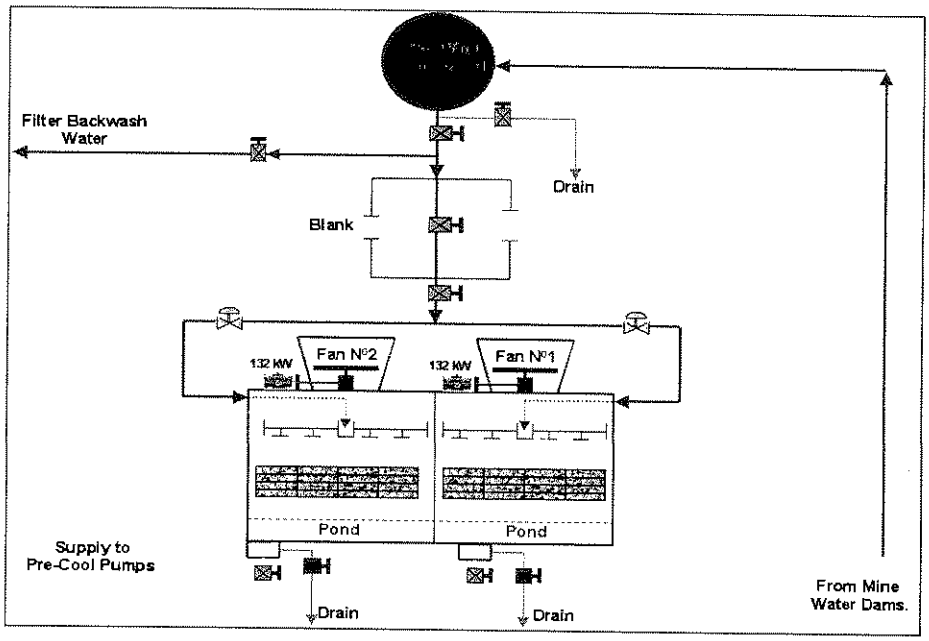

Figure C.1: Pre-cooling tower configuration

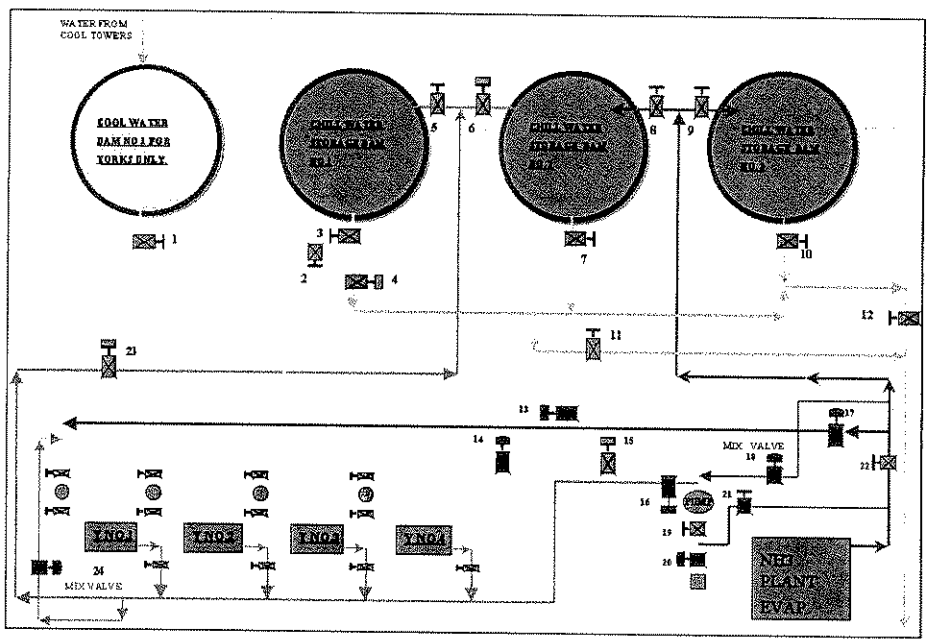

Figure C.2: Surface cooling plant

C.1.1 Dams

Dam	Purpose	Volume [m^3]	Open/ Closed	Controlled by
Mine Water	Collect water from mine	3817.7	Open	-
Hot Water	Hot water pumped from Mine water dam	2709	Open	Level
Pre-Cool	Collect water from Pre-cool Towers	318.1	Open	Level
Cool Water	Store water after Pre-cool Towers	2709	Closed	Level
Chill 1	Store water after York chillers	2709	Closed	Level
Chill 2	Store water after York or Howden chillers	2709	Closed	Level
Chill 3	Store water after Howden chiller	2709	Closed	Level

Table C.1: Summary of dam

C.1.2 Pumps

Table C.2 presents a summary of the pumps used in the surface cooling cycle. The various pump curves are shown in the following pages.

Pump description	Pump (Type)	Impeller diameter (m)	Flow [l/s]	Power [kw]	Cotrolled by:
Mine Water	KSB ETA 250/50	0.41	300	200	Hot dam level
Filter pumps - A	Sulzer AZS 200/250	0.25	75	15	Cool dam Level
Filter pumps - B	Allis-Chalmer	0.3	120	30	Cool dam Level
York Evaporator	Salweir SDB 200/250	0.32	114	55	Chill 1 dam Level
York Condensor	Salweir SDB 10/12	0.36	280	132	Chill 1 dam Level
Howden Evap	Salweir SDB 350/450	0.415	420	160	Chill 2&3 dam Level
Howden Cond	Salweir SDB 350/450	0.475	420	185	Chill 2&3 dam Level

Table C.2: Summary of pump specifications

C.1.3 Cooling Towers

There are basically two sets of cooling towers. Firstly is the pre-cooling tower used to cool the water from the hot water dam. Secondly, there are the cooling towers on the condenser sides of the chillers. The two types are almost the same, therefore only one tower, the pre-cooling tower, will be discussed. Table C.3 shows all the data of the pre-cooling tower.

Performance Data	
Inlet Water Temp. (°C)	28
Outlet Water Temp. (°C)	18.5
Inlet WB Air Temp. (°C)	16
Outlet WB Air Temp. (°C)	23.3
Pressure (kPa)	85
Losses (%)	1.63
Water Flow (m^3/h)	1728
Per Cell (m^3/h)	864
Air flow/cell (m^3/s)	525.8
Static Pressure drop (Pa)	136.8
Heat Exchanged (MW)	19.06

Fan Details	
Diameter (m)	7.315
RPM	161
Number of blades	6
Pitch of blades (°)	16.3
Manufacturer	Howden
Type	ENF

Motor Details	
Power per motor (kW)	132
RPM	1480
Absorbed power (kW)	117.4
Manufacturer	ZEST/WEG

Construction Details	
Number of cells	2
Total Plot area (m^2)	14.85x28.75
Fill Area (m^2)	14.34x14
Induced draught	
Air opening (m^2)	80
Pitch of fill (m)	0.25
Fill Depth (m)	3.25
Height to bottom of fill (m)	3

Table C.3: Specifications for Pre-cooling Tower

C.1.4 Chillers

The specifications for the York chillers are shown in Table C.4 and for the Howden in Table C.5.

Design Details

Voltage (V)	11000	Chilled water inlet Temp. (°C)	14.5
Amps (A)	85.5	Chilled water outlet Temp. (°C)	4
Bearing Temp. - DE (°C)	60	Chilled water Delta T (°C)	10.5
Bearing Temp. - NDE (°C)	60	Chilled water flow (l/s)	114
Stator Temperature - Phase1	100	Evaporator duty (kW)	5012
Stator Temperature - Phase2	100	Condenser water outlet Temp.(°C)	27.5
Stator Temperature - Phase3	100	Condenser water inlet Temp. (°C)	22
Barometric Pressure (kPa)	84	Condenser water Delta T (°C)	5.5
% Vane opening	100	Condenser water flow (l/s)	270
Oil Level	Halftop	Condenser duty (kW)	6217
Oil Temp. (°C)	60	Compressor shaft power (kW)	1264
Oil Press. (kPa)	450	Coeffiesient of performance	3.96
Differantial oil Press. (kPa)	210	Carnot COP	9.5
Suction Temp. (°C)	2	Cycle efficiency (%)	41.71
Suction Press. - Gauge (kPa)	240	Power to cooling Ratio	0.25
Suction Press. - Absolute (kPa)	324	LMTD Condenser	4.73
Corresponding Temp. (°C)	1.62	LMTD Evaporator	6.21
Suction Superheat (°C)	0.4		
Discharge Temp. (°C)	50.5		
Condenser Press.-Gauge (kPa)	670		
Condenser Press.-Absolute(kPa)	754		
Corresponding Temp. (°C)	30.52		
Discharge superheat (°C)	20.5		
High Pressure Liquid Temp. (°C)	30		
Degrees system Air	0.5		

Table C.4: Specifications for York Chillers

Design Details - Normal running

Voltage (V)	11000	Evap. Ammonia Inlet Temp. (°C)	1
Amps (A)	160	Evap. Ammonia Outlet Temp. (°C)	10
Bearing Temp. - DE (°C)	45	Evap. Water Inlet Temp. (°C)	11
Bearing Temp. - NDE (°C)	34	Evap. Water Outlet Temp. (°C)	5
Stator Temperature - Phase1	59	Chilled water Delta T (°C)	5.5
Stator Temperature - Phase2	63	Chilled water flow (l/s)	420
Stator Temperature - Phase3	60	Evaporator duty (kW)	8300
Barometric Pressure (kPa)	84	Cond. Ammonia Inlet Temp. (°C)	40
% Vane opening	100	Cond.Ammonia Outlet Temp.(°C)	28
Oil Level	Halftop	Cond. water outlet Temp.(°C)	30
Oil Temp. in Seperator (°C)	40	Cond. water inlet Temp. (°C)	21
Oil Temp. in Manifold (°C)	40	Cond. water Delta T (°C)	9
Oil Filter Diff. Press. (kPa)	10	Cond. water flow (l/s)	350
Differantial oil Press. (kPa)	440	Cond. duty (kW)	11340
Suction Temp. (°C)	3	Compressor shaft power (kW)	1462
Surge drum Press. (kPa)	417	Coeffiesient of performance	5.7
Surge drum Level (%)	7	Carnot COP	13.434
Discharge Temp. (°C)	40-50	Cycle efficiency (%)	42.3
Discharge Press. (kPa)	1230	Power to cooling Ratio	0.1761

Table C.5: Specifications for Howden Chiller

C.2. VERIFICATION OF TEMPERATURES, LEVELS AND FLOWS

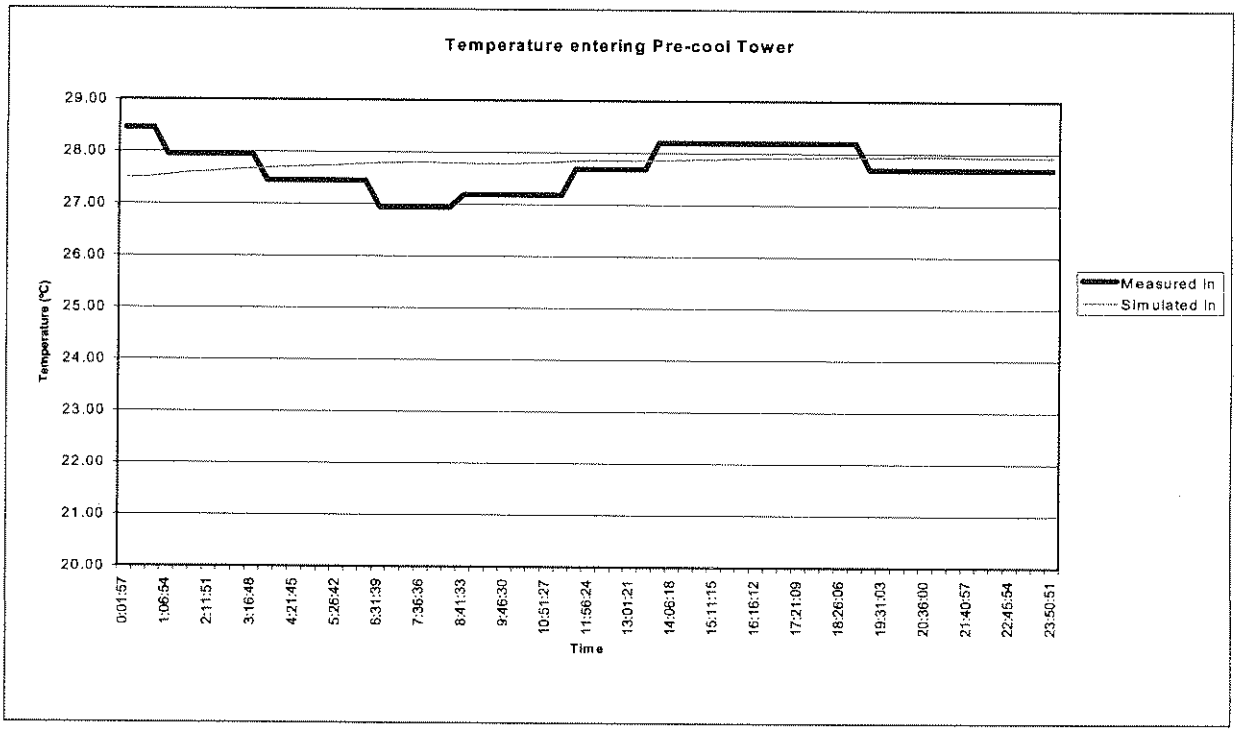

Figure C.3: Pre-cool towers inlet temperature verification

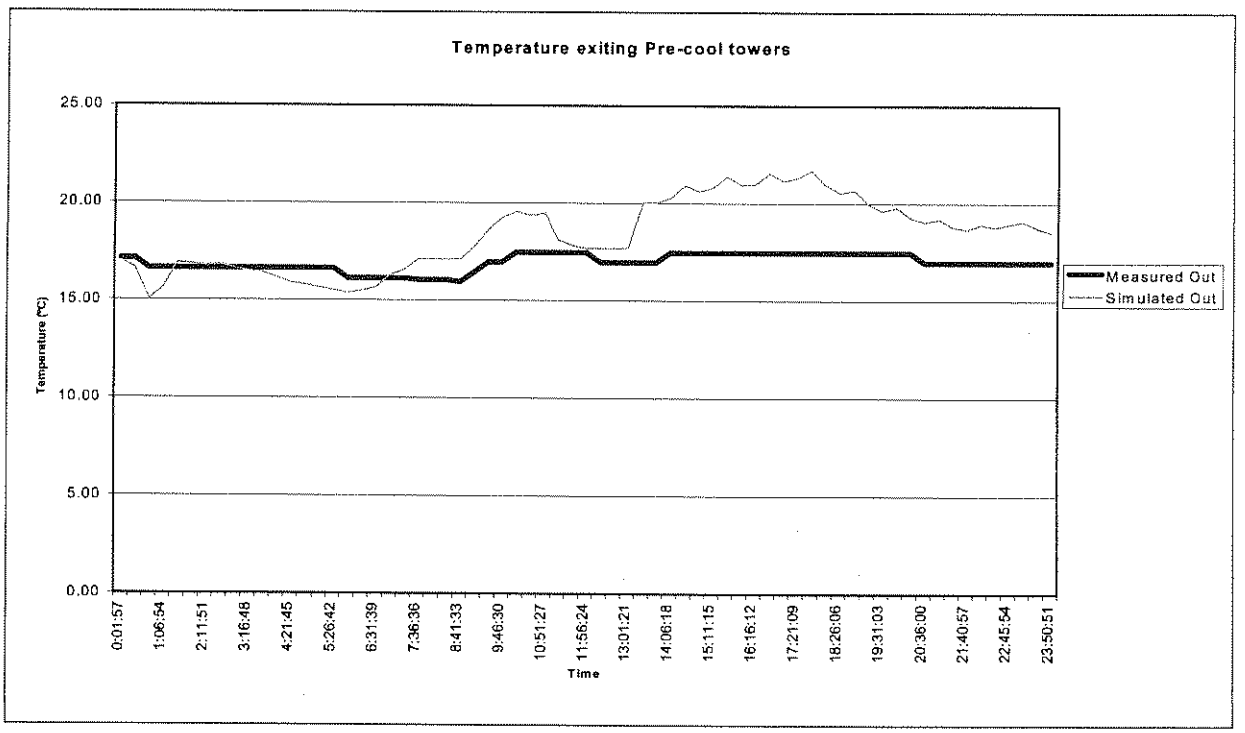

Figure C.4: Pre-cool tower exiting water temperature verification

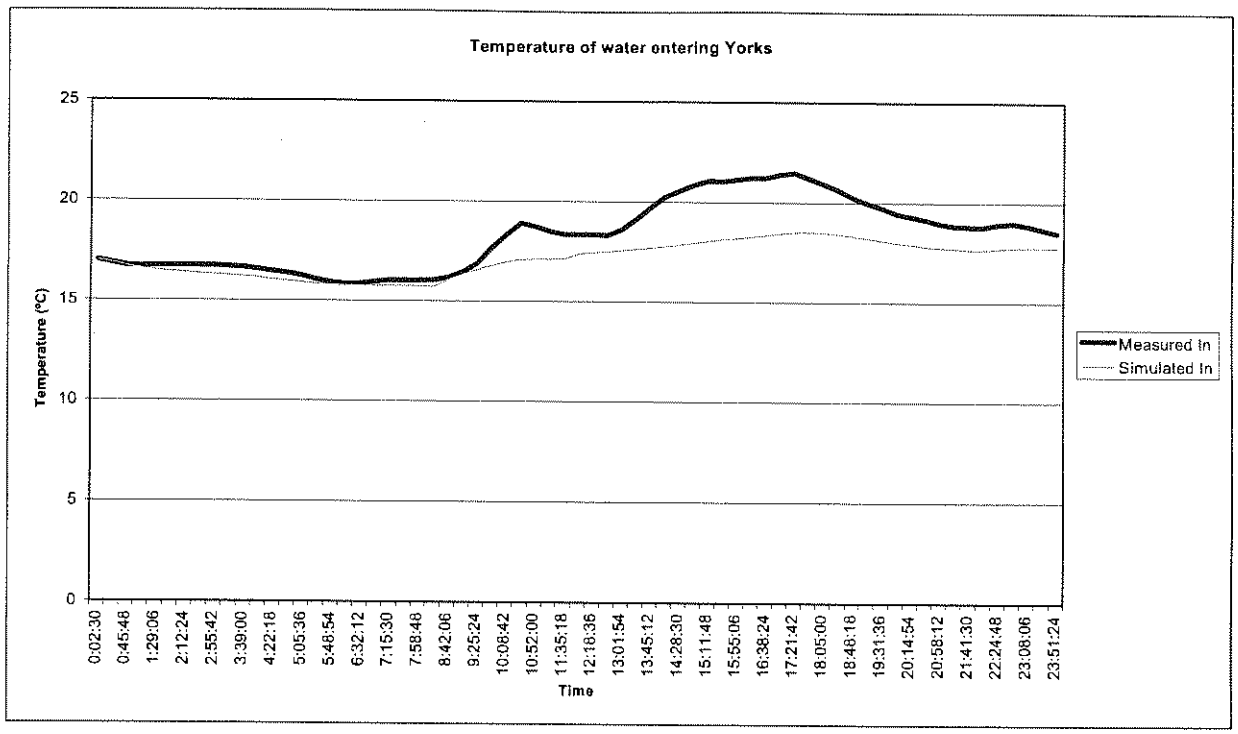

Figure C.5: Temperature of water entering the York chillers

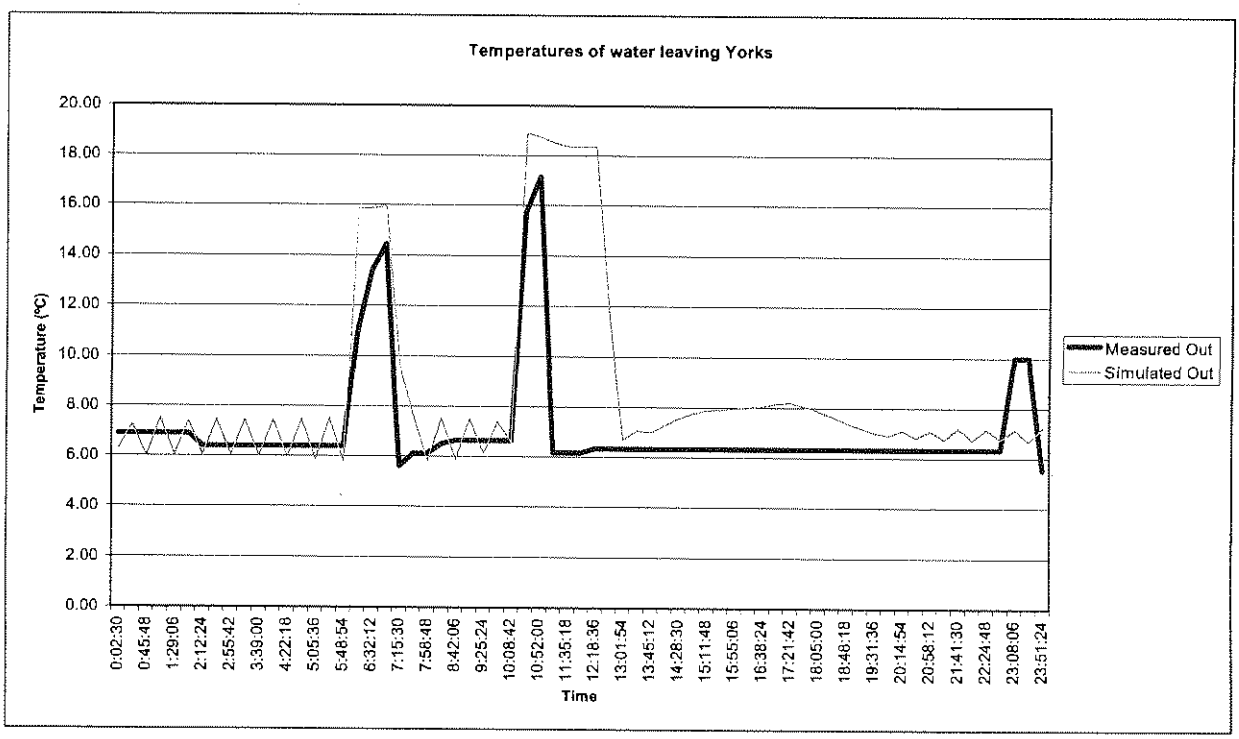

Figure C.6: Temperature of water exiting York chillers

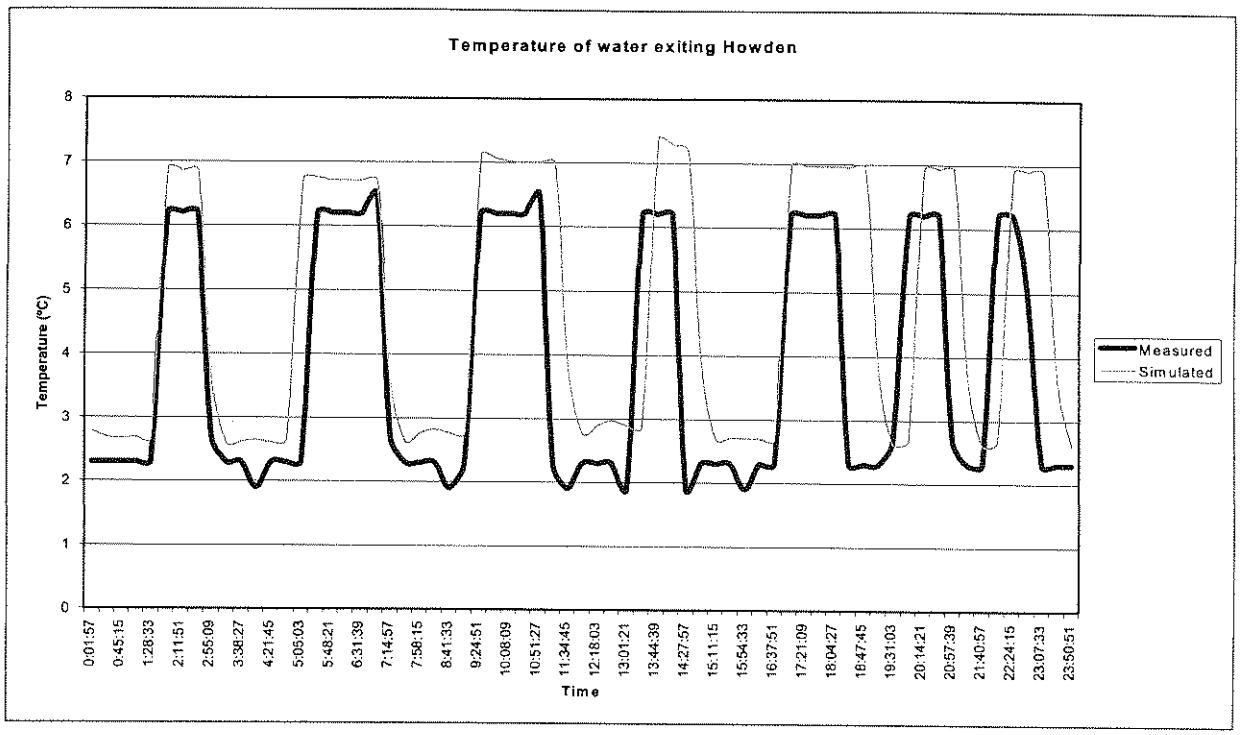

Figure C.7: Temperature of water exiting Howden chiller

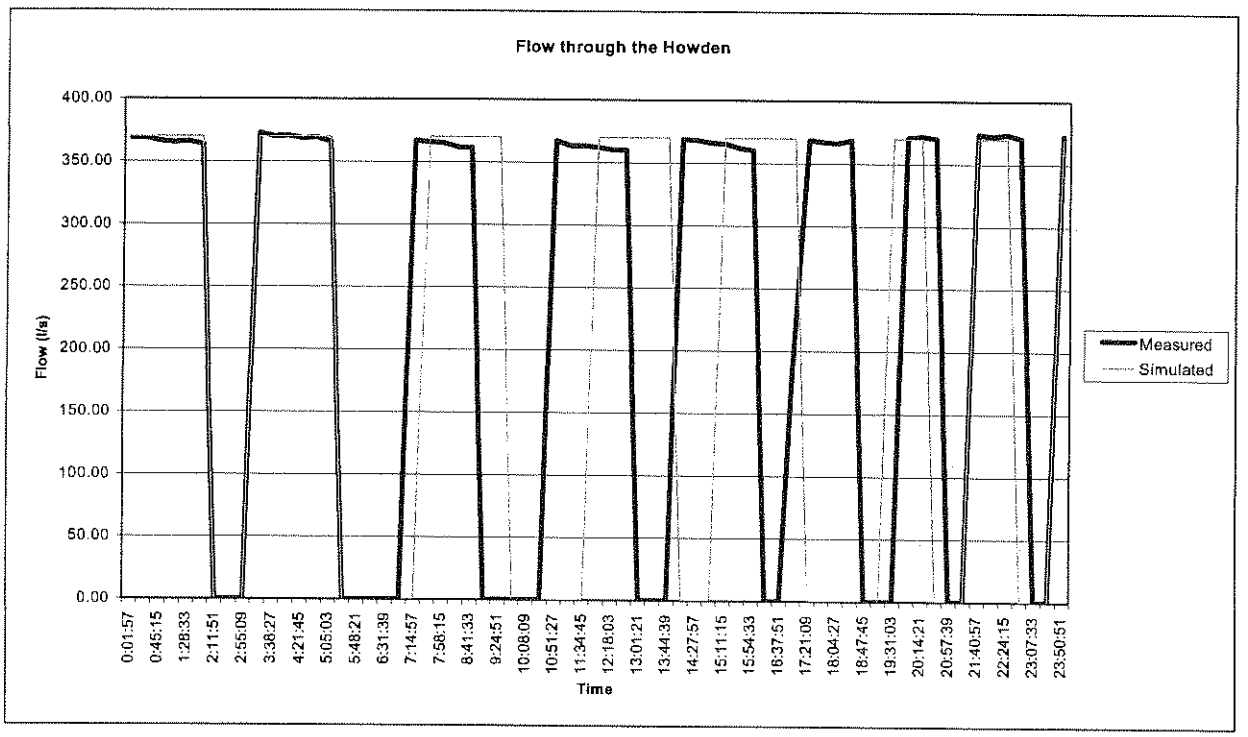

Figure C.8: Flow through the Howden Chiller

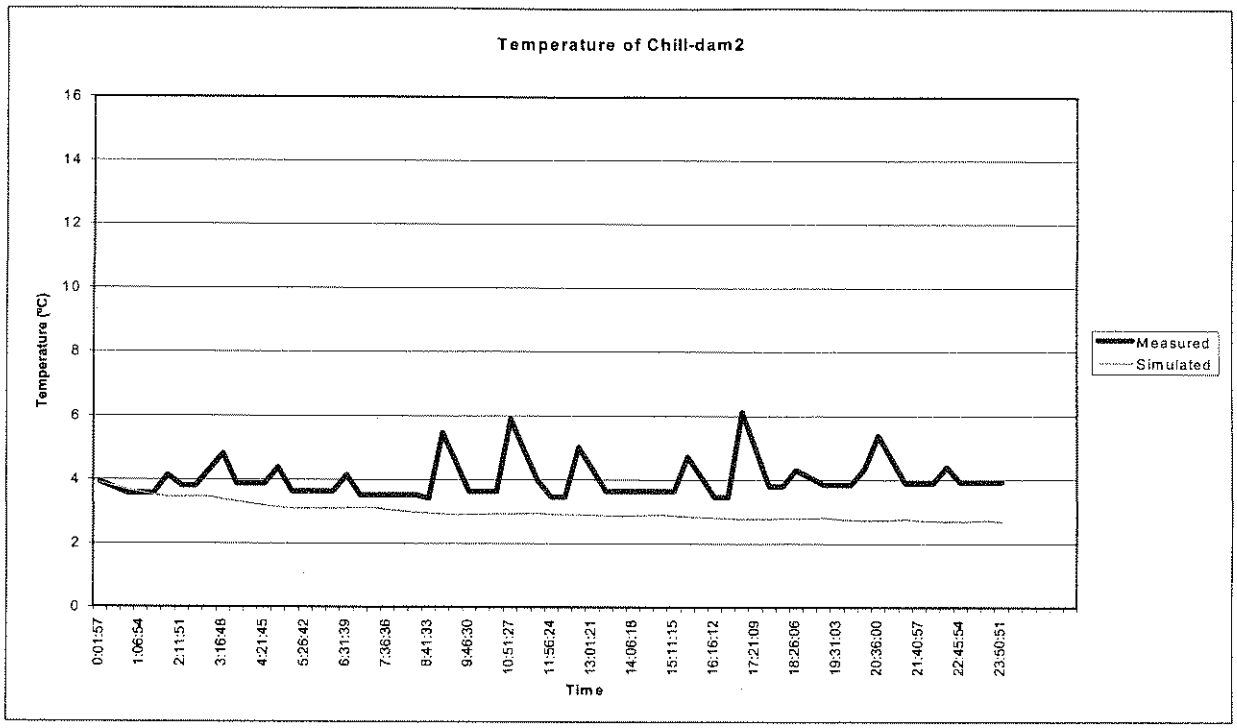

Figure C.9: Temperature of Chill-dam2

C.3. VERIFICATION OF POWER CONSUMPTION

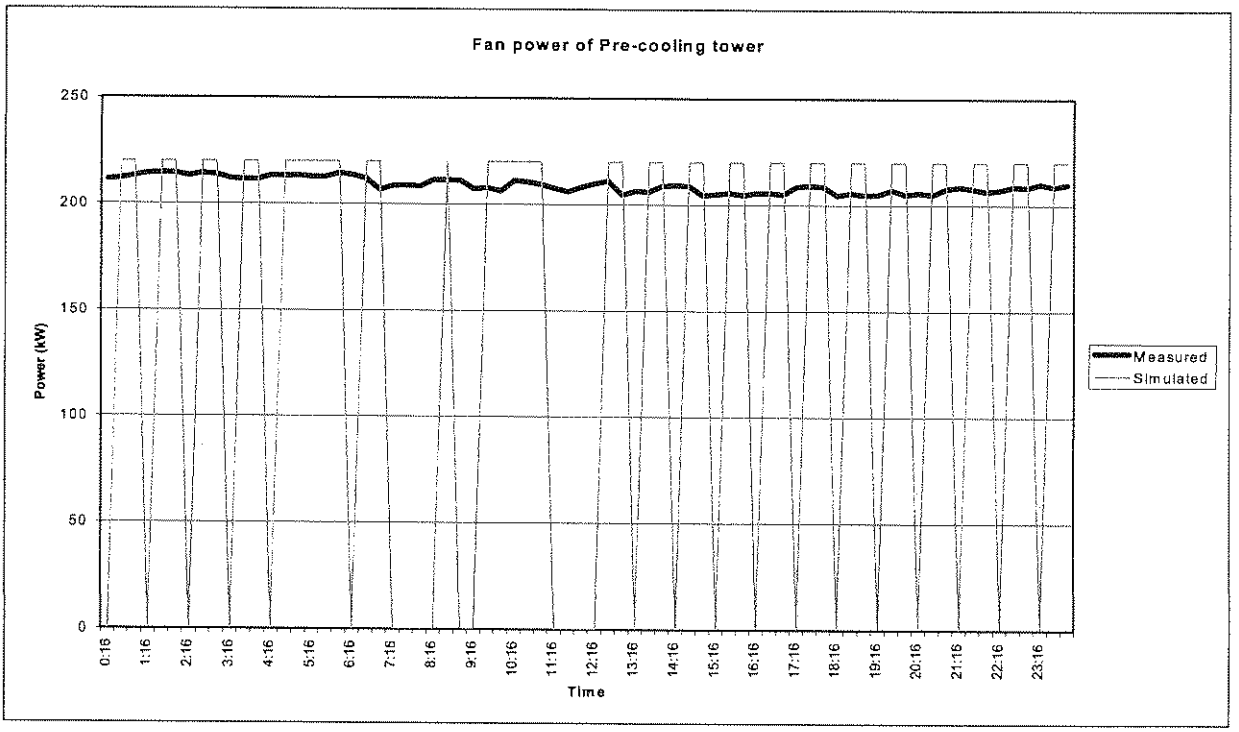

Figure C.10: Pre-cooling tower fan power verification result

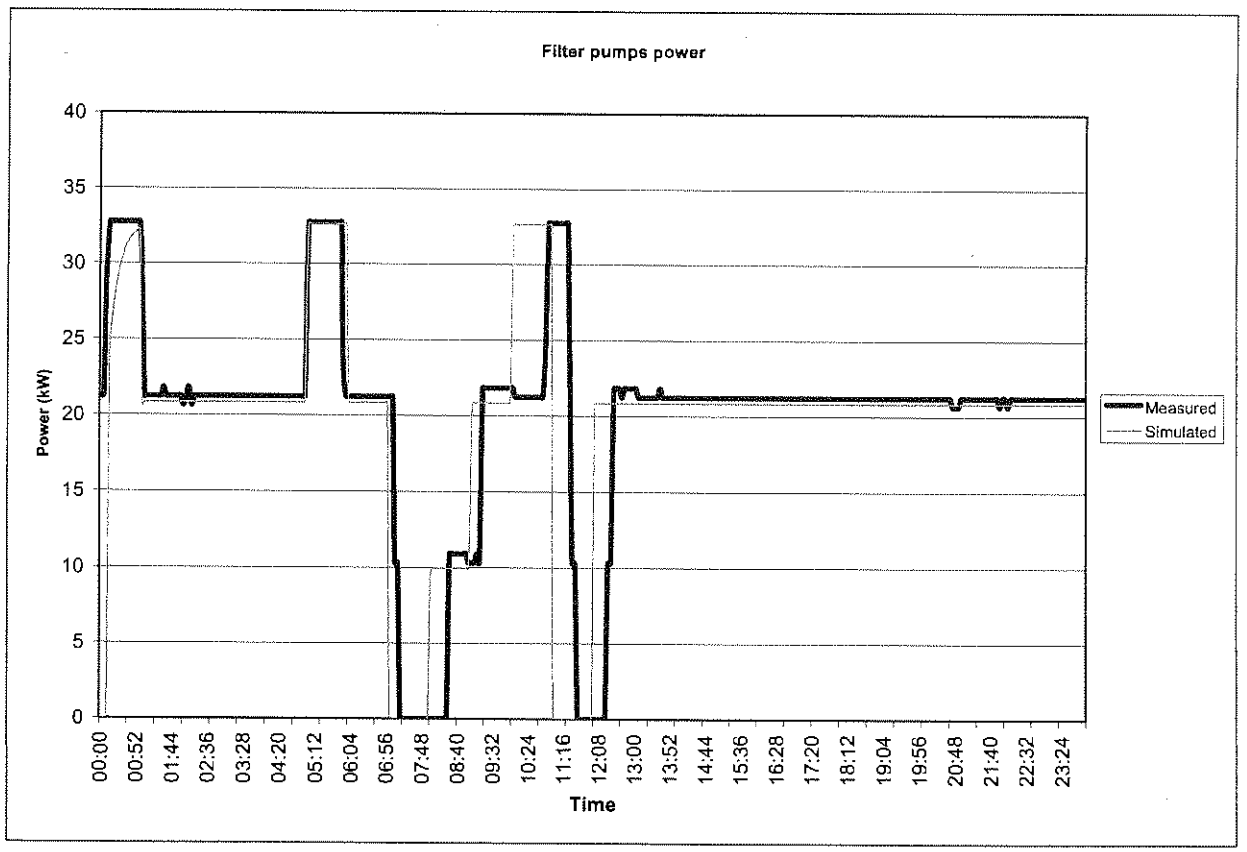

Figure C.11: Filter pumps power verification results

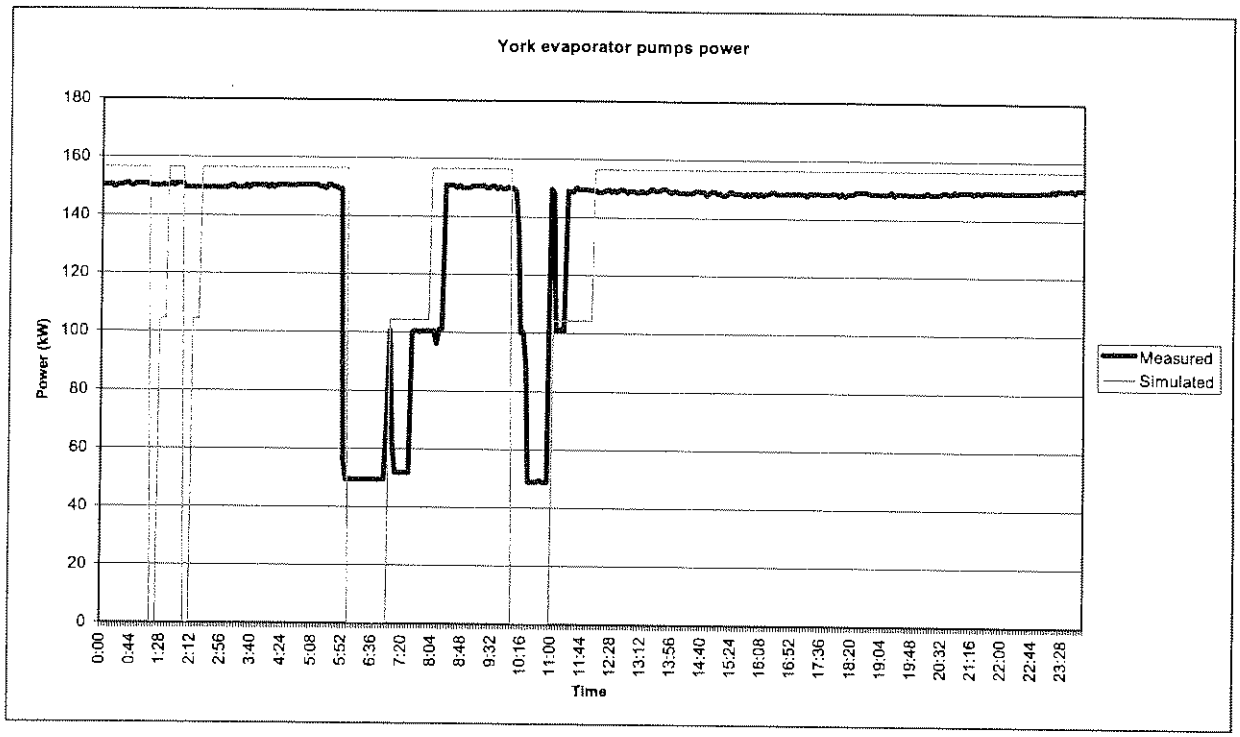

Figure C.12: York evaporator pumps power verification results

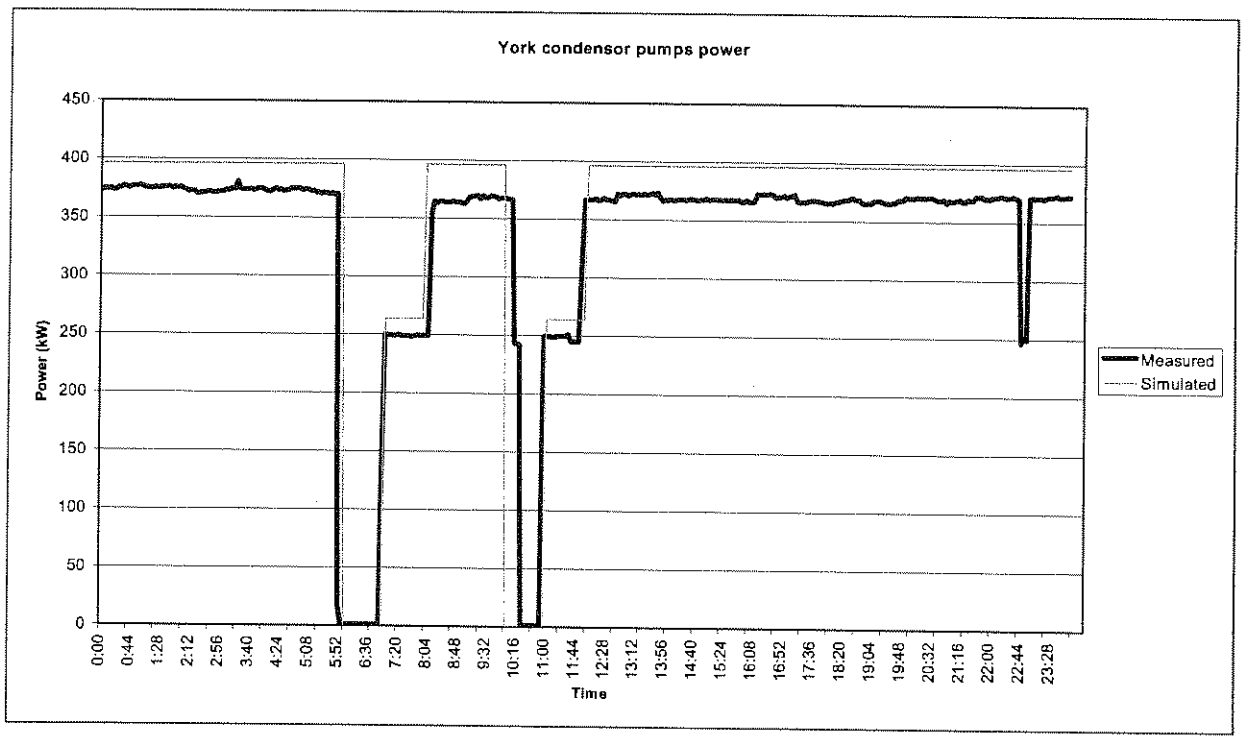

Figure C.13: York condenser pumps power verification results

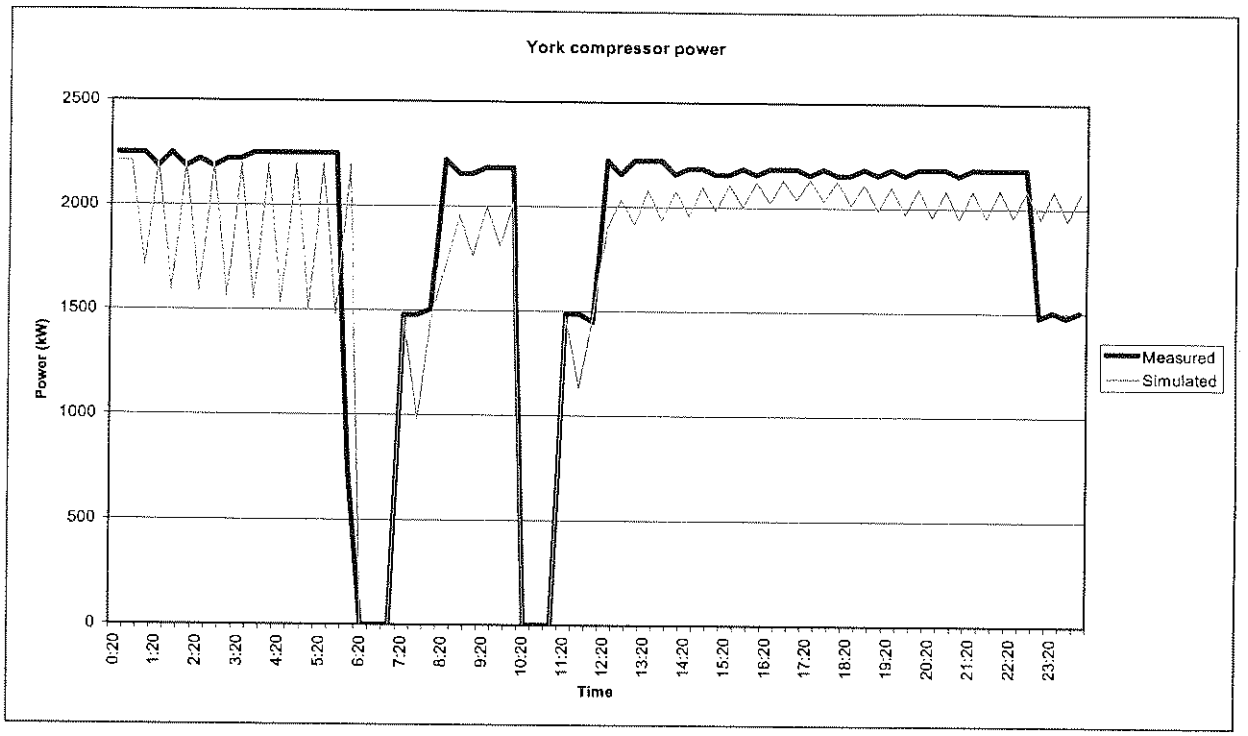

Figure C.14: York chiller compressor power verification results

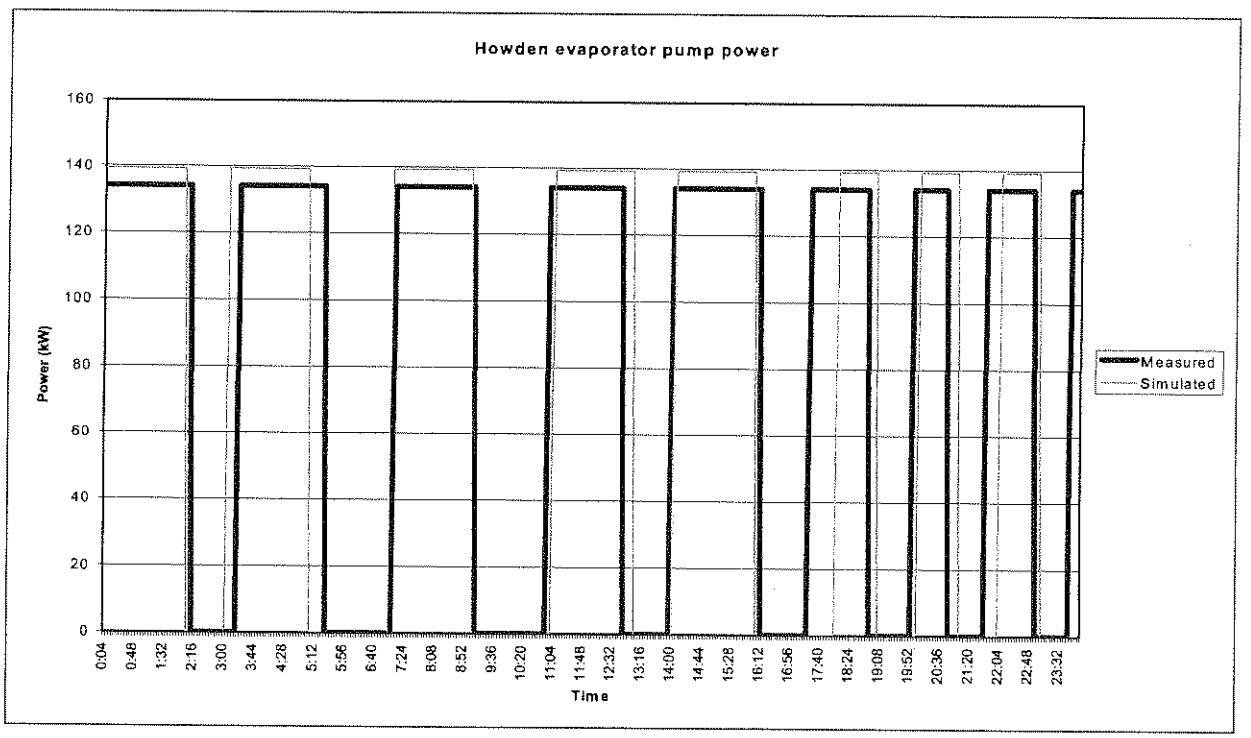

Figure C.15: Howden evaporator pump power verification results

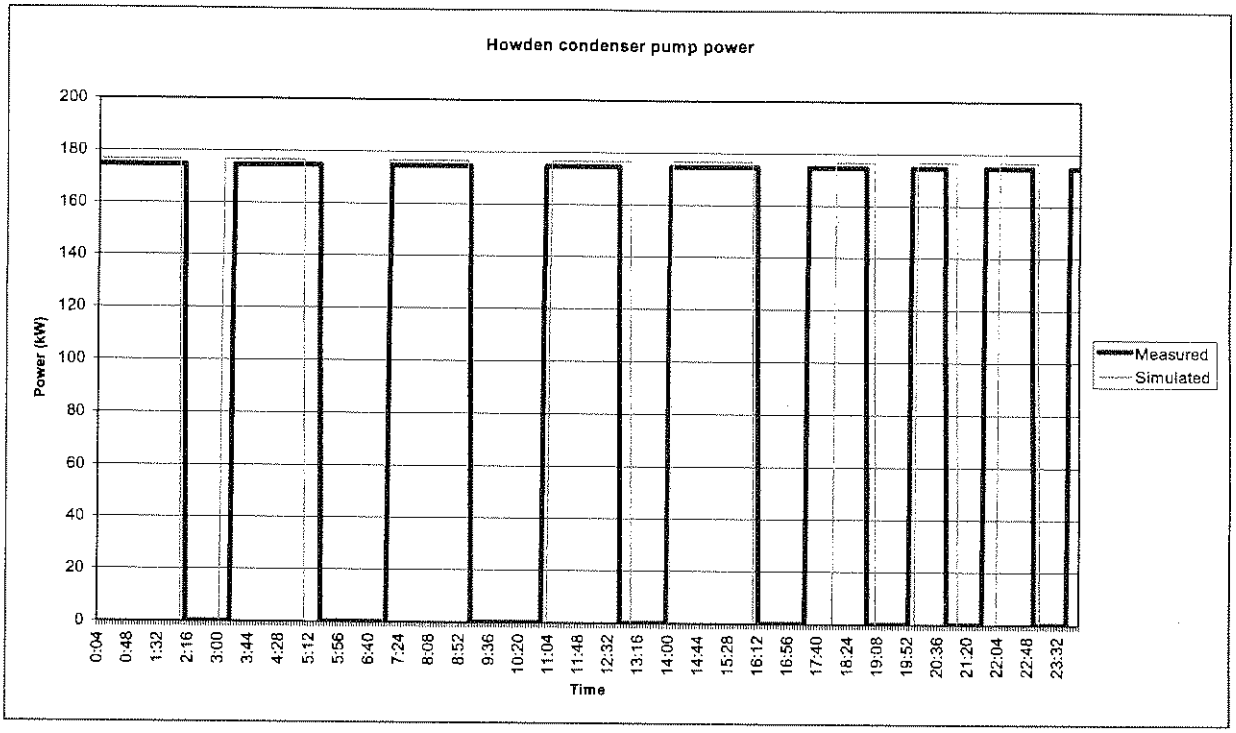

Figure C.16: Howden condenser pump power verification results

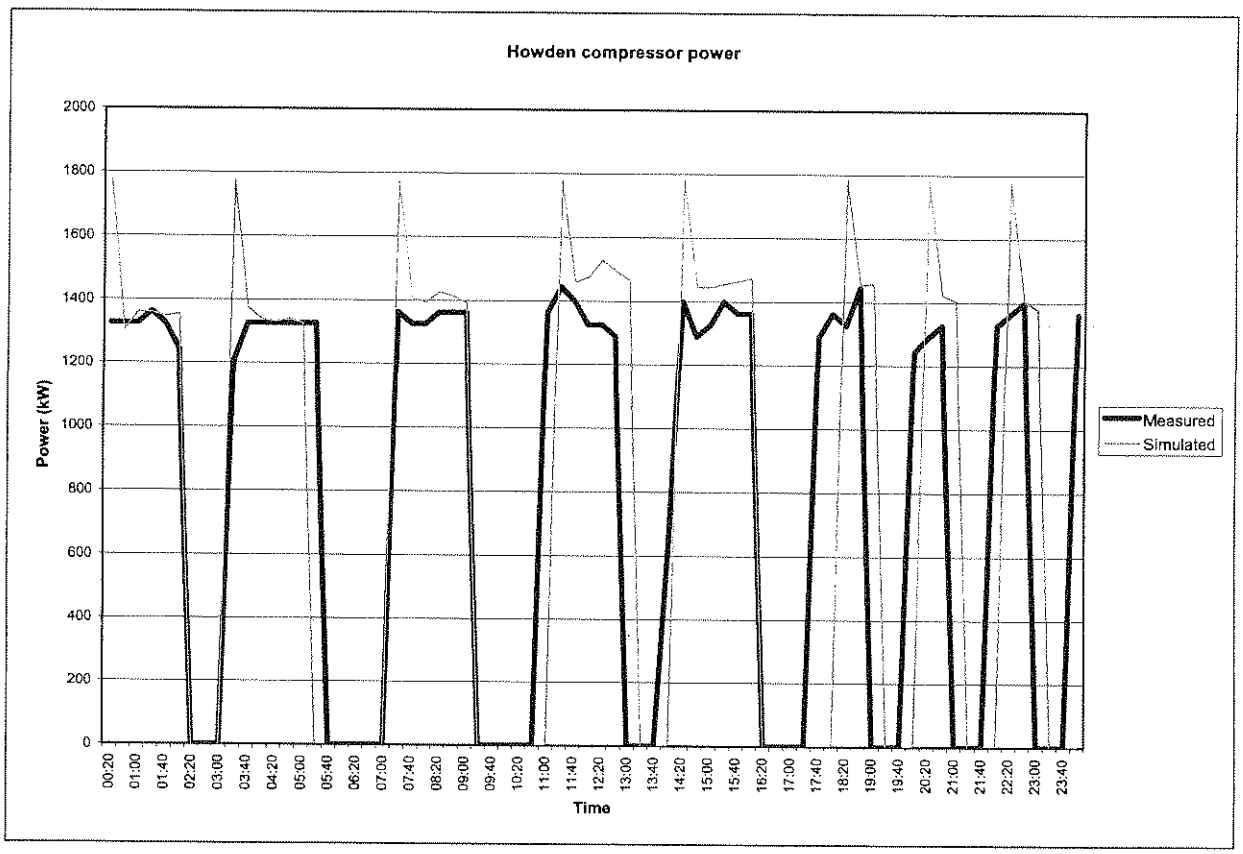

Figure C.17: Howden compressor power verification results

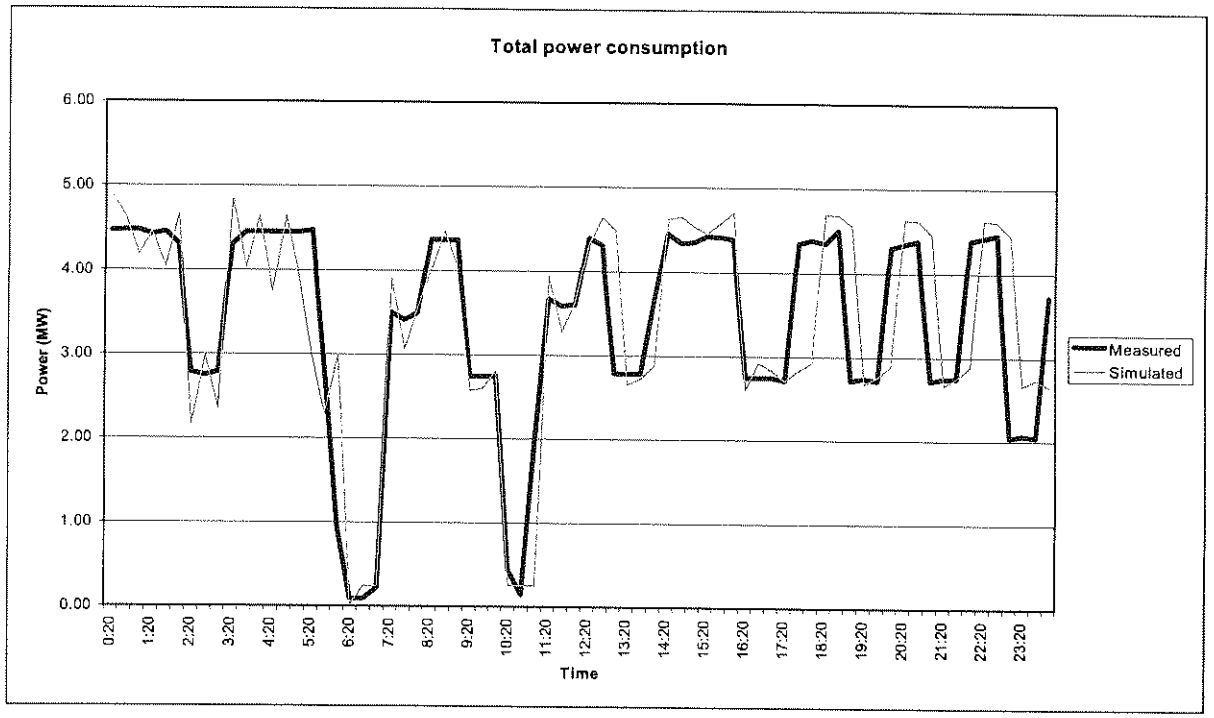

Figure C.18: Total power consumption verification results

C.4. LOAD SHIFTING POTENTIAL FOR RTP

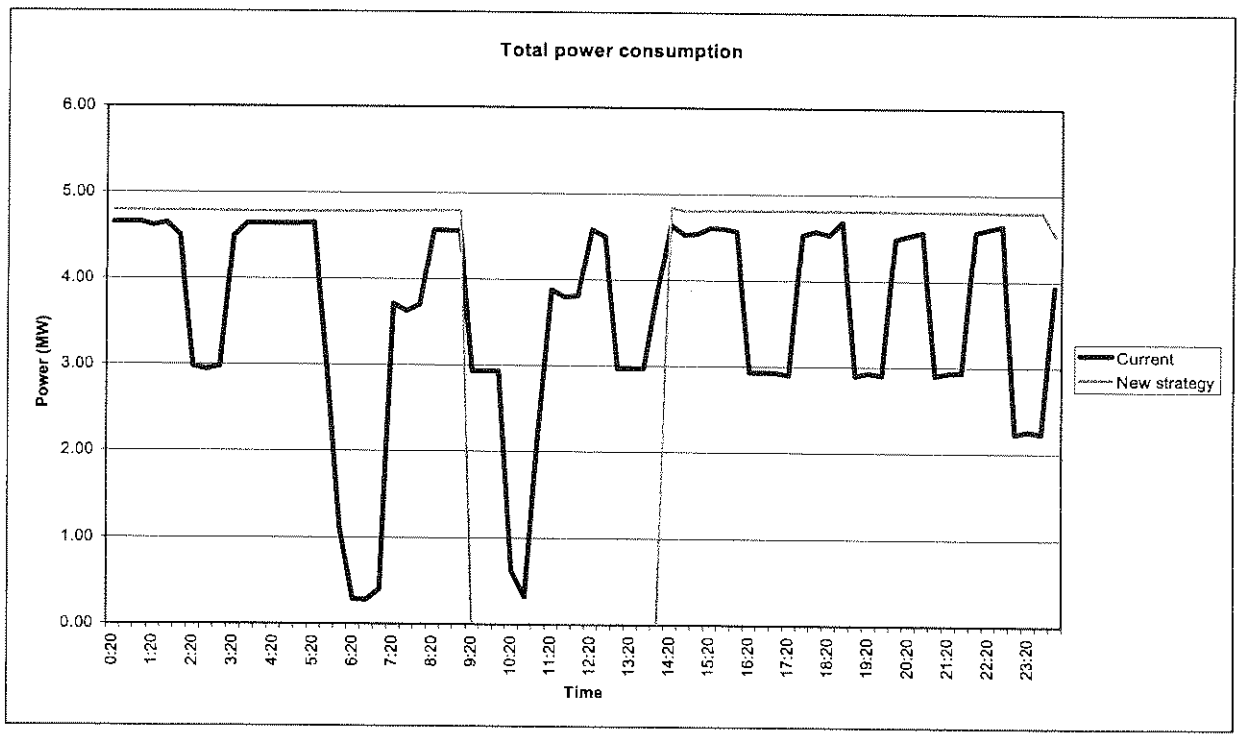

Figure C.19: The potential load shift of surface plant

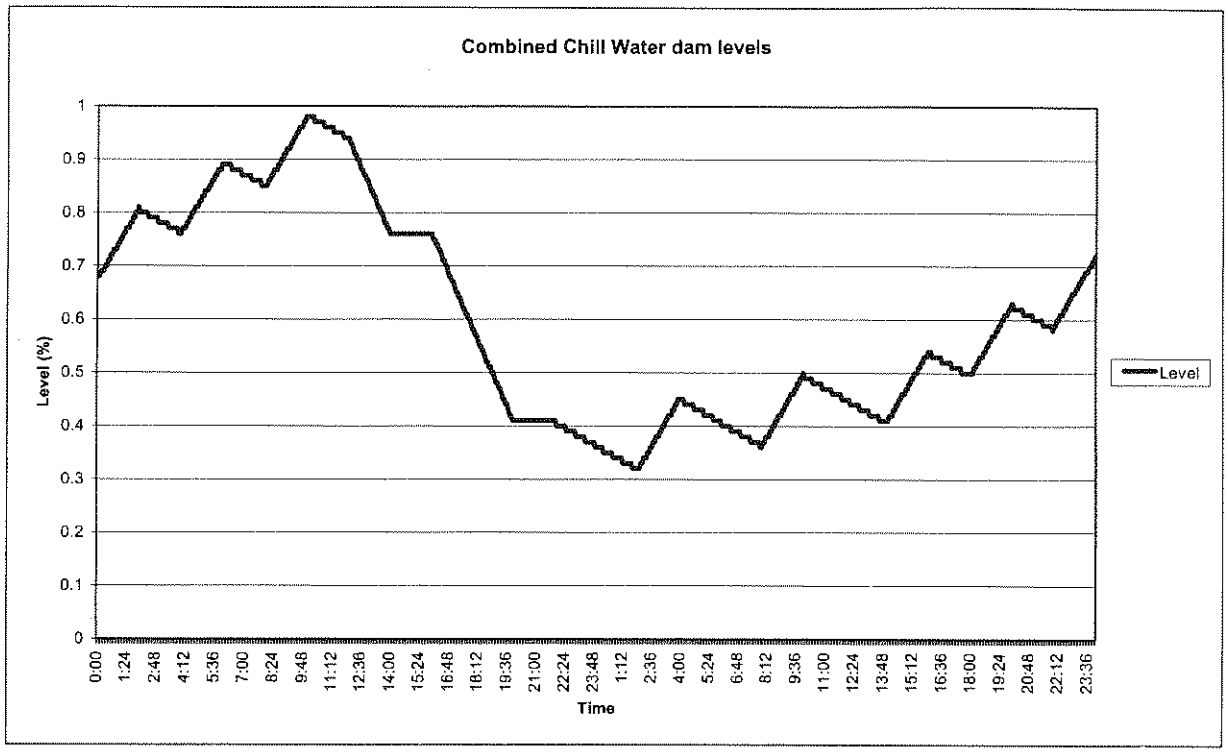

Figure C.20: The combined dam levels for the Chilled Water dams

APPENDIX D

POTENTIAL FOR DSM ON MINE PUMPING SYSTEMS

This appendix presents all the equipment specifications and base year verification results of chapter 9.

D.1. EQUIPMENT SPECIFICATIONS

The schematic layout of the Underground Pumping Stations can be seen in Figure D-1. This shows the pumps' mass flow capacity and the dams' storage capacity.

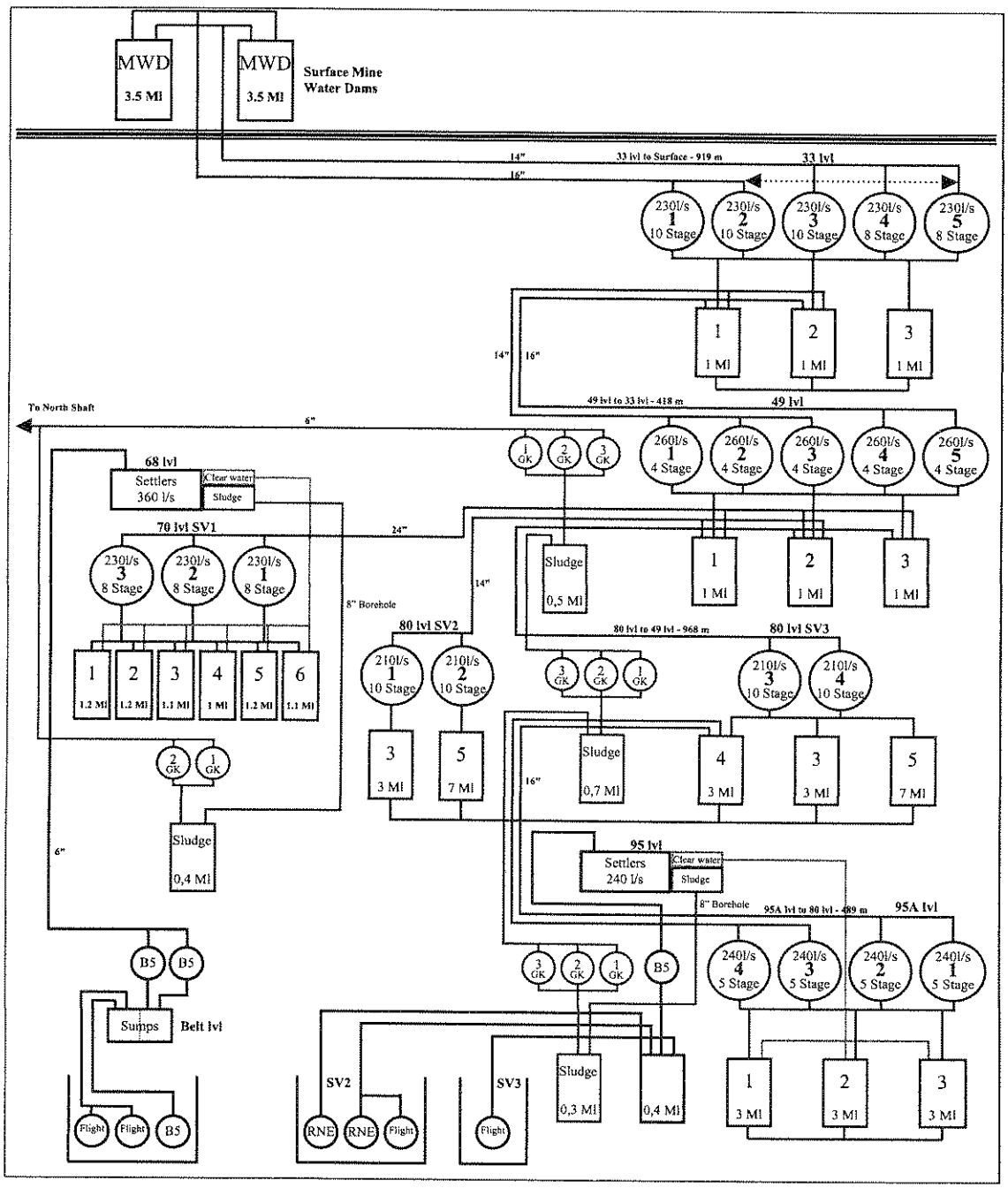

Figure D.1: Schematic layout of Underground Pumping Stations

D.1.1 Dams

Level	Depth [m]	Number of Dams	Total Capacity [m^3]
Surface	0	2	7000
33	919	3	3000
49	1337	3	3000
70	2000	6	6800
80	2305	5	23000
95A	2794	3	9000

Table D.1: Specifications of Underground Dams

D.1.2 Pumps

Level	Pumps details	Quantity	Flow [l/s]	Power [kW]	Controlled by:
33	GRIFO 10-Stage, GHP 53-29	5	230	3000	Dam level
49	GRIFO 4-Stage, GHP 58-29	5	260	1160	Dam level
70	GRIFO 8-Stage, GHP 53-29	3	230	2200	Dam level
80	GRIFO 10-Stage, GHP 53-29	4	210	3000	Dam level
95A	GRIFO 5-Stage, GHP 58-29	4	240	1600	Dam level

Table D.2: Specifications of Underground Pumps

D.2. BASE YEAR VERIFICATION

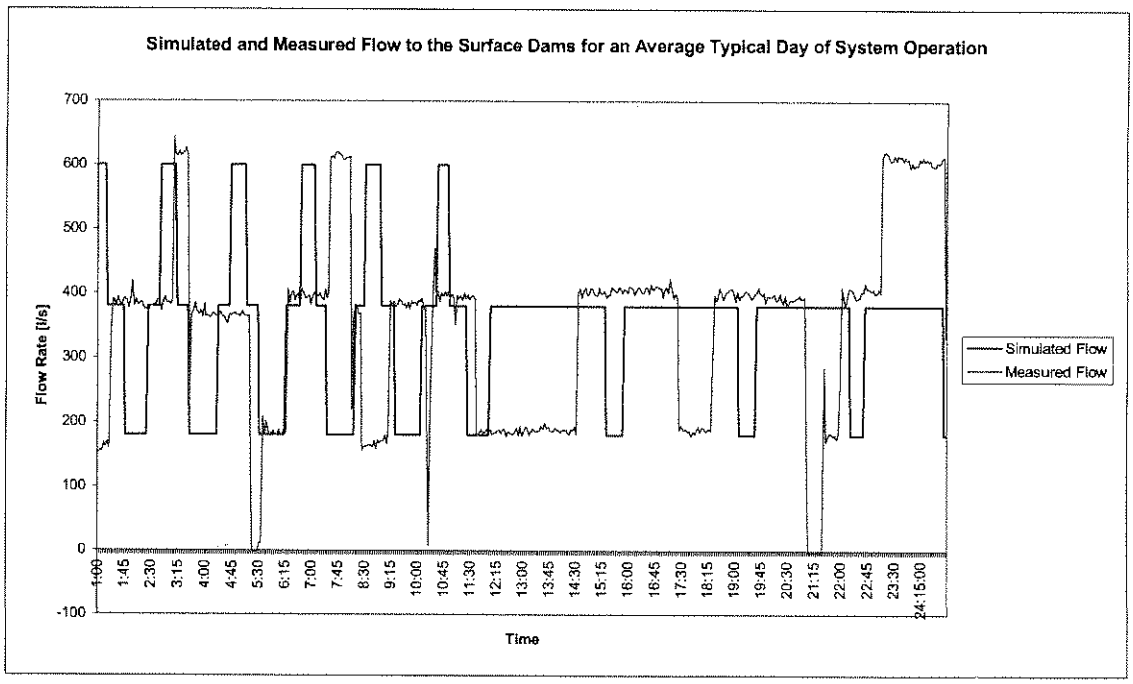

Figure D.2: Graph showing the base year verification results of the predicted flow rate from the underground workings to the surface mine water dams for an average typical day of system operation.

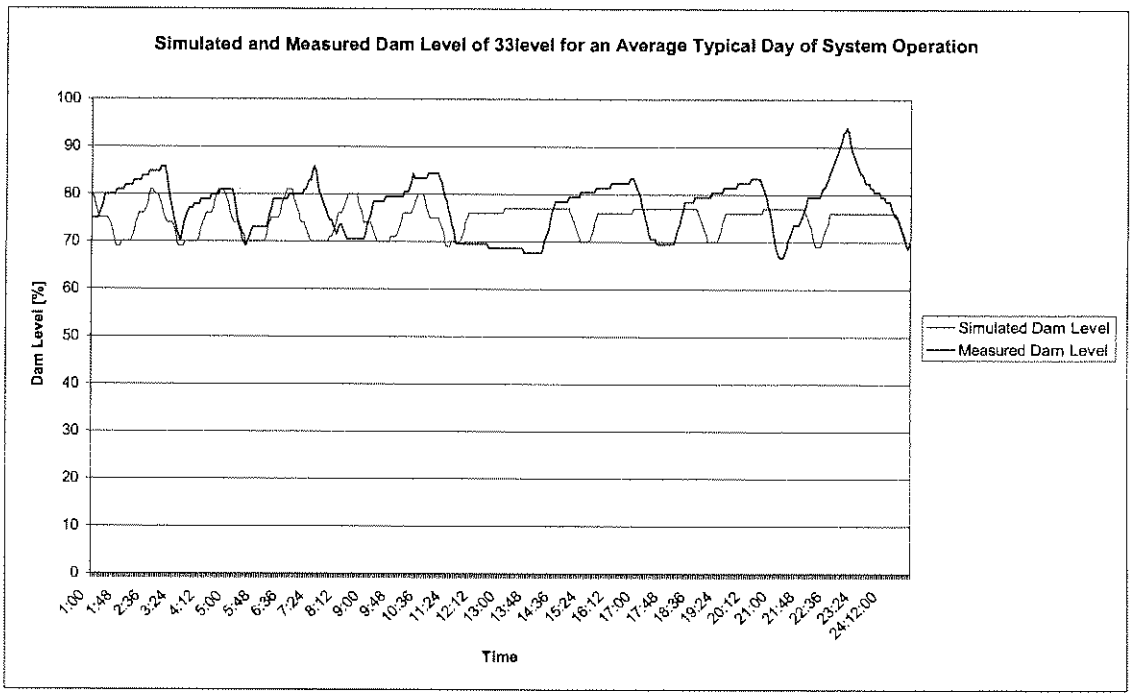

Figure D.3: Graph showing the base year verification of the predicted dam level of 33level against the actual measured dam level for an average typical day of system operation.

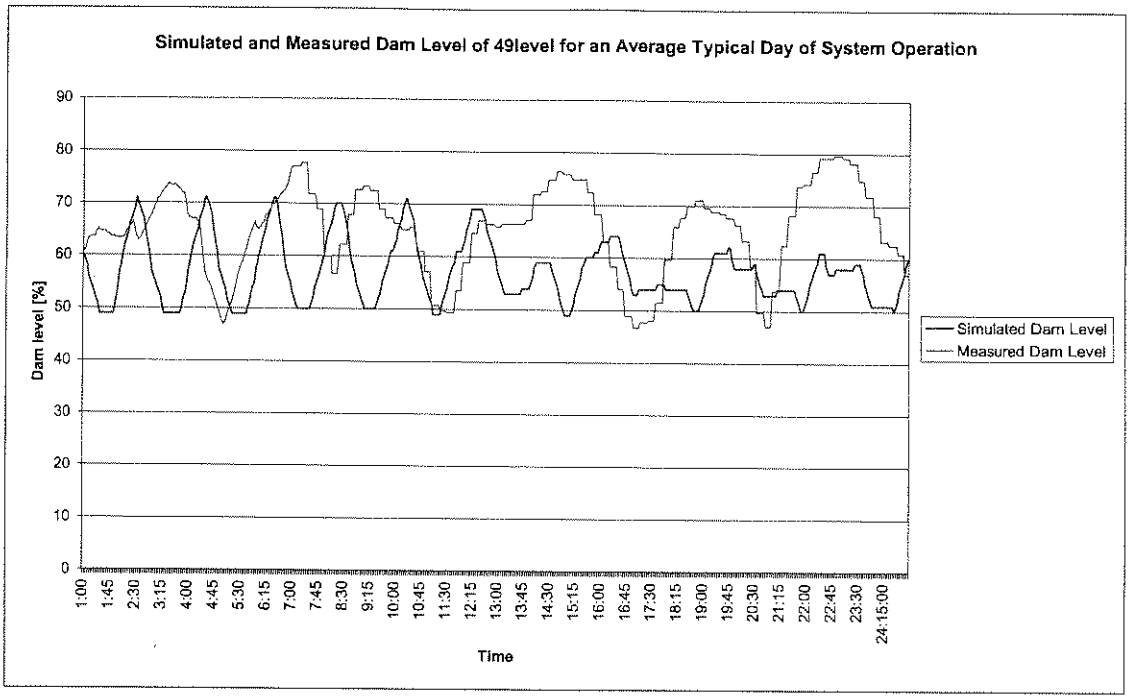

Figure D.4: Graph showing the base year verification of the predicted dam water level of 49level against the actual measured dam level for an average typical day of system operation.

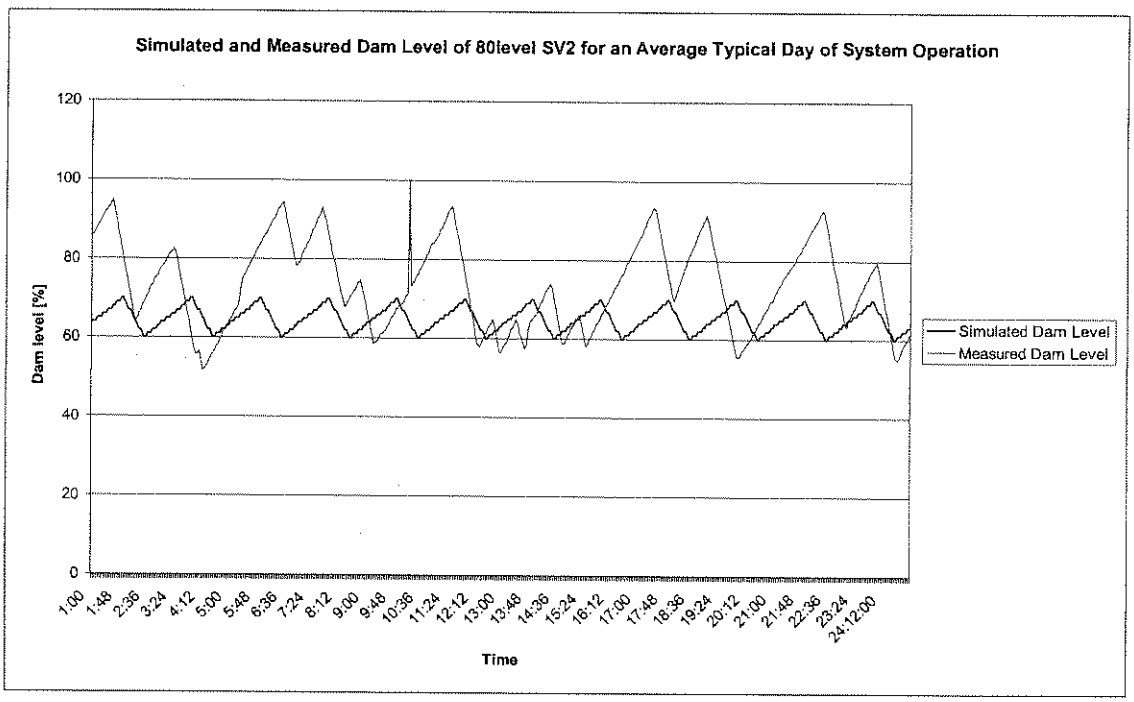

Figure D.5: Graph showing the base year verification of the predicted dam water level of 80level SV2 against the actual measured dam level for an average typical day of system operation.

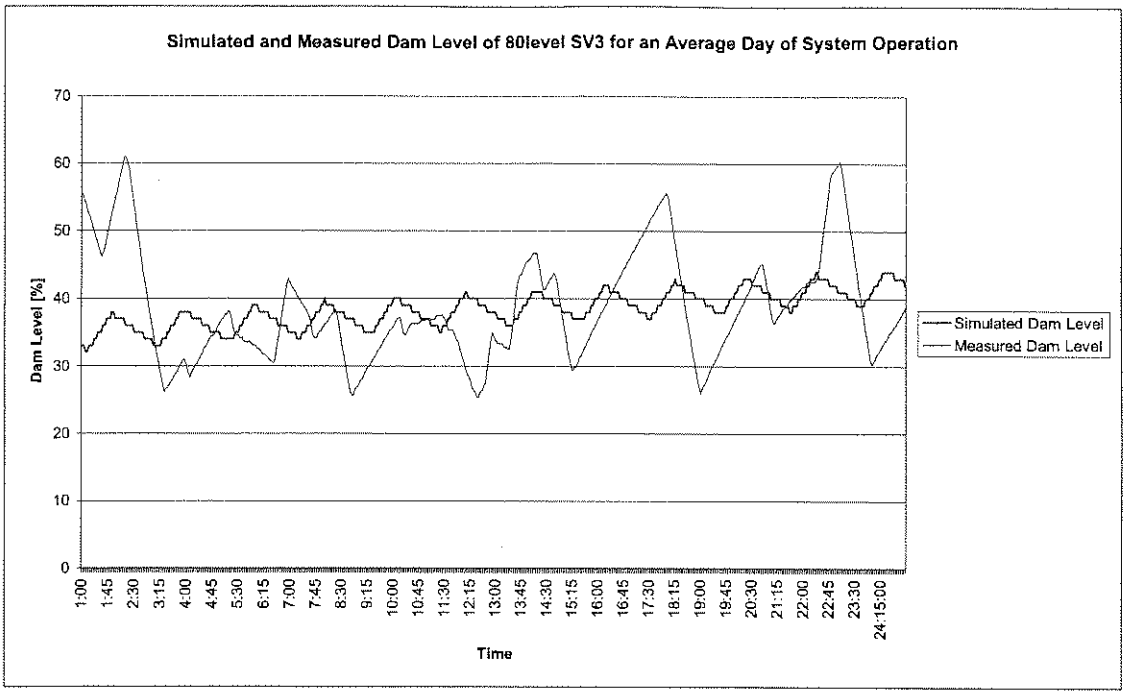

Figure D.6: Graph showing the base year verification of the dam water level of 80level SV3 against the actual measured dam level for an average typical day of system operation.

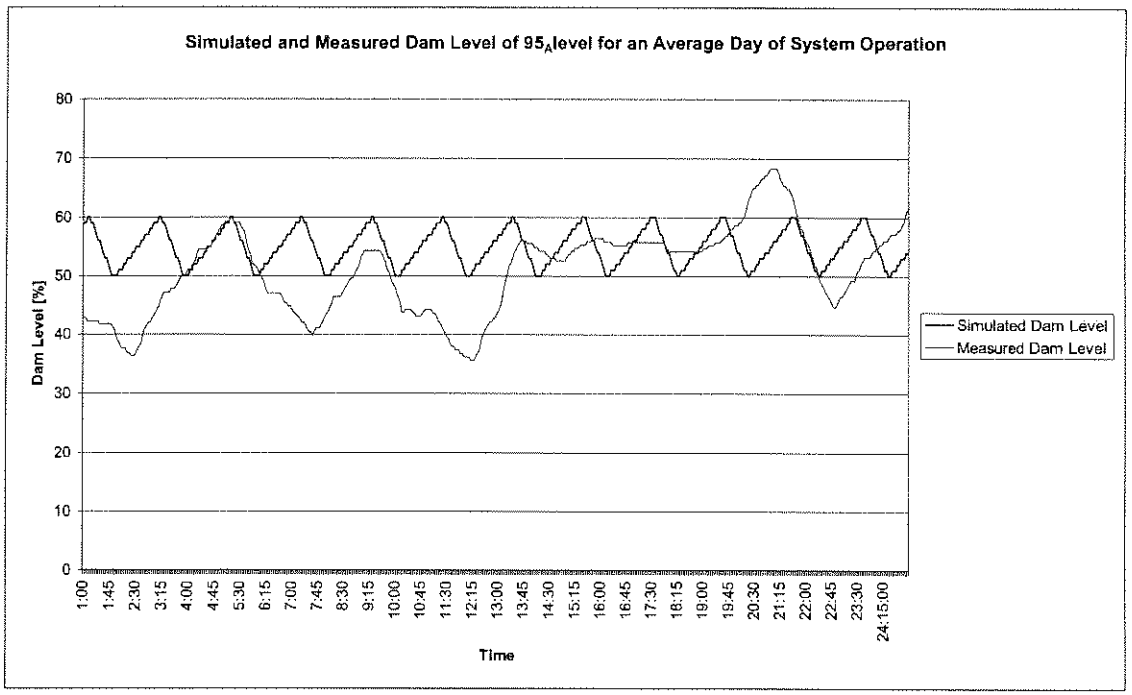

Figure D.7: Graph showing the base year verification of the predicted dam water level of 95_Alevel against the actual measured dam level for an average typical day of system operation.

APPENDIX E

ESCO PROTOCOL EVALUATION

In this appendix two ESCO protocols were evaluated. The one protocol is based on the building and HVAC system energy simulation software VisualDOE and the other one on QUICKcontrol.

ESCO PROTOCOL EVALUATION

Parties involved:

ESKOM

TEMM International

Persons involved:

S F van Geems

DC Arndt

E.1. INTRODUCTION

In this short report two ESCO (Energy Service Company) protocols were evaluated. The one protocol is based on the building and HVAC system energy simulation software VisualDOE, and the other one on QUICK*control*.

The evaluation was conducted during a period of one week and was based on the requirements of the two evaluators. In this investigation a point out of five was given by the two evaluators for each step of a typical ESCO study. Five means that the tool satisfies the required specification of the evaluators completely. The evaluators' requirements were based on the following criteria from most important to least important:

- Time to perform each step
- Level of knowledge and needed information to perform each step
- Shortcomings to perform each step
- Accuracy of assumptions made during each step

E.2. SUMMARY OF RESULTS

Total points from evaluation questionnaire out of 125:

VisualDOE: 83/125 (66%)

QUICK*control*: 107/125 (86%)

VisualDOE shortcomings:

- It is time consuming to construct the building model.
- It is only possible to configure pre-constructed typical HVAC system types.

- It is only possible to implement the control options available in the program.
- It is time consuming to create a new weather file via DOE in the USA.
- It is almost impossible to verify the simulation model without the correct climate data.
- The program does not include a report writer to complete the final report in a short period of time.
- Software support is only available in the USA or via email.
- No new software extensions can be made or initiated by the user.
- Error messages can appear regularly due to the quantity of information processed.
- The model size is limited in terms of the zones per block that can be created.
- If the programme is not used on a regular basis it requires some time to orientate oneself within the package.
- Typical equipment used in South Africa must be created.

QUICK*control* shortcomings:

- The system must be configured on a component basis. There are no typical system types to select from.
- Detailed control parameters are needed for input. There are no typical control strategies to select from, only typical controllers (PID and Step controllers).
- Typical system components (fuel boiler, air/air heat exchangers) still need to be implemented into the software.
- The simulation currently runs in excess of 20 minutes for a year simulation. The software is currently being revised which will also reduce the time required for simulations.
- The programme relies on the inputs given by the operator in terms of correctness.

E.3. EVALUATION QUESTIONNAIRE

1. General	**Point**
1.1 Simulation engine	
VisualDOE: Use the transfer function method to calculate hourly heating and cooling loads. From there it is a hand–down method from component to component to calculate the energy consumption of the system. The influence of the system control parameters can therefore not be seen in the indoor conditions. The dynamic response of the system cannot be simulated and real life control simulation is not possible.	2
QUICK*control:* Is a fully integrated building, system and control simulation program. The response of the system and building can be simulated on a minute basis to predict the effect control has on the indoor comfort. Any change in a component effect therefore the entire integrated system and building network. This makes real life control simulation possible.	5
1.2 Simulation time	
VisualDOE: A 19-zone year simulation takes about 2 minutes on a Pentium II 233 MHz PC.	5
QUICK*control:* A 10-zone year simulation takes about 9 minutes on a Pentium II 233 MHz PC.	2
1.3 Support	
VisualDOE: Support is only available from the USA via email and one local SA user.	2
QUICK*control*: Support is locally available via telephone, email and personal contact.	5
1.4 Future extensions	
VisualDOE: The program cannot be extended to satisfy new requirements of the user.	1
QUICK*control:* The program can be extended to satisfy any new requirements of the user. The program can also be extended to make provision for new areas, like mine ventilation and cooling energy simulation.	4

2. BUILDING INPUT DATA	Point
2.1 Obtain Structure information	
VisualDOE: Detail building structure data is needed for input, which involves detail building drawings. Typical structure data for South Africa is not available in the library and material properties and structure thicknesses must be obtained.	2
QUICK*control:* All needed input data can be gathered on site. No drawings are needed. A complete structure database is available for typical South African constructions. Sheets are available to gather all the relevant information.	5
2.2 Obtain building dimensions	
VisualDOE: The dimensions of each surface (including glazing) must be obtained from building drawings or measured in the building. The model will therefore reflect accurate building detail.	2
QUICK*control:* Only the internal floor area, north wall length, wall height and % glazing of each zone is needed for input. All this information can be gathered by walking through the building. Sheets are available to gather all the relevant information.	5
2.3 Obtain or measure zone air flows	
VisualDOE: Zone air is specified in terms of the supply air options: Let programme size Total flow Flow/area Air changes/hour This is again linked with options, which specify the outside air. Thermostat types together with a throttling range are specified for control purposes. Typical min & max zone temps are displayed with max supply air and outside air quantities.	4
QUICK*control:* Supply and fresh airflow rates must be obtained or measured for each zone. Sheets are available to gather all the relevant information.	3
2.4 Obtain ventilation schedules	
VisualDOE: Yearly ventilation schedules must be obtained for each	3

zone.	
QUICK*control:* Yearly ventilation schedules must be obtained for each zone. Sheets are available to gather all the relevant information.	4
2.5 Obtain lighting and other internal loads	
VisualDOE: Lighting and internal heat generation fixtures and schedules must be obtained through a walk through audit. Custom data sheet used.	4
QUICK*control:* Lighting and internal heat generation fixtures and schedules must be obtained through a walk through audit. Sheets are available to gather all the relevant information.	4
2.6 Obtain occupancy	
VisualDOE: Occupancy numbers and schedules must be obtained through a walk through audit. Custom data sheet used.	3
QUICK*control:* Occupancy numbers and schedules must be obtained through a walk through audit. Sheets are available to gather all the relevant information.	3
3. HVAC SYSTEM INPUT DATA	**Point**
3.1 Air distribution system	
VisualDOE: Component performance data, flow rates, pressures and the configuration of system must be obtained. Sheets are available to gather all the relevant information.	3
QUICK*control:* Component performance data, flow rates, pressures, the configuration of system and the control parameters must be obtained. Sheets are available to gather all the relevant information.	4
3.2 Water distribution system	
VisualDOE: Component performance data, flow rates, pressures and the configuration of system must be obtained. Sheets are available to gather all the relevant information.	3
QUICK*control:* Component performance data, flow rates, pressures, the configuration of system and the control parameters must be obtained. Sheets are available to gather all the relevant information.	4
4. VERIFICATION MEASUREMENTS	**Point**

VisualDOE: A number of conditions and the consumption of component power must be monitored to identify problem areas and to calibrate the simulation model.	3
QUICK*control:* A number of conditions and the consumption of component power must be monitored to identify problem areas and to calibrate the simulation model. Sheets are available to ensure the correct measurements are taken and for automatic data processing.	5
5. VERIFICATION SIMULATIONS	**Point**
5.1 Structure input	
VisualDOE: Each surface's dimensions and construction with its properties must be read into the program in detail. No South Africa pre-constructed library is available.	3
QUICK*control:* Only the internal floor area, north wall length and the wall height need to be read into the program. South African pre-constructed structure database is available for selection. This input can be completed on site while doing the walk through audit.	5
5.2 Occupancy input	
VisualDOE: Occupancy numbers and scheduling must be read into the program for each zone type.	3
QUICK*control:* Occupancy numbers and scheduling must be read into the program for each day type. This input can be completed on site while doing the walk through audit.	3
5.3 Internal load input	
VisualDOE: The equipment power density (w/m^2) of fixtures and the lighting power density of lights (w/m^2) and other equipment must be read into the program for each zone type.	4
QUICK*control:* The wattage fixtures and number of lights and other equipment must be read into the program for each day type. This input can be completed on site while doing the walk through audit.	4
5.4 Weather input	
VisualDOE: Weather data can be collected form the weather station or measured on site for the verification day. All new weather data including typical year data must first be sent to DOE to be transformed	2

into BIN data. This was done by Eskom.	
QUICK*control*: Weather data can be collected form the weather station or measured on site for the verification day. All new weather data including typical year data can directly be entered into the program's climate database. Typical year data is already available for all the climate regions of South Africa.	5
5.5 System input	
VisualDOE: Only typical HVAC system configurations and control options are available for selection. The user must have the necessary knowledge of system types to select the closest one to the real one. The components of the systems need not to be configured or linked.	3
QUICK*control:* Any existing system type or new type can be constructed. The system can be built exactly the same in the model as in real life. Any control logic can be modelled. Each component of the system, including the control, must be configured and linked correctly.	5
5.6 Calibrate simulation model and compare to measurements	
VisualDOE: Only average hourly verification and calibration on the main component types is possible. It is difficult to obtain the correct weather data for the verification period. Without the correct weather data it is impossible to verify.	3
QUICK*control:* Real life minute verification and calibration on component basis is possible. This implies that each component can be calibrated to ensure that the existing system and building is modelled correctly. The correct dynamics of the system can therefore be incorporated into the simulations. A logic and simple method is available to perform the calibration.	4

6. RETROFIT SIMULATIONS	**Point**
6.1 Base year simulation	
VisualDOE: Hourly year simulations can be executed which include weekday, Saturday, Sunday and public holiday schedules. Peak demand and energy consumption are therefore based on average hourly values.	3
QUICK*control:* Minute year simulations can be executed which include weekday, Saturday and Sunday schedules. Peak demand and energy consumption are therefore based on integrated hourly values as used in South Africa.	4
6.2 Retrofit simulations: Structure changes	
VisualDOE: Structural changes (insulation, shading devices) can be implemented into the simulation model with ease.	4
QUICK*control:* Structural changes (insulation, shading devices) can be implemented into the simulation model with ease.	4
6.3 Retrofit simulations: Equipment scheduling	
VisualDOE: The dynamic effect of equipment scheduling can only be investigated on an hourly basis. It is therefore difficult to ensure indoor comfort for optimal scheduling.	3
QUICK*control:* The dynamic effect of equipment scheduling can be investigated on a minute basis. It is therefore possible to ensure indoor comfort for optimal scheduling.	5
6.4 Retrofit simulations: New control strategies	
VisualDOE: The user has the option to select from a menu typical energy efficient control strategies. However the user is not always sure of the strategy implemented by the software. The user cannot implement new customised inventions. The effect of new control setpoints is displayed in terms of min & max temps.	3
QUICK*control:* Energy efficient control must be implemented with the typical controllers available in the software. This implies that any new control inventions can be implemented into the software and the user will be sure of the logic involved. The effect new control has on indoor comfort can be predicted by the software.	4

6.5 Retrofit simulations: New tariff structure	
VisualDOE: The effect of new tariff structures can be investigated.	4
QUICK*control:* The effect of new tariff structures can be investigated. Relative easy to create new structures. Certain assumptions need to be made in terms of kVAr charges.	2
6.6 Retrofit simulations: Plant upgrades	
VisualDOE: Plant changes can be implemented by initiating standard futures. i.e. variable speed, inlet vanes, discharge dampers.	5
QUICK*control:* Plant changes must physically be constructed which might be time consuming.	2
6.7 Retrofit simulations: Combination of options	
VisualDOE: This can easily be achieved after the verification stage of the process.	4
QUICK*control:* It requires the construction of a new layout. From a time point of view it will take longer to construct. Standard models can however be generated on request.	3
7 REPORT WRITING	**Point**
VisualDOE: The package does not include any type of report writer. The user must therefore build his own report templates in MS Word. This can take up to a week to complete the report.	2
QUICK*control:* This protocol provides a report writer, which is based on a master and standard template database structure. The master database can be updated after each project and pulled into the template database of each new project. Simulation results can be linked to the database in graph or table format for import. The report writer automatically generates the report in MS Word. It will only take 2 days to finalise the report.	4

NOTES TO THE READER:

The writers' opinions within this ESCO protocol evaluation are in no way a final judgement on any of the two packages. Both packages offer unique features, which makes the application thereof acceptable.

The opinions offered in this document do not necessarily reflect the opinion of Eskom, and therefore Eskom does not accept responsibility for the comments by the authors.